Pertanika Journal of Science & Technology
Vol. 19 (1) Jan. 2011

Contents

Research Management Centre (RMC)
1st Floor, IDEA Tower II
UPM-MTDC Technology Centre
Universiti Putra Malaysia
43400 UPM Serdang
Selangor Darul Ehsan
Malaysia

http://www.rmc.upm.edu.my
E-mail : ndeeps@admin.upm.edu.my
Tel : +603 8947 1622 /1620

UPM Press
Universiti Putra Malaysia
43400 UPM Serdang
Selangor Darul Ehsan
Malaysia

http://penerbit.upm.edu.my
E-mail : penerbit@putra.upm.edu.my
Tel : +603 8946 8855/8854
Fax : +603 8941 6172

ISSN 0128-7680
9 770128 768083 01

Pertanika JST
Vol. 19 (1) Jan. 2011
UPM Press, Malaysia

Pertanika Journal of

SCIENCE & TECHNOLOGY

JST

VOL. 19 (1) JAN. 2011

PERTANIKA JOURNALS

A scientific journal published by Universiti Putra Malaysia Press

About the Journal

Pertanika is an international peer-reviewed journal devoted to the publication of original papers, and it serves as a forum for practical approaches to improving quality in issues pertaining to tropical agriculture and its related fields. *Pertanika* began publication in 1978 as the Journal of Tropical Agricultural Science. In 1992, a decision was made to streamline *Pertanika* into three journals to meet the need for specialised journals in areas of study aligned with the interdisciplinary strengths of the university. The revamped Journal of Science & Technology (JST) aims to develop as a pioneer journal focusing on research in science and engineering, and its related fields. Other *Pertanika* series include Journal of Tropical Agricultural Science (JTAS); and Journal of Social Sciences and Humanities (JSSH).

JST is published in **English** and it is open to authors around the world regardless of the nationality. It is currently published two times a year, i.e. in **January** and **July**.

Goal of *Pertanika*

Our goal is to bring the highest quality research to the widest possible audience.

Quality

We aim for excellence, sustained by a responsible and professional approach to journal publishing. Submissions are guaranteed to receive a decision within 12 weeks. The elapsed time from submission to publication for the articles averages 5-6 months.

Indexing of *Pertanika*

Pertanika is now over 30 years old; this accumulated knowledge has resulted in Pertanika journals being indexed in SCOPUS (Elsevier), EBSCO, AGRICOLA, and CABI. etc. JST is indexed in EBSCO.

Future vision

We are continuously improving access to our journal archives, content, and research services. We have the drive to realise exciting new horizons that will benefit not only the academic community, but society itself.

We also have views on the future of our journals. The emergence of the online medium as the predominant vehicle for the 'consumption' and distribution of much academic research will be the ultimate instrument in the dissemination of research news to our scientists and readers.

Aims and scope

Pertanika Journal of Science and Technology aims to provide a forum for high quality research related to science and engineering research. Areas relevant to the scope of the journal include: *bioinformatics, bioscience, biotechnology and biomolecular sciences, chemistry, computer science, ecology, engineering, engineering design, environmental control and management, mathematics and statistics, medicine and health sciences, nanotechnology, physics, safety and emergency management,* and related fields of study.

Editorial Statement

Pertanika is the official journal of Universiti Putra Malaysia. The abbreviation for *Pertanika* Journal of Science & Technology is *Pertanika J. Sci. Technol.*

Editorial Board

Editorial Board

Pertanika Editorial Office

Research Management Centre (RMC)
1st Floor, IDEA Tower II, UPM-MTDC Technology Centre
Universiti Putra Malaysia, 43400 Serdang, Selangor, Malaysia
Tel: +603 8947 1622, 8947 1620
E-mail*:* ndeeps@admin.upm.edu.my

Publisher

The UPM Press
Universiti Putra Malaysia
43400 UPM, Serdang, Selangor, Malaysia
Tel: +603 8946 8855, 8946 8854 • Fax: +603 8941 6172
penerbit@putra.upm.edu.my
URL *:* http://penerbit.upm.edu.my

Pertanika Journal of Science & Technology
Vol. 19 (1) Jan. 2011

Contents

ISSN: 0128-7680
Pertanika J. Sci. & Technol. **19 (1)**: 1 – 9 (2011)

Effects of Different Environmental Parameters on the Respiratory Metabolism of the Larvae of Malaysian Horseshoe Crab, *Tachypleus gigas* (Müller)

Suniza, A. M. S., Zaleha Kassim and Anil Chatterji*
Institute of Tropical Aquaculture, Universiti Malaysia Terengganu, 21030 Kuala Terengganu, Terengganu, Malaysia
**E-mail: anilch_18@yahoo.co.in*

ABSTRACT

Respiratory metabolism of the larvae of Malaysian horseshoe crab *Tachypleus gigas* (Müller) was studied under different salinities, pH, and temperature. The trend in oxygen consumption was uniform at all salinities, ranging from 10-40 ppt, indicating insignificant influence on the oxygen consumption by the larvae. Similarly, the correlation coefficient values showed that the relationship between oxygen consumption and salinity was not significant ($P > 0.05$; $r = 0.245$). During the first three hours, the oxygen consumption was 8.89, 10.72, 17.4, and 12.06% at 10, 20, 30, and 40 ppt salinities, respectively. Meanwhile, the maximum oxygen consumption was recorded after 12 hrs, i.e. at salinity 20 ppt. A sudden drop in oxygen consumption was recorded during 3-6 hours of the experiment. This was followed by a gradual increase in the consumption of oxygen up to 12 hours of experiment. A similar trend in the oxygen consumption was observed in different pH levels, ranging from 5 to 9. At pH 6 and 9, during the first six hour, a moderate consumption of oxygen was observed. However, at pH 6, 7 and 8, the rates of oxygen consumption were found to be relatively greater after six hours, indicating unfavourable conditions. The data were statistically tested and it was found that a high degree of correlations existed between pH and oxygen consumption ($r = 0.97$). The analysis of covariance showed a significant relationship between oxygen consumption and pH ($P < 0.05$). Meanwhile, minimal variation in oxygen consumption was recorded between 30 and 40°C, with a gradual decrease in dissolved oxygen concentration up to 12 hours of experimental time. At 50°C, almost all dissolved oxygen was consumed by the larvae. The rate of oxygen consumption between 30 and 40°C was low during the first 9 hours of the experiment but it was significantly increased at later hours. A sudden increase in the oxygen consumption was recorded at 50°C, suggesting that it might be the most unfavourable temperature condition. Meanwhile, a significant relationship was observed between temperature and oxygen consumption ($P < 0.05$; $r = 0.98$).

Keywords: Environmental parameters, respiratory metabolism, larvae, Malaysian horseshoe crabs

INTRODUCTION

Respiration is a process where marine organisms obtain sufficient quantity of oxygen and release carbon dioxide. It is also an important phenomenon in controlling different physiological activities of the animals, such as maintenance of the blood pH, proper oxygen tension of the blood and normal body temperature. The most frequently parameter used to assess crustacean respiratory metabolism

*Corresponding Author

is oxygen consumption by the animal. It is important to note that respiratory metabolism of marine organism is dependent on many environmental factors. Among other, salinity, temperature, and pH are the main external factors controlling the respiratory metabolism of the marine organisms (Wolvekamp and Waterman, 1960). In addition, there are also some other important intrinsic factors, like body size of the animal, that also play an important role in the organisms' metabolic rate (Gaudy and Sloane, 1981).

Horseshoe crabs have well-developed external gills in the form of appendages which are known as gill lamellae. These gill lamellae have well-developed circulating system with blood vessels that help the animal in respiration (Chatterji, 1994). Gases diffuse from the surrounding water through the moist epithelium of the gill and circulate these to the blood vessels. In the present study, the effects of salinity, pH and temperature on the respiratory metabolism of larvae of the Malaysian horseshoe crab, *Tachypleus gigas* (Müller) were assessed.

MATERIALS AND METHODS

For the purpose of this study, fertilized eggs of the Malaysian horseshoe crab (*T. gigas*) were directly collected from the nest made on the breeding beach of Balok in Kuantan, Pahang (Lat 3° 56.915' N; Long 103° 21.933' E). The experiments were carried out at Akuatrop Plankton Laboratory and Institute Oceanography (INOS) Biotech Laboratory, Universiti Malaysia Terengganu (UMT). The eggs were kept for incubation at a constant temperature of 27±1°C. The trilobite larvae were hatched between 42 and 45 days of incubation and this was followed by the first moulting after 75 days. The larvae were collected and divided into several groups immediately after the first moulting.

Seawater was collected from the marine hatchery of the Institute of Tropical Aquaculture and kept in a circular tank under the sun for evaporation to achieve a salinity of 40 ppt. Different salinities of water were prepared by diluting 40 ppt of seawater with sterilized freshwater. Meanwhile, a salinometer (Atago, S/Mill, Japan) was used to determine the salinity. A portable pH meter (Thermo Russel RL060P) was used to record the pH of the seawater after calibrating it with standard pH Buffers of 4.2, 7.0, and 9.2. The pH of seawater was adjusted from 5-7 by 1 N HCl and 7-9 by 1 N NaOH solutions with the help of a portable pH meter. A constant temperature water bath was used to control the temperatures of the experimental tanks ranging from 30-50°C. Oxygen consumption in larvae was studied in specially designed glass respiratory chambers of 2 L capacity. A small PVC tube was fitted at one end of the glass respiratory chamber to insert the oxygen probe. The oxygen concentration was recorded using a pinpoint dissolved oxygen monitor (YSI Hand Operated Oxygen: Temperature Meter Model 550 A).

In order to study the effect of salinity on respiratory metabolism, larvae that ranged in the weight from 0.63 to 0.89 g were initially acclimatized for one hour in 5 L seawater of different salinities, i.e. from 10, 20, 30, and 40 ppt. A batch consisting of 30 larvae each were then transferred from the acclimatization tank to the respective respiratory chamber. Dissolved oxygen concentrations were recorded immediately after transferring the larvae into the respiratory chambers. This was followed by sealing the surface of respiratory chamber with liquid paraffin so as to avoid any diffusion of oxygen from the air. The respiratory chamber was kept inside a constant temperature room, where the temperature was maintained at 24±1°C. Meanwhile, the pH of the water was maintained at 7.0 in each set of the experiment.

In the second set of the experiment, 30 larvae were acclimatized in 5 acclimatization tanks of 5L capacity and at a salinity of 30 ppt. The respiratory metabolism of larvae was studied under 5, 6, 7, 8, and 9 pH.

In the third set of experiment, the effects of temperature at 30, 40, and 50°C on the respiratory metabolism of the larvae were studied. About 10L of filtered seawater, at a salinity of 30 ppt and pH 7.0, was aerated for two hours at the beginning of the experiment. A batch of 30 larvae was then transferred into a respiratory chamber. The respiratory chamber was kept in a temperature-controlled water bath. The temperature of the water bath was slowly adjusted to the desired level to avoid any physical stress to the larva. Before sealing the surface of the respiratory chamber with liquid paraffin, dissolved oxygen concentration was recorded using an oxygen meter.

All the experiments were conducted in replicate and in all sets of the experiment; the values of dissolved oxygen were recorded at 3-h intervals for 12 hours. The decrease in dissolved oxygen level was considered as the amount of oxygen (mg/l per 3 hour) used by the larvae during the experimental period.

RESULTS

During the acclimatization and experimental period, no larval mortality indicating the sturdiness of the animal under different stress conditions was observed. The influence of salinity on the respiratory metabolism of the larva is presented graphically in *Fig. 1*. The trend in oxygen consumption was more or less uniformed at all salinities, ranging from 10-40 ppt indicating insignificant influence of salinity on the oxygen consumption by larvae. The correlation coefficient values showed that the relationship between oxygen consumption and salinity was not significant ($P > 0.05$; $r = 0.245$). During the first three hours of the experiment, the oxygen consumption by 30 larvae was 8.89, 10.72, 17.4, and 12.06% of the initial dissolved oxygen concentrations at 10, 20, 30 and 40 ppt, respectively (*Fig. 2*). The maximum oxygen consumption during the first three hours was recorded at 20 ppt. A sudden drop in the oxygen consumption was recorded at 3-6 hours of the experiment. This was followed by a gradual increase in the consumption of oxygen, while the maximum value of 26.29% was recorded at salinity 20 ppt after 12 hours of the experiment (*Fig. 2*).

A similar trend in oxygen consumption was observed at different pH ranges of 5 to 9. At pH 6 and 9 during the first six hours, a moderate consumption of oxygen was observed (*Fig.3*). After 6 hours, however, at pH 6, 7 and 8, the rates of oxygen consumption were suddenly increased and this indicated the most unfavourable conditions (*Fig. 4*). The consumption rate suddenly dropped after 9 hours at pH 8, whereas it continued to increase at pH 6 and 7 after 9 hours and up to 12 hours. The data were tested statistically and it was found that a high degree of correlations existed between pH and oxygen consumption ($r = 0.97$). The analysis of covariance showed a significant relationship between oxygen consumption and pH ($P < 0.05$).

The effects of temperature on the oxygen consumption are presented in *Fig. 5*. The variation in the consumption of oxygen was minimal, i.e. between 30 and 40°C, whereby a gradual decrease in the dissolved oxygen value was recorded up to 12 hours of the experimental time. At 50°C, almost all dissolved oxygen was consumed by the larvae. Initially at 30 and 50°C, the rate of oxygen consumption was low, but it was considerably increased after 9 hours of experiment (*Fig. 6*). A sudden increase in the oxygen consumption was recorded at 50°C after 6 hours, and this showed the most unfavourable conditions. The data were tested statistically using the analysis of variance (ANOVA), where a significant relationship was observed between temperature with oxygen consumption ($P < 0.05$; $r = 0.98$).

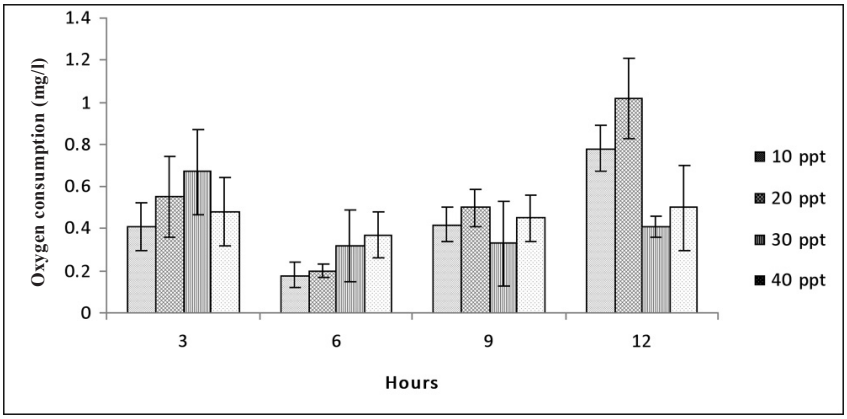

Fig. 1: Oxygen consumption (mg/l) by the larvae of T. gigas *at different salinities*

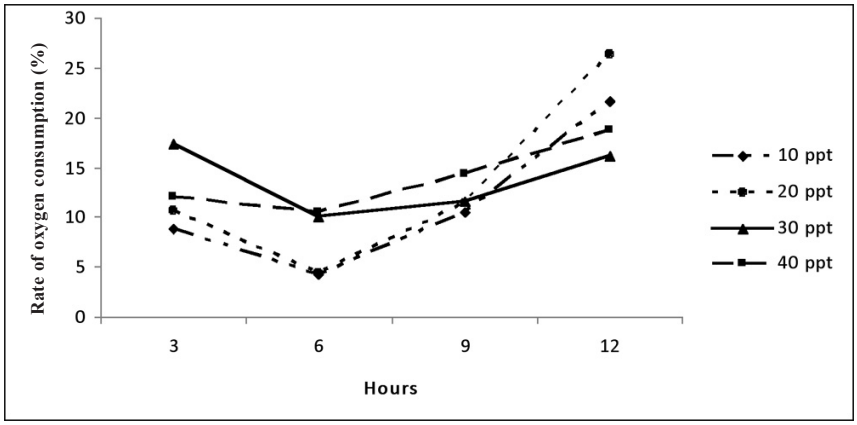

Fig. 2: The rate of oxygen consumption (%) by the larvae in different salinities

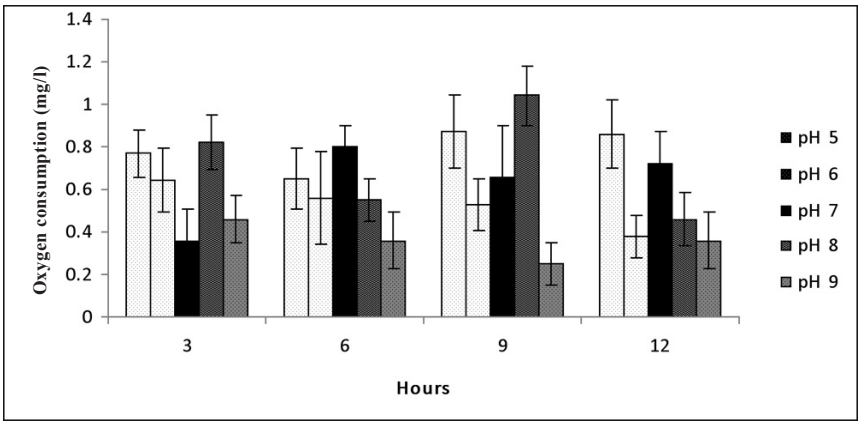

Fig. 3: Oxygen consumption (mg/l) by the larvae of T. gigas *at different pH levels*

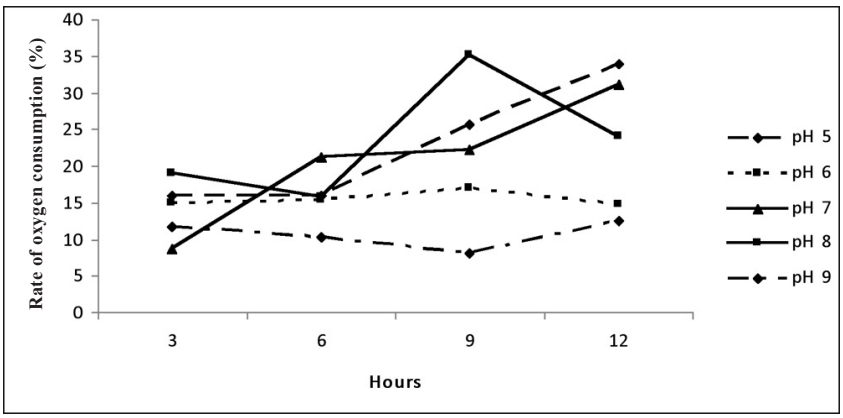

Fig. 4: Rate of oxygen consumption (%) by the larvae in different pH

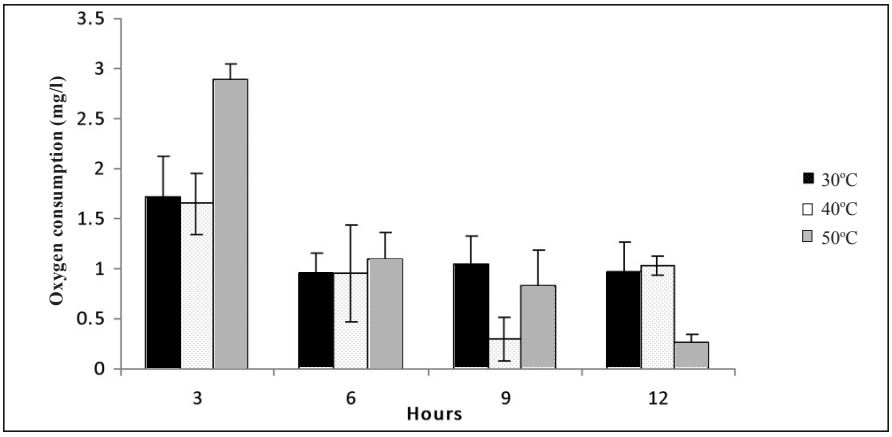

Fig. 5: The oxygen consumption (mg/l) by the larvae of T. gigas *at different temperature*

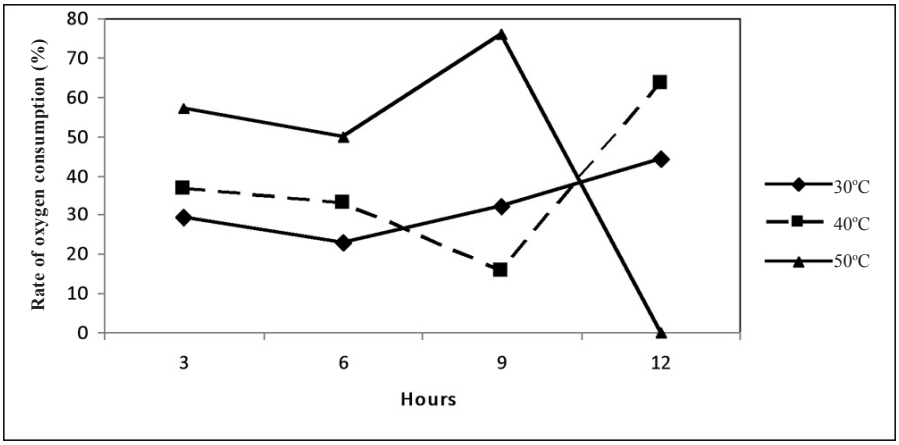

Fig. 6: The oxygen consumption rate (%) by the larvae in different temperatures

DISCUSSION

It is important to note that oxygen requirements and oxygen consumption rates are dependent on both biotic and abiotic factors (Brett, 1987). The most important abiotic factors affecting the oxygen consumption in aquatic organisms are temperature and salinity. Meanwhile, temperature directly affects the rate of all biological processes, whereas salinity influences osmoregulatory demand by the organisms. Both the factors have effects on the oxygen content of the medium. However, the interaction between salinity and temperature can be rather complex, with one variable acting as a modulating factor on the effects of the other (Vernberg, 1983).

When a marine organism is exposed to unfavourable temperature or salinity conditions, it must accommodate in some ways with this physiological stress. Short-term adjustments require additional expenditure of metabolic energy which can be measured by an increase in respiration. On the other hand, some organisms respond to sub-optimal conditions by reducing their metabolic rates, and this is either by withdrawing into a shell or as a result of lowered enzymatic activity (Gaudy and Sloane, 1981). Marine organisms can respond to the changes in salinities as osmoregulators or osmoconformers. Regulation is an active process which usually results in an increase in metabolic rate.

Meanwhile, metabolic rate varies with the changes in salinity, temperature and pH. In addition to these parameters, other factors such as the size of the animal, light condition and the amount of oxygen present in the environment also play significant roles in controlling the oxygen consumption in aquatic animals. Several studies have demonstrated that the oxygen consumption varies in juveniles and post-larvae of the penaeid prawns in relation to changes in salinity (Kutty *et al*., 1971; Gaudy and Sloane, 1981, Janakiraman *et al.*, 1985; Diwan *et al*., 1989), temperature (Kutty *et al*., 1971; Yagi *et al*., 1990; Villarreal and Rivera, 1993) and body weight (Kurmaly *et al*., 1989). Similarly, for *P. monodon*, the influence of salinity on the oxygen consumption has not been found to be significant (Gaudy and Sloane, 1981; Lei *et al*., 1989). In *P. stylirostris*, however, an increase in the oxygen consumption was observed at low salinities (Gaudy and Sloane, 1981).

In the present study, salinity was found to have no significant effect on the oxygen consumption in larvae of *T. gigas*. This indicates that the animal can thrive well in wide range of salinity changes. Nonetheless, salinity was found to affect the metabolism of decapod crustaceans, and this has been well studied through the measurement of oxygen consumption (Lemos *et al*., 2001). Similarly, the rate of oxygen consumption by *Amphibola crenata* has been reported to be unaffected by the salinity of the external medium in the range 0-125% seawater (Shumway and Sandra, 1981). However, *A. crenata* showed an increase in respiratory rate during exposure to anaerobic conditions, and a declining oxygen trend at higher salinity revealed almost no ability to regulate the rate of oxygen consumption (Shumway and Sandra, 1981). Therefore, when the animal has been exposed to both salinity and anoxic stress conditions, they can reach the maximum degree of oxygen dependence (Shumway and Sandra, 1981).

Not much work has been carried out on the respiratory metabolism of crustaceans under different pH conditions. In the present study, the larvae of *T. gigas* were found to be influenced by the changes in pH of seawater, whereby a wide fluctuation in the oxygen consumption was observed. The normal oxygen consumption was found at pH 6 and 9 up to six hours, but this was shown to have a sudden increase in the consumption rate at pH 6, 7 and 8. This revealed that up to 6 hours, the respiration of the larvae was normal, but they underwent a stress condition which resulted in a high consumption of oxygen after 6 hours.

Meanwhile, temperature was found to show a profound effect on the metabolic rate of aquatic animals. Endothermic animals expend extra energy to maintain their body temperature as the environmental temperature increases or decreases (Villarreal and Rivera, 1993). Nevertheless,

exothermic organisms can not alter their internal temperature and they usually show an increased metabolism as temperature rises, within a zone of tolerance. Outside of the tolerance zone, however, their metabolism falls as enzymatic process can no longer work properly.

Pagurus longicarpus or mussels (*Mytilus edulis*) are common intertidal animals and they are capable of surviving with fluctuations in temperature and salinity. Hermit crabs respond to stress by withdrawing into their shell. Several attempts have been made by several researchers to demonstrate the effects of temperature on the survival of the larvae of marine animals (Costlow *et al*., 1960: 1962: 1966; Choudhury, 1971; Young and Hazlett, 1978; Moreira *et al*., 1980). However, in adult penaeid prawns, the respiratory metabolism was found to be moderate between the temperatures of 20 and 30°C (Dall, 1986; Liao and Murai, 1986). In the present study, the oxygen consumption was the maximum at 40 and 50°C after 9 hours. These conditions are not suitable for the larvae of *T. gigas*. Therefore, the present study has demonstrated that temperature plays a significant role in influencing the respiratory metabolism, specifically at higher temperatures (>40°C).

There has always been a controversy to interrelate the respiratory metabolism with osmotic regulation in marine animals (Gross, 1957; Panikkar, 1969). However, most of the work carried out on the energy spent during osmotic regulation is based on the consumption of oxygen by the animals in a particular environment (Rao, 1968). Hence, the respiratory metabolism is considered to be an important biological process, especially for the aquatic cultivable animals which help in assessing the organism's oxygen requirement under different environmental conditions. It is also the best indicator to precisely evaluate the energetic expenditure in the osmotic regulation process of any aquatic organism.

Horseshoe crabs have a relatively high tolerance for a wide range of salinity. Normally, salinities for larvae and adults range from 8 ppt to natural seawater (36 ppt). According to Humberto and Jorge (1993), salinity and temperature are the most important external parameters but dissolved oxygen (DO) is the major limiting factor since biochemical reactions of an organism are controlled by the level of available oxygen, which is essential for aerobic metabolism.

CONCLUSIONS

The estimation of oxygen consumption during a brief experimental period does not seem to be a reliable index of respiratory metabolism as compared to natural condition which is primarily a culture system for extended periods. However, oxygen is an important environmental constituent and the scarcity of oxygen in the environment results in various phenotypic and physiological changes in the animals for their survival in a particular environment due to stress which is caused by depletion of oxygen. In the present study, the respiratory metabolism of the larvae of Malaysian horseshoe crab *Tachypleus gigas* (Müller) was investigated under different salinities (10-40 ppt), pH (5-9) and temperature (30-50°C). The oxygen consumption was found to be normal under different salinities for the first three hours, but the maximum oxygen consumption rate was recorded at salinity 20 ppt after 12 hrs. Meanwhile, a moderate consumption of oxygen was observed at pH 5-9, i.e. during the first six hours, and this was suddenly increased at pH 6, 7 and 8 after 6 hours, indicating unfavourable conditions. A gradual decrease in dissolved oxygen value was recorded up to 12 hours of the experimental time at all temperatures and almost all dissolved oxygen was consumed by the larvae of *T. gigas* at 50°C. The present study has proven that temperature (>40°C) and pH are the limiting factors influencing the oxygen consumption rates in the larvae of *T. gigas*.

ACKNOWLEDGEMENTS

The authors are grateful to Prof. Dr. Faizah Shaharom, the Director of the Institute of Tropical Aquaculture for providing the laboratory facilities, and University Malaysia Terengganu for the Research Fellowship Award to one of the authors (AC).

REFERENCES

Brett, J. (1987). Environmental factors affecting growth. In W.H. Hoare, D.J. Randall and S.R. Brett (Eds.), *Fish Fisiology*, *8*(528), 252-259.

Chatterji, A. (1994). *The Horseshoe Crab – A Living Fossil*. India: Swarajya Publication.

Choudhury, P. (1971). Responses of larval *Macrobrachium carcinus* (L.) to variation in salinity and diet (Decapoda*:* Palaemonidae). *Crustaceana*, *20*, 113-120.

Costlow, J. D., Bookout, C. G. and Monore, R. (1960). The effect of salinity and temperature on the larval development of *Sesarma cinererum* (Bosc.) reared in the laboratory. *Biological Bulletin Marine Biology*, *118*, 118-202.

Costlow, J. D., Bookout, C. G. and Monore, R. (1962). Salinity-temperature effects on the larval development of the crab *Panopeus herbstii* Milne-Edwards, reared in the laboratory. *Physiology Zoology*, *35*, 79-93.

Costlow, J. D., Bookout, C. G. and Monore, R. (1966). Studies on the larval development of the crab *Rhithropanopeus harrisii* (Gould.) I. The effect of salinity and temperature on the larval development. *Physiology Zoology*, *39,* 81-100.

Dall, W. (1986). Estimation of routine metabolic rate in a penaeid prawn*, P. esculentus* (Haswell). *Journal of Experimental Marine Biology and Ecology*, *96*, 57-74.

Diwan, A. D., Laxminarayana, A. and Kakati, V. S. (1989). Osmoregulatory ability of *P. monodon* (Fabricius) in relation to varying salinities. *Indian Journal of Fisheries*, *36*(1), 53-57.

Gaudy, R. and Sloane, L. (1981). Effect of salinity and oxygen consumption in postlarave of the penaeid shrimps, *P. monodon and P. stylirostris* without and with acclimation. *Marine Biology*, *65*, 297-301.

Gross, W. J. (1957). An analysis of response to osmotic stress in selected decapod crustacean. *Biological Bulletin Marine Biology*, *112*, 43-62.

Humberto, V. and Jorge, A.D. (1993). Effect of temperature and salinity on the oxygen consumption of laboratory produced *Penaeus californiensis* Postlarvae. *Comparative Biochemistry and Physiology*, *106*, 103-107.

Janakiraman, B., Venkateswarlu, Y., Rajarami Reddy, G. and Sasira Babu, K. (1985). Oxygen uptake rhythm in penaeids prawns, *P. indicus* (H. Milne Edwards) in different salinities. *Indian Journal of Marine Sciences*, *14*, 222-223.

Kurmaly, K., Yule, B. A. and Jones, D. A. (1989). Effect of body size and temperature on the metabolic rate of *P. monodon. Marine Biology*, *103*, 25-30.

Kutty, N. M., Murugapoopathy, G. and Krishnan, T. S. (1971). Influence of salinity and temperature on the oxygen consumption in young juveniles of the Indian prawn *P. indicus. Marine Biology*, *111*, 125-131.

Lei, C. H., Hsieh, L. Y. and Chen, C. K. (1989). Effect of salinity on the oxygen consumption and ammonia-N excretion of young juveniles of the grass shrimps, *P. monodon* (Fabricius). *Bulletin of the Institute of Zoology Academia Sinica*, *28*, 245-256.

Lemos, D., Phan, V.N. and Alvarez, G. (2001). Growth, oxygen consumption, ammonia-N excretion, biochemical composition and energy content of *Farfantepenaeus paulensis* Pe´rez-Farfante (Crustacea, Decapoda, Penaeidae) early postlarvae in different salinities. *Journal of Experimental Marine Biology and Ecology*, *261*, 55-74.

Liao, I. C. and Murai, T. (1986). Effects of dissolved oxygen temperature and salinity on the oxygen consumption of the grass shrimp *P. monodon.* In J.L. Maclean, L.B. Dizon and L.V. Hosillos (Eds.), *The First Asian Fisheries Forum* (pp.641-646). Asian Fisheries Society, Manila, Phillipines.

Moreira, G. S., Mcnamara, J. C., Moreira, P. S. and Weinrich, M. (1980). Temperature and salinity effects on the respiratory metabolism of the first zoeal stage *Macrobrachium holthusi* Genofre and Loboa (Decaposa: Palaemonidae). *Journal of Experimental Biology and Marine Ecology*, *47*, 141-148.

Panikkar, N. K. (1969). New perspectives in estuarine biology. *First All India Symposium in Estuarine Biology*, Madras, Dec. 27-30, (Mimeo), 8 pp.

Rao, G. M. P. (1968). Oxygen consumption in rainbow trout (*Salmo gairdneri*) in relation to activity and salinity. *Canadian Journal of Zoology*, *46*, 781-786.

Shumway and Sandra, E. (1981). Factors effecting oxygen consumption in marine pulmonate, *Amphibola crenata* (Gmelin, 1971). *The Biological Bulletin*, *160*(2), 332-347.

Vernberg, F.J. (1983). *Respiratory Adaptations. The Biology of Crustacean, Environment Adaptations* (Vol 8). New York: Academic Press.

Villarreal, H. and Rivera, J. A. (1993). Effect of temperature and salinity on the oxygen consumption of laboratory produced *P. californiensis* post larvae. *Comparative Biochemistry and Physiology*, *106*(1), 103-107.

Wolvekamp, H. P. and Waterman, T. H. (1960). *Respiration in Physiology of Crustacean*. New York: Academic Press.

Yagi, H., Ceccaldi, H. J. and Gaudy, R. (1990). Combined influence of temperature and salinity on the oxygen consumption of the larvae of the pink shrimp, *Palaemon serratus* (Pennant) (Crustacea: Decapoda Palaemon). *Aquaculture*, *86*, 77-92.

Young, A. M. and Hazlett, J. L. (1978). The effect of salinity and temperature on the larval development of *Clibanarius vittalus (Bosc.).* (Crustacea: Decapoda: Diogenidae). *Journal of Experimental Marine Biology and Ecology*, *34*, 131-141.

ISSN: 0128-7680
Pertanika J. Sci. & Technol. **19 (1)**: 11 – 17 (2011)

In vitro Antiplasmodial Properties of Selected Plants of Sabah

S. Khozirah[1*], A. Noor Rain[2], M.J. Siti Najila[2], Z. Imiyabir[3], L. Madani[3], C. Rohaya[2], M. Rosilawati[2], H. Nuziah[4], S.H. Goh[4] and I. Zakiah[2]

[1]Laboratory of Natural Products, Institute of Bioscience, Universiti Putra Malaysia, 43400 UPM, Serdang, Selangor, Malaysia
[2]Herbal Medicine Research Center, Institute for Medical Research, Jalan Pahang, 50588 Kuala Lumpur, Malaysia
[3]Forest Research Center, Sepilok, Sandakan, Sabah
[4]Forest Research Institute of Malaysia (FRIM), Kepong, Selangor, Malaysia
[*]E-mail:khozirah@yahoo.com.my

ABSTRACT

The antiplasmodial activity of the crude extracts of thirty plant species collected from Sabah was evaluated using chloroquine-sensitive strain (D10) and chloroquine-resistant strain (Gombak A) of *Plasmodium falciparum*. Significant activities were observed for the bark extract of *Polyalthia insignis* (IC_{50} 3.89 and 11.89 μg/ml against Gombak A and D10, respectively), the leaf extracts of *Kopsia dasyrachis* (4.62 μg/ml against Gombak A) and *Litsea elliptibacea* (IC_{50} 8.88 μg/ml against Gombak A), as well as the leaf and bark extracts of *Neouvaria acuminatissima* (IC_{50} 6.90-10.08 and 0.69 μg/ml against Gombak A and D10, respectively), and the bark extract of *Polyalthia microtus* (IC_{50} 9.0 and 12.12 μg/ml against Gombak A and D10, respectively).

Keywords: ***Plasmodium falciparum*, lactate dehydrogenase assay, *Polyalthia insignis, Kopsia dasyrachis, Neouvaria acuminatissima*, antimalarial**

INTRODUCTION

Malaria, one of the most important tropical diseases, is caused by pathogenic strains of *Plasmodium* (WHO, 2000). According to the latest statistics on the disease, half of the world population is at risk of malaria. In 2008 alone, an estimated 243 million cases were reported to have caused an estimated of 863,000 deaths (WHO, 2009). The emergence of multi-drug resistant strains of *Plasmodium* exacerbates the situation further, posing a major obstacle to successful chemprophylaxis and chemotherapy of the disease (Solomon *et al*., 2009). In Malaysia, several reports of the parasite resistance to common antimalarial drugs have been documented (*see* Montgomery and Eyles, 1963; Clyde *et al*., 1973; Dondero *et al*., 1976, Black *et al*., 1982; Ponnampalam, 1982). A more recent study has also reported the widespread resistance of falciparum malaria to both chloroquine and sulfadoxine/pyrimethamine (SDX/PYR) in several areas of Peninsular Malaysia (Hakim *et al.*, 1996; Cox-Singh *et al*., 2001). This rapid spread of parasite resistance has spurred a renewed interest in the search for new alternative antiplasmodial agents (Winstanley, 2000; Siti Najila *et al.*, 2002; Noor Rain *et al*., 2007; Wan Omar *et al*., 2007). To this end, tropical rain forest plants represent a fertile source of the new candidates for development into new alternative antimalarial drugs for therapy.

In the search for plants with anti-malarial properties, the authors have conducted an *in-vitro* screening for plants with activity against the malaria parasite, *Plasmodium falciparum*. For this

Received: 20 February 2010
Accepted: 23 April 2010
[*]Corresponding Author

purpose, thirty plant species collected from Tabun Wildlife Reserve in Sabah were evaluated for antiplasmodial activity using the lactate dehydrogenase (LDH) assay (Makler *et al*., 1993). The enzymatic assay is based on the observation that the LDH enzyme of *Plasmodium falciparum* has the ability to use 3-acetyl pyridine NAD as a coenzyme in the reaction leading to the formation of pyruvate from lactate. This assay has been tested for its applicability in assessing parasite density and drug sensitivity. In drug sensitivity testing, the inhibition profiles and IC_{50} values that were obtained using this assay were directly comparable to those that were determined by the radioactive uptake and microscope methods. The assay is relatively easy to perform and rapid compared to the radioactive uptake and microscopy methods. This paper reports the primary screening results obtained on the thirty species.

MATERIALS AND METHODS

Plant Materials

Plants were collected from the Tabun Wildlife Reserve located in Sabah, East Malaysia. Voucher specimens (*see* Table 1) were lodged at the Sepilok Forest Research Centre in Sandakan, Sabah.

The plant materials for testing were air-dried and ground to a fine mesh using a Wiley mill, and they were then directly soaked in dichloromethane:methanol 1:1. The extract that was obtained from 3 overnight soakings was collected, pooled and evaporated to dryness, lyophilized and stored at –4°C prior to testing.

Parasite Strain and Its Preparation

Two strains of *P. falciparum* were used. Gombak A is a Malaysian isolate and it is known to be resistant to chloroquine (Slamet Trijono *et al.*, 1991). It was originally isolated form an Orang Asli patient who was admitted to the Gombak Hospital in 1982. Meanwhile, the chloroquine-sensitive strain (D10) was obtained from the Institute of Medical Microbiology, University of Milan.

A continuous culture of the chloroquine sensitive (D10) and a Malaysian strain of the chloroquine resistant parasite (Gombak A) was maintained in a suspension consisting of RPMI 1640 culture medium that was supplemented with HEPES (25mM), sodium bicarbonate (0.2%) and gentamycin (40 μg/ml) at pH 7.4, and A or O type of red blood cells. The method of culturing is similar to that described by Trager and Jansen (1976: 1977).

Antiplasmodial Activity

The *in vitro* testing of the antiplasmodial activity was done by measuring the lactate dehydrogenase (LDH) activity of the parasite, as described by Makler *et al.* (1993) with slight modifications. Briefly, 190 μl of the *P. falciparum*-infected erythrocyte suspension, which had been prepared with 1.5% parasitemia and 2% haematocrit, were seeded into each well of the prepared test plate. The final concentration of the test ranged from 64 μg/ml to 0.006 μg/ml (lowest). Meanwhile, the highest concentration of DMSO that the parasites were exposed to, i.e. 0.3%, was shown to have no measurable effect on parasite viability. All the test samples were done in duplicate. Control readings of parasitized red blood cells devoid of plant extracts/drugs and non-parasitized red blood cells were done simultaneously. The positive and negative control wells containing 10 μl of diluted DMSO in 1:16 dilution which had been prepared earlier were added into 190 μl of each *P. falciparum*-infected and non-infected erythrocytes (2% hematocrit), respectively. Similarly, 190 μl of the parasite material were added into the different concentrations of the test extracts. Later, the test and the control plates were placed in a candle jar (with an approximate gas environment

TABLE 1
In vitro antiplasmodial activity of plant extracts against *Plasmodium falciparum*

No	Plant species	Family	Voucher specimen no:	Plant part tested	IC_{50} µg/ml	
					D10 (sensitive strain)	Gombak A (resistant strain)
1	*Alangium griffithii*	Alangiaceae	143521	Bark	1.54	*
2	*Alpinia fraseriana*	Zingiberaceae	145379	stem	4.40	13.68
3	*Borneodendron aenigmaticum*	Euphorbiaceae	145393	leaf	*	*
4	*Callicarpa havilandii var rispida*	Verbenaceae	145389	bark	1.88	*
5	*Calophyllum blancoi*	Guttiferae	145398	leaf	*	*
				bark	0.75	46.34
6	*Calophyllum gracilipes*	Guttiferae	145377	bark	*	*
7	*Calophyllum nodosum*	Guttiferae	145385	bark	*	*
8	*Chionantus crispus*	Oleaceae	145396	bark	*	*
9	*Chisoceton erythrocarpus*	Meliaceae	143512	bark	*	40.75
				fruit	14.85	19.03
10	*Clausena excavata*	Rutaceae	145366	leaf	*	40.32
11	*Canarium hirsutum*	Burseraceae	143522	leaf	*	*
12	*Decaspermum fruticosum*	Myrtaceae	145397	bark	*	*
13	*Dendrocnide elliptica*	Urticaceae	145375	bark	*	*
14	*Diospyros cauliflora*	Ebenaceae	143504	bark	*	*
15	*Diospyros tuberculata*	Ebenaceae	143519	bark	*	*
16	*Diplectria sp.*		143515	bark	*	*
17	*Kopsia dasyrachis*	Annonaceae	145362	leaf	*	4.62
				stem	*	*
18	*Leea indica*	Vitaceae	145370	bark	*	*
19	*Leucosyke winklerii*	Urticaceae	145387	bark	*	*
20	*Litsea elliptibacea*	Lauraceae	145380	leaf	*	8.88
				bark	*	*
21	*Neouvaria acuminatissima*	Annonaceae	143506	bark	0.69	10.08
				leaf	*	6.90
22	*Orophea corymbosa*	Annonaceae	143509	leaf	*	33.00
23	*Polyalthia insignis*	Annonaceae	143511	leaf	*	*
				bark	11.89	3.89
24	*Polyalthia microtus*	Annonaceae	145376	bark	9.01	12.12
25	*Polyalthia rumpii*	Annonaceae	143524	root	*	*
26	*Melicope subunifoliolata*	Rutaceae	145390	leaf	25.02	*
27	*Sauralia sp.*	Sauraliaceae	143505	bark	*	*
28	*Schima wallichii*	Theaceae	145383	bark	*	*
29	*Sterculia stipulata*	Sterculiaceae	145381	bark	49.96	*
30	*Xylopia malayana*	Annonaceae	143507	bark	30.58	*
-	Chloroquine	-	-	-	0.017 (±0.0009)	1.78 (±0.116)

* - parasite inhibition > 50µg/ml

of about 3% O_2, 6% CO_2 and 91% N_2). The test samples were incubated for 72 hrs at 37°C for maximum parasite growth.

After 72 hours, the plates were placed at –20°C for a minimum of 24 hours. Then, an aliquot (20 μl) of the blood lysate, from every concentration, was added into 100 μl of Malstat (Flow Inc., Portland, OR, USA), which had been dispensed into a new microtitre plate. The mixtures were mixed well before any further addition of aliquots of 20 μl of a mixture of 1:1 Nitro Blue Tetrazolium (NBT) and Phenazine ethosulphate (PES) (Sigma Chemicals, USA). The plates were placed in the dark for 2 hours, after which the absorbance was read at 630 nm using an ELISA plate reader (MRX Microplate Reader, Dynex Technologies, USA). The 50% growth inhibition concentration or IC_{50} value was estimated from a dose response curve. The plants with IC_{50} values less than 8 μg/ml were considered as having potential antiplasmodial activities and were suggested for further investigations in an animal model. On the contrary, the plants with IC_{50} values > 50 μg/ml were considered as inactive.

RESULTS AND DISCUSSION

Of the thirty plant species tested, the crude extracts of fourteen species showed significant antiplasmodial activity, *in vitro*, with IC_{50} values ranging between 0.6 to 49 μg/ml (*see* Table 2). Of the fourteen, six species (namely *Alpinia fraseniana, Calophyllum blancoi, Chisocheton erythrocarpus, Neovaria acuminatissima, Polyalthia insignis*, and *Polyalthi microtus*) displayed varying degrees of activity towards both the sensitive and resistant *P. falciparum* strains. The other eight species (*Alangium griffithii, Callicarpa havilanda var rispida, Kopsia dasyrachis, Litsea elliptibacea, Orophea corymbosa, Melicope subunifoliolata, Sterculia stipulata* and *Xylopia malayana*) were active, with varying degrees of activity towards either one of the strains.

The bark extract of *Polyalthia insignis* and the leaf extract of *Kopsia dasyrachis* seemed to be the most potent species against the resistant Gombak A strain (IC_{50} 3.89 and 4.62 μg/ml, respectively). At the same time, *P. insignis* also exhibited a moderate inhibition of the sensitive D10 strain (IC_{50} 11.89 μg/ml), whereas *K. dasyrachis* was inactive towards the strain. A significant inhibition of the resistant strain was also shown by the leaf extracts of *Neouvaria acuminatissima* (IC_{50} 6.90 μg/ml) and *Litsea elliptibacea* (IC_{50} 8.88 μg/ml), while the bark extract of *Polyalthia microtus* inhibited both strains with the IC_{50} values between 9 – 12 μg/ml.

The bark extract of *Neouvaria acuminatissima* exhibited the greatest potency towards the sensitive *P. falciparum* strain (D10, IC_{50} 0.69 μg/ml), while showing significant, albeit lower, potency against the resistant strain (Gombak A, IC_{50} 10.08 μg/ml) at the same time. On the other hand, the bark extract of *Calophyllum blancoi* was almost equally potent towards D10 (IC_{50} 0.75 μg/ml) but showed a weak activity towards Gombak A (IC_{50} 46.34 μg/ml). The bark extracts of *Alangium griffithi* and *Callicarpa havilanda var rispida* significantly inhibited the sensitive strain (IC_{50} 1.54 and 1.88, respectively) but did not inhibit the resistant strain. The other active species exhibited a moderate to weak activities against both or either one of the parasite strains. The only fruit extract in the collection exhibited a moderate inhibition of both strains with the IC_{50} values between 14 – 19 μg/ml.

In conclusion, this preliminary screening has identified several species with potential for further investigations of their bioactive constituents. In particular, *Polyalthia insignis, Kopsia dasyrachis* and *Neouvaria acuminatissima* deserve special attention due to their potent activity against both resistant and sensitive strains of *P. falciparum*. *Polyalthia microtus, Litsea elliptibacea* and *Alpinia frasesiana* are also of interest for further study since they have shown a quite significant inhibition of the resistant strain. Although they have no significant activity towards the resistant strain, *Alangium griffithii, Callicarpa havilanda* var *rispida* and *Calophyllym blancoi* should also be investigated further in view of their very potent activity towards the sensitive strain.

It is interesting to note that three of the active species (*P. insginis, P. microtus* and *K. dasyrachis*) are of the genera *Polyalthia* and *Kopsia*, with both belonging to the Annonaceae family. From the literature, it seems that the two genera are rich sources of isoquinoline and indole type alkaloids. The compounds belonging to these two classes of alkaloids have previously been reported to exhibit potent antiplasmodial activities (Xiao *et al*., 2002; Addae-Kyereme *et al*., 2001; Iwasa *et al*., 2001; Long *et al*., 1999). *Polyalthia insignis* contains seco-benzyltetrahydroisoquinoline alkaloids as the major constituents (Kee-Huat Lee *et al*., 1997). The species is used by the Murut tribe in Sabah as an antipyretic (Fasihuddin and Hasmah, 2001). Although no ethnomedicinal use was recorded for *P. microtus*, the phytochemical investigation on the species showed the major constituents to be alkaloids of the aporphinoid type (Lee *et al*., 1997). Meanwhile, the *Kopsia* species was not traditionally used to treat fever but it came into use as a treatment for ulcers and syphilitic sores (Mat Saleh and Latif, 2002). *K. dasyrachis* has been found to be rich in indole and monoterpene alkaloids (Kam *et al*., 1999a, b). *Litsea,* belonging to the family of Lauraceae, is also known to yield aporphine alkaloids (Borthakur and Rastogi *et al*., 1979; Uprety *et al*., 1972; Tewari *et al*., 1972).

Apart from alkaloids, it is also possible that the antiplasmodial activity is exerted by the other components in the bioactive plants. In particular, *diterpenoids* is known to co-occur with alkaloids in several *Polyalthia* species (Hao *et al.*, 1995; Hara *et al*., 1995; Ma *et al*., 1994; Kijjoa *et al.*, 1993) while *Neouvaria acuminatissima* has also been reported to elaborate labdane diterpenoids although it is not known whether the alkaloids is also present in the species (Lee *et al.*, 1995). Similarly, an Annonaceae, *Neouvaria* is a chemically understudied genus of this family. It is of interest to examine the class of alkaloids and other chemical constituents present in this particular Annonaceae. The isolation of the antiplasmodial components must be carried out for identification and bioactivity evaluation.

ACKNOWLEDGEMENTS

The authors wish to thank the Director of Blood Bank, Kuala Lumpur for the provision of human serum and blood for the *P. falciparum* continuous culture, and Prof. Donatella Taramelli of the Institute of Medical Microbiology, University of Milan, for the provision of the chloroquine-sensitive strain, D10.

REFERENCES

Black, F., Bygbjerg, I., Effersoe, P., Gomme, G. and Jepsen, G. A. (1982). Fansidar resistant falciparum malaria acquired in South-East Asia. *Transactions of the Royal Society of Tropical Medicine and Hygiene*, *75*, 715-716.

Borthakur, N. and Rastogi, R.C. (1979). Laetanine, a new noraporphine alkaloid from *Litsea laeta*. *Phytochemistry*, *18*, 910-911.

Clyde, D.F., Han, C.M. and Huang, Y.S. (1973). Resistance to chloroquine *of P. falciparum* from Sabah. *Transaction of the Royal Society of Tropical Medicine and Hygiene*, *67*, 146.

Cox-Singh, J., Robaiza Zakaria, Mohd. Shukri Abdullah, Hasan Abdul Rahman, Nagappan, S. and Singh, B. (2001). Short report: Differences in dihydrofolate reductase but not dihydropteroate synthase alleles in *Plasmodium falciparum* isolates from geographically distinct areas in Malaysia. *American Journal of Tropical Medicine and Hygiene*, *64*(1, 2), 28-31.

Dondero, T.J. Jr., Parsons, R.E. and Ponampalam, J.T. (1976). Studies on the resistant of malaria chloroquine and combination of chloroquine in Peninsular Malaysia. *Transaction of the Royal Society of Tropical Medicine and Hygiene*, *70*, 149-154.

Fasihuddin, A. and Hasmah, R. (2001). Medicinal plants of the community in Sabah. Retrieved from http// www.borneofocus.com/vaic/R&D/article42.htm.

Hakim, S.L., Sharifah Roohi, S.W.A., Zurkunai, Y., Noor Rain, A., Mansor, S.M., Palmer, K., Navaratnam, V. and Mak, J.W. (1996). *Plasmodium falciparum*: Increased proportion of severe resistance (RII and RIII) to chloroquine and high rate of resistance to sulfadoxine-pyrimethamine in Peninsular Malaysia after two decades. *Transactions of the Royal Society of Tropical Medicine & Hygiene*, *90*, 924-927.

Hao, X.-J., Yan, X.-S., Zhang, Z. and Shang. L.-J. (1995). Clerodane diterpenes from *Polyalthia cheliensis. Phytochemistry*, *39*, 447-448.

Hara, N., Asaki, H., Fujimoto, Y., Gupta, Y.K., Singh, A.K. and Sahai, M. (1995). Clerodane and ent-halimane diterpenes from *Polyalthia longifolia. Phytochemistry*, *38*, 189-194.

Kam, T.-S., Subramaniam, G. and Chen, W. (1999a). Alkaloids from *Kopsia dasyrachis. Phytochemistry*, *51*, 159-169.

Kam, T.-S., Choo, Y.-M., Chen, W. and Yao, J.-X. (1999b). Indole and monoterpene alkaloids from the leaves of *Kopsia dasyrachis. Phytochemistry*, *52*, 959-963.

Kijjoa, A., Pinto, M.M.M., Pinho, P.M.M. and Herz, W. (1993). Clerodanes from *Polyalthia viridis*. *Phytochemistry*, *34*, 457-460.

Lee, I.-S., Ma, X., Chai, H.-B., Madulid, D.A., Lamont, R.B., O'Neill, M.J., Besterman, J.M., Farnsworth, N.R., Soejarto, D.D., Cordel, G.A., Pezzuto, J.M. and Kinghorn, A.D. (1995). Novel cytotoxic labdane diterpenoids from *Neouvaria acuminatissima*. *Tetrahedron*, *51*, 21-18.

Lee, K.H., Chuah, C.H. and Goh, S.W. (1997). Seco-benzyltetrahydroisoquinolines from *Polyalthia insignis* (Annonaceae). *Tetrahedron Letters*, *38*, 1253-1256.

Ma, X., Lee, I.-S., Chai, H.-B., Zaw, K., Farnsworth, N.R., Soejarto, D.D., Cordell, G.A., Pezzuto, J.M. and Kinghorn, A.D. (1994). Cytotoxic clerodane diterpenes from *Polyalthia barnesii. Phytochemistry*, *37*, 1659-1662.

Makler, M.T., Ries, J.M., Williams, J.A., Bancroft, J.E., Piper, R.C., Gibbins, B.L. and Hinrichs, D.J. (1993). Parasite lactate dehydrogenase as an assay for *Plasmodium falciparum* drug sensitivity. *American Journal of Tropical Medicine and Hygiene*, *48*(6), 739-741

Mat Saleh, K. and Latif, A. (2002). Tumbuhan Ubatan Malaysia. Universiti Kebangsaan Malaysia, pp. 503-505.

Montgomery, R. and Eyles, D.E. (1963). Chloroquine resistant falciparum malaria in Malaya. *Transaction of the Royal Society of Tropical Medicine and Hygiene*, *57*, 409-416.

Noor Rain, A., Khozirah, S., Mohd. Ridzuan, M.A.R., Ong. B.K., Rohaya, C., Rosilawati, M., Hamdino, I., Badrul Amini and Zakiah, I. (2007). Antiplasmodial properties of some Malaysian medicinal plants. *Tropical Medicine*, *24*(1), 29-35.

Ponnampalam, J.T. (1982). Falciparum malaria resistant to Fansidar (sulfadoxine-pyrimethamine) occurring in three children of the same family. *Singapore Medical Journal*, *23*, 37-38.

Siti Najila, M.J., Noor Rain, A., Mohamad Kamel, A.G., Syed Zahir, S.I., Khozirah, S., Lokman Hakim, S., Zakiah, I. and Azizol, A.K. (2002). The screening of extracts from *Goniothalamus scortechinii. Aralidium pinnafitidum* and *Andrographis paniculata* for antimalarial activity using the lactate dehydrogenase assay. *Journal of Ethnopharmacology*, *82*, 239-242.

Slamet, T., Lim, P.K.C., Mak, J.W., Storey, J. and Noor Rain, A. (1991). Sensitivity of Malaysian isolates *Plasmodium falciparum* to a number of antimalarials. *Tropical Biomedicine*, *8*, 85-87.

Solomon, A.W., Nayagam, S. and Pasvol, G. (2009). Recent advances in tropical medicine. *Transaction of the Royal Society of Tropical Medicine and Hygiene*, *103*, 647-652.

Tewari, S., Bhakuni, D.S. and Dhar, M.M. (1972). The aporphine alkaloids of *Litsea glutenosa. Phytochemistry*, *11*, 1149-1152.

Trager, W. and Jensen, J.B. (1976). Human malaria parasite in continuous culture. *Science*, *193*(4254), 673-675.

Trager, W. and Jensen, J.B. (1977). *Plasmodium falciparum* in culture: Use of outdated erythrocytes and description of the candle jar method. *Journal of Parasitology*, *63*(5), 883-886.

Uprety, H., Bhakuni, D.S. and Dhar, M.M. (1972). Aporphine alkaloids of *Litsea sebifera, L. wightiana* and *Actinodaphne obovata. Phytochemistry*, *11*, 3057-3059.

Wan Omar, A., Ngah, Z.U., Zaridah, M.Z. and Noor Rain, A. (2006). *In vitro* and *in vivo* antiplasmodial properties of some Malaysian plants used in traditional medicine.

Winstanley, P.A. (2000). Chemotherapy for falciparum malaria: The armoury, the problems and the prospects. *Parasitology Today*, *16*, 146-153.

World Health Organization. (2000). Severe falciparum malaria. *Transaction of the Royal Society of Tropical Medicine and Hygiene*, *94*, 36-37.

World Health Organization. (2009). The World Malaria Report 2009. 78 pages.

ISSN: 0128-7680
Pertanika J. Sci. & Technol. **19 (1)**: 19 – 24 (2011)

Quantification of Total Phenolics in Different Parts of *Pluchea indica* (Less) Ethanolic and Water Extracts

Normala H.[1*] and Suhaimi M.I.[2]
[1]Department of Environmental Sciences,
Faculty of Environmental Studies, Universiti Putra Malaysia,
43400 UPM, Serdang, Selangor, Malaysia
[2]Faculty of Biotechnology and Life Sciences,
Universiti Industri Selangor,
40000 Shah Alam, Selangor, Malaysia
[*]E-mail: mala_upm@putra.upm.edu.my

ABSTRACT

One of the compounds present in *Pluchea indica* extracts is antioxidant which plays an important role in inhibiting free radicals and thus protects humans against infections and degenerative diseases, such as cancer, arthritis, and ageing process. The main objective of this study was to investigate and determine the total phenolic compounds of *Pluchea indica* in different concentrations of ethanolic extracts. This species was chosen because of its high phytonutrient compounds with potential medicinal properties. There was a significant difference ($P \leq 0.05$) in the total phenolic among the different parts of the tested plant. 50% of the ethanolic extract produced the highest total phenolic compounds (1775.00±86.00 to 658.95±5.00 µmol/g), followed by water extract (759.79±1.53 µmol/g) and 100% ethanol extract (352.72±22.30 to 249.29±5.37 µmol/g), respectively. In terms of the plant parts, the leaves contained the highest phenolic compounds (1775.00±86.00 µmol/g in 50% ethanol extract, 759.79±1.53 µmol/g in 100% aqueous extract and 352.72±22.30 µmol/g in 100% ethanol extract), followed by the stems (990.22±24.00 µmol/g in 50% ethanol extract, 990.22±24.59 µmol/g in 100% aqueous extract and 293.48±0.00 µmol/g in 100% ethanol extract). Meanwhile, lower total phenolic compounds were detected in the flowers (727.71±11.00 µmol/g in 50% ethanol extract, 603.81±8.46 µmol/g in 100% aqueous extract and 249.29±5.37 µmol/g in 100% ethanol extract) and roots (658.95±5.00 µmol/g in 50% ethanol extract, 450.00±10.76 µmol/g in 100% aqueous extract and 272.28±0.53 µmol/g in 100% ethanol extract). Based on these findings, *Pluchea indica* has potential medicinal properties that can be further developed to produce neutraceutical products, diet supplements or cosmetic products. However, further research should first be conducted on the effects of these compounds on laboratory animals.

Keywords: Antioxidant, phenolics, *Pluchea indica,* herbal medicines

INTRODUCTION

Food provides energy needed to perform daily functions and maintain normal metabolic processes. It contains neutraceutical compounds that are essential to prevent diseases. For example, phenolics are one of the groups of antioxidative compounds that can scavenge free radicals in human body and are continually needed in human diet. Bleary of eye problems can occur where diets are deficient in β-carotene (Beecher, 1999). The essential nutrients, such as antioxidants other than vitamins that are needed to prevent specific diseases, have been a major focus of human nutrition research for the past century. Through research, scientists have determined the amount of each essential

Received: 13 March 2009
Accepted: 25 March 2010
[*]Corresponding Author

nutrient required to prevent illnesses. The interesting part of food is the linkage between diet and illnesses. It cannot be entirely explained by the absence or presence of the various essential nutrients in our diets. A multitude of components found in food have been investigated to determine the role they play in maintaining health and reducing the risk of diseases. Numerous phytochemicals (plant chemicals) occurring in fruits and vegetables are taking centre stage in this research, as more evidence accumulates regarding their health-promoting properties (Beecher, 1999).

The importance of plants in nutrition research is the re-evaluation of the medicinal practices of past and present cultures (Zeisel, 1999). The traditional medicines are based largely on the use of plant extracts. For example, Chinese medicines predate modern medicine by thousands of years. It employs a vast array of botanical extracts for the treatment of diseases and maintenance of health. Meanwhile, East Indian Ayurvedic medicine, early European folk medicines, and native North American medicines are based largely on the use of plant extracts (Huang *et al.*, 2005).

Pluchea indica is a common herbal plant found in Malaysian coastal areas. It grows as an erect shrub. In Malaysia, Indonesia and Thailand, it is consumed as vegetable and post-natal treatment (Smith *et al.*, 1996). Other potential uses of this plant include reduction of muscle pain, haemorrhoids, dissolving kidney stones, lowering blood sugar, diuretic, promoting digestion, and elixir of longevity. Many researchers have identified that herbs have high contents of nutraceutical compounds. Meanwhile, antioxidant in herbs of plant origin is the substance that reduces oxidative damage caused by free radicals (Huang *et al.*, 2005). Free radicals are highly reactive chemicals that attack molecules by capturing electrons and thus modifying chemical structures. Antioxidants include a number of enzymes and other substances, such as vitamins C and E and beta carotene that are capable of counteracting the damaging effects of oxidation (Wright and Carpenter, 2001). Antioxidants are commonly added to food products, such as vegetable oils and prepared food, to prevent or delay their deterioration. Free radical generation is directly related with oxidation in food and biological systems.

The objectives of this study were to extract and determine the total phenolics content in different solvent extracts of *Pluchea indica.* This plant is believed to contain high phenolic compounds but limited research on nutraceutical compounds of this plant has been reported. This research may lead to further investigation on the potential of this particular plant as neutraceutical products, diet supplements or cosmetics.

MATERIALS AND METHODS

The leaves, stems, flowers, and roots of *Pluchea indica* were harvested from Kampung Kuala Kangkong, Simpang Empat, which is located in Alor Setar, Kedah, Malaysia. The samples were washed with water to remove all debris, as well as damaged and diseased portions. The leaves, stems, flowers and roots were dried in an oven at 45°C for 48 hours until a constant weight was obtained. After that, 0.2g of the dried leaves, stems, flowers and roots were separately ground using a warring blender. Each of the different plant parts of fine powder was extracted using 20 ml of distilled water, 50% ethanol, and 100% ethanol. The samples were centrifuged using Eppendorf Centrifuge at 4500 rpm for 30 minutes, and they were later stored in -20°C freezer for determination of the total phenolic compounds.

The total phenolic compounds were determined using the Folin Ciocalteu (Fluca Biochemical) reagent using the procedure proposed by Gao *et al*. (2000). 100µl extract of each different vegetative part was mixed with 200µl of Folin Ciocalteu reagent. 2000µl distilled water was then added to the mixture. Each sample was mixed with 1000µl sodium carbonate (Systerm ChemAr) and vortexes. The sample mixture was then incubated for two hours at the room temperature. All the samples were diluted into two series of dilution, 1:5 dilution and 1:10 dilution. This was to ensure the reading within the standard curve range of between 0.0 and 350mg/L gallic acid equivalent. The

determination was done in three replications. Gallic acid was used as a standard. The concentration of the total phenolics in the blue mixture was then measured at wavelength 765 nm using UV-spectrophotometer.

A stock solution of gallic acid was prepared by dissolving 2.5 mg gallic acid (Sigma) in 1.0 ml of distilled water. The test tubes were labelled according to the concentrations of solution. Standards of varying concentrations were prepared by serial dilution, as shown in Tables 1 and 2. The analysis of variance was used to detect the differences in the total phenolic compounds in the different parts of *Pluchea indica* at significant difference of $P \leq 0.05$.

TABLE 1
Dilution for gallic acid standards

Final concentration (ppm)	Volume stock (µL)	Volume of dH_2O (µL)
0	-	1000
5	2	998
10	4	996
50	20	980
75	20	970
100	40	960
250	100	900
300	20	880
375	150	850
500	200	800

TABLE 2
Sample solution dilution

Dilution factor	Volume of sample (µL)	Volume of solvent (µL)
5	200	800
10	100	900

RESULTS AND DISCUSSION

Total Phenolic Compounds

All the different solvent extraction systems used showed a wide range of the total phenolic compounds, i.e. from 249 to 1775 µmol/g, in the different vegetative parts depending on the solvent used (see *Fig. 1*).

The 50% ethanol extract contained significantly ($P \leq 0.05$) higher amounts of the total phenolic compounds compared with 100% ethanol extract and aqueous extract. It was found that the leaves contained 1775.00 ± 86.00 µmol/g, while the stems contained 990.22 ± 24.00 µmol/g of the total phenolic compounds. The total phenolic compounds in the flowers were 727.71 ± 11.00 µmol/g. There was a significantly ($P \leq 0.05$) lower phenolic compound in 50% ethanol solvents in the roots.

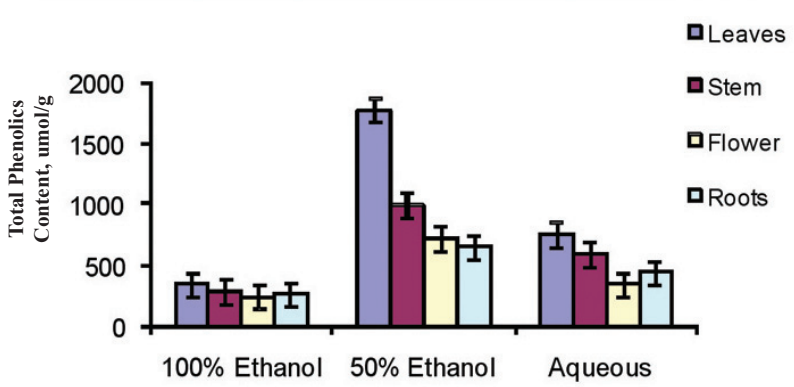

Fig. 1: Total phenolics in different solvent extractions of Pluchea indica*. The values were expressed as mean ± standard deviation (n = 3), significantly different at P ≤ 0.05*

The total phenolic compounds in the roots were 658.95 ± 5.00 µmol/g. This was due to the fact that the solvent in all different vegetative parts of *Pluchea indica* could be dissolved in 50% ethanol extract. The 50% ethanol extract allowed more extracts to form hydrogen bonds with phenolic compounds and thus, extracted more phenolic compounds than the 100% ethanol and water extract. Adding water to ethanol allows compounds that are able to bind with the oxygen molecule in the water to be extracted (Carey, 2003). From the statistical test, it could be concluded that the total phenolic compounds content was significantly influenced by the solvent and different vegetative parts. Meanwhile, water is able to form the hydrogen bonds with phenolic compounds that may not have numerous hydroxyl groups and therefore can extract more phenolic compounds than methanol alone (Carey, 2003). Extracting aqueous methanol increased the phenolics content as compared to pure methanol. These results are consistent with the previous findings of several researchers (e.g. Yen *et al*., 1996; Fukumoto and Mazza, 2000; Siddhuraju and Beecker, 2003).

The concentration of the total phenolic compounds in the leaves of water extract was 759.79 ± 1.53 µmol/g higher than that of the stems, while the concentration of total phenolic compounds was of 603.81 ± 8.46 µmol/g. The phenolic compounds in the flowers were 350.55 ± 34.58 µmol/g and this was 450.00 ± 10.76 µmol/g in the roots. The lowest phenolic compounds in aqueous was in the flowers. The aqueous extract allows the compounds to bond with the oxygen molecules in the water. This is because of the ability of the aqueous extract to form the hydrogen bonds with the phenolic compounds. From the statistical test, it was found that the total phenolic compounds content was significantly influenced by solvent and different vegetative parts. Water allowed the compounds to bind with the oxygen molecules in the water. In addition, water is also able to form hydrogen bonds with phenolic compounds that may not have numerous hydroxyl groups, and therefore, extracting more phenolic compounds than methanol alone (Carey, 2003). Water can also extract compounds such as sugar. As such, phenolic compounds that are bound to sugar may be extracted with the addition of water.

The lowest total phenolic compounds were found in 100% ethanol solvents. The leaves showed 352.72 ± 22.30 µmol/g. In the stems, the phenolic compounds were 293.48 ± 0.00 µmol/g. The phenolic compounds in the roots were 272.28 ± 0.53 µmol/g. Meanwhile, the lowest phenolic compounds in *Pluchea indica* was detected in the flowers (249.29 ± 5.37 µmol/g). The 100% ethanol extracts allowed less compounds bonding with the oxygen molecules as compared to water extract and 50% ethanol extract. Therefore, 100% ethanol solvent may cause inability to the

compounds to bond with phenolic compounds that may have numerous hydroxyl groups. It could be concluded that the total phenolic compounds content was significantly influenced by solvent and different vegetative parts. Tanaka *et al*. (1998) suggested that polyphenolic compounds have inhibitory effects on mutagenesis and carcinogenesis in humans when ingested up to 1.0 g daily from a diet rich in fruits and vegetables.

This result shows that the polarity of the phenolics in aqueous extracts of *Pluchea indica* was higher compared to 100% ethanolic solvent which has redox properties that make it act as reducing agents. Meanwhile, the phenolic compounds in plants are the largest group of compounds with antioxidative properties. Nagai *et al*. (2003) and Yang *et al*. (2002) reported that the phenolic compounds have the redox properties which allow them to act as reducing agents, hydrogen donators and singlet oxygen quenchers. The redox potential of phenolic compounds plays an important role in determining the antioxidant capacity (Rice-Evans *et al.*, 1997). The plant phenolics constitute one of the major groups of compounds acting as primary antioxidants or free radical terminators. Therefore, it is important to determine the total amount of phenolics in selected plant extracts. As one of the most diverse and widespread group of natural compounds, polyphenol is probably the most important natural phenolics (Agrawal, 1989). These compounds possess a broad spectrum of chemicals and biological activities including radical scavenging properties, and such properties are especially distinct for flavonols.

This study showed that the variation in the total phenolic compounds of various extracts varied widely, depending on the polarities of the solvent used. The aqueous solvents were more efficient in extracting the total phenolics as compared to their corresponding absolute ones. Similar observations were also reported in a previous study by Wang *et al.* (2004), in which various concentrations of ethanol (ranging from 15% to 96%) were investigated for the extraction of phenolic compounds.

CONCLUSIONS

The study showed that *Pluchea indica* vegetative parts have high total phenolic compounds. The highest total phenolic compounds were in 50% ethanol, followed by aqueous and the least in 100% ethanol. In the 50% ethanolic extracts with different vegetative parts, the leaves showed the highest phenolic compounds, followed by the stems, flowers, and roots. In 100% water extracts, the highest content of the total phenolics was found in the stems, and this was followed by the leaves, flowers, and roots. Finally, in 100% ethanolic extracts, the leaves had the highest total phenolics content, followed by the stems, and roots, while the lowest phenolic compound was found in the flowers.

Extraction by ethanol solvents is more efficient for phenolic compounds, and this is probably correlated to their antioxidative activity. The antioxidant of phenolics in *Pluchea indica* could act as a substance that significantly decreases the adverse effects of the reactive species, such as reactive oxygen and nitrogen species, on normal physiological functions in humans. This antioxidant can scavenge reactive oxygen species to stop radical chain reactions or inhibit the radical. The extract can be used as the production of food supplements and cosmetic products.

ACKNOWLEDGEMENT

This research project was supported through a grant from University Industri Selangor (UNISEL), Malaysia.

REFERENCES

Agrawal, P.K. (1989). Carbon-13 NMR of flavonoids. *Elsevier*. New York. 37-52.

Beecher, G.R. (1999). "Phytonutrients" role in metabolism: Effect on resistance to degenerative processes. *Nutrition Reviews*, *57*(9), S3–S6.

Carey, F. (2003). *Organic Chemistry* (5th Edn.). New York. McGraw-Hill Co.

Fukumoto, L. and Mazza, G. (2000). Assessing antioxidant and prooxidant activities of phenolic compounds. *Journal of Agricultural and Food Chemistry*, *48*, 3597-3604.

Gao, X., Bjork, L., Trajkovski, V. and Uggla, M. (2000). Evaluation of antioxidant activities of rosehip ethanol extracts in different test systems. *Journal of the Science of Food and Agriculture*, *80*, 2021–2027.

Huang, D., Ou, B. and Prior, R. (2005). The chemistry behind antioxidant capacity assays. *Journal of Agricultural and Food Chemistry*, *53*, 1841-185.

Nagai, T., Reiji, I., Hachiro, I. and Nobutaka, S. (2003). Preparation and antioxidant properties of water extract of propolis. *Food Chemistry*, *80*, 29–33.

Rice-Evans, C.A., Miller, N.J. and Paganga, G. (1997). Antioxidant properties of phenolic compounds. *Trends in Plant Science*, *2*, 152-159.

Siddhuraju, P. and Becker, K. (2003). Antioxidant properties of various solvent extracts of total phenolic constituents from three different agroclimatic origins of Drumstick tree (*Moringa oleifera* Lam.) leaves. *Journal of Agricultural and Food Chemistry*, *57*, 2144-2155.

Smith, M.A., Perry, G., Richey, P.L., Sayre, L.M., Anderson, V.E., Beal, M.F. and Kowal, N. (1996). Oxidative damage in Alzheimer's. *Nature*, *382*, 120-121.

Tanaka, M., Kuei, C.W., Nagashima, Y. and Taguchi, T. (1998). Application of antioxidative milland reaction products from histidine and glucose to sardine products. *Nippon Suisan Gakkaishil*, *54*, 1409-1414.

Wang, S.Y. and Lin, H.S. (2004). Antioxidant activity in fruits and leaves of blackberry, raspberry, and strawberry varies with cultivar and developmental stage. *Journal of Agricultural and Food Chemistry*, *48*, 140–146.

Wright, J., Johnson, E. and Carpenter, D. (2001). Predicting the activity of phenolic antioxidants: Theoretical method, analysis of constituent effects, and application to major families of antioxidants. *JACS*, *123*, 1173-1183.

Yang, J.H., Lin, H.C. and Mau, J.L. (2002). Antioxidant properties of several commercial mushrooms. *Food Chemistry*, *77*, 229–235.

Yen, G., Wu, S. and Duh, P. (1996). Extraction and identification of antioxidant components from the leaves of mulberry (*Morus alba* L.). *Journal of Agricultural and Food Chemistry*, *44*, 1678-1690.

Zeisel, S.H. (1999). Regulation of "Nutraceuticals". *Science*, *285*, 185-186.

ISSN: 0128-7680
Pertanika J. Sci. & Technol. **19 (1)**: 25 – 32 (2011)

Pressurized Liquid Extraction of Polycyclic Aromatic Hydrocarbons from Soil Samples

Noorashikin Md Saleh[1*] and M. Marsin Sanagi[2]
[1]Department of Chemical Sciences, Faculty of Science and Technology,
Universiti Malaysia Terengganu,
21030 Kuala Terengganu, Terengganu, Malaysia
[2]Department of Chemistry, Faculty of Science,
Universiti Teknologi Malaysia,
81310 UTM Skudai, Johor, Malaysia
[*]E-mail: noorashikin@umt.edu.my

ABSTRACT

A Pressurized Liquid Extraction (PLE) method was developed by using conventional High Performance Liquid Chromatography (HPLC). It was found that all of the PAHs have been successfully extracted with dichloromethane-acetone with high percentage recovery. A high temperature of 180°C gave the highest recovery for fluoranthene (94.4%). Meanwhile, fluorene showed the highest recovery at 150 bar, with 94.6% recovery. It is noted that there is no significant day-to-day difference in the efficiency of the developed method, with the R.S.D. values averaging at 0.02. The optimized conditions applied to the soil samples were analysed using the High Temperature High Performance Liquid Chromatography (HT-HPLC) with chromatographic conditions: Octadecylsilyl-silica (ODS-silica) column (100 mm × 4.6 mm I.D.); mobile phase acetonitrile:water 40:60 (v/v); flow rate 2.5 mL/min; temperature 70°C; UV absorbance 254 nm; injection volume 5µL.

Keywords: Polycyclic Aromatic Hydrocarbons (PAHs), pressurized liquid extraction, high temperature high performance liquid chromatography

INTRODUCTION

Accelerated solvent extraction (ASE), which is also known as pressurized liquid extraction (PLE), was first described by Richter *et al.* (1995). The PLE uses organic solvents at elevated temperatures and pressures to obtain a complete extraction of analytes from solid or semi-solid samples in shorter periods of time and with smaller quantities of solvents, as compared to conventional extraction procedures. According to Wan and Wong (1996), one of the major driving forces is the increasing demand from the regulatory bodies to reduce the large volumes of organic solvents consumed by the classical extraction methods such as Soxhlet.

In this study, the PLE method was developed using the conventional HPLC instrument for the analysis of the samples. The PLE has demonstrated advantages for automation, reduced extraction time and lower solvent use as compared to the conventional soxhlet extraction. Recently, the PLE with sub-critical heated water has been used to extract polar to moderately polar organic compounds from the sediment samples. The extraction of non-polar high molecular weight compounds, such as PAHs, PCBs, and brominated flame retardants at temperatures greater than 250ºC, has also been reported (Scott, 1984).

Received: 30 March 2009
Accepted: 1 March 2010
[*]Corresponding Author

Saim *et al.* (1997) discussed the effect of extraction solvents. A selection of organic solvents, single or in combination, was chosen to investigate their influence on the recovery of PAHs. The results indicate that the solvent has an effect on the recovery of PAHs, except for hexane. Meanwhile, poor recovery obtained for hexane was attributed to its lower polarity.

Richter *et al*. (1999) explained that temperature has a pronounced effect on the performance of PLE from the standpoint of solubility and mass-transfer. They studied the effect of temperature on the recovery of the total petroleum hydrocarbons (TPHs). The temperature was varied from room temperature, which was 27ºC to 100ºC. The researchers noted that using elevated temperatures and pressures, in combination with organic solvent, improved precision and recovery for the extraction of analytes from solid samples. In particular, the PLE gave a recovery that was comparable to those obtained from the soxhlet extraction and other techniques in use, while requiring only a fraction of the time and solvents needed for those techniques. Thus, the PLE has shown good potential for the recovery of volatile and semi-volatile compounds.

PAHs (Polycyclic Aromatic Hydrocarbons) are one of the typical persistent organic compounds (POPs) featured in regional and global cycling. PAHs are emitted mainly into the atmosphere and have been detected at long distances from their source. Compounds with five or more aromatic rings that exist are mainly adsorbed in to airborne particulate matter, such as fly ash and soot, due to their low vapour pressures. PAHs have been reported to have mutagenic and/or carcinogenic effects. The ability of polycyclic aromatic hydrocarbons (PAHs) to induce cancer has been documented by epidemiological studies of workers in coal tar, creosote, coal gas, coke, and cutting oil industries (Claessens and Straten, 2004).

MATERIALS AND METHODS

Reagents and Chemicals

HPLC grade solvent acetonitrile was obtained from Scharlau AC0340 (Barcelona, Spain). Meanwhile, methanol solvent was obtained from HyperSolv, BDH Laboratory, EC No. 200-659-6 (England). The polycyclic aromatic hydrocarbons (napthalene, fluorene (EC No. 2016955), phenanthrene (EC No. 2015815), and fluoranthene (EC No. 2059124) were obtained from Fluka Chemika, Sigma-Aldrich Chemic, Steinheim, (Switzerland). Double-distilled deionized water of at least 18 MΩ was purified using the Nano ultra pure water system (Barnstead, USA).

Chromatographic Conditions

The high temperature HPLC systems consisted of a conventional HPLC system that is coupled with a column oven of a Shimadzu GC-8A Gas Chromatography (Shimadzu Kyoto, Japan). In this study, the HPLC separations were carried out using Waters 515 HPLC pump (Mildford, USA) for mobile phase delivery. The samples were injected into the system using a 25µL loop for sample introduction. The analyte peaks were detected using a Shimadzu SPD- 6A UV detector (Kyoto, Japan) and were recorded on a Waters 746 Data Module integrator (Mildford, USA).

Pressurized Liquid Extraction Method

Extractions were carried out using a JASCO PU 980 HPLC pump. The samples (7g) were accurately weighed into a 11 mL cell. The sample cell was then closed to finger tightness and placed in a Shimadzu GC 8A oven. *Fig. 1* shows a schematic diagram of the pressurized liquid extraction system. The extractions were carried out using dichloromethane-acetone. In addition, the extractions were performed using a preheated method. In this procedure, the sample cells were heated to the

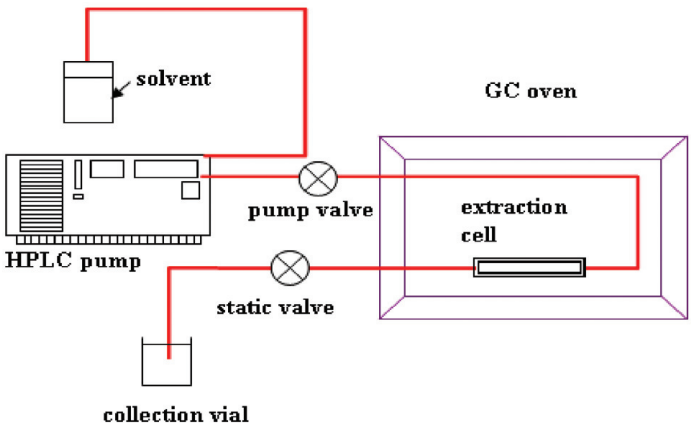

Fig. 1: Schematic diagram of pressurized liquid extraction system

extraction temperature (the range of 60°C to 250°C was tested). When a gas chromatograph oven was used, the cell was allowed to equilibrate for 10-15 min after the oven had reached the set point temperature. The static valve was opened during the preheating step.

The pump valve was opened after the heat-up time, whereas the solvent was introduced into the cell at 2.0 mL/min until about 1 mL was accumulated in the collection vial. At that point, the static valve was closed and the cell continued to pressurize to the set point (50-250 bar). The static period for these studies was 5 min. because longer periods did not show improvement in term of recovery. After the static period, the static valve was reopened, fresh solvent was introduced to flush the lines and cell, and the extract was collected in the vial. During this solvent flush step, 50-100% of the extraction cell volume of solvent was pumped into the cell.

Day to Day Experiments

The soil samples were analysed using the optimized method of the PLE to study the efficiency of the developed method.

Procedure

The samples of four PAHs, with a concentration of 20 ppm (napthalene, fluorine, phenanthrene, and fluoranthene), were dissolved in acetonitrile and kept in the freezer. Mixed solutions were prepared by mixing specific quantities of analytes from each stock solution. The prepared solution was injected in triplicates onto the column.

The separation was carried out using different compositions (acetonitrile-water: 70-30; 60-40; 50-50; 40-60, v/v). The eluent flow rate was 1.0 mL/min and the sample injection volume was 1µL. Meanwhile, the UV detection of analytes for the comparison study was at 254 nm.

RESULTS AND DISCUSSION

In this study, the optimized PLE conditions were investigated to be applied for the extraction of the PAHs from the soil samples. The extraction solvents, extraction pressure, and extraction temperature were optimized and the reproducibility of the method was also investigated. In the PLE, the soil was mixed with anhydrous sodium sulphate. The advantages of mixing the soil with anhydrous

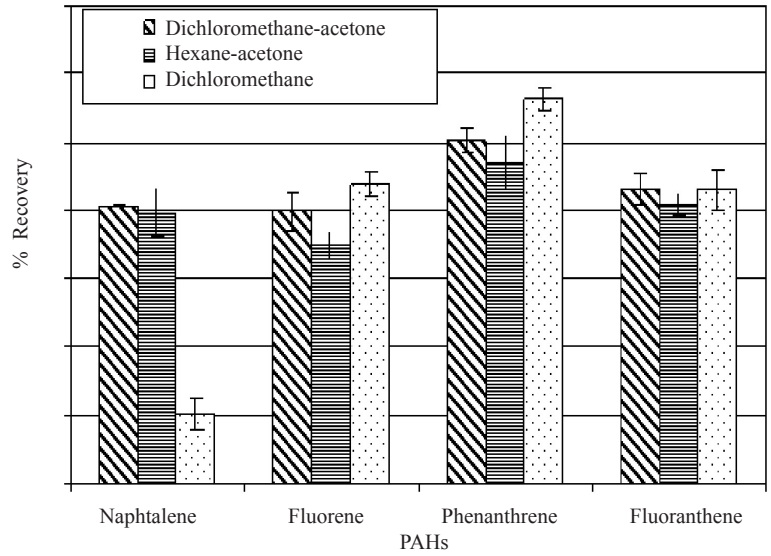

Fig. 2: Average percentage recoveries of spiked 50 ppm PAHs in soil samples using different extraction solvent

sodium sulphate include trapping of water through binding to sodium sulphate, minimized soil exposure to laboratory air, stopping the microbial activity due to the high salt concentration, and a longer storing period for the sample that was treated in this way.

Liquid chromatographic analysis of the extracts that were obtained from the PLE of spiked soil samples was also carried out. It was found that different extraction solvents gave different recovery percentages (*Fig. 2*). The recovery of PAHs ranged from 80% to 101% for dichloromethane-acetone, 70% to 94% for hexane-acetone and 21% to 113% for dichloromethane as extractant. The highest recovery percentages were observed for phenanthrene (113%) and fluorene (88%) using dichloromethane as the extraction solvent. All relative standard deviations for the spiked standard PAHs were acceptable (R.S.D. 0.3-9.3). Low recovery was obtained for naphthalene with dichloromethane as single solvent extractant, indicating that the solvent was not suitable for naphthalene as compared to other analytes. Similar results have also been reported by Burkhardt *et al.* (2005) who obtained a mean recovery of 67% for naphthalene, as compared to phenanthrene (102%), and fluoranthene (111%), using water-isopropanol as extraction solvents. Meanwhile, Fisher *et al.* (1994) found that spiking in more polar solvent resulted in a higher recovery. Similar results were also obtained by Eschenbach *et al.* (1994) who explained that acetone showed a greater efficiency than toluene or dichloromethane.

Temperature has a significant influence on the diffusion coefficient of solvents; hence, the kinetics of an extraction process and its overall efficiency is strongly dependent on this parameter. In this work, the recovery of PAHs from the spiked samples was determined using different extraction temperatures, in the range of 100°C-180°C, with the mixture of dichloromethane-acetone 50:50 (v/v) as the extraction solvent.

In general, higher recovery of all the PAHs studied was obtained at higher temperatures (*see* Table 1). For example, at 100°C and 180°C, the recovery of phenanthrene was found to be 83% and 89%, respectively. A high temperature of 180°C gave the highest recovery for fluoranthene (94%), followed by fluorene (92%), phenanthrene (89%), and naphthalene (82%). The higher

TABLE 1
The recovery percentages of the spiked standard PAHs at 20 ppm in 7g of the soil samples at different extraction temperatures

Compound	% Recovery (R.S.D.)		
	Temperature		
	100°C	150°C	180°C
Naphthalene	42(±2.5)	68(±1.0)	82(±1.0)
Fluorene	87(±1.3)	92(±1.4)	92(±1.1)
Phenanthrene	83(±1.7)	88(±7.7)	89(±1.8)
Fluoranthene	87(±1.1)	87(±1.5)	94(±0.2)

(R.S.D. %) was based on triplicate injections

recovery for the more hydrophobic compounds (phenanthrene and fluoranthene) can be explained because these compounds are generally more thermally stable. Hawthorne *et al*., 2000 reported that increasing the extraction temperature gave a higher recovery for higher molecular weight of the PAH extracted. Meanwhile, PAHs with high-molecular weight may have stronger adsorption and formation of non-extractable residues (Hawthorne *et al.*, 2000). Hence, fluoranthene with the highest molecular weight shows the highest recovery and naphthalene with the lowest molecular weight reveals the lowest recovery.

The high recovery at 180°C for the PAHs studied can be explained by the fact that at higher temperatures, there is a decrease in the viscosity of liquid solvents, which allow a better penetration of the matrix particles and enhance extraction. Thus, an increase in the temperature can disrupt the strong solute-matrix interactions caused by the van der Waals forces, hydrogen bonding, and dipole interactions of the solute molecules and active sites on the matrix. In addition, increased temperatures can also decrease the surface tension of the solvent that facilitates a better contact of the solvent with the analytes and enhance extraction (Bruce, 2000).

The results obtained are in good agreement with those reported by Jaska *et al.* (2004) who suggested that in order to enhance the efficiency of recovery, extractions need to be performed at an elevated temperature within the range of 50-180°C, depending on the boiling point of the analytes studied. In the PLE, the samples were extracted at the temperatures well above the boiling point of the extractant used. The kinetics of the mass transfer can greatly be improved at elevated temperatures. Therefore, it is highly possible that a poor extraction solvent in a conventional extraction method, such as Soxhlet extraction, can be a good solvent in the PLE at high temperatures.

Meanwhile, the use of pressure facilitates the extraction of analytes from the samples, in which the analytes are trapped in the matrix pores. In this case, an elevated pressure, along with an elevated temperature, reduces the solvent surface tension that helps force the solvent into the sample pores to contact the analytes. In this study, the following pressures were used to determine the effects of pressure on the extraction efficiency: 50 bar, 100 bar, and 150 bar. However, higher pressure was not attempted in this study because only modest pressure in the range of 100-150 bars (10-15MPa) is usually needed to maintain the solvents as liquid in the PLE (Jaska, 2004). The results show that the recovery percentage of the analytes improves with the increase in pressure (Table 2). All the analytes studied showed the highest recovery at 150 bar. In particular, fluorene showed the highest recovery percentage (95%), followed by phenanthrene (94%), fluoranthene (87%), and naphthalene (52%). These results confirm the hypothesis that the increased pressures would allow the analytes

TABLE 2
The recovery percentage of the analyte studied at different extraction pressures (temperature: 180°C)

Compound	% Recovery (R.S.D.)		
	Pressure (bar)		
	50	100	150
Naphthalene	45 (±5.8)	49 (±0.20)	52 (±0.04)
Fluorene	83 (±4.2)	88 (±0.03)	95 (±0.08)
Phenanthrene	79 (±1.1)	83 (±0.03)	94 (±0.03)
Fluoranthene	77 (±2.6)	82 (±0.20)	87 (±0.04)

TABLE 3
Relative recovery percentages and standard deviation of the analytes studied on daily basis

	% Recovery			Mean % recovery	% R.S.D.
Compound	Day 1	Day 2	Day 3		
Naphthalene	88	63	68	73	$\pm 0.1_1$
Fluorene	95	97	91	94	$\pm 0.0_4$
Phenanthrene	90	93	89	91	$\pm 0.0_2$
Fluoranthene	91	89	88	89	$\pm 0.0_1$

which were found in pores effectively blocked by solvent to be more rapidly extracted than what is possible at the room temperature and atmospheric pressure.

From the results obtained (Table 3), it is noted that there are no significant day-to-day differences in the efficiency of the developed method, while the day-to-day R.S.D. values were lower. The highest value was obtained for fluorene (95%) at Day 1, while the lowest recovery was naphthalene (63%) at Day 2. The result showed that the three-ring PAHs (fluorene, phenanthrene) appeared to be more efficiently extracted by the PLE as compared to the two-ring PAH (naphthalene), and this was probably due to its higher volatility of naphthalene which had caused more analyte loss during extraction.

The results indicate that the developed method for the PLE of PAHs has good reproducibility. The RSDs were good, i.e. ranging from 0.0_1 to 0.1_1. Therefore, the PLE method is proven to be readily applicable as a standard method for the extraction and analysis of PAHs. Currently available US EPA methods for the extraction of PAHs from contaminated soil include Method 3540 for Soxhlet extraction, Method 3541 for SFE and Method 3545 for PLE. Conte *et al*. (1997) reported that the PLE is advantageous because the parameters involved include the ease of total automation that adds to better reproducibility, reduced time direct contact between operator and solvent vapour, reduced consumption of organic solvents, the subsequent storage and disposal.

CONCLUSIONS

A method for the determination of PAHs has been developed using a homemade pressurized liquid extraction (PLE) system and elevated temperature RPLC. In particular, the PLE has shown an excellent efficiency in term of the total extraction time, total solvent usage, and reproducibility. In fact, the PLE method has demonstrated an outstanding performance with dichloromethane-acetone 50:50 (v/v) as solvent extraction, pressure 150 bar, and extraction temperature of 180°C. Data showing the method R.S.D. and reproducibility have proven the suitability of the method for routine monitoring of the compounds of interest in samples of soil. Although not all classes of environmentally-important compounds have been covered, the PLE of representative semi-volatile compounds in the soil matrixes indicate this technique as a viable technique for extraction, among the new regime of rapid method. In short, recovery with the use of the PLE in all cases was found to be satisfactory, offering a good agreement with the established data reported.

ACKNOWLEDGEMENTS

The authors wish to thank Universiti Teknologi Malaysia and the Ministry of Science, Technology and Innovation, Malaysia (MOSTI), for the financial support through the IRPA Project 09-02-06-0074 EA211 Vote No. 74255.

REFERENCES

Bruce, R.E. (2000). Extraction of hydrocarbons contamination from soils using accelerated solvent extraction. *Journal of Chromatography A*, *874*, 217-224.

Burkhardt, M.R., Revello, R.C., Smith, S.G. and Zaugg, S.D. (2005). Pressurized liquid extraction using water/isopropanol coupled with solid-phase extraction cleanup for industrial and anthropogenic waste-indicator compounds in sediment. *Analytica Chimica Acta*, *534*, 89-100.

Claessens, H.A. and Straten, M.A.V. (2004). Review on the chemical and thermal stability of stationary phases for RP-HPLC. *Journal of Chromatography A*, *1600*, 23-41.

Conte, E., Milani, R., Morali, G. and Abballe, F. (1997). Comparison between accelerated solvent extraction and traditional extraction methods for the analysis of the herbicide diflufenican in soil. *Journal of Chromatography A*, *765*, 121-125.

Eschenbach, A., Kastner, M., Bierl, R., Schaefer, G. and Mahro, B. (1994). Evaluation of a new, effective method to extract polycyclic aromatic hydrocarbons from soil samples. *Chemosphere*, *28*, 683-692.

Fisher, R., Kreuzig, R. and Bahadir, M. (1994). Extraction behaviour of polycyclic aromatic hydrocarbons absorbed on waste incinerator fly ash. *Chemosphere*, *29*, 311-317.

Hawthorne, S.B., Grabanski, C.B., Martin, E. and Miller, D.J. (2000). Comparisons of soxhlet extraction, pressurized liquid extraction, supercritical fluid extraction and subcritical water extraction for environmental solid: Recovery, selectivity and effects on sample matrix. *Journal of Chromatography A*, *592*, 421-433.

Jaska, M., Tomaniora, M., Hajslova, J. and Kocourek, V. (2004). Appraisal of classic and novel extraction procedure efficiencies for the isolation of polycyclic aromatic hydrocarbons and their derivatives from biotic matrices. *Analytica Chimica Acta*, *520*, 93-103.

Richter, B.E., Jones, B.A., Ezzell, J.L. and Porter, N.L. (1999). Accelerated solvent extraction: A technique for sample preparation. *Analytical Chemistry*, *68*, 1033-1039.

Saim, N., Dean, J.R., Abdullah, M.F. and Zakaria, Z. (1997). Extraction of polycyclic aromatic hydrocarbons from contaminated soils using soxhlet extraction, pressurized and atmospheric microwave-assisted extraction, supercritical fluid extraction and accelerated solvent extraction. *Journal of Chromatography A*, *791*, 361-366.

Scott, R.P.W. (1984). *Small Bore Liquid Chromatography Columns: Their Properties and Uses*. New York: John Wiley and Sons.

Wan, H.B. and Wong, M.K. (1996). Minimization of solvent consumption in pesticide residue analysis. *Journal of Chromatography A*, *754*, 43-47.

ISSN: 0128-7680
Pertanika J. Sci. & Technol. **19 (1)**: 33 – 43 (2011)

Properties of Laterite Brick Reinforced with Oil Palm Empty Fruit Bunch Fibres

Sallehan Ismail[1*] and Zaiton Yaacob[2]
[1]Department of Building,
Faculty of Architecture, Planning & Surveying,
Universiti Teknologi MARA, Seri Iskandar Campus,
32610 Seri Iskandar, Perak, Malaysia
[2]Department of Building,
Faculty of Architecture, Planning & Surveying,
Universiti Teknologi MARA Malaysia,
40450 Shah Alam, Selangor, Malaysia
[*]E-mail: salle865@perak.uitm.edu.my

ABSTRACT

The development of a new, low-cost building material that is composed of non-fired, pressed laterite bricks incorporating oil palm empty fruit bunches (OPEFB) fibre was investigated in this study. The main aim of this research was to study the physical and mechanical properties of laterite brick reinforced with OPEFB fibre, including dimensions, weight, density, water absorption and compressive strength. The tests were carried out according to BS 3921:1985 for water absorption and compressive strength tests. The mix proportion of the control bricks was 70% soil, 24% sand, and 6% cement. Meanwhile, the OPEFB fibre contents ranged from 1% to 5% by weight of cement. The specimens were taken from a total of 120 bricks. The findings withdrawn from this research were: firstly, the density of laterite bricks was decreased with the increase in the OPEFB fibre content of the bricks. Secondly, it was found that the addition of the OPEFB fibres improved the compressive strength of the bricks, and the maximum compressive strength determined in this study for bricks was with 3% fibre content. Finally, the water absorption results indicated a small increase in water absorption with the increase in the OPEFB fibre content in laterite bricks.

Keywords: Natural fibre, OPEFB fibre, laterite bricks

INTRODUCTION

Cheap building materials are necessary for the development of low cost housing in Malaysia. In particular, non-fired laterite bricks are an attractive building material because they are inexpensive to manufacture. These bricks are manufactured by sun-baking pressed earth from laterite soil that is mixed with sand and cement as composites. With earth being affordable, environment-friendly, and abundantly available, the production of blocks and bricks made from earth has been used in home construction in many countries for a long time (Binici *et al*., 2004). Earth has been extensively used for wall construction around the world, particularly in developing countries (Ren and Kagi, 1995). Several studies have focused on improving and stabilising the development and production of these kinds of bricks and on the properties of these bricks in terms of strength, shrinkage, thermal

Received: 12 June 2009
Accepted: 9 April 2010
[*]Corresponding Author

conductivity, and durability of soil to meet building standards (e.g. Heathcote, 1991; Ren and Kagi, 1995; Walker, 1995; Ogunye and Boussabaine, 2002; Khedari *et al.*, 2005; Achenza and Fenu, 2006; Morel *et al.*, 2007).

The concept of using natural fibres is not new in the construction industry, as the utilisation of fibres in materials and construction can be traced back to many centuries ago. During the Egyptian times, straws or horsehairs were added to mud bricks, while straw mats were used as reinforcements in early Chinese and Japanese housing construction (Li, 2002). The application of natural fibres has been widely used in cement composites and earth blocks as construction materials for many years in developing countries due to the availability and low cost of fibres (e.g. Nilsson, 1975; Aziz *et al.*, 1984; Coutts and Ni, 1995; Aggarwal, 1995; Ghavami *et al.*, 1999; Bouhicha *et al.*, 2005; Binici *et al*., 2005). Furthermore, several studies have proven the advantages of the use of natural fibres in soil, concrete, and cement composites; they can increase the flexural strength, post-crack load bearing capacity, impact toughness, and bending strength of these composites (e.g. Ramaswamy *et al*., 1983; Aziz *et al*., 1984; Swamy, 1988; Brandt, 1995; Coutts and Ni, 1995; Ghavami *et al*., 1999; Toleˆdo Filho *et al*., 2000). Due to their light weight, good chemical resistance (e.g. alkali in cement), corrosion resistance, and high strength-to-weight ratio, natural fibre-based composites are becoming an important composite material in the building and civil engineering fields. Therefore, this research made an attempt to turn natural fibres that are easily found in Malaysia into laterite bricks.

Oil palm production is a major agricultural industry in Malaysia. In 2007, 4.3 million hectares of land were planted with palm oil trees (MPOB, n.d.). Large quantities of palm waste, known as empty fruit bunches (EFB), are left in plantations where palm oil is produced. The abundance of oil palm EFB (OPEFB) has created crucial environmental issues, such as fouling and attraction of pests. In the past, this residue was often used as fuel to generate steam at the mills (Ma *et al.*, 1993). Unfortunately, burning these materials creates air pollution, which is prohibited by the Environment Quality Act (EQA) (1974). Nowadays, however, valuable fibre can be obtained from OPEFB, which has found its use in manufacturing board and paper.

Thus, this research investigated the physical and mechanical characteristics of laterite bricks that are reinforced with OPEFB fibres. In particular, the purpose of this research was to determine the potential and feasibility of laterite bricks that are reinforced with OPEFB fibres in increasing the added value of these products, especially in building materials. Moreover, the recycling or utilisation of solid wastes that are generated from most agro-based industries is currently very rewarding. The anxiety caused by enormous waste production, resource preservation, and material cost has focused the attention on the reuse of solid waste. Material recovery from the conversion of agricultural wastes into useful materials has not only led to environmental gains but it may also preserve natural resources. In addition, the use of waste materials is a potential alternative in the construction industry due to the increasing cost of raw materials and the continuous reduction of natural resources. Waste materials, when properly processed, have been shown as effective construction materials which readily meet design specifications (Mannan and Ganapathy, 2004). This research attempted to propose the use of these seemingly waste products as construction materials in low-cost housing as well as to encourage housing developers to invest in house construction incorporating these materials.

EXPERIMENTAL WORK

Material Used

All the materials used in this specimen were local products that had been supplied by local manufactures. The materials that were used to produce brick specimens were laterite soil, sand, cements and OPEFB fibres.

Soils

The type of soil used in this research is laterite soil, which was supplied by Majpadu Sdn. Bhd. The soil was taken from the nearby factory area and kept under roof cover to ensure that it was neither too dry nor too wet. The moisture content for the laterite soil was found to be 16.6%, as tested according to BS 1377: 1990. After sieving, the size of the soil particles was less than 2 mm in diameter, according to the manufacturer's requirements. The physical properties and chemical composition of these soils are given in Table 1.

TABLE 1
The physical properties of the soils used

Characteristics of laterite soil	Value
Specific gravity	2.66
Liquid limit (%)	63
Plastic limit (%)	32
Plasticity index (%)	31
Activity coefficient	80
Clay (%)	16
Silt (%)	37
Fine sand (%)	41
Coarse sand (%)	6

Sand

The sand used for this study was obtained from a tin mine in Puchong. The average sand particle size was below 5mm, while the moisture content recorded was 2.36%.

Cement

The cement used in this research was the ordinary Portland cement manufactured by Associated Pan Malaysia Sdn. Bhd. Cement, as specified in the Malaysian Standard specification MS 522:Part 1:2003 for concrete work.

The fibres

The OPFB fibres were obtained from the Sabutek (M) Sdn. Bhd. factory that is located in Teluk Intan, Perak. They were sun dried for one week prior to cutting them manually. The fibres were long and circular in shape. However, these fibres must be short and straight so as to ensure a quick dispersal without clinging. The fibres were then cut at an average of 25 mm length intervals. In this research, the fibres were used as additives, whereby they were added at a volume fraction of 1-5% to produce stable and improved laterite bricks. The typical physical and chemical compositions of the OPEFB fibres are presented in Tables 2 and 3.

TABLE 2
The properties of the OPEFB fibres

Properties	Value
Length (single fibre) (mm)	100- 280
Diameter (single fibre) (mm)	0.25 – 0.6
Moisture content (%)	11
Density (g/cm^3)	1.3
Breaking elongation (%)	30
Tensile strength (MPa)	21
Compression of strength (MPa)	36
Bending stress (MPa)	38

TABLE 3
Chemical composition of OPEFB fibre

Chemical composition	Value (%)
Hot water solubles	12.8
Hemi-cellulose	2.1
Lignin	25
Cellulose	59
Alkali soluble	28
Pentosans	8.7
Ash	3.2

Mix Design

The design mix proportion of all the OPEFB fibre brick specimens was 70% soil, 24% sand, and 6% cement for the matrix. All the constituent materials for the OPEFB bricks were prepared in 6 sample groups, with 20 bricks in each group, to determine the compressive strength and water absorption. Meanwhile, the total number of bricks was 120 pieces. In this study, 5 groups of the brick samples were added, with various percentages of fibre contents ranging from 1-5%, calculated based on the weight of cement. The remaining group of bricks had no fibres and served as the control samples. These control samples were used as a guide for comparison with other bricks containing fibres to determine the comparison of the physical and mechanical properties of laterite bricks. The wastage allowance was 45%, allowing for wastage in double handling (from hand mixing to pressing machine) and for error in soil weight during materials pressing. The total of the overall quantities for constituents, such as soil, sand, and cement (matrix) in the bricks, were 353, 121, and 30 kg, respectively. The total quantity of the fibres used was 750g.

Preparation of the Brick Specimens

Laterite bricks with OPEFB fibres were manufactured at the factory known as Majpadu Sdn. Bhd., which is located at Jalan Kebun, Shah Alam. The material was prepared in the laboratory of the Faculty of Architecture, Planning, and Surveying at Universiti Teknologi MARA (UiTM), before it was brought to the factory. Generally, laterite bricks are not fired but hardened from a chemical reaction and from mechanical compaction. Chemical reactions occur when the added cement reacts with the minerals in the soil. When compacted by mechanical force, soil grains and soil aggregates are bonded tightly, decreasing the pore rate of the bricks and increasing their density. As a result, water permeability and capillarity absorption are reduced. The processes involved in the OPEFB fibre brick fabrication include mixing, pressing, wrapping, and curing.

The mixing of the constituent materials

The Portland cement and OPEFB fibres were mixed beforehand in a laboratory at UiTM before they were mixed with soil and sand in the factory. The cement and fibres were weighed according to the mix design before mixing. The cement and fibres were mixed by hand to ensure an even dispersion of the fibres in the cement to prevent balling up. After that, the cement fibre mixes were packed separately in plastic bags based on the different types of fibres and brick samples. Afterwards, the cement and fibre mixtures were transported to the factory. At the factory, the cement and fibres were mixed with laterite soil and sand, according to the specified mix proportion using a hand shovel, on a piece of plywood at ground level. The mixing process took approximately 5-10 min to ensure an even dispersion of all the matrix and fibres. The production of brick samples began with the control samples, and this was followed by the mixture content with fibre.

The pressing of bricks

After mixing by hand shovel, the materials were scooped into a gunny sack, poured into the mini mixer at the pressing machine to press out the bricks and transported by conveyor. The pressure used for pressing the bricks was 9 kN/m^2. The pressed bricks were then moulded by using a mould size of 216 mm in length, 97 mm in width, and 68 mm in depth.

The wrapping and curing of bricks

After pressing, the bricks were stacked on timber palettes and marked according to their fibre contents and material composition. The bricks were then wrapped with a plastic film to avoid rapid drying and stored under a sheltered area for 24 h prior to spraying with water. The bricks were then stored in open air for 14 days and they were also allowed to cure for 28 days prior to use in the investigation carried out in this study.

Test Methods

All the tests were executed after the bricks had been cured for 28 days. A series of tests was conducted to determine the physical and mechanical properties of the bricks; these included dimension, density, compressive strength, and water absorption, which were conducted according to BS 3921:1985. In order to determine the dimension measurement of the bricks, deviations were taken from 10 bricks of each sample. Their length, height, and thickness were also measured. Meanwhile, the density of the brick specimens was calculated by dividing the weight with volume. The compressive strength test was carried out by imposing the bricks on a compression load until breakage to examine the variation of strengths, allowing the researchers to categorise the bricks by their strength level. Compressive strength was calculated by dividing the maximum load by the load area of the specimen according to the standards. Ten specimens from each sample group were

taken to determine their compressive strength to compute the average strength. Meanwhile, the water absorption test was carried out to determine the permeability of the bricks. The specimens were first dried in an oven for 76 h at 110°C and later cooled at room temperature before weighing. After that, the specimens were placed inside a curing tank and were boiled in water for 6 h. The specimens were removed after they had been immersed in the tank for 16 h and then weighed. The ratio of the water content to the dry mass of bricks determines the quantity of the water absorption of specimens.

RESULTS AND DISCUSSION

Brick Dimension

Brick dimension is influenced by material content and the density of the constituent materials. In this study, the average brick dimension was calculated from 10 samples for each group. The brick dimensions evaluated were length, width, depth, area, and volume. A summary of the average brick dimensions is given in Table 4. The average OPEFB fibre brick was 216.17 mm long, 97.17 mm wide and 68 mm thick. The standard deviations for all the samples were 0.41 for length, 0.41 for width, and 0 for depth. The average brick area for all the samples was 0.021 m^2, with a standard deviation of 0.0001m^2, and the average volume was 0.00143 m^3 with a standard deviation of 0.00001 m^3. The standard deviation for average length, width, depth, area, and volume for bricks with the OPEFB fibre content was from 0 to 0.41. It can be summarised that bricks with OPEFB fibre had a uniform size and a surface area that is similar to fibreless bricks.

TABLE 4
The dimensions of the OPEFB fibre bricks

Type (R)	Length (mm)	Width (mm)	Depth (mm)	Area (m^2)	Volume (m^3)
R0 (0% FIBRE)	216	97	68	0.0210	0.00145
R1 (1% FIBRE)	216	97	68	0.0210	0.00142
R2 (2% FIBRE)	216	97	68	0.0210	0.00142
R3 (3% FIBRE)	216	97	68	0.0210	0.00142
R4 (4% FIBRE)	216	97	68	0.0210	0.00142
R5 (5% FIBRE)	217	98	68	0.0213	0.00143
AVERAGE	216.17	97.17	68	0.0210	0.00145
STANDARD DEVIATION	0.41	0.41	0.00	0.0001	0.00001

Brick Density

The average value for the brick density, with various levels of fibre content, is shown in *Fig. 1*. In all cases, it can be concluded that the average density of the OPEFB fibre bricks was lower than that of the control bricks. *Fig. 1* shows the decreased density of the bricks with fibres due to the fact that the OPEFB fibre replaced the heavier constituent materials, i.e. either sand or soil in laterite bricks. Meanwhile, the average density for the control bricks was 2086.29 kg/m^3, whereas the average density of bricks with 1% fibre content was 2037.36 kg/m^3, with a reduction of about

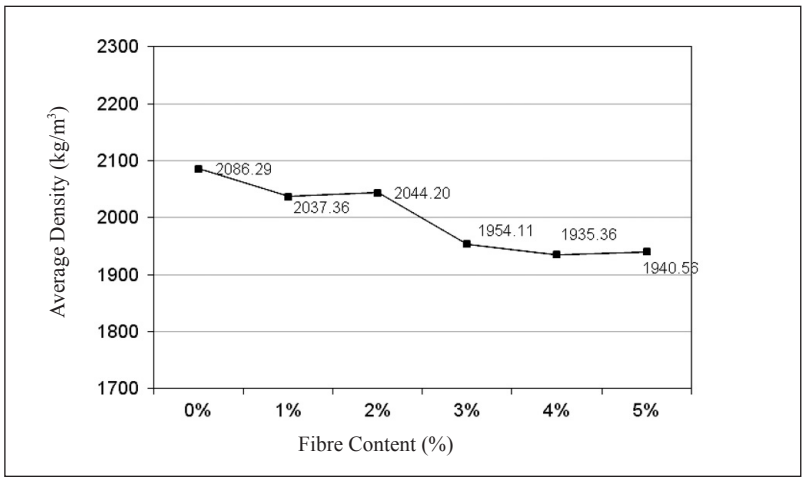

Fig. 1: Density of OPEFB fibre bricks

2.3% as compared to the density of the control bricks. There was an increase of 0.3% for the bricks with 2% fibre content as compared to the bricks with 1% fibre content. A higher reduction density was shown by the bricks with 3%, 4%, and 5% fibre contents, with a reduction in density of about 6.3%, 7.2%, and 7%, respectively, in comparison to the density of the control bricks.

Compressive Strength of the OPEFB Fibre Bricks

The compressive strength of a material determines the load-carrying capacity of that material before breakage. The compressive strength for all brick types is illustrated in *Fig. 2* below.

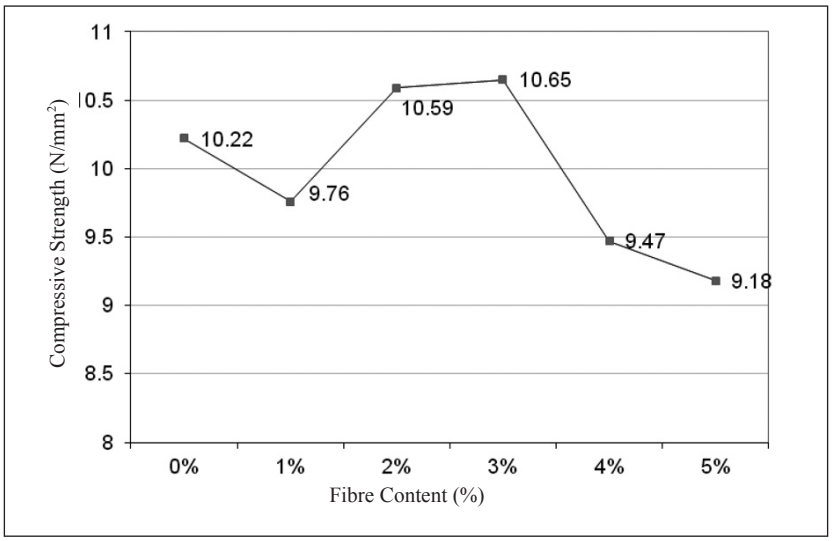

Fig. 2: The compressive strength of the OPEFB fibre bricks

As illustrated in *Fig. 2*, the compressive strength of the control bricks was 10.22N/mm². When the control was compared with the OPEFB fibre bricks with the fibre contents of 1, 4, and 5%, a slight reduction was found in strength for the bricks, that is, 9.76, 9.47, and 9.18 N/mm², respectively. However, the results for the bricks with 2 and 3% fibre contents showed that the fibres began to reinforce the bricks successfully and increase the compressive strength to 10.59 and 10.65N/mm², respectively. The increase in the compression strength for the bricks with 2% and 3% fibre contents was 3.6% and 4.2%, respectively as compared to the control bricks. Thus, it can be concluded that the optimum OPEFB fibre percentage that can successfully increase the maximum compressive strength of bricks is 3% of the fibre content. In this case, an increase in the compression strength occurs because the fibres can withstand stresses (Binici *et al*., 2005) and successfully reinforce and hold the matrix. Based on the researchers' observation of the crack appearance of the specimens, the decrease in the compressive strength of bricks with 4% and 5% fibre contents occurred because the space occupied by the fibres acted like voids in the matrix. Such a void space could be attributed to the high volume fraction of the fibres, and the non-uniform fibre distribution tended to make fibres ball or clump together. When the fibres are not evenly distributed and orientated in the matrix, they can clump together with less matrix material in between to hold them together, creating more voids and making the bricks weak. Juárez *et al*. (2010) reported that the ultimate compressive strength of the fibre-reinforced masonry value is dependent upon the aspect ratio of the fibre. A lower fibre aspect ratio leads to a higher compressive strength in masonry pieces, but a higher addition of fibre decreases the value of compressive strength (Yetgin *et al*., 2008).

Water Absorption

Brick density is a function of the water absorption, fibre content, and porosity. Overall, the results indicate that the density due to water absorption for bricks with OPEFB fibres is higher as compared with that for the control bricks and that it is possible for the bricks with OPEFB fibres to be more permeable to water. The relationship between water absorption and density is presented in *Fig. 3*. The higher water absorption capacity of OPEFB bricks may be attributed to the amount of water absorbed by the cellulose fibres, which is influenced by void volume and the amount of cellulose material present, and both these parameters affect density. Thus, one can expect the density to decrease and the water absorption to increase as the fibre content is increased due to the nature of the hydrophilic and low-density OPEFB fibres. At the same time, the packing of the fibres and the matrix becomes less efficient as the fibre content is increased, and causes the void volume to increase, followed by a decrease in density and an increase in water absorption (Coutts and Ni, 1995). In other words, this result is compatible with the density theory, which predicts that samples of higher original density are less likely to absorb water, and vice versa. Another result shows the same trend as the observation previously conducted by Ghavami *et al*. (1999) which indicates that the fibres absorb water and expand during mixing and drying of soil. The swelling of the fibres pushes the soil away, at least at the micro-level. At the end of the drying process, the fibres lose the moisture and shrink back almost to their original dimensions, leaving very fine voids around them.

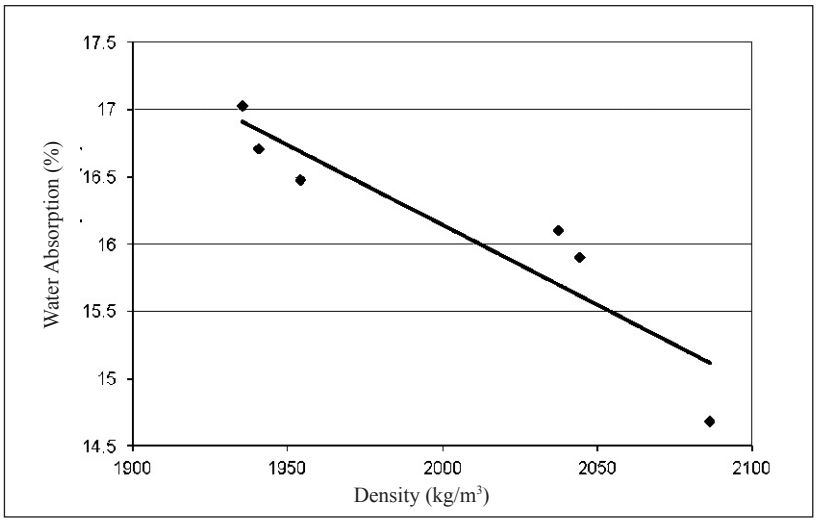

Fig. 3: The relationship between density and water absorption for the OPEFB fibre bricks

CONCLUSIONS

The following conclusions can be drawn from the findings of this research;

1. The density of the OPEFB fibre-reinforced laterite bricks decreases with the increase in fibre content. This may be due to the fibres displacing heavier constituent materials, such as cement and soil, from the laterite bricks.
2. The addition of OPEFB fibres at 3% successfully increases the compressive strength of laterite bricks. During mixing, it was observed that the OPEFB fibres at this level were well-distributed in the bricks and were able to take more loads. Moreover, they were successfully reinforced and held by the matrix, but the addition of more fibre was found to reduce the strength of bricks.
3. Bricks with OPEFB fibres have a slightly higher water permeability or absorption than fibreless bricks. In more specific, the OPEFB fibres are believed to be responsible for the absorption of more water and increase brick permeability to water.

Overall, the OPEFB fibres have the potential as reinforcement for laterite bricks. The result showed that the addition of OPEFB fibres produced lighter bricks and improved the compressive strength. However, the incorporation of fibres resulted in more permeable bricks. Hence, more study is required to determine the effect of fibre orientation in the matrix in order to understand the bond between the soil matrix and fibres better, while a study of the microstructure is also needed. Another study which can be expanded from this research is to find the special treatment of OPEFB that can improve the physical properties of the fibres so that they become less permeable to water.

REFERENCES

Achenza, M. and Fenu, L. (2006). On earth stabilization with natural polymers for earth masonry construction. *Materials and Structures*, *39*, 21–27.

Aggarwal, L.K. (1995). Bagasses-reinforced cement composites. *Cement Concrete Composites*, *17*, 107–12.

Agopyan, V. (1988). Vegetable fibre reinforced building materials developments in Brazil and other Latin American countries. In R.N. Swamy (Ed.), *Natural fibre reinforced cement and concrete Glasgow: Blackie* (pp. 208–42). Concrete Technology and Design, 5.

Aziz, M. A., Paramasivam, P. and Lee, S.L. (1981). Prospects for natural fibre reinforced concretes in construction. *The International Journal of Composites and Lightweight Concrete*, *3*(2), 123-132.

Binici, H., Aksogan, O. and Shah, T. (2005). Investigation of fibre reinforced mud brick as a building material. *Construction and Building Materials*, *19*, 313–318.

Bouhicha, M., Aouissi, F. and Kenai, S. (2005). Performance of composite soil reinforced with barley straw. *Cement and Concrete Composite*, *27*, 617.

Brandt, A.M. (1995). *Cement-based Composite: Materials, Mechanical Properties and Performance.* London: E & FN SPON.

British Standards Institution. (1985). *BS 3921: 1985 Specification for Clay Bricks*. BSI, London.

British Standards Institution. (1990). *BS 1377: Part 4: 1990 Methods of Testing Soils for Civil Engineering Purpose*. BSI, London.

Coutts, R.S.P. and Ni, Y. (1995). Autoclaved bamboo pulp fibre reinforced cement. *Cement Concrete Composites*, *17*, 99–106.

Ghavami, K., Filho, R.D.T. and Barbosa, N.P. (1999). Behaviour of composite soil reinforced with natural fibres. *Cement Concrete Composite*, *21*, 39–48.

Heathcote, K. (1991). Compressive strength of cement stabilised pressed earth blocks. *Building Research and Information*, *19*(2), 101-105.

Khedari, J., Watsanasathaporn, P. and Hirunlabh, J. (2005). Development of fibre-based soil–cement block with low thermal conductivity. *Cement and Concrete Composites*, *27*, 111–116.

Juárez, C., Guevara, B., Valdez, P. and Durán-Herrera, A. (2010). Mechanical properties of natural fibers reinforced sustainable masonry. *Construction and Building Materials*, Article in Press, Corrected Proof.

Law of Malaysia. (Act 127) Environmental Quality Act (EQA) 1974, *Section 29A*. Retrieved on March 20, 2009 from http://www.doe.gov.my/v2/files/legislation/a0127.pdf.

Lee, S.M., Cho, D., Park, W.H., Lee, S.G., Han, S.O. and Drzal, L.T. (2005). Novel silk/poly(butylene succinate) biocomposites: The effect of short fibre content on their mechanical and thermal properties. *Composites Science and Technology*, *65*, 647-657.

Li, V.C. (2002). Large volume, high-performance applications of fibers in civil Engineering. *Journal of Applied Polymer Science*, *83*(3), 660-686.

Ma, A.N., Cheah, S.A. and Chow, M.C. (1993). Current status of palm oil processing waste management. In Yeoh *et al.* (Eds.), *Waste management in Malaysia: Current status and prospects for bioremediation*, 111-136.

Malaysian Palm Oil Board. (n.d). Malaysian Oil Palm Statistics, 2007. Retrieved June 25, 2008 from http:// econ.mpob.gov.my/ economy/annual/stat 2007/Area1.1.htm.

Malaysian Standards. (2003). *MS 522: Part 1:2003 Portland Cement (Ordinary and Rapid-hardening): Part 1: Specification (Second revision)*. SIRIM.

Mannan, M.A. and Ganapathy, C. (2004). Concrete from an agricultural waste-oil palm shell (OPS). *Building and Environment*, *39*, 441 – 448.

Morel, J.C., Pkla, A. and Walker, P. (2007). Compressive strength testing of compressed earth blocks. *Construction and Building Materials*, *2*, 303–309.

Nilsson, L.H. (1975). Reinforcement of concrete with sisal and other vegetable fibres. Swedish Council for Building Research, Document DIY, Stockholm, Sweden.

Ogunye, F.O. and Boussabaine, H. (2002). Diagnosis of assessment methods for weatherability of stabilised compressed soil blocks. *Construction and Building Materials*, *16*, 163–172.

Ramaswamy, H.S., Ahuja, B.M. and Krishnamoorthy, S. (1983). Behavior of concrete reinforced with jute, coir, and bamboo fibres. *International Journal Cement Concrete Composites*, *5*(1), 3–13.

Reddy, B.V. (1998). Steam-cured stabilised soil blocks for masonry construction. *International Journal Energy and Buildings*, *29*, 29–33.

Ren K.B. and Kagi D.A. (1995). Upgrading the durability of mud bricks by impregnation. *Building and Environment*, *30*, 433-440.

Sastra, H.Y., Siregar, J.P., Sapuan, S.M., Leman, Z. and Hamdan, M.M. (2005). Flexural properties of *Arenga pinnata* fibre reinforced epoxy composites. *American Journal of Applied Sciences*, (Special Issue), 21-24.

Swamy, R.W. (1988). *Natural Fibre Reinforced Cement and Concrete*. Glasgow, Great Britain: Bell & Bain.

Toleˆdo Filho, R.D., Scrivener, K., England, G.L. and Ghavami, K. (2000). Durability of alkali-sensitive sisal and coconut fibres in cement mortar composites. *Cement Concrete Composite*, *22*(6), 127–43.

Yetgin, S., Cavdar, O. and Çavdar, A. (2008). The effects of the fiber contents on the mechanic properties of the adobes. *Construction and Building Materials*, *22*(3), 222-227.

Walker, P.J. (1995). Strength, durability and shrinkage characteristics of cement stabilised soil blocks. *Cement Concrete Composites*, *17*, 301–10.

ISSN: 0128-7680
Pertanika J. Sci. & Technol. **19 (1)**: 45 – 55 (2011)

Prediction of Water Table in an Alluvial Aquifer Using Modflow

Saleh A. Al-Hassoun[1] and Thamer Ahmed Mohammad[2*]
[1]Department of Civil Engineering, College of Engineering,
King Saud University, Riyadh 11421, Kingdom of Saudi Arabia
[2]Department of Civil Engineering, Faculty of Engineering,
Universiti Putra Malaysia, 43400 UPM, Serdang,
Selangor, Malaysia
[*]E-mail: thamer@eng.upm.edu.my

ABSTRACT

Groundwater is the main source of water in the Kingdom of Saudi Arabia (KSA). A larger part of groundwater is founded in alluvial (unconfined) aquifers. Prediction of water table elevations in unconfined aquifers is very useful in water resources planning and management. During the last two decades, many aquifers in different regions of the KSA experienced significant groundwater decline. The declines in these aquifers raised concerns over the quantity and quality of groundwater, as well as concerns over the planning and management policies used in KSA. The main objective of this study was to predict water table fluctuations and to estimate the annual change in water table at an alluvial aquifer at wadi Hada Al Sham near Makkah, KSA. The methodology was achieved using numerical groundwater model (MODFLOW). The model was calibrated and then used to predict water table elevations due to pumping for a period of 5 years. The output of the model was found to be in agreement with the previous records. Moreover, the simulation results also show reasonable declination of water table elevations in the study area during the study period.

Keywords: Water table, elevations, alluvial aquifer, prediction, validation

INTRODUCTION

Groundwater constitutes the most important natural water resource in the Kingdom of Saudi Arabia. It exists in two different types of formation. The first type is deep confined aquifer that exists throughout the two thirds of the eastern part of the country. These aquifers contain huge amounts of water. The second type is shallow unconfined aquifer. This type is scattered throughout the country and it is mainly found under wadis. They are normally unconsolidated and of limited thickness. Meanwhile, alluvial (unconfined) aquifers have been developed in the country for hundreds of years to sustain agriculture before drilling of wells in the vast confined aquifers which was started only in the last few decades. These supply substantial amounts of water to agricultural areas that are located around many wadis in the Kingdom. Groundwater flow and water table fluctuations in the alluvial aquifer can be numerically simulated if adequate hydrologic and geologic data are available. These models and concepts, on which they are based on, are well-accepted by researchers and engineers dealing with groundwater flow.

A simulation of groundwater flow that takes into consideration the parameters and properties variability of aquifer is only possible through mathematical modelling. Most models that are usually employed to simulate groundwater flow are based on the Partial Differential Equation (PDE) which can be solved numerically through Finite Difference (FD) or Finite Element (FE) techniques. These methods discreet the time and flow domains, and require computing the hydraulic head in each cell

Received: 13 July 2009
Accepted: 27 April 2010
[*]Corresponding Author

by dividing the stress periods into smaller time steps. Several studies with the use of the FD and FE methods have been carried out by many researchers (Wang and Chunmaio, 1998; Bakker, 1999; Gupta *et al*., 1984; Mazzia and Putti, 2002).

The development of high speed computers may ease solving the PDE in groundwater modelling using numerically-based models such as MODFLOW. MODFLOW is a fully-distributed three dimensional groundwater model which uses a block-centred approach and a modular structure consisting of a main program and a series of subroutines that are grouped into packages (McDonald and Harbaugh, 1988). MODFLOW has been updated and it comprises different refinements such as the revised version in 1996 (Harbaugh and McDonald, 1996).

MODFLOW is widely used to either predict groundwater flow or head fluctuations (Pulido-Velazquez *et al*., 2007) or to verify other groundwater simulation methods, such as spreadsheet simulation model (Karahan and Ayvaz, 2005). Due to its capability, MODFLOW is widely used to simulate different types of groundwater problems in different geographical regions, such as the arid, semi-arid and tropical areas. It is a well known model in the field of groundwater. In this study, MODFLOW was applied to simulate the fluctuation in water table at the semi-arid region. This is considered as an example to present the capability of the model.

MODFLOW has been used in groundwater simulation and management scenario analysis in Jordan (Al-Kharabsheh, 2000), simulation and well field operation in discontinuous layers in Kuwait (Szekely *et al*., 2000), investigation of possible alternatives for effective groundwater management in eastern Saudi Arabia (Rasheeduddin *et al*., 2001), simulation and modelling of groundwater in multilayer aquifer system in the valley (wadi) area of south-west Egypt (Ebraheem, 2002), and the prediction of the effect of irrigation and water abstractions on the piezometric levels in the Murzuq aquifer in the south-west of Libya (Shaki and Adeloye, 2007).

STUDY AREA AND CHARACTERISTICS OF AQUIFER

The application of the groundwater model was done on the unconfined aquifer underneath wadi Hada Al Sham, which is located in north Makkah, Saudi Arabia. The study area is located between the longitudes of 39° 40' and 40° 15' in the east and the latitudes of 21° 45' and 22° 10' in the north, as shown on the location map in *Fig. 1*. Wadi Hada Al Sham flows into wadi Usfan that runs in the east-west direction having its outlet towards the Red Sea at a distance of 105km in the north of Jeddah. It consists of Wadis sub-basins Madrakah, Zabyah, Hishash, and Wadi Al Lusub. The area is bound by Wadi Khulays in the north and Wadi Fatimah in the south.

Agriculture is the main activity in the region, particularly private farms. The main source of water in the area is the groundwater from aquifers. Many wells of different types and diameters are used and most of them are exploiting the unconfined (alluvial) aquifer.

The study area is a part of the Western Arabian Shield which comprises complex of metamorphic and plutonic rocks. The central part of the area consists of sedimentary rocks of Tertiary age which are overlain by basaltic lava flows. The sedimentary rocks cover about 50% of the total surface area. Cretaceous Hada Al Sham formation is composed of sandstone, siltstone, and alluvial deposits. According to Kotb *et al*. (1983), the upstream area of the valley has deposits of layers of pebbles and coarse sand. It gradually changes to silt and clayey silt at the downstream. The thickness of the alluvium deposit in the middle portion varies in the range of 35 to 75 m.

The region of the study area is presumed as an arid basin with a low precipitation of about 100-300 mm annually. The meteorological data (mainly rainfall) were measured and collected by the Ministry of Water (MoW) from seven stations covering the region of the study area. There are two stations located with the basin of the study area. The potential evapotranspiration is at its maximum in July, i.e. around 300 mm. It decreases to 130 mm in December and January.

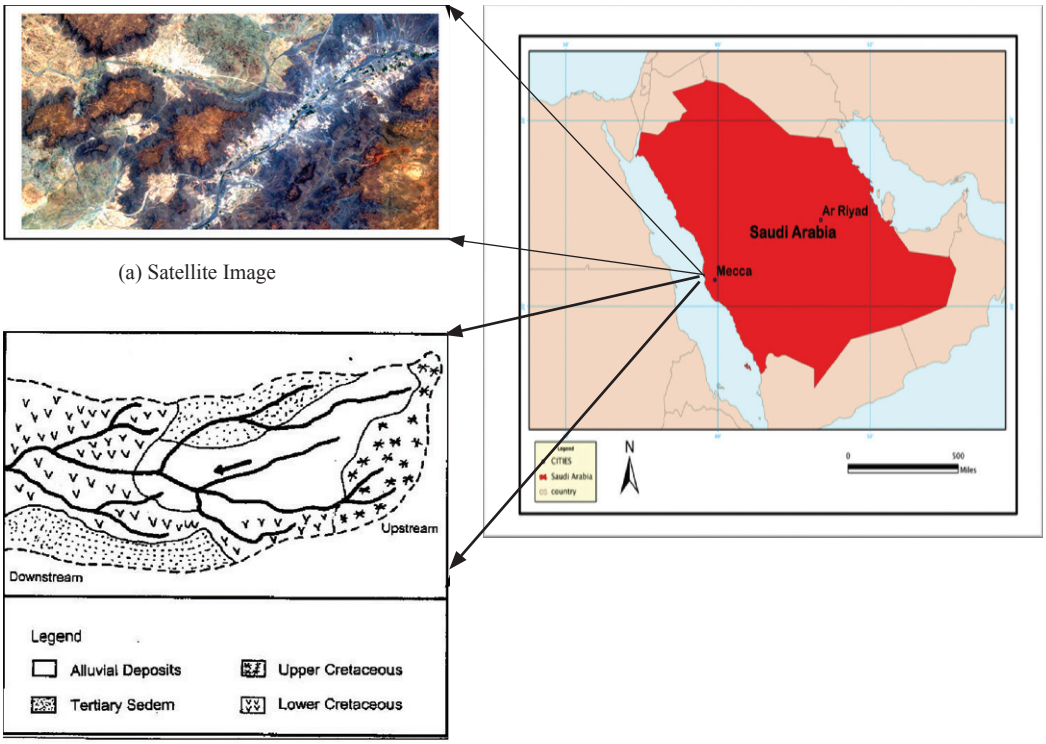

(a) Satellite Image

(b) Geo-Topographic Map

Fig. 1: Map showing the location of Wadi Hada Al-Sham Aquifer

Groundwater occurs in the area within two geological units, namely the alluvial deposits of the wadi system and the classic members of Cretaceous-Tertiary sedimentary succession (Hussien *et al*., 1993).

In this study, the application of MODFLOW was only done for the alluvial (unconfined) aquifer. The aquifer properties were investigated by MoW and found to be (on average), as follows:

- The effective porosity (Φ)= 0.18
- The vertical hydraulic conductivity (k) = 0.56 m/day
- The aquifer transmissivity (T) = 212 m^2/day
- The specific yield (S_y) = 0.15
- The average thickness of the aquifer (b) = 380 m

MODELLING SETUP

The numerical finite-difference model (MODFLOW) was used to simulate groundwater flow with initial and boundary conditions. The input data for the simulation model may be classified as spatial and temporal. The spatial input includes aquifer characteristics, such as water levels, boundaries, hydraulic conductivity, storage coefficient, location of wells, recharge area, drainage area, etc., whereas the temporal input includes time dependent data. The period of simulation is divided into a series of "stress periods" within which specified stress calculates an overall water budget and controls model output according to user's specification.

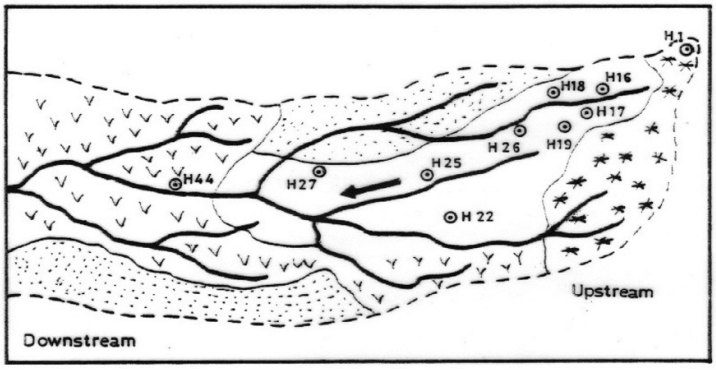

(a) Location of wells before converting the area to grids

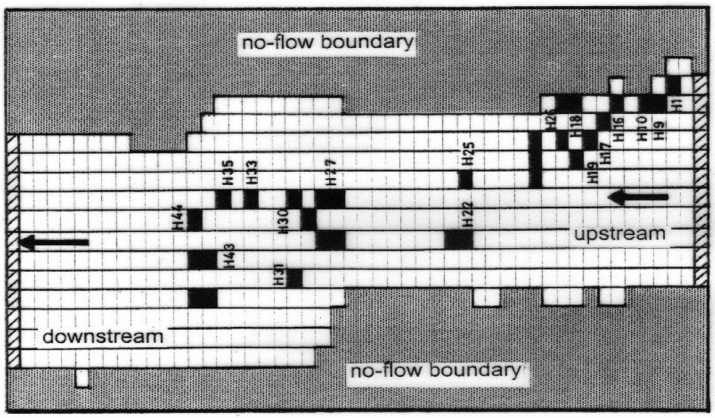

(b) Location of wells after converting the area to grids

Fig. 2: The location of the wells

The modelled area is replaced by a set of discrete nodes in a grid pattern covering the modelled area. The grid consists of 50 rows and 20 columns (1000 cell) overlaying on the (50 x 30 km) or 1500 km^2 study area, as shown in *Fig. 2a*. The model area is divided into cells, with each consisting of 1.0 x 1.5 km (see *Fig. 2b*). The necessary data for each cell were entered, i.e. top and bottom of the aquifer, hydraulic conductivity, specific yield coefficient, and porosity of the formation, etc.

The initial (i.e. at the beginning of the simulation) water table levels, obtained from the observation wells in the study area, were used to retrieve the initial water level contour map, as shown in *Fig. 3*. Meanwhile, the discharge pumping rates from the 18 wells in the area are presented in Table 1.

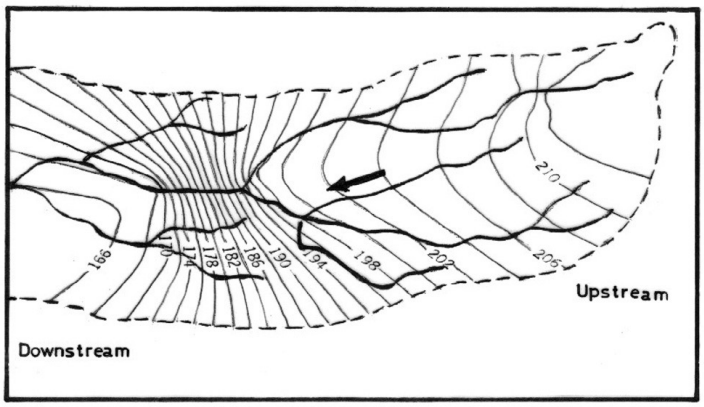

(a) Observed

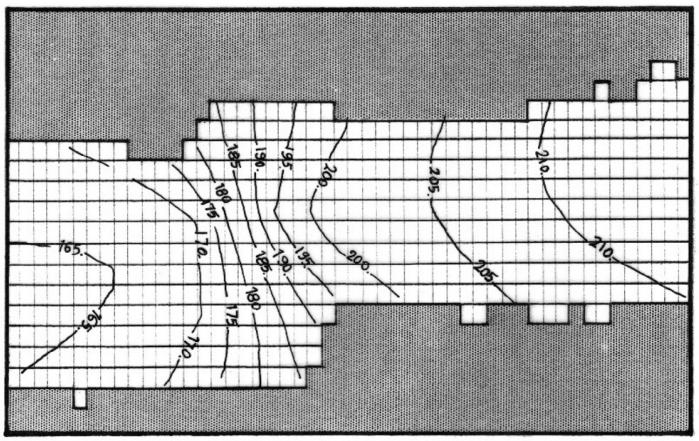

(b) Simulated

Fig. 3: The initial observed and simulated water table contours (in m)

TABLE 1

The pumping rates from the different wells

Well no. (H-)	1	7	8	9	10	16	17	18	19	22	26	27	30	31	33	35	43	44
Q (m^3/ day)	280	420	400	370	380	400	450	420	400	350	430	450	500	510	470	400	450	510

These values were included in the model to predict the water table elevations in the aquifer. On the other hand, the recharge to the aquifer in the area was estimated as 0.41 mm/day or 0.00041 m/day, reflecting the annual average infiltration depth due to the flow in the wadi.

Meanwhile, the boundary conditions used in the model simulation and calibration include the upstream and downstream of the wadi that were assumed to be constant head boundary, where head fluctuation is minor. The upstream inflow was estimated as 300 m^3/day, and this was 200 m^3/day for the downstream outflow. The banks of the wadi are assumed as no-flow boundary. These boundaries are displayed in *Fig. 2*.

The simulation of the model was started in 1998 and ended in 2003, with a stress period of 5 years (1825 days). The time step that was used in both calibration and simulation was set as one day.

MODEL CALIBRATION

The calibration of a groundwater model can be defined as a trial and error procedure which is done by matching the computed groundwater potentials from the simulation with the observed potentials in the field. The process is completely based on the availability of historical field data of water level in the aquifer. The calibration was done for the adjustment of the aquifer parameters. These parameters are initially imperfectly known and there is usually a certain range of possible values for them that may be valid. The model is said to be calibrated when the difference between the computed and observed potentials is less than a certain specified value.

Once the field has been discretized, the model grids must be initialized. This involves assigning the starting values of the hydraulic parameters and specific yield. The initial value of the hydraulic conductivity was 0.56 m/day, while the specific yield was 0.15. The other data that are necessary for the MODFLOW calibration process are aquifer type (in the case of the present study, it is unconfined), initial water levels, top and bottom elevations, porosity and other aquifer properties and temporal data (discharge rates and general boundary head).

The model was run with a steady state calibration for the study area, with a one day simulation period. The values of the hydraulic conductivity, i.e. K, were chosen in the range from 0.10 up to 1.0 m/day. A comparison of the water level contour maps, using different values of K, was then performed until it was found from the trials that the K value of 0.60 m/day had produced the best matching between observed (*Fig. 3a*) and calibrated water level contours map. This map was achieved as shown in *Fig. 3b*.

RESULTS OF THE MODEL SIMULATION

Water Level Contour Maps

The groundwater flow model MODFLOW was used, with calibrated parameters, to predict and map water table contours of the study area after different durations (1, 2, 3, 4, and 5 years), as respectively shown in *Figs. 4* through *8*. The predicted water table levels were found with a reasonable distribution in the area. Meanwhile, a continuous declination in water table levels can be attributed to the continuous extraction of water from the aquifer through different wells in the study area. However, there are small differences in the contour lines from year to year which indicate that the groundwater storage in the area is huge and the impact of exploitation (by pumping wells) is not significant. A comparison between the observed and predicted water table elevations for the study area was also conducted. It was found that the absolute error between the observed and MODFLOW could predict the ranges from 0 to 6 m, as shown in Table 2.

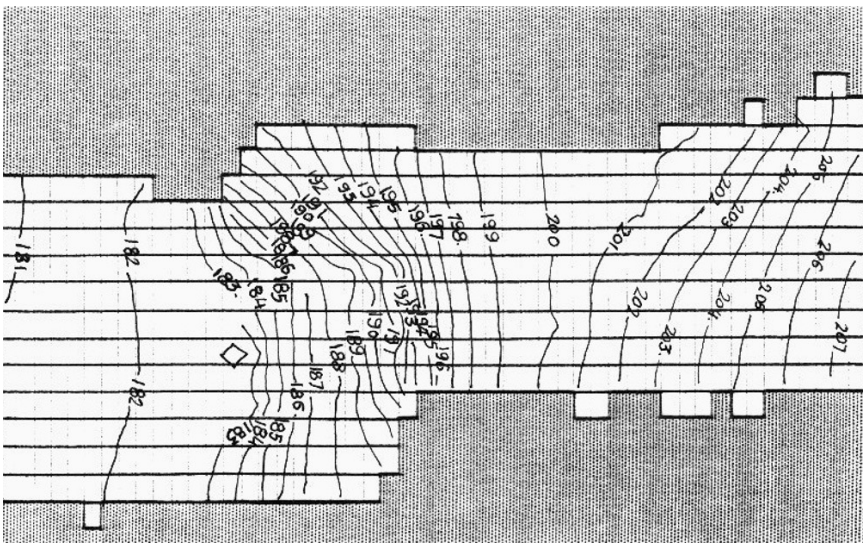

Fig. 4: The predicted water table contours (in m) at the end of Year 1

TABLE 2
Observed and predicted water table elevations for the study area

Distance form down stream border (km)	Observed water table elevation (m)	Predicted water table elevation (m)	Absolute error (m)
8	210	210	0
14	205	205	0
18	202	200	2
21	194	195	1
28	185	186	1
31	176	170	6
39	165	166	1

Well Water Levels

As shown in *Fig. 2*, there are many wells located in the study area. The water table in the selected wells at the study area was predicted. Table 3 and *Fig. 9* show the model output for the 5-year period.

The results show the declining levels of the water table in most wells. Pumping from the wells has been found to produce drawdown in the aquifer. However, the decline in the water levels is not significant, suggesting that the groundwater storage at the area is very large as compared to the discharge pumped from the wells (low use to yield ratio).

TABLE 3
Simulated water table in the wells (m)

Well year	H-1	H-16	H-17	H-18	H-19	H-22	H-25	H-26	H-27	H-44
1	203.73	204.30	204.02	203.31	203.43	202.05	198.99	203.31	191.75	193.80
2	201.92	202.55	202.33	201.71	201.84	200.67	197.11	201.50	191.22	191.99
3	201.36	202.01	201.81	201.21	201.34	200.24	196.59	200.94	191.12	191.53
4	201.19	201.83	201.64	201.05	201.18	200.10	196.43	200.76	191.10	191.39
5	201.11	201.76	201.57	200.98	201.11	200.04	196.37	200.69	191.09	191.33

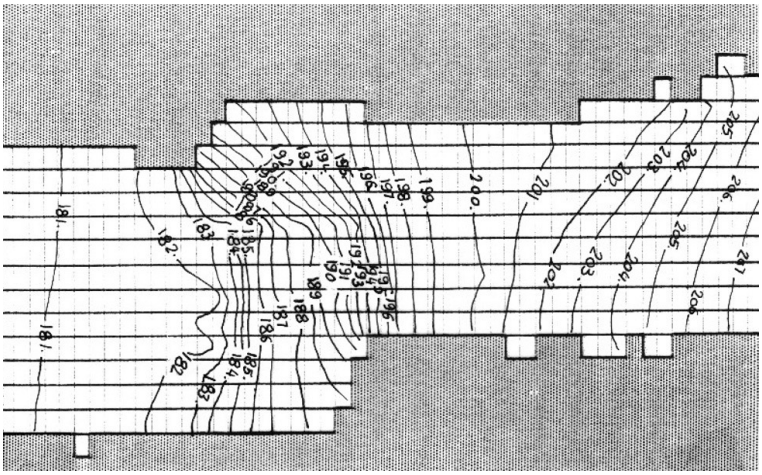

Fig. 5: The predicted water table contours (in m) at the end of Year 2

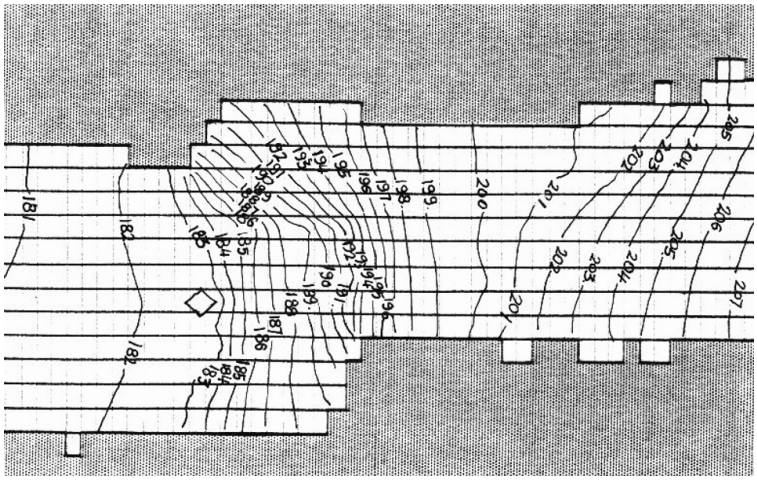

Fig. 6: The predicted water table contours (in m) at the end of Year 3

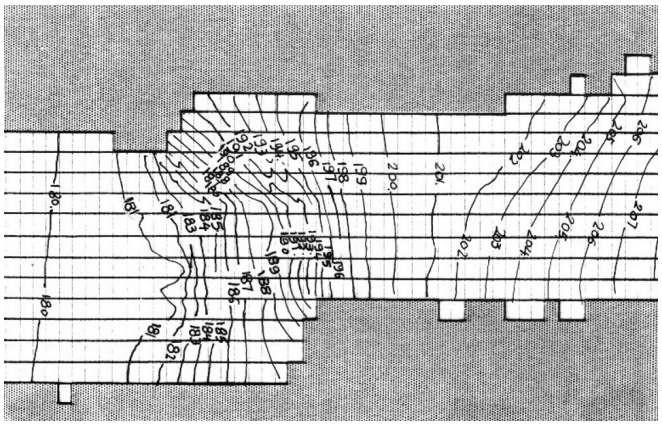

Fig. 7: The predicted water table contours (in m) at the end of Year 4

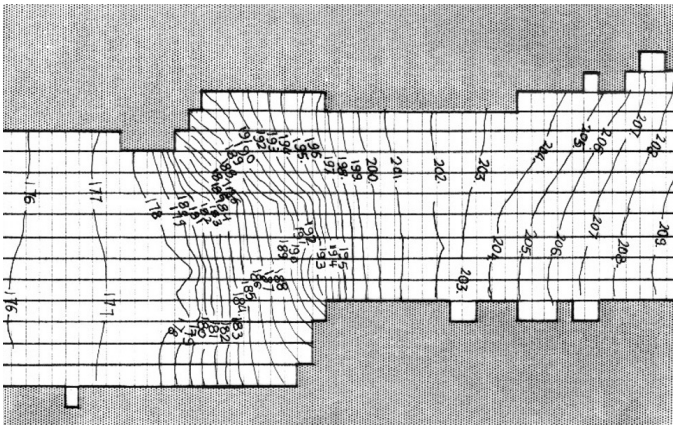

Fig. 8: The predicted water table contours (in m) at the end of Year 5

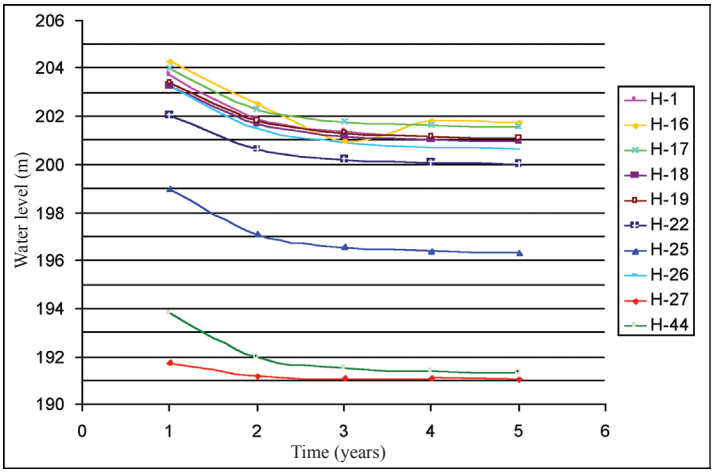

Fig. 9: The simulated water levels in different wells

CONCLUSIONS

The groundwater model MODFLOW was performed to predict the water table in alluvial aquifer located in the Kingdom of Saudi Arabia known as Hada Al Sham region. Based on the findings of the present study, the following conclusions can be drawn:

1. MODFLOW can successfully simulate the elevations of water table for an alluvial aquifer in the semi-arid region with reasonable accuracy.
2. Model calibration indicates that the predicted hydraulic conductivity of the aquifer is 0.60 m/day, which is not radically different from the observed one, i.e. given as 0.56 m/day.
3. The absolute errors between the observed and predicted water table elevations were found to be between 0 – 6 m.
4. Model simulation results for a period of 5 years confirm the low use to yield ratio for the studied aquifer (Hada Al Sham).
5. The simulated maps for 5 years water table counters confirm the abundant groundwater storage in the studied area and the possibility of digging more well without any serious impact on the storage. This can be attributed to the minor changes in the elevations of water table at the study area.

REFERENCES

Al-Kharabsheh, A. (2000). Groundwater modelling and long-term management of the Azraq Basin as an example of Arid area conditions (Jordan). *Journal of Arid Environments*, *44*, 143-153.

Bakker, M. (1999). Simulating roundwater flow in multi-aquifer systems with analytical and numerical Dupuit-Models. *Journal of Hydrology*, *222*(1-4), 55-64.

Ebraheem, A.M. (2002). A groundwater flow model for the new valley area with a telescoping mesh on Kharga Oasis, Western Desert of Egypt. *Proceedings of the International Conference on Water Resources Management*, Arid Regions, Kuwait, 23-27.

Gupta, S.K., Cole, C.R. and Pinder, G.F. (1984). A Finite Element Three-Dimensional Groundwater (FE3DGW) Model for a Multi-aquifer System. *Journal of Water Resources Research*, *20*(5), 553-63.

Harbaugh, A.W. and McDonald, M.G. (1996). "Programmer's Documentations for MODFLOW-96: An Update to the US Geological Survey Modular Finite-Difference Groundwater Flow Model", US Geological Survey Open-File.

Hussein, M.T., Bazuhair, A. and Al-Yamani, M.S.T. (1993). Groundwater availability in the Khulais Plain, Western Saudi Arabia. *Journal of Hydrological Sciences*, *38*(3), 203-213.

Karahan, H. and Ayvaz, M.T. (2005). Transient groundwater modelling using spreadsheets. *Journal of Advances in Engineering Software*, *36*, 374-384.

Kotb, H., Hakimm, H. and Zaidi, S. (1983). A geochemical and geophysical investigation of groundwater in Wadi Fatimah. *Bulletin of Faculty of Earth Sci*ence, *5*, 135-152. K.A.U., Saudi Arabia,

Mazzia, A. and Putti, M. (2002). Mixed-finite element and finite volume discretization for heavy brine simulations in groundwater. *Journal of Computer and Applied Mathematics*, *147*(1), 191-213.

McDonal, M.G. and Harbaugh, A.W. (1988). A Modular Three-Dimensional Finite – Difference Groundwater Flow Model" Report Book 6, Chapter A1. USGS, Denver, CO, USA.

Pulido-Velazquez, D. A., Sahuquillo, J. A. and Pulido- Velazques, M. (2007). A general methodology to simulate groundwater flow of unconfined aquifers with a reduced computational cost. *Journal of Hydrology*, *338*, 42-56.

Rasheeduddin, M., Abderrahman, W.A. and Lloyd, J.W. (2001). Management of groundwater resources in Eastern Saudi Arabia. *Journal of Water Resources Development*, *17*(2), 185-210.

Shaki, A.A. and Adeloye, A.J. (2007). Mathematical modelling of effects of Irawan Irrigation Project Water Abstractions on the Murzuq Aquifer Systems in Libya. *Journal of Arid Environment*, *71*, 133-156.

Szekely, F., Senay, Y., Al-Rashed, M., Al-Sumait, A. and Al-Awadi, E. (2000). Computer simulation of the hydraulic impact of water well fields in Kuwait. *Journal of Hydrology*, *235*, 205-220.

Wang, P.P. and Chunmaio, Z. (1998). An efficient approach for successively perturbated groundwater models. *Journal of Advances in Water Resources*, *21*(6), 499-508.

ISSN: 0128-7680
Pertanika J. Sci. & Technol. **19 (1)**: 57 – 66 (2011)

Optimization of Polymerase Chain Reaction (PCR) of Mitochondrial Cytochrome c Oxidase I (COI) Gene in Two Bornean Fanged Frogs

Ramlah Zainudin* **and Dency Flenny Ak Augustine Gawin**
Department of Zoology,
Faculty of Resource Science and Technology,
University Malaysia Sarawak,
94300 Kota Samarahan, Sarawak, Malaysia
**E-mail: zramlah@frst.unimas.my*

ABSTRACT

Limnonectes kuhlii and *Limnonectes leporinus* are two of the Bornean fanged frogs (without advertisement call) which are widely distributed, thus thought to exhibit different evolutionary lineages and the existence of genetically cryptic species. Yet, the two species are still under study especially at the molecular level. Hence, cytochrome c oxidase I (COI) of mitochondrial gene was used to investigate suitable parameters for DNA amplification using the Polymerase Chain Reaction (PCR) method. Three PCR programmes (varied in the temperatures and period of each PCR step) were employed to identify the most efficient parameters in amplifying PCR products for both species. From the three programmes, Programme B (Initial denaturation: 96°C for 5 min; denaturation: 95°C for 45 sec; annealing: 48-53°C for 1 min 30 sec; extension: 72°C for 1 min 30 sec; final extension: 72°C for 10 min, 30 cycles) showed the highest percentage (53%) of optimal PCR products. The other two programmes showed non-specific products or "primer-dimers". The results also suggest that the annealing temperature of 52°C, 0.025-0.05 units/µl of 1.5mM *Taq* polymerase, 0.04 mM of dNTPs mix and optimal concentrations of magnesium in 50 µl of reaction mixture were sufficient enough to amplify high quality PCR products for both species. However, using Programme B, the re-amplification of the PCR products yielded "primer-dimer". In addition, a 'Hot-Start' PCR method was also applied and mostly yielded in an optimal PCR amplification. Nevertheless, further research on the second amplification of the two species should be conducted to determine the causes of the primer-dimer production.

Keywords: **Polymerase Chain Reaction (PCR) conditions, optimization, annealing temperature, Hot-Start PCR**

INTRODUCTION

Bornean fanged frogs, categorized under the sub-genus *Limnonectes* in the family of Ranidae (Dubois, 1992; Emerson and Ward, 1998; Frost *et al*., 2006) are divided into four species, namely *Limnonectes leporinus*, *L. ingeri*, *L. kuhlii*, and *L. ibanorum* (Inger, 1996; Emerson and Inger 1992; Dubois, 1992; Frost *et al*., 2006). Most of the *Limnonectes* species (except for *L. kuhlii*) are grouped in the *grunniens* (Emerson and Ward, 1998), and consist all the putative species which are difficult to identify due to the high similarity in their external morphology. Hence, there is confusion in taxonomically categorizing the species and its systematic relationship using the conventional methods (Emerson and Ward, 1998). With the revolution of the molecular techniques, the studies on the phylogenetic and taxonomy of the Bornean fanged frogs can be applied as an alternative method (Avise, 1994; Duellman and Trueb, 1994).

Received: 1 October 2009
Accepted: 21 December 2009
*Corresponding Author

One of the steps which are essential in any molecular technique is the polymerase chain reaction (PCR) amplification (Mullis, 1990; Mullis and Faloona, 1987). Polymerase chain reaction (PCR) is a technique which is used to amplify the number of copies of a specific region of DNA to produce enough DNA to be adequately tested (Mullis and Faloona, 1987). Basically, it works on two designated and oriented primers; anneal complementary to the 'targeted' regions of the denatured DNA templates that are to be amplified and continued with primer extension (Mullis, 1990; Mullis and Faloona, 1987). The cycle of denaturation, annealing and extension is repeated, resulting in exponential copies of the targeted regions, approximately 2^n where n is the number of performed amplification cycles (Mullis, 1990; Mullis and Faloona, 1987). A PCR mixture reaction contains DNA template, primers, *Taq* polymerase, deoxynucleotide triphosphates mix (dATP, dCTP, dGTP, and dTTP), 10X reaction buffer that contains Tris-HCL (pH 7.5-9.0), KCl and additive(s) to increase the PCR reaction, and finally $MgCl_2$ (Erlich *et al*., 1991). Previous studies (Saiki, 1989; Erlich *et al*., 1991) showed that the components of PCR, as well as the PCR protocols such as temperature and duration of each step, could influence the yield of the PCR amplification.

The main objective of this study is to optimize the PCR amplification of *Limnonectes leporinus* and *Limnonectes kuhlii* by modifying the concentrations of certain components in the reaction mixtures, the annealing temperatures and duration of each phase of the COI primers.

MATERIALS AND METHODS

Samples Collection

Samples of *Limnonectes leporinus* and *Limnonectes kuhlii* were collected from Santubong (1°44'00.00"N 110°20'00.00"E), Matang Ranges including Matang Wildlife Center and Kubah National Park (1°36'44.61"N 110°11'38.47"E) and Bau District (1°21'05.45"N 110°14'16.81"E), which are in the Kuching Division. Muscle tissues were extracted from the hind legs of the captured frogs and these were then preserved in vials containing 20% DMSO, and 0.25M EDTA before they were kept in -20°C freezer.

PCR Analysis

Total genomic DNA was extracted following the protocols of Pure-Gene™ Tissue DNA Kit (BioSynTech, Subang Jaya). The extracted DNA was subsequently amplified using the Whatman Biometra® (050-551 T-*personal* 48). Two universal mitochondrial DNA primers, namely COI-f (forward) and COI-e (reverse) with the sequences of '5-CCTGCCGGAGGAGGTGAYCC-3'and '5-CCAGTAAATAACGGGAATCAGTG-3' (Palumbi *et al*., 1991), were used in the study. The optimization of the PCR amplification was done by varying the concentrations of Mg^{2+} and *Taq* DNA polymerase (Fermentas) (*see* Table 1), following Arnheim (1992). Three PCR programmes were designated for the optimization procedures (Table 2), following Emerson and Ward (1998) and Ramlah (1998). The amplification products were electrophorese to check for successful amplification products. Successful PCR products were excised from the gel (without purification) and re-amplified for the second PCR amplification (weight, per comm.).

TABLE 1
PCR reaction mix used for DNA amplification

PCR component	Volume in a 50 µl reaction mix, µl	Final concentration in a 50 µl reaction mix, mM except *Taq* in units/µl
10X PCR reaction buffer[a]	5	1X (10 mM of Tris-HCl; 50 mM KCl)
$MgCl_2$	2.0-4.0	1.0-2.0 mM
Deoxynucleotide triphosphates mix (dATP, dCTP, dGTP and dTTP)	1.0	0.04 mM of each dATP, dTTP, dCTP and dGTP
Taq polymerase	0.25-0.5	0.025-0.05 units /µl
Primer CO1-e	2.5	$7.56X10^{-3}$ mM
Primer CO1-f	2.5	$3.28X10^{-2}$ mM
DNA template	1-4	Variable[b]

[a]1 ml of 10X PCR Reaction Buffer contains 100mM Tris-HCl, 500 mM KCl, and 0.8% Nonidet P40.
[b]Depending on the concentration of the total genomic DNA extraction.
Note: Sterile distilled water was added for each PCR reaction mix to maximize the volume of 50 µl.

TABLE 2
Three PCR programmes with different sets of parameters, the number of reaction performed and cycling temperatures, following Emerson and Ward (1998) and Ramlah (1998)

PCR programme	Cycling temperature	
A	Denaturation: 94˚C for 30 sec Annealing: 43˚C for 30 sec Extension: 72˚C for 45 sec	5 cycles
	Denaturation: 94˚C for 30 sec Annealing: 45˚C for 30 sec Extension: 72˚C for 45 sec	25 cycles
	Storage: 4˚C for forever	
B	Initial denaturation: 96˚C for 5 min Denaturation: 95˚C for 45 sec Annealing: 48-53˚C for 1 min 30 sec Extension: 72˚C for 1 min 30 sec Final extension: 72˚C for 10 min	30 cycles
	Storage: 4˚C for forever	
C	Initial denaturation: 95˚C for 5 min Denaturation: 94˚C for 45 sec Annealing: 52˚C for 1 min 30 sec Extension: 72˚C for 1 min 30 sec Final extension: 72˚C for 10 min	30 cycles
	Storage: 4˚C for forever	

Note: Programmes A and C were tested on 2, and 52 PCR reactions, respectively. In Programme B, an amount of the PCR reactions in the bracket was prepared based on the respective annealing temperatures: 48˚C (2); 49˚C (2); 50˚C (3); 51˚C (17); 51.5˚C (33); 52˚C (78); 52.5˚C (5); and 53˚C (5).

The visualization step was repeated and the successful PCR product was then purified to remove any excess of reaction components. For the Hot-Start PCR, *Taq* polymerase was added into an uncompleted reaction mixture incubated in a thermal cycler at a temperature between 80°C- 82°C before entering the annealing stage of the first cycle.

The PCR results were calculated as the percentage of the total positive reaction products (positive results that consist either single or multiple bands and primer dimer) per total reaction samples. In addition, positive results were further divided into three categories of single band, multiple bands and primer dimer. Meanwhile, the percentage was calculated as the total products (single band/ multiple band or primer dimer) per total positive results. Only single band PCR products were considered to be successful.

RESULTS AND DISCUSSION

Cycling Parameter and Mg^{2+} Concentration

The results showed that the annealing temperatures between 48°C and 52°C (*Figs 1* and *2a,b*) were sufficient to produce PCR products (*see* Table 3). However, the 500bp PCR products produced the brightest band at 52°C (*Fig. 3*). Programme B was more preferable than Programme C due to the highest occurrence of primer–dimer products (69.1% out of 30.9 % of positive results) in the latter programme (*see* Table 4). The magnesium concentrations of 1.5 mM and 1.75 mM yielded good PCR products, either using the Programme B, or C with an annealing temperatures ranging from 51°C to 52°C (*Fig. 3*). The result is consistent with the cycling parameter and Mg concentration used by Ramlah (1998: 2009) in producing good PCR products.

TABLE 3

Overall results of PCR products in three various programmes; A, B and C

No. of PCR reaction	Program (Annealing temperatures, °C)	Positive result (%)	Negative result (%)
2	A (43-45˚C)	-	100
132[a]	B (48-53˚C)	53.3	44.7
52	C (52.0˚C)	33.9	66.6

[a]refer to the note listed under Table 2

TABLE 4

Detail results of PCR products using Programmes B and C (with annealing temperature of 51-52°C)

No. of reaction samples	PCR programme	Parameter (°C)	Obtained results in %				
			Positive results	Single band		Multiple bands	Primer-dimer
				Good	Poor		
15	B	51.0	60.0	-	20.0	40.0	40.0
30		51.5	73.3	-	20.0	53.3	26.7
72		52.0	59.7	26.4	29.2	4.1	40.3
55	C	52.0	30.9	23.6	7.3	-	69.1

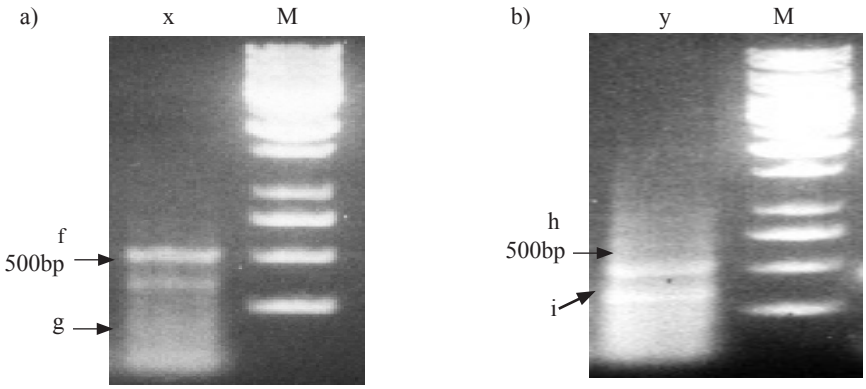

Fig.1: PCR products (bands f and h) and truncated products (bands g and i) of L. leporinus *of Matang obtained at annealing temperatures of 49˚C (lane x) and 48˚C (lane y). The PCR products in lane y were the least purified as compared to lane x. M= 1kb Ladder (Fermentas)*

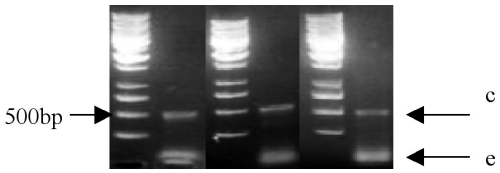

(a) Annealing temperature

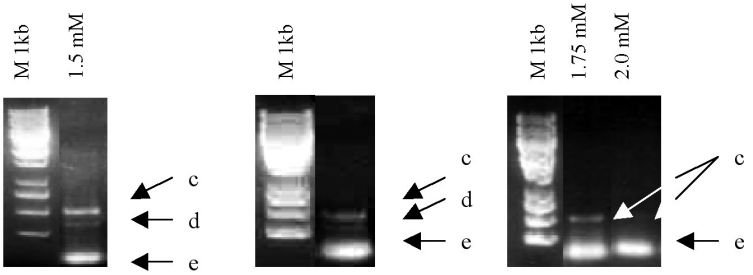

(b) [Mg^{2+}]

Fig. 2: (a) Reaction mixtures of Limnonectes leporinus *from Bau contained 0.025 units/µl Taq polymerase, 10 mM Tris HCl, 50 mM KCl, 0.04 mM dNTPs, 1.5 mM Mg^{2+}, and 3µl template. Amplification used Programme B with annealing temperature ranging from 51˚C to 52˚C. (b) Reaction mixtures were prepared as in (a) except with a variation in Mg^{2+} concentrations from 1.5 mM (o), 1.5mM with HS (p), 1.75mM (r) to 2.0 mM (s). Amplification was at 52˚C (H. S. = Hot-Start PCR). Bands c were first amplification products and Bands d were non-specific products. Bands e were primer-dimers. M= 1kb Ladder (Fermentas)*

Enzyme Concentration and Hot-Start PCR

An amount of 0.025 units/µl of *Taq* successfully amplified eight PCR products of *L. kuhlii* from the Santubong area (*Fig. 3*). However, poor products were mostly produced when it was tried on *L. leporinus* (*Fig. 4*). The optimization of *Taq* polymerase concentrations, ranging from 0.035 units/µl to 0.05 units/µl, successfully produced PCR products (*Fig. 4*) at the 0.025 units/µl. This is consistent with the result obtained by Ramlah (2009) when the same concentration of *Taq polymerase* used was found to produce good PCR products of the *Hylarana* frog. Additionally, the Hot-Start PCR produced far better results than the conventional PCR method (see *Fig. 4*).

PCR Cycle Profile and Hot-start Method

The success of the PCR amplification in generating clean products is determined by the PCR cycling system. Temperature and duration time for each step in a PCR profile must be perfectly suitable to initiate the amplification processes. Some previous studies showed that the success of amplification was determined by the annealing temperature which ranged between 50°C to 72°C (Ramlah, 1998; Ramlah, 2009; Roux, 1995; Innis and Gelfand, 1990). Hoelzel and Green (1992) reported that annealing temperature is influenced by the sequence and length of the primers used and the targeted DNA. In this study, the amplified products were detected at the annealing temperature above 48°C (*Figs. 2* and *3*) although they were contaminated with background smear and non–specific products. The emergence of the unwanted or false products was due to mis-incorporation between the primer(s) and template, or mis-extension of incorrect nucleotides at the 3' end of the primer(s) (Innis and Gelfand, 1990; Kidd and Ruano, 1995).

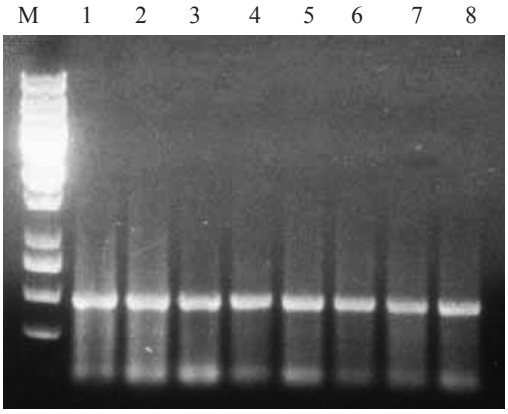

Fig. 3: PCR products of Limnonectes kuhlii *of Santubong from the first successful amplifications using programme B (52˚C). The reaction mixtures were 10 mM Tris-HCl; 50 mM KCl, 1.5 mM Mg^{2+}, 0.025 units/µl Taq and 3.5 µl of template. M= 1kb Ladder (Fermentas)*

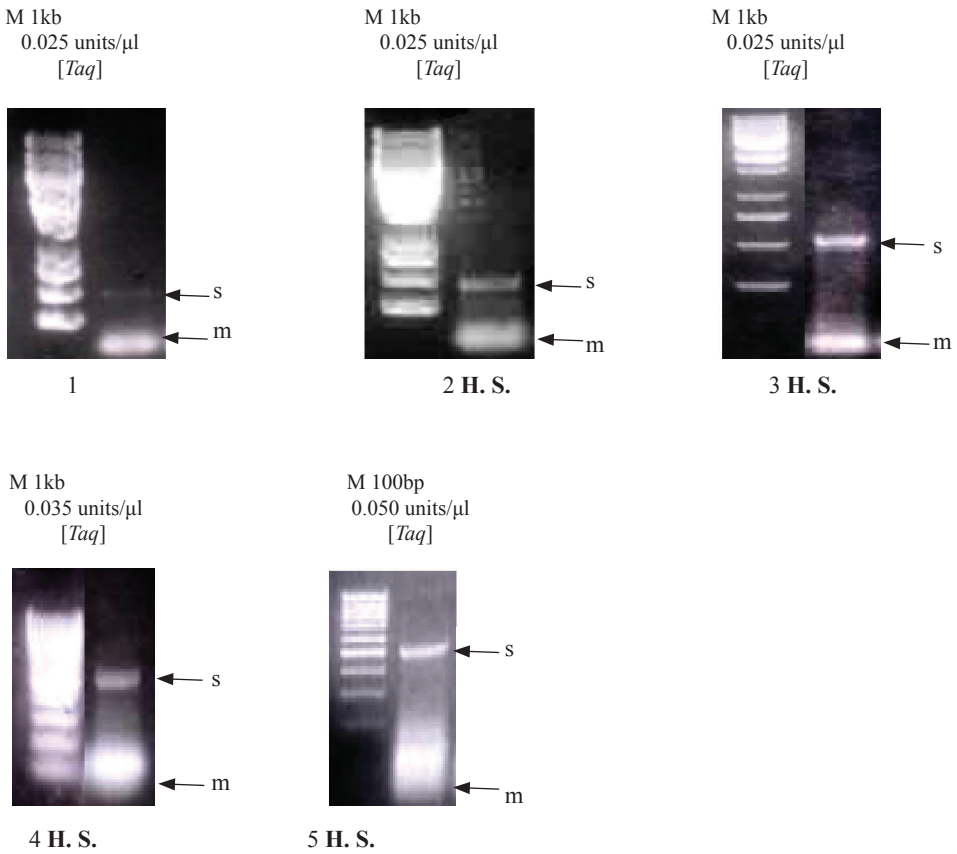

Fig. 4: The reaction mixtures of Limnonectes leporinus *samples taken from Bau were prepared as in Fig. 3, with a range of enzyme variations from 0.025-0.050 units/µl and concentrations of template (s= 500 bp PCR products; m= primer-dimer; Lanes 1, 2 and 4= First amplification products; Lanes 3 and 5= Second amplification products; H.S.= Hot-Start PCR). The template volumes of 3.5 µl, 3.0 µl, 1.0 µl, 4.0 µl, and 2.0 µl were pipetted respectively in the reaction mixtures of lanes 1, 2, 3, 4, and 5. M= Gene Ladder (Fermentas)*

When, the temperature was increased to 52°C, no production of spurious products was observed (*Fig. 3a*). In addition, the duration of annealing time within a range of 30 sec to 2 min could avoid the disturbances of the secondary structure in the template and the concentration of primer(s) although other study showed that shorter time was sufficient for hybridization (Hoelzel and Green, 1992). Hence, the duration of 1 min and 30 sec was sufficient to permit all the primers to bind to the target regions.

The denaturation step can influence the PCR amplification as incomplete separation of the targeted template and/or amplified products in initial denaturation, and further cycles will cause a formation of "primer-dimer", while an amplified double-stranded fragment was short in length, i.e. roughly 50bp. Therefore, both Programmes B and C had 5 min initial denaturation before the first cycle was begun. Preference of Programme B than C may be due to the longer strands, and/or the target region of the COI gene of those two species which are rich in G+C bases (Kidd and Ruano,

1995). The temperature and period of denaturation in Programme B was not too high and too long, respectively, for a *Taq* polymerase to degrade quickly as it has a half-life activity of about 5-6 min (Gelfand and White, 1990). The extension step, at 72°C for 45 sec, was seemingly sufficient to polymerize complementary all annealed temperatures.

The number of cycles may have an impact on the efficiency of the PCR amplification. Thirty cycles in the three programmes were proven to yield enough amplification products; however, some of them were very low in yield or contaminated, which were probably due to fewer cycles or excess in the initial DNA template in the sample reactions (Kidd and Ruano, 1995). For the re-amplified PCR products, substantial primer-dimers could be seen, which might be due to the emergence of a "plateau effect" after 20-25 cycles in the secondary amplification (Innis and Gelfand, 1990). Many factors, such as competition for reactants between primer-dimers and targeted products, re-annealing of targeted product at concentrations above 10^8 M, and insufficient denaturation of DNA at higher DNA concentration may contribute to the effect. Hence, it is essential to maintain the copied template at a lower concentration. The application of the Hot-Start PCR method (Roux, 1995; Brownie *et al.*, 1997) can halt the non-specific hybridization of primer and template by mixing the reaction mixture together at a temperature above the annealing temperature. The substitute method has been proven to be efficient in producing outstanding results in most sample reactions in this study.

Optimization of the Buffer Components

Generally, the concentration of $MgCl_2$, *Taq* polymerase and template DNA can influence the specificity, and efficiency of the PCR amplification (Saiki, 1989). According to Kidd and Ruano (1995), too much magnesium will initiate spurious binding of primer(s) to incorrect template region that will lead to an accumulation of undesired products, while too little will disturb the extension reaction, and lead to amplified products reduction. Gelfand (1989) and Chamberlain and Chamberlain (1994) reported that the exact requirement of the ionic concentration was dependent on the concentration of dNTPs. As for the *Taq* concentration, a range within 0.025-0.050 units/µl can seemingly be used; however, it depends on the initial template or/and copied template concentration in the PCR reaction buffer. Too much template could inhibit the amplification although a maximum amount of 0.050 units/µl of the enzyme had been used. In other cases, an amount of 0.035 units/µl of *Taq* had been tried, but the outcomes were non-specific products (*Fig. 4*). In this experiment, the amount of 0.050 units/µl produced desired products in some sample reactions. It is assumed that the DNA template is not the only main factor for the amplification of non-specifics products, as it may also be due to the primer itself (Innis and Gelfand, 1990), or the concentration of magnesium (Viguera *et al*., 2001).

Additionally, storage buffer (20% DMSO) used for preserving frogs' muscle tissues might not be fully washed out from the DNA extraction and carried into the PCR reaction mixture, and this thus disturbed the activity of *Taq* to polymerize annealed primer(s). More than 10% of DMSO could lessen *Taq* activity by 50%, and thereby decreased the yield (Hoelzel and Green, 1992). Moreover, the addition of an additive, Nonidet P40 in PCR reaction buffer could reverse the DMSO effect. Previous experiments had proved that 5% of NP40 could increase the *Taq* activity (Hoelzel and Green, 1992).

CONCLUSIONS

PCR parameters and cycling temperatures of initial denaturation: 96°C for 5 min; denaturation: 95°C for 45 sec; annealing: 48-53°C for 1 min 30 sec; extension: 72°C for 1 min 30 sec; final extension: 72°C for 10 min, 30 cycles) were adequate to produce optimal PCR products. The results also suggest that the annealing temperatures of 52°C, 0.025-0.05 units/µl of 1.5mM *Taq* polymerase, 0.04 mM of dNTPs mix and optimal concentrations of magnesium in 50 µl of reaction mixture were sufficient to amplify high quality of PCR products for both species. Moreover, the Hot-Start PCR was found to be effective in yielding intended PCR products.

ACKNOWLEDGEMENTS

This research was supported by Universiti Malaysia Sarawak through its Research Foundation Grant 270/2002 (08). The researchers wish to thank all the staff of the Faculty of Resource Science and Technology for their invaluable information and advice.

REFERENCES

Arnheim, N. (1994). Polymerase chain reaction strategy. *Annual Review of Biochemistry*, *61*(XIV+1359P), 131-156.

Avise, J. C. (1994). *Molecular Markers, Natural History and Evolution*. New York: Chapman and Hall.

Brownie, J., Shawcross, S., Theaker, J., Whitcombe, D., Ferrie, R., Newton, C. and Little, S. (1997). The elimination of primer-dimer accumulation in PCR. *Nucleic Acids Research*, *25*(16), 3235-3241.

Chamberlain, J. S. and Chamberlain, J. R. (1994). Optimization of multiple PCRs. In K. B. Mullis, F. Ferre and R.A. Gibbs (Eds.), *The polymerase chain reaction* (pp. 38-46**)**. Boston: Birkhauser.

Duellman, W. E. and Trueb, L. (1994). *Biology of Amphibians*. USA: The John Hopkins University Press.

Dubois, A. (1992). Notes sur la classification des Ranidae (Amphibiens Anoures). *Bull.Mens. Soc. Linn. Lyone*, *61*, 305-352.

Erlich, H. A., Gelfand, D. and Sninsky, J. J. (1991). Recent advances in the polymerase chain reaction. *Science*, *252*(5013), 1643-1651.

Emerson, S. B. and Ward, R. Y. K. (1998). Male secondary sexual characteristics, sexual election, and molecular divergence in fanged ranid frogs of Southeast Asia. *Zoological Journal of the Linnean Society*, *122*, 537-553.

Emerson, S. B. and Inger, R. F. (1992). The comparative ecology of voiced and voiceless Bornean frogs. *Journal of Herpetology*, *26*(4), 482-490.

Frost, D. R., Grant, T., Faivovich, J., Bain, R.H., Haas, A., Haddad, C. F. B., De Sa R.O., Channing, A., Wilkinson, M., Donnellan, S.C., Raxworthy, C. J., Campbell, J. A., Blotto, B. L., Moler, P., Drewes, R. C., Nussbaum, R. A., Lynch, J. D., Green, D. M. and Wheeler, W. C. (2006). The amphibian tree of life. *Bulletin of the American Museum of Natural History*, *297*, 1-370.

Gelfand, D. H. (1989). *Taq* DNA polymerase. In H. A. Erlich (Ed.), *PCR technology* (pp. 17-22). New York: Stockthon Press.

Gelfand, D. H. and White, T J. (1990). Thermostable DNA polymerase. In H. A. Erlich (Ed.), *PCR technology* (pp. 129-141). New York: Stockthon Press.

Hoelzel, A. R. and Green, A. (1992). Analysis of population-level variation by sequencing PCR-amplified DNA. In A. R. Hoelzel (Ed.), *Molecular genetic analysis of populations: A pratical approach* (pp. 159-187). New York: Oxford University Press.

Inger, R. F. (1996). The systematics and zoogeography of the amphibian of Borneo. *Fieldiana Zoology*, *52*, 1-402.

Innis, M. A. and Gelfand, D. H. (1990). Optimization of PCRs. In M. A. Innis (Ed.), *PCR protocols: A guide to methods and applications* (pp. 3-12). New York: Academic Press Inc.

Kidd, K. K. and Ruano, G. (1995). Optimizing PCR. In M. J. McPherson, B. D. Hames and G. R. Taylor (Eds.), *PCR: A practical approach* (pp. 1-21). New York: Oxford University Press.

Mullis, K. (1990). The unusual origin of the polymerase chain reaction. *Scientific American*, *262*(4), 56-65.

Mullis, K.B. and Faloona, F.A. (1987). Specific synthesis of DNA *in vitro* by a polymerase catalysed chain reaction. *Methods in Enzymology*, *155*, 335-350.

Palumbi, S., Martin, A., Romano, S., McMillan, W.O., Stice, L. and Grabowski, G. (1991). *The Simple Fool's Guide To PCR (Version 2)*. Honolulu: Department of Zoology and Kewalo Laboratory, University of Hawaii.

Ramlah, Z. (1998). Microgeographic variation of mitochondrial DNA in populations of Sarawak riparian frogs. MSc thesis (Unpublished). University of Illinois at Chicago.

Ramlah, Z. (2009). Ecology and Molecular phylogenetics of Bornean frogs from the genus *Rana* Linnaeus 1758. PhD thesis (Unpublished). Universiti Kebangsaan Malaysia.

Roux, K. H. (1995). Optimization and troubleshooting in PCR. In C. W. Dieffenbach and G. S. Dveksler (Eds.) *PCR primer: A laboratory manual* (pp. 53-61). New York: Cold Spring Habor Laboratory Press.

Saiki, R. K. (1989). The design and optimization of the PCR. In H. A. Erlich (Ed.), *PCR technology* (pp. 7-16). New York: Stockthon Press.

Viguera, E., Canceill, D. and Ehrlich, S. D. (2001). *In vitro* replication slippage by DNA polymerase from thermophilic organisms. *Journal of Molecular Biology*, *312*, 323-333.

ISSN: 0128-7680
Pertanika J. Sci. & Technol. **19 (1)**: 67 – 76 (2011)

Effects of Image Processing Techniques on Mammographic Phantom Images: A Pilot Study

Mostafa Langarizadeh[1*], Rozi Mahmud[1], Abd. Rahman Ramli[2], Suhaimi Napis[3], Mohammad Reza Beikzadeh[4] and Wan Eny Zarina Wan Abdul Rahman[5]

[1]Faculty of Medicine and Health Sciences,
[2]Faculty of Engineering,
[3]Information and Communication Development Centre (iDEC),
Universiti Putra Malaysia,
43400 UPM, Serdang, Selangor, Malaysia
[4]MIMOS BHD, Malaysia
[5]Faculty of Mathematics and Quantitative Research, UiTM, Malaysia
[*]E-mail: langarizadeh2001@yahoo.com

ABSTRACT

Breast cancer is one of the most important diseases among females. According to the Malaysian Oncological Society (Wahid, 2007), about 4% of women who are 40 years old and above are suffering from breast cancer. Masses and microcalcifications are two important signs for breast cancer diagnosis on mammography. In this research, the effects of different image processing techniques which include enhancement, restoration, segmentation, and hybrid methods on phantom images were studied. Three different phantom images, which were obtained at 25kv (63.2 MAS), 28kv (29.8 MAS) and 35kv (9.5 MAS), were manipulated using image processing methods. The images were scored by two expert radiologists and the results were compared to explore any significant improvements. Meanwhile, the Wilcoxen Rank test was used to compare the quality of the manipulated images with the original one (alpha=0.05). Each image processing method was found to be effective on some particular criteria for image quality. Some methods were effective on just one criterion while some others were effective on a few criteria. The statistical test showed that there was an average improvement of 41 percent when the images were manipulated using the histogram modification methods. It could be concluded that different image processing methods have different effects on phantom images which generally improve radiologists' visualization. The results confirm that the histogram stretching and histogram equation methods lead to higher improvement in image quality as compared to the original image ($p < 0.05$).

Keywords: Image processing, enhancement, mammogram, breast phantom

INTRODUCTION

Cancer is one of the most important causes of death around the world. In USA, the second cause of death is cancer (American Cancer Society, 2006). Cancer is not limited to a specific gender or a group of people. It can involve anybody and no one is spared. In USA, one out of two men and one out of three women have some forms of cancer (American Cancer Society, 2006; World Health Organization, 2008).

World Health Organization reported that in 2005, cancer caused 7.6 million deaths and more than 70% of these deaths occurred in non-rich countries. It is expected that deaths due to cancer would increase up to nine million in 2015 and 11.4 million in 2030 (World Health Organization, 2008).

Received: 5 November 2009
Accepted: 22 March 2010
[*]Corresponding Author

In the women population, breast cancer is one of the most important diseases (Cheng and Xu, 2002). It was reported that 8% of the women population in the USA and 5% in the UK have breast cancer (Cancer Help, 2002; Cheng and Xu, 2002; Wahid, 2007). According to the Malaysian Oncological Society, about 4% of Malaysian women have breast cancer (Elm, 2005; Wahid, 2007). This malignancy was the 10th cause of hospitalization and 3rd cause of deaths in Malaysia in 2006 (Ministry of Health, 2006).

Masses and microcalcifications are two important signs for breast cancer diagnosis on mammograms. Mass detection is more difficult than microcalcification because the earlier may have almost the same density as normal breast tissue and they have different shapes and possibly ill-defined boundaries than the latter (Cheng and Xu, 2002; Kang *et al*., 2006).

Phantom refers to a test object that is used to simulate radiographic characteristics of compressed tissue and contains components that are radio-graphically model aspects of breast disease and cancer (Collectible, 2008). The mammographic phantom was designed to simulate x-ray attenuation of 4.2 cm compressed human breast comprising of 50% adipose and 50% glandular tissue. The test objects of different sizes, shapes and densities are embedded in a wax insert, which is enclosed in an acrylic base. These test objects consist of five circles which represent masses, six lines which represent fibrils and there are five groups of specks (micro-calcifications).

Cheng and Xu (2002) argued that "(1) low-contrast of mammographic images, (2) hard to read masses in mammogram, (3) the general variation of the intensities of the masses such that radiopaque mass with high-density and radiolucent mass with low-density in comparison with the background". These issues are the basis for image manipulation to increase enhancement and easier detection of the signs of breast cancer. He further stated that an important stage in low level image processing is pre-processing. He concluded that histogram modification is one of the methods used for image enhancement. However, Computer Assisted Diagnosis (CAD) can increase the accuracy of cancer detection, and hopefully to differentiate lesions which are benign and malignant (Cheng and Xu, 2002).

Singh and Bovis (2005) compared different enhancement methods to improve the quality of mammogram. They used different techniques, such as the following:

1. Histogram equation (HISTEQ)
2. Adaptive Contrast Enhancement (ACE)
3. Density Weighted Contrast Enhancement (DWCE)
4. Adaptive Contrast Enhancement based on Local Entropy (ACELE)
5. Adaptive Contrast Enhancement based on Fractal Dimension (ACEFD)

The researchers applied these techniques on 200 mammograms which had been extracted from a screening database. Based on the results of their research, ACE and ACELE methods could not improve the contrast of the target area against its background. Although the ACEFD could not obtain a good enhancement score for contrast enhancement, it could distinguish between the target and background. The DWCE method has better effect, and fuzzy even have better contrast enhancement of the background. HISTEQ has a clear enhancement on the target against its background.

Meanwhile, other researchers have suggested using texture, segmentation or wavelet methods. Li *et al*. (2001) suggest a new morphological enhancement algorithm. They tested this method on 200 mammograms consisting of 50 normal and 150 abnormal images which had been confirmed by biopsy. The results showed that the suggested method has effects in the suspected mass patterns and reduced noises, as well as removing background noises. The researchers further claimed that using this method twice could be effective on dense mammograms and useful to remove fibroglandular background.

Based on other research carried out in Malaysia, different wavelet filters were applied to enhance the mammograms which had been obtained from a group of Malaysian women. The investigators used 35 images that were derived from the 3 main races in Malaysia, namely, Malay, Chinese, and Indians (Al-qdah *et al*., 2003). These images were taken from different breast density categories. The researchers further applied three different wavelet methods (DB4, SYM4, and COIF2) and concluded that the DB4 method is the best technique, particularly to detect microcalcifications (Al-qdah *et al*., 2003); however, no exact report has been given on the improvement rate of this particular technique.

The main purposes of this paper are to study the effects of different image processing techniques on phantom standard images and to identify more useful and helpful method for a better image visualization and thus increase the level of sensitivity and specificity to detect abnormalities on digital mammogram images.

METHODS AND MATERIALS

Three different phantom images, which had been produced using 25kv (63.2 MAS), 28kv (29.8 MAS), and 35kv (9.5 MAS), were collected from the National Cancer Society of Malaysia (NCSM) and used in this research (*Fig. 1*).

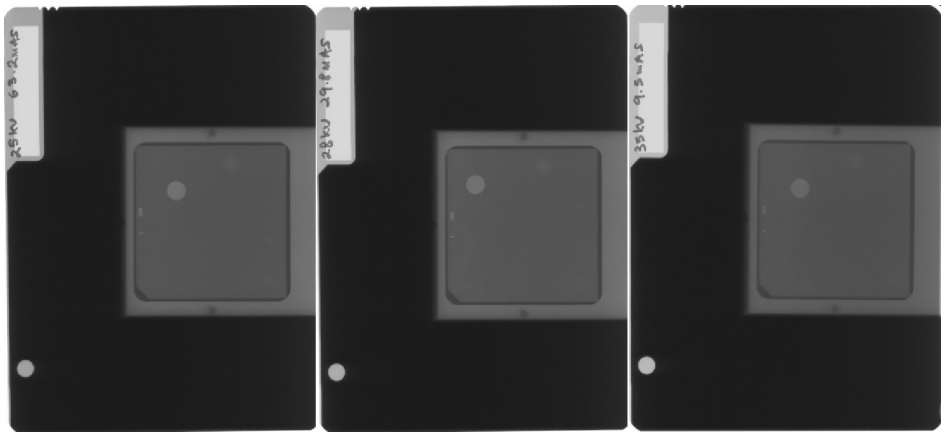

(a) (b) (c)

Fig. 1: Original phantom images, (a) 25kV, (b) 28kV, (c) 35kV

As clearly shown in *Fig. 1*, there is a very large unnecessary area (which does not have any information) in the original images. All these areas were cropped to make processing faster. The images were then resized (256 by 256 pixels as in *Fig. 2*), while different image processing methods, such as histogram equation, border slicing, histogram stretching, median filter, gray map, wavelet, sharpening, and some hybrid methods, were applied on these phantom images.

The manipulated images were scored by two expert radiologists from the Imaging Department, UPM and Hospital Serdang, and the results were analyzed using SPSS version 15. Meanwhile, the Wilcoxen ranked test was used to study the improvement in the quality of the images.

(a) (b) (c)

Fig. 2: Original resized phantom images: (a) 25kV, (b) 28kV, (c) 35kV

"The present criteria for the number of objects to pass the ACR Mammography Accreditation are the minimum of the four largest fibrils, three largest speck groups, and the three largest masses" (Collectible, 2008). The scoring criteria are shown in Table 1. The total score for a good image quality should be more than 10. All the procedures are summarized in *Fig. 3*.

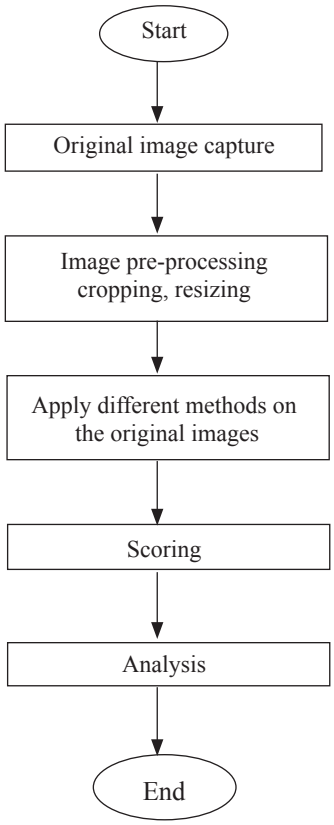

Fig. 3: Flowchart of the research material

TABLE 1
Phantom minimum requirements for image quality

CRITERIA	FIBRIL	SPECKS	MASS
MIN. REQUIREMENT	4	3	3

RESULTS

The manipulated images having very poor quality were excluded from the study. Many of the methods have caused artefacts on the images. This could be harmful because it could cause image degradation (not clear). In the original image of 25kv (Table 2), four fibrils, one speck and four masses were seen. As there were just four fibrils in the phantom images of the present study, it is not surprising that there was no improvement in this criterion after manipulation. Only one speck could be seen in the original image. Based on the results of this study, the number of specks which observed in the image of 25kv were improved using histogram equation (with a gray level of 153), histogram stretch, filter + histogram stretch, histogram equation +border slicing, gray map (with gray level of 102) +border slicing, and sharpening. The authors found that many of the methods could increase the number of masses that were seen in the image. These include histogram equation (with gray level of 51, 102, 153, 204, 255), histogram stretch, filter + histogram, filter +histogram equation, filter + gray map (with gray level of 102, 153, 204, 255), histogram equation (with gray level of 51, 204) + border slicing, and histogram equation + wavelet. The improvement for each method used is as shown in Table 2.

TABLE 2
Phantom 25kv image improvement

Criteria / Method		Fibril	Specks	Mass	Total	Artifact	Quality percent	Quality improvement %
Original image		4	1	4	9	0	81.82	0
Histogram Equation	51	4	1	5	10	1	90.91	9.09
	102	4	1	5	10	1	90.91	9.09
	153	4	2	5	11	1	100	18.18
	204	4	1	5	10	1	90.91	9.09
	255	4	1	5	10	1	90.91	9.09
Histogram stretch		4	2	5	11	0	100	18.18
Filter + Histogram		4	2	5	11	1	100	18.18
Filter +Histogram Equation	51	4	1	5	10	1	90.91	9.09
	102	4	1	5	10	1	90.91	9.09
	153	4	1	5	10	1	90.91	9.09
	204	4	1	5	10	1	90.91	9.09
	255	4	1	5	10	1	90.91	9.09
Filter + Gray Map	204	4	1	5	10	0	90.91	9.09
Gray Map	102	4	2	5	11	0	100	18.18
	153	3	2	5	10	0	90.91	9.09
	204	4	2	5	11	0	100	18.18
	255	4	2	5	11	0	100	18.18
Histogram Equation + Border	51	4	2	5	11	1	100	18.18
	102	4	2	4	10	1	90.91	9.09
	153	4	2	4	10	1	90.91	9.09
	204	4	2	5	11	1	100	18.18
	255	4	2	4	10	1	90.91	9.09
Gray Map + Border	102	4	2	4	10	1	90.91	9.09
Histogram Equation + Wavelet	153	4	1	5	10	1	90.91	9.09
	255	3	2	5	10	1	90.91	9.09
Sharpening		4	2	4	10	0	90.91	9.09

In the original image of 28kv (Table 3), two fibrils, two speck and four masses were seen. The methods which gave a better visualization of the fibrils were histogram equation (with gray level of 255), filter +histogram equation (with gray level of 51, 153, 204), and histogram equation (with gray level of 51, 102, 153, and 204) + border slicing. Nonetheless, none of the methods could increase the number of specks that were observed in the manipulated images as compared to the original one. Many manipulation methods have been shown to increase the visualization of the masses, and these include histogram equation (with gray level of 51, 102, 153, 204, 255), histogram stretch, filter + histogram, filter +histogram equation, filter + gray map (with gray level of 102, 153, 255), gray map (with gray level of 102, 153, 204, 255), histogram equation (with gray level of 51, 102, 153, 204, 255) + border slicing, and histogram equation + wavelet. Table 3 shows the experimental data and percentages of improvement.

TABLE 3
Phantom 28kv image improvement

Criteria / Method		Fibril	Specks	Mass	Total	Artifact	Quality percent	Quality improvement %
Original image		2	2	4	8	0	72.73	0
Histogram Equation	51	3	2	5	10	1	90.91	18.18
	102	3	2	5	10	1	90.91	18.18
	153	3	2	5	10	1	90.91	18.18
	204	3	2	5	10	1	90.91	18.18
	255	4	2	5	11	1	100	27.27
Histogram stretch		3	2	5	10	1	90.91	18.18
Filter + Histogram		3	2	5	10	1	90.91	18.18
Filter +Histogram Equation	51	4	2	5	11	1	100	27.27
	102	3	1	5	9	1	81.82	9.09
	153	4	2	5	11	1	100	27.27
	204	4	1	5	10	1	90.91	18.18
	255	3	2	5	10	1	90.91	18.18
Gray Map	153	2	2	5	9	0	81.82	9.09
	204	3	1	5	9	0	81.82	9.09
Histogram Equation + Border	51	4	2	5	11	1	100	27.27
	102	4	2	5	11	1	100	27.27
	153	4	2	5	11	1	100	27.27
	204	4	2	5	11	1	100	27.27
	255	3	2	5	10	1	90.91	18.18
Gray Map + Border	102	3	2	4	9	0	81.82	9.09
Histogram Equation + Wavelet	51	2	2	5	9	1	81.82	9.09
	102	2	2	5	9	1	81.82	9.09
	153	3	2	5	10	1	90.91	18.18
	204	2	2	5	9	1	81.82	9.09
	255	2	2	5	9	1	81.82	9.09

In the original image of 35kv (Table 4), zero fibrils, zero specks, and four masses were also observed. All the manipulation methods have been found to improve the visualization of the fibrils, except for border slicing, filter + border slicing, filter + gray map (with gray level of 51 and 102), gray map (with gray level of 51), gray map (with gray level of 51, 153, 204 and 255) + border slicing, wavelet, filter + wavelet, border slicing + wavelet, gray map (with gray level of 51, 102, 153, 204, 255), and sharpening. As for the original image, no specks were detected. All the manipulation methods improved the number of specks detected, except for border slicing, median filter, filter + border slicing, filter + histogram equation (with gray level of 51, 102, 153, 255), filter + gray map, gray map (with gray level of 51, 102, 255), gray map (with gray level of 51, 153, 204, 255) + border, wavelet, filter + wavelet, border slicing + wavelet, gray map + wavelet.

Many manipulation methods could increase the number of masses that have been observed in the original image except border slicing, median filter, filter + border, filter + gray map, gray map (with gray level of 51, 102, 255), gray map (with gray level of 51, 204, 255) + border slicing, wavelet, filter + wavelet, border slicing + wavelet, gray map + Wavelet. The percentages of the improvement are shown in Table 4.

DISCUSSION

The results have shown that some of the pre-processing techniques as well as median filter, histogram stretching and histogram equation are more effective for mammogram phantoms ($p<0.05$). In addition, in 25kv and 28kv images, many techniques such as sharpening and gray map may have more effects on the phantom image quality; however, the author found that none of the methods had improved the quality of image for all the criteria. In addition, the authors found that the median filter was effective since it reduced the noise and produced a better visualization for radiologists. This technique changes all the pixels values based on the median of each pixel neighbours. On the other hand, the histogram stretching tries to reform the pixels between the minimum of 0 and the maximum of 255. It means that the contrast between the different parts of the image will be increased. In addition, this particular technique also produces higher contrast in mammographic phantom images and gives a better visualization for radiologists and consequently a better detection of objects.

CONCLUSIONS

With the various image processing methods, the ideal image quality and resolution present a challenge to radiologists to examine mammogram images, analogue, as well as digital. The research aims to explore the effects on the mammographic phantom using different image processing methods. The ideal contrast and axial resolution of image were selected to represent the most effective methods. The effects of the selected methods on the actual mammographic images were explored for further study. In particular, the image processing method has different effects on the phantom images and it gave a better visualization for the radiologists for early detection of masses and classifications. It explores the positive effects of image processing method; however, some methods could not improve all the image quality criteria. Thus, the histogram stretching and histogram equalization were the most effective methods on mammographic phantom images, especially on 35kv ($p<0.05$).

TABLE 4
Phantom 35kv image improvement

Criteria / Method		Fibril	Specks	Mass	Total	Artifact	Quality percent	Quality improvement %
Original image		0	0	2	2	0	18.18	0
Histogram Equation	51	3	2	5	10	1	90.91	72.73
	102	4	1	4	9	1	81.82	63.64
	153	3	2	5	10	1	90.91	72.73
	204	3	2	5	10	1	90.91	72.73
	255	3	2	5	10	1	90.91	72.73
Histogram stretch		3	1	5	9	1	81.82	63.64
Median Filter		1	0	2	3	0	27.27	9.09
Filter + Histogram		3	2	5	10	1	90.91	72.73
Filter +Histogram Equation	51	2	0	4	6	1	54.55	36.37
	102	2	0	4	6	1	54.55	36.37
	153	3	0	5	8	1	72.73	54.55
	204	3	1	4	8	1	72.73	54.55
	255	3	0	4	7	1	63.64	45.46
Filter + Gray Map	153	2	0	2	4	0	36.36	18.18
	204	2	0	1	3	0	27.27	9.09
	255	2	0	2	4	0	36.36	18.18
Gray Map	102	1	0	2	3	1	27.27	9.09
	153	1	1	3	5	0	45.45	27.27
	204	3	1	5	9	0	81.82	63.64
	255	2	0	2	4	0	36.36	18.18
Histogram Equation + Border	51	3	1	5	9	1	81.82	63.64
	102	3	1	4	8	1	72.73	54.55
	153	4	1	4	9	1	81.82	63.64
	204	3	1	4	8	1	72.73	54.55
	255	3	1	5	9	1	81.82	63.64
Gray Map + Border	102	1	1	3	5	0	45.45	27.27
	153	0	0	3	3	0	27.27	9.09
Histogram Equation + Wavelet	51	3	2	5	10	1	90.91	72.73
	102	2	2	4	8	1	72.73	54.55
	153	2	2	5	9	1	81.82	63.64
	204	2	2	5	9	1	81.82	63.64
	255	3	2	5	10	1	90.91	72.73
Sharpening		0	1	3	4	0	36.36	18.18

LIMITATIONS

1. Phantom has no breast parenchyma background as compared to human breast tissues. Therefore, the real representation of cancer detection is not challenged in phantom images.
2. Cropped images are small sized. Larger mammogram images may take time to referent the results.
3. More radiologists should score the images.

REFERENCES

Al-Qdah, M., Ramli, A. R., Wirza, R., Mahmud, R. and Taysir, M. (2003). Detection of calcifications in mammography using wavelets. Paper presented at the *Student Conference on Research and Development*.

American Cancer Society. (2006). What is Cancer? Retrieved on February 6, 2008 from http://www.cancer.org/docroot/CRI/content/CRI_2_4_1x_What_Is_Cancer.asp.

Cancer Help. (2002). The mammogram. Retrieved on February 6, 2008 from www.cancerhelp.org.uk.

Cheng, H. D. and Xu, H. (2002). A novel fuzzy logic approach to mammogram contrast enhancement. *Information Sciences*, *148*(1-4), 167-184.

Collectible, Q. A. (2008). Mammography phantom image quality evaluation. Paper presented at the *Conference of Radiation Control Program Directors*, Frankfort.

Elm, H. (2005). Accreditation in Mammography – Pain or Gain? *Biomedical Imaging and Intervention Journal*, *1*(1), e6-18.

Kang, H. K., Ro, Y. M. and Kim, S. M. (2006). A microcalcification detection using adaptive contrast enhancement on wavelet transform and neural network. *IEICE Transactions on Information and Systems, E89-D*(3), 1280-1287.

Li, H., Wang, Y., Liu, K. J. R., Lo, S. C. B. and Freedman, M. T. (2001). Computerized radiographic mass detection. i. lesion site selection by morphological enhancement and contextual segmentation. *IEEE Transactions on Medical Imaging*, *20*(4), 289-301.

Ministry of Health. (2006). Health facts 2006. Retrieved on February 6, 2008 from http://www.moh.gov.my/MohPortal/index.jsp?lang=en.

Singh, S. and Bovis, K. (2005). An evaluation of contrast enhancement techniques for mammographic breast masses. *IEEE Transactions on Information Technology in Biomedicine*, *9*(1), 109-119.

Wahid, M. I. (2007). Breast cancer. Retrieved on February 6, 2008 from www.malaysiaoncology.org.

World Health Organization. (2008). Cancer. Retrieved on February 6, 2008 from http://www.who.int/cancer/en/.

ISSN: 0128-7680
Pertanika J. Sci. & Technol. **19 (1)**: 77 – 92 (2011)

Product Structure Initialization, the Bottleneck of ERP Implementation in Customer Driven Environments: A Case Study

S. Abedi Niestanak*, A. A. Faieza, S. Sulaiman and M.Y. Rosnah
Department of Mechanical and Manufacturing,
Faculty of Engineering, Universiti Putra Malaysia,
43400 UPM, Serdang, Selangor, Malaysia
**E-mail: abedi.saied@gmail.com*

ABSTRACT

This study of the implementation of enterprise resource planning (ERP) in a customer driven environment analyzes the critical success factors throughout the initialization phase. The dynamic and stochastic nature of customer driven environments results in a massive workload of product structure configuration tasks related to new arrivals on one hand and a constant updating process on the other. Meanwhile, the development and implementation of an ERP system was studied from the very first step (i.e. the feasibly study for implementing an ERP) to the last step (i.e. testing the outputs of the implemented system) in an office furniture company for three years. The study involved analyzing of the data collected that were from a series of interviews, as well as direct observations and reviewing of the company's documents. Based on the output of the analysis phase, a top-down hierarchical analysis of goals and CSFs were carried out according to the CSF analysis method. Three top level objectives included reducing project failure risk, project cost, and project time. Analysing the primary results of the study (i.e. activity model, data flow diagram DFD of different levels, system problems and potential solutions descriptions, etc.) revealed that the critical phase of the implementation project would be product structure initialization and this should be taken into consideration as the bottleneck of production planning in customer driven environment, which dramatically reduced the ERP efficiency in this kind of environment. Moreover, initializing issues of the same process is the main obstacle to the success of the ERP implementation, as it considerably raises the project failure risk and cost. Therefore, the simplification, facilitation, and automation of the PSCM process, which lead to acceleration of this process, are the most significant success factors for the ERP implementation projects in customer driven environment.

Keywords: ERP implementation, critical success factor, make-to-order, customer driven manufacturing, product structure configuration

INTRODUCTION

Customer satisfaction is the most significant objective for all goods and services producers in the contemporary competitive market. Today, many manufacturers depend on the enterprise's product characteristics and their customer expectations in related markets to decide whether to accept a customer's orders for producing products that are not in their standard product range or whether to customize their available products to have more satisfied customers.

Received: 18 November 2009
Accepted: 30 April 2010
*Corresponding Author

Furthermore, rapid changes in customer taste and the essential need to offer proper goods to satisfy the customer's new taste have driven the manufacturers to extend their offered product list. At the same time, they must maintain the history of their previous products, which is necessary for providing customers with after-sale support and for future references. This situation leads to the creation of customer-driven manufacturing enterprises that may produce goods and services which are more compatible with customers' requirements, but their performance is seriously affected by an ever-growing volume of product information (Jianxin Jiao and Tseng, 2004; Olsen *et al.*, 1997; Hegge and Wortmann, 1991).

On the other hand, emerging manufacturing tools and techniques require continuous adjustments to be made to the present manufacturing conditions. This then forces a manufacturer to design new products so their production processes are more compatible with or to design new manufacturing equipment and adjust old products to fit the new manufacturing conditions. Therefore, managers are constantly under pressure to improve their enterprises' performance and adapt to this wide range of change and uncertainty in order to perform better than their rivals in such a volatile and competitive market.

It is important to note that responsiveness and agility are two significant competitive advantages (Koh and Simpson, 2007) that should be taken into consideration in conjunction with satisfying a customer's desired quality, design, and functionality. In other words, delivering a customized product according to the customers' requests within a shorter lead time is desirable (Jodlbauer, 2007).

Enterprise resource planning (ERP) systems, due to their comprehensive coverage of the vast majority of an enterprise's business processes, have attracted managers' attentions as the most effective tools to be used in increasing an enterprise's agility, particularly in production planning and control processes (Koh and Simpson, 2007).

Many surveys have revealed that despite the potential value of ERP as a business process management tool, volatile manufacturing conditions in make-to-order (MTO) environments and, consequently, heavy and unpredictable workloads, result in poorly utilized ERPs. These surveys also indicate that a production planning process (including production scheduling and material resource planning), as the heart of the system, deals with more problems than other functions (Koh and Simpson, 2007; Berglund and Karltun, 2007; Vollmann *et al.*, 1997). It is obvious that product structure information is so important that without sufficient and accurate product structure information, all kinds of planning (including material requirements, human resource requirements, scheduling and financial resource planning) are actually impossible.

Hence, product structure initialization is a mandatory prerequisite for all the other tasks in the implementation project, so it should be taken into account as a critical task (Hernandez Matias *et al.*, 2008; Koh and Simpson, 2007; Persona *et al.*, 2004). Improving the product structure configuration and modification (PSCM) process performance through simplifying, facilitating, and automating this process in possible areas is expected to pave a way for an ERP implementation project and reduce the project risk and its cost.

Considering the fact that material requirements planning (MRP) has a fundamental role for manufacturing resource planning (MRPII) and ERP, using these systems as a type of production planning and control tool leads to an identical outcome (Koh and Saad, 2003: 2002; Enns, 2001), and that the PSCM process has been located at the heart of this group (i.e. MRP, MRPII, and ERP), while all these systems can benefit from any attempt on the PSCM process improvement.

From a different angle, Berglund and Karltun (2007) surveyed a production-scheduling process in four companies and concluded that the outcome of the scheduling process was influenced by the scheduler adding human capabilities that could not be automated. This means that the improvement

in the system performance will positively affect the scheduler's efficiency as a human resource, which is expected to raise the overall performance of the enterprise.

In sum, the conclusion drawn from reviewing the literature of ERP employment in MTO manufacturing environments (Hernandez Matias *et al.*, 2008, Berglund and Karltun, 2007; Koh and Simpson, 2007; Beheshti, 2006; Persona *et al.*, 2004, etc.) implies that this kind of environment is mainly facing problems related to product structures in two separate phases, as follows:

- Product structure database initialization
- PSCM process throughout ERP utilization

Meanwhile, problems in the initialization phase are related to processing a massive volume of information on product structures that must be entered into the database quickly and under the pressure of a constant and heavy flow of new arrivals. The difficulties in this particular phase considerably raise the implementation failure risk and its cost. In addition, problems in the utilization phase also originated from this heavy workload as well as a modification workload arising from internal elements that aggravated the pressure on the PSCM process and created a bottleneck in the production planning process. This bottleneck increases the delivery lead time, which is the most significant performance indicator for customer driven enterprises and paralyzes the scheduler as a human resource.

The expected results of simplifying, facilitating, and automating the PSCM process are as follows:

- Implementation failure risk and cost reduction
- Delivery lead-time reduction
- Increased scheduler performance and enhanced system reliability through a reduction of the amount of inaccurate and defective information
- Enhanced system reliability through a reduction of the amount of information that is not reflected in the system

This paper focuses on the ERP problems in connection with the PSCM process through the initialization phase. In addition, an analysis of the potential destinies of the implementation project and the risks and success factors, which are expected to reduce the failure risk and cost of the project, will also be given.

MATERIALS AND METHODS

Method

Manufacturing systems in the wood industry are some of the finest types of systems to track and investigate business management tool issues and customer driven manufacturing systems. This is due to the complexity of production processes, as they deal with products with many variants (e.g. colour, material, options, dimensions, etc.) and they have a make-to-order attitude. Many other studies have already chosen the wood industry to test their hypotheses (e.g. Hernandez Matias *et al.*, 2008; Carlson and Yao, 2008; Berglund and Karltun, 2007).

The development and implementation of an ERP system were studied from very first step (i.e. the feasibly study for implementing an ERP) to the last step (i.e. testing the outputs of the implemented system) in an office furniture company for three years. The case company was one of the pioneer office furniture manufacturers in Iran. When its Board of Directors decided to considerably extend their offered product list and accept the newly-designed customer orders, a measure was taken to

defeat their rivals in the market, and they were no longer able to use only the Excel spreadsheets in their production planning process.

After a comprehensive feasibly study, the company came to the conclusion to invest in a tailored ERP. This was because none of available ERPs on the market could match the company's requirements within its budget. The first author had participated in the ERP development as a system analyst and consultant through system development and different stages of the implementation. This direct engagement with the related issues provided the author with a comprehensive overview of the problems and the success factors in this scope. As the development project was carried out according to the structured systems analysis and the design method (SSADM V4), the outputs of the analysis and modelling phase provided the authors with all critical success factors (CSFs) analysis requirements.

A brief review of the analysis phase may provide a better perception of references on CSF analysis. According to the SSADM method, the analysis phase includes analyzing the current situation to find out how the current system works and to diagnose the current problems (Weaver *et al.*, 1998). This process involves analyzing the data collected from a series of interviews and direct observations and reviewing of the company's documents. The following steps are parts of this stage:

- Develop a business activity model: A model of the business activity is built, while business events and rules are investigated as inputs to the specification of the new automated system.
- Investigate and define requirements: The objective of this step is to identify problems associated with the current environment that are to be resolved by the new system. It also aims to identify the additional services to be provided by the new system and users of the new system.
- Investigate the current processing: The information flow associated with the services currently provided is investigated and described in the form of a data flow model. At this point, the data flow model represents the current services with all their deficiencies.
- Investigate the current data: This step is to identify and describe the structure of the system data independently of the way the data are currently held and organized. It produces a model of data that supports the current services.
- Derive a logical view of current services: The objective of this step is to develop a logical view of the current system that can be used to understand problems with the current system.

Based on the output of the analysis phase, a top-down hierarchical analysis of the goals and CSFs were carried out according to the CSF analysis method. The mission statement was "implementing the developed ERP within one year and with a determined budget." Thus, three top level objectives were defined (i.e. reducing project failure risk, project cost, and project time). Having in-depth system specifications (i.e. activity model, data flow diagram DFD of different levels, system problems, and potential solutions descriptions, etc.) showed that the critical phase of the implementation project would be product structure initialization. A detailed analysis revealed that simplifying, facilitating, and automating this process in the ERP could directly satisfy the top-level objectives. This was shown later in practice through the implementation project. The sequence of the methodology is clearly illustrated in *Fig. 1*.

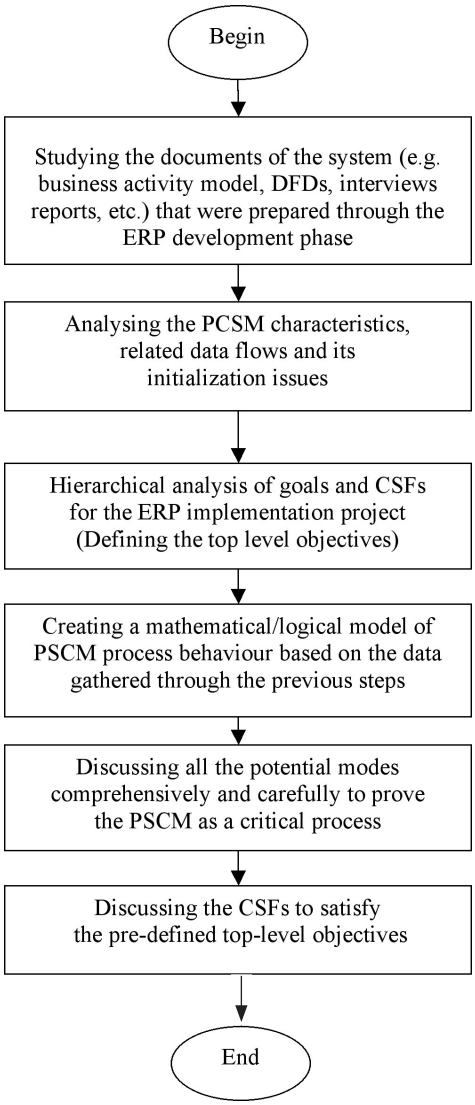

Fig. 1: The flowchart of the methodology

Company's Description

In this section, the case study company is briefly described, including a brief history of the company's improvements in connection to its information systems. The case company is one of the pioneer office furniture manufacturers in Iran which was founded in 1996. The development of the company was quicker than expected because of the special attention paid by its founders to exploiting modern managerial tools and methods.

The company attained the ISO 9001 certificate in fall 2002, as a result of practicing the standard requirements throughout the company. Two years later, the company was granted "the best product quality manufacturer" and was given a crystal statue by the HOFEX council during the Annual Office and Home Furniture Fair in 2004.

The company offered a range of computer and printer desks and a limited range of office furniture at that time. The production planning process was manipulated by three workers (the scheduler, his assistant, and the production planning supervisor) using several MS Excel spreadsheets.

The fair in 2004 was a critical point in company's history, in which the Board of Directors had decided to extend the range of products offered to compete against other companies. They did this by adding more office furniture models and office partitions.

In addition, the company also accepted all the new design requests and big furnishing projects (including purpose-designed products). This main competitive policy led to a substantial increase in production planning workload. A backlash was expected at this time because the workload was no longer manageable with the available resources.

Apart from the effects of the above strategic decision, the normal increase in production planning workload caused new problems in this process, originating primarily from its major sub-process (i.e. PSCM). Increasing the workload on the PSCM process partially paralyzed the spreadsheet-based production planning system. Eventually, the Board of Directors decided to conduct a feasibility study to implement an ERP system as a way of addressing the situation. Thus, a six-month analysis was carried out on the company's workflow and its production planning characteristics, as well as the requirements and an evaluation of available ERP systems on the market which revealed that none of the available alternatives could cover all of the company's requirements. This was particularly true in the PSCM process and the Board of Directors came to the conclusion in early 2005 that they should invest in developing a tailor-made ERP system.

At that time, the company already had approximately one hundred employees, of which twenty were white-collared. The company also had approximately 50 basic products, excluding different colours (i.e. each item was available in five colours on average), and out of which five were available in two different dimensions, which made the total 300 distinctive products. In addition, the same products might be available with different options in terms of functionality and some of them were available in two different materials (i.e. chipboards and medium-density fibreboards or MDF). This further increased the total number of variants to 450 distinctive items in terms of their model, colour, material, options, and dimensions.

Although many of components were used in several products, the available system did not allow the production planning team to re-use them in several structures. This meant that one product structure per variant was to be filed and thus, there was an archive of one hundred thousand data records, considering the fact that each product underwent 220 production processes on average.

Obviously, dealing with such a large volume of data was too demanding and caused many mistakes, which further spread to other parts of the system in spite of the hard efforts on the part of the production planning team. This massive amount of data, all of which needed to be entered into the new ERP database, were the main obstacles to implementing the available ERPs.

The trends in the company's performance indicators were not desirable, and putting more pressure on the system would have caused them to become even more negative. From the annual inspection reports of ISO9001, one could see that the promised delivery time, a main key performance indicator (KPI) of the company, was seven working days during this era (including one day for taking orders, five days for production planning, out of which, four days were used for product structure configuration and one day was used for the final assembling and delivery). This length of time caused them to be overdue in 42% of the cases, out of which 33% were due to issues related to product structure configuration. As product structure information was a mandatory prerequisite for any planning activity, utilizing the ERP was impossible prior to the launching of the PSCM process, so product structure initialization was apparently and undeniably a critical task.

Beyond the company's performance indicators, delays statistics and overall workflow diagrams suggested that the PSCM was the main bottleneck of the business processes and its performance directly affected the company's overall performance. This situation drove us towards paying particular attention to analyzing the PSCM issues and their essential role in the success of ERP implementation.

RESULTS AND DISCUSSION

The PSCM Process Characteristics

The term "product structure" in the case company is a collection of all the required resource information for producing a specified product, including the related production process characteristics that are presented in a hierarchical manner with defined process priorities.

The product structure was documented in a tree format, where every non-leaf node was representative of a production process (e.g. E, I, F, etc. in *Fig. 2*) related to a corresponding workstation and had a specified duration. In this format, the result of any production process comes out as part of its direct parent. The nodes located in the lowest level in any branch (i.e. leaf nodes) of this structure are raw materials (e.g. L, M, N, K, C in *Fig. 2*) and this provided the production planner with the information required for material resource planning. Parent-child relationships define process priorities that located at the different levels of the structure.

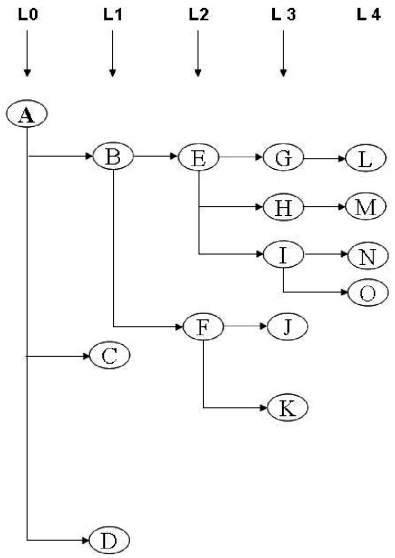

Fig. 2: A conceptual scheme of the product structure in the case company

Each node was recorded as a row in the company's Excel spreadsheets, bearing its specifications, including the process code, the work station, the process time, the parent node code, the consumption rate, the outcome component code for non-leaf nodes, as well as the raw material code for the leaf nodes, and a descriptive data field in some cases. The parent code of each node established a hierarchical relationship among the nodes, which was interpretable in a tree structure manner (see *Fig. 2*).

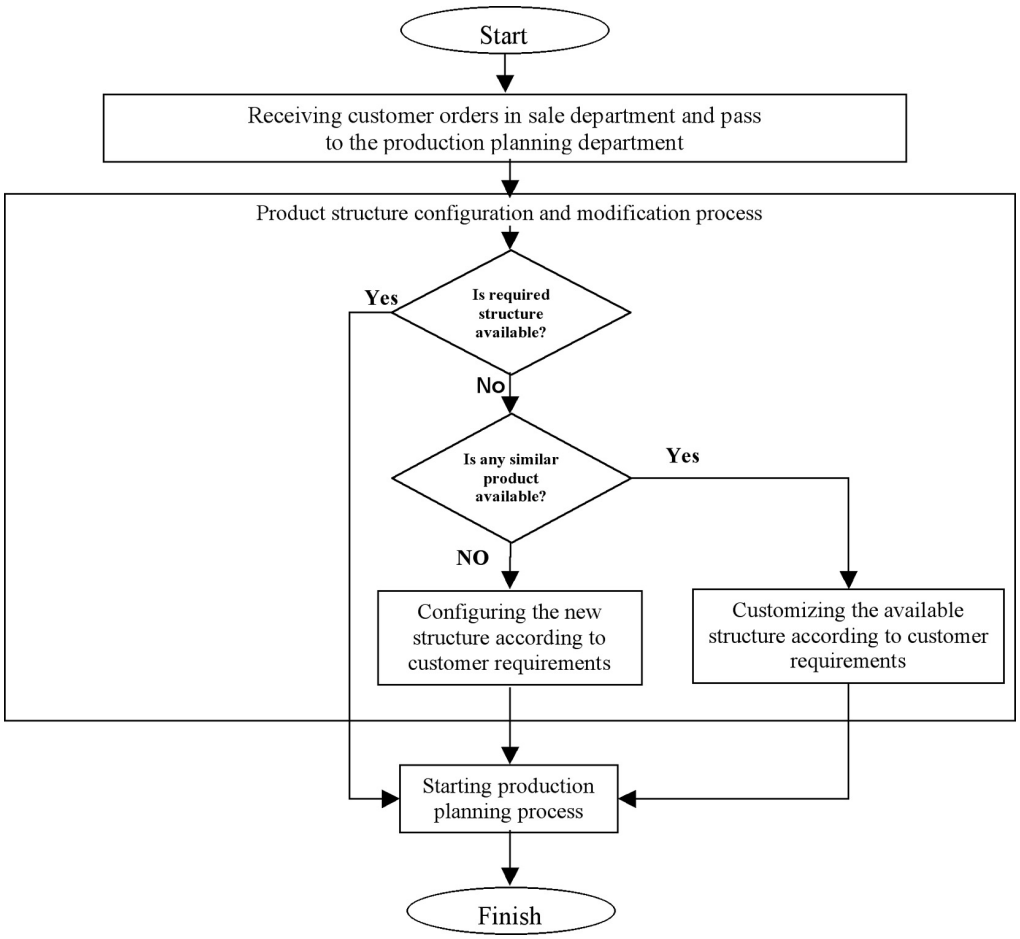

Fig. 3: Routine workflow of the PSCM in the case company

The number of nodes varied from approximately one hundred (for some plain computer desks) to more than four hundred (for some of more complicated models of office furniture), depending on the complexity of the products. The average number of rows per product was 220, as previously reported. The structure information of the products was independently archived in separate worksheets, despite the fact that there were many identical components in the different products which could have been summarized. *Fig. 3* illustrates the PSCM routine workflow in the company.

As illustrated in *Fig. 3*, the PSCM process includes technically comparing customers' requirements with available products to find an identical or similar product. Meanwhile, minor or major modification or a complete configuration might be required, depending on the differences of the volume.

Configuration of a new product comprised of a range of decision making tasks based on the information available that is scattered among several worksheets and the personal experience of the production planning team members. The output of the process included in-depth manufacturing specifications for a given product. These specifications comprised of the required materials, production processes, production priorities, input and output of each process, consumption rates, and basic materials.

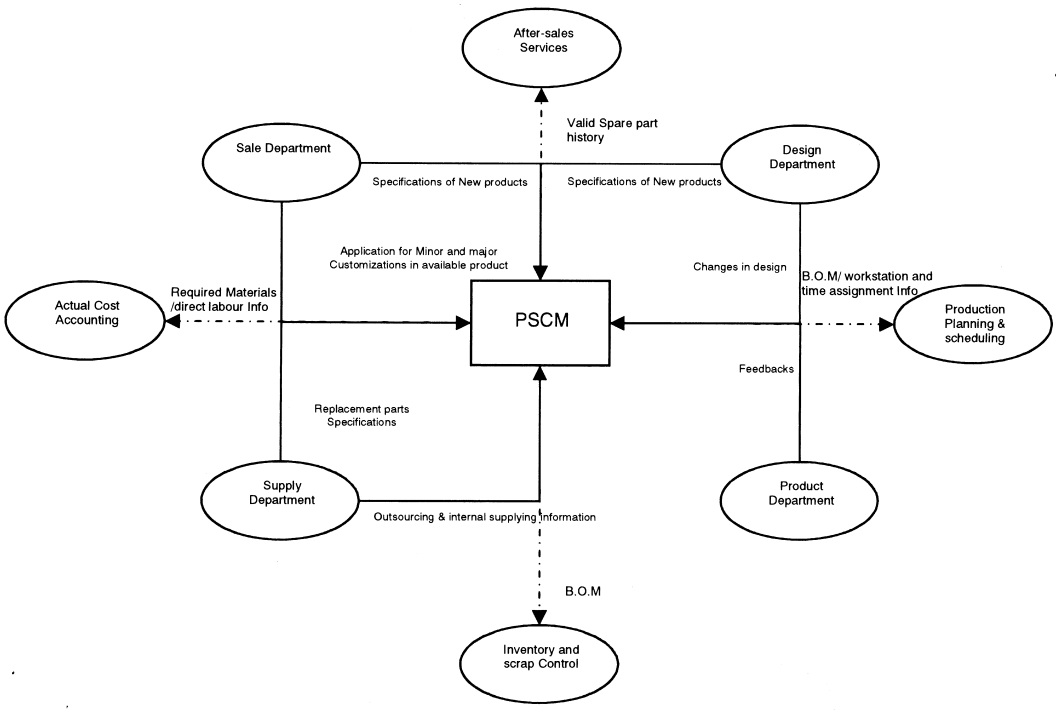

Fig. 4: Context-level data flow diagram (DFD) related to the PSCM process

According to the concept of the customer-driven manufacturing, the customer is the most significant source of data for the product structure configuration and modification (PSCM) process. Unlike make-to-stock environments or mass production, the production planning department in the make-to-order environment is dealing with a continuous flow of customer requests that may lead to specifying a completely new product structure, as well as minor or major customizations in the structures of the available products.

As stated earlier, the company's competitive strategy entails offering new, designed products to the customers and improving available products according to the market feedbacks. This means that the Design Department has to send additional internal workflow towards the PSCM process. Moreover, the Design Department also increases the workflow because of the extensive modifications to the available product structures that are necessary because of the changes in technology, new machinery, modern production methods, and new components and raw materials.

In practice, the Supply Department also triggered a workflow due to the problems in providing the manufacturing process with desirable resources. In many cases, it was not possible to find compatible resources with enterprise standards due to the supplier's market constraints. In these cases, similar parts were used instead. It is obvious that without reflecting these changes in the information systems, tracing the valid product structure to provide the customers with proper after-sale services and analyzing the supplier's market was impossible. In addition, the avoidance of reflecting minor changes in the system gradually undermined the reliability of the system. Therefore, an additional workload would develop to track these kinds of changes in the system.

The last mentionable workflow towards the PSCM process was the change in the system which was caused by decision making in relation to outsourcing a component or producing a component which was once obtained from the supplier. Despite the strict supervision done to ensure the

accuracy of the provided product structure information, on many occasions, the product department were still facing deficient and inaccurate product information. This could include items missing in the bill of the material (B.O.M), dedicating the wrong raw material, an incorrect consumption rate, an incorrect workstation, etc. These deficiencies triggered a reverse workflow of revision requests targeted to the PSCM process. The context-level DFD in *Fig. 4* illustrates all the data flowing towards the PSCM process.

However, the modification of a component might affect several product structures. The impact of the modification depends on the number of products that contained the component in their structure. The communal modification should be reflected in many worksheets. This was a demanding and time consuming task that sometimes caused information incompatibility.

Potential Modes Analysis

The normal functionality of the PSCM (i.e. serving all of the above-mentioned workflows) could not stop for a long period of time before initializing the new system or the routine workload interfered with the initialization process and reduced its rate of progress.

Once a product structure has been initialized, it should be frequently updated during the project in both the new and the old systems to achieve desirable level of system reliability at the end of the project. This intervening updating process would make the project progress rate dwindle while the initialization phase was progressing. The more project proceeds, the more often information should be updated so that the proceeding velocity will reduce along the time vector and this reduction begins shortly after the start of the initialization process (see *Fig. 5*). The resulting nominal rate turns into the actual rate, as follows:

Actual Progression Rate = Nominal Progression Rate - Intervening Processes Increment

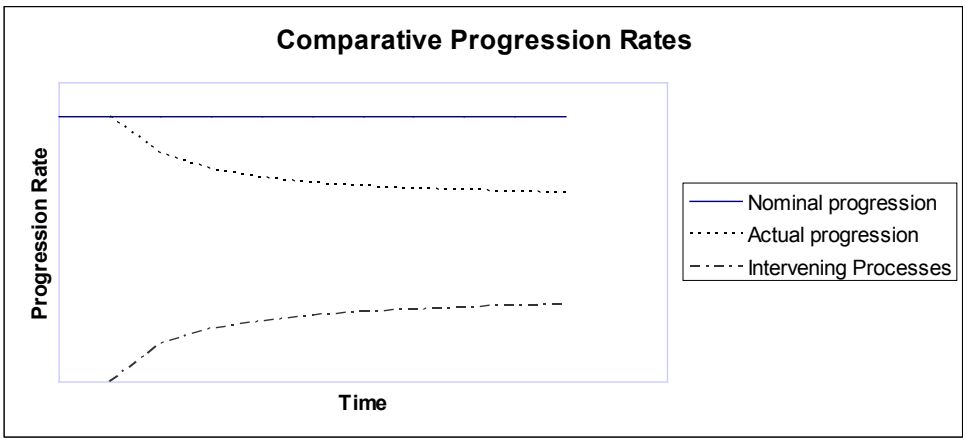

Fig. 5: Intervening task's effect on project progression rate

On the other hand, the initialization process deals with a growing stockpile of product structures which should be entered to the new system. Thus, the project progression velocity should be discussed as a relative element instead of an absolute one. The equations below describe the 'nominal relative progression rate' and the 'actual relative progression rate'.

Nominal Relative Progression Rate = Nominal Progression Rate - Input Rate

and

Actual Relative Progression Rate = Nominal Relative Progression Rate - Intervening Process Growth

Meanwhile, *Fig. 6* depicts how the input rate affects the nominal and the actual progression rates, as well as how it shifts them to a lower level (i.e. nominal relative and actual relative progression rates).

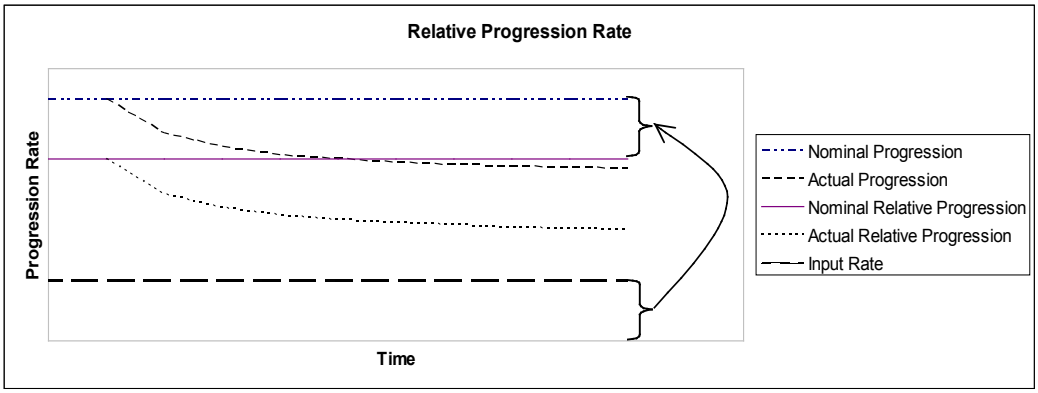

Fig. 6: Absolute and relative project progression rates

The "actual relative progression rate" is the final form of the project proceeding curve that has been affected by almost all of the typical factors and it gives a good representation of the actual project proceeding velocity. The shape and slope of the curve are apparently dependent on many unpredictable factors. Nonetheless, they could be ignored in this context or case because they do not affect the analysis in this scope. Similarly, the input rate and the nominal progression rate have been assumed to be constant rates, but they are not constant in the real world practices.

Some factors have been ignored, such as the changes in the volume of customer demands, changes in the working calendar (i.e. the number of working hours in different days or number of holidays in different months), seasonal changes in demand, the complexity of the products ordered during different periods, human resource availability, software bugs, problems occurring during the data entry process, hardware breakdowns, intervening activities (e.g. receiving a phone call, attending meetings, etc.) that are not part of the scheduler's official job description. Including these factors would make the situation more complicated, and it is unnecessary because this simplified curve is able to cover all of the required aspects of the initialization phase and to analyze all the possible destinies of the project. Regardless of the shape and slope of the curves, the following equation is valid based on the concept of integrals in calculus (Apostol, 1967):

$$\int_0^t h(t) = \int_0^t f(t)\,dt - Area_A$$

As it is obvious, the surface of area A is equal to the surface of area B (see *Fig. 7*), while, $Area_B = \int_0^t g(t)\,dt$ so the original form of the equation can be modified as follows:

$$\int_0^t h(t) = \int_0^t f(t)\,dt - \int_0^t g(t)\,dt$$

In which:

f(t) = Nominal Relative Progression Rate
g(t) = Intervening Process Growth
h(t) = Actual Relative Progression Rate

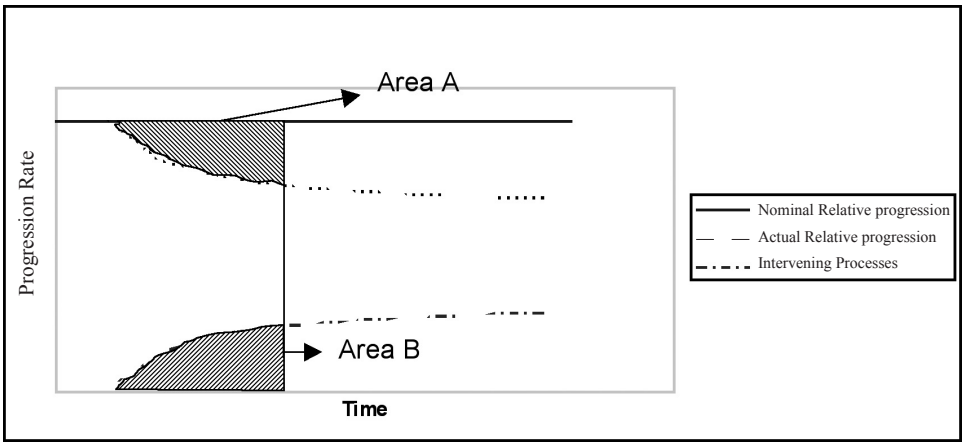

Fig. 7: Equal surfaces

At the theoretical finish line of the project, where t = t_f in the above equation, the finish line would be equal to the first stockpile (FS) (i.e. the amount of data that should be entered into database at the beginning of the initialization phase) and the equation would therefore change, as follows:

$$\int_0^{t_f} h(t) = \int_0^{t_f} f(t)\,dt - \int_0^{t_f} g(t)\,dt = FS$$

Fig. 8 illustrates a typical project progression model of an initialization phase, whereby two different modes can be assumed, in which the destiny of the project should be separately analyzed, as follows:

1. The 'intervening process growth' curve goes along the 'nominal relative progression rate' curve and they never meet. In this condition, regardless of the shape of the curves and their relative distance, the initialization phase can theoretically finish at point "t_f", in which:

$$\int_0^{t_f} f(t)\,dt - \int_0^{t_f} g(t)\,dt = FS$$

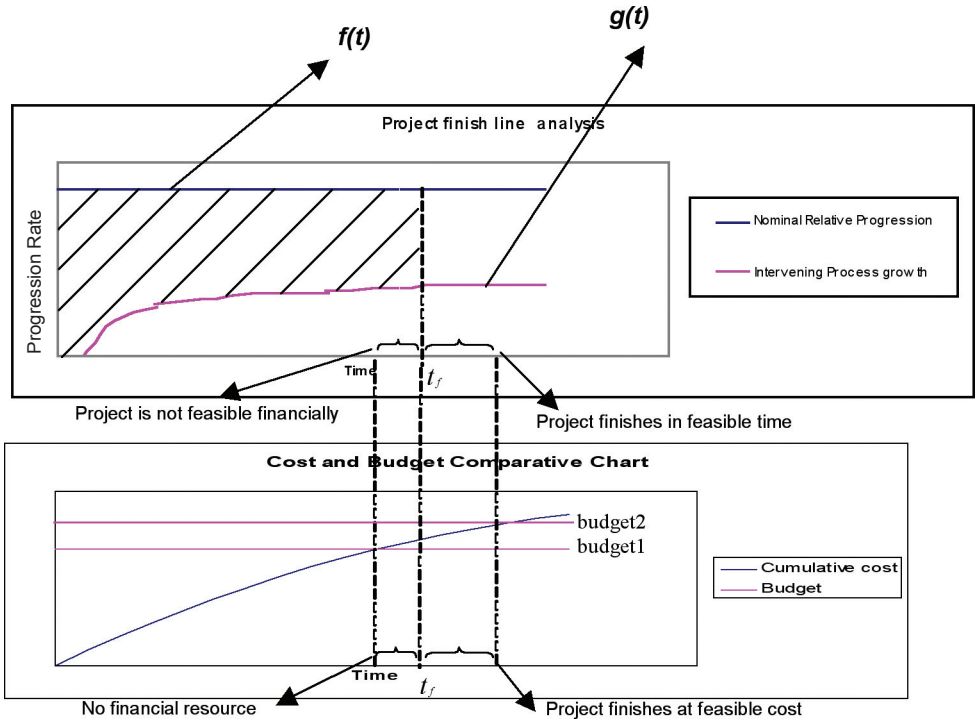

Fig. 8: Technical and financial analysis of the project finish line

In this mode, a cost and budget analysis helps to predict the feasibility of the project.

- If the cost of the initialization phase exceeds the budget at point "t_f" (i.e. the theoretical finish point), it can be inferred that the project is technically feasible, but it is financially infeasible at the same time.
- If the initialization phase finishes before its cost exceeds the budget, the project is taken as both technically and financially feasible.

Even if a project is feasible from a theoretical point of view, the overall feasibility is dependent upon the project budget and cost scheme. Instead of moving the theoretical finish point forward and backward to analyze the situation, two different budget lines (i.e. budget1, budget2) are illustrated in *Fig. 8* to have both modes in a single figure, though the project budget scheme is fixed in practice.

2. The 'intervening process growth' curve crosses the 'nominal relative proceeding rate curve'. The project destiny should be discussed by taking three significant aspects into account, as follows:
   - The project theoretical finish line, t_f;
   - The project budget scheme;
   - The critical point (i.e. *cp*) in which the project progression rate becomes negative.

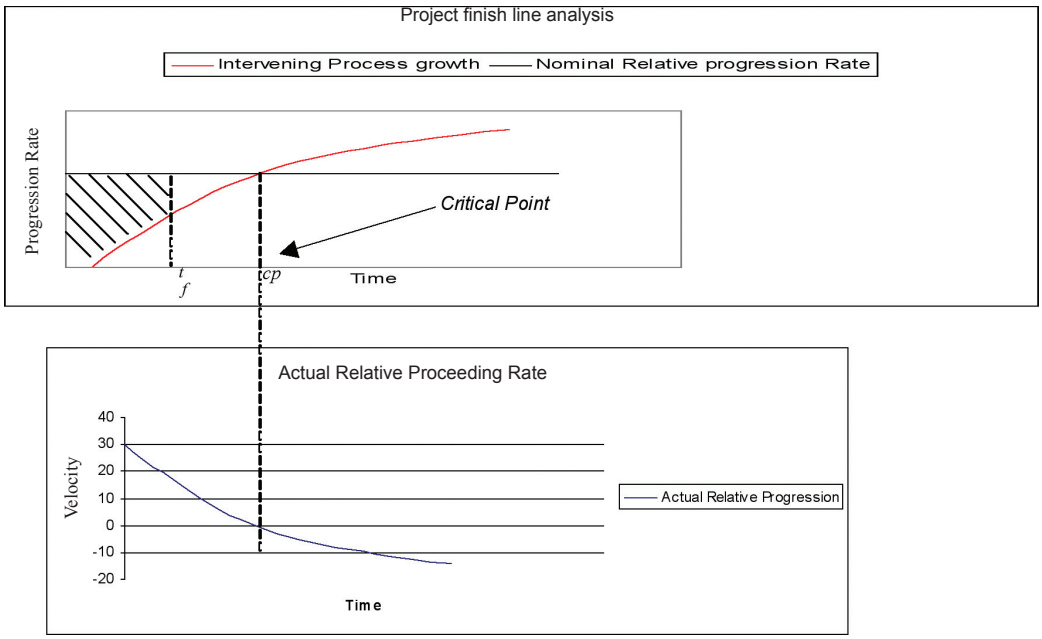

Fig. 9: Critical point analysis

Thus, three different situations can be assumed in this mode when all of the above-mentioned aspects are included:

$$\int_0^{cp} f(t)\,dt - \int_0^{cp} g(t)\,dt < FS \tag{2.1}$$

As shown in *Fig. 9*, the project will be never actually finish because in passing the critical point, the progression rate will turn into a negative rate. Therefore, the more time passes, the more the stockpile of the un-entered data grows.

$$\int_0^{cp} f(t)\,dt - \int_0^{cp} g(t)\,dt > FS \tag{2.2}$$

In this condition, everything is dependent upon the position of the theoretical finish point of the project, which is located somewhere before '*cp'* in relation to the financial finish point. This is similar to the first mode and two different destinies can be derived in this condition, namely:

- If the cost of the initialization phase exceeds the budget at this point, it can be inferred that the project is theoretically feasible, but it is financially infeasible.
- If the initialization phase finishes before its cost exceeds the budget project, it is accepted as both theoretically and financially feasible.

$$\int_0^{cp} f(t)\,dt - \int_0^{cp} g(t)\,dt = FS \tag{2.3}$$

The final situation is where the critical point is the final line of the project at the same time. In other words, $cp = t_f$. A financial analysis can again shed light on the destiny of the project. If the project cost does not exceed the budget at the '*cp'* point, the project is therefore feasible. Otherwise,

it is not feasible from a financial perspective despite the fact that the project is theoretically feasible.

Meanwhile, finding solutions for raising the proceeding velocity and reducing the effects of intervening processes on the progression rate can result in moving the theoretical end of project backward. Moving this point backward when the project budget is fixed can lead to a change in the project destiny, i.e. from infeasible to feasible or simply to finishing the project at a lower cost, depending on the project condition. Considering the fact that the PSCM process initialization is a mandatory prerequisite for all the other tasks in an ERP implementation project, particularly in customer driven environments, moving the theoretical finish point of this phase backward will reduce project failure risk by changing the destiny of previously infeasible modes to feasible and reducing the overall project cost and duration.

As such, enhancement of the proceeding velocity is possible through simplifying and facilitating the PSCM process, while data accuracy will be guaranteed through reduction of the manual data entry and the embedding of strict constraints within graphical user interface (GUI).

CONCLUSIONS

The simplification, facilitation, and automation of the PSCM process, which lead to the acceleration of this process, are significant factors that can reduce the failure risks and cost of ERP implementation in the customer-driven environment. Moreover, it can be expected that improving the performance of this process can lead to an enhancement in the overall company's performance as the empirical results of the case company also admit this claim as the PSCM process is the bottleneck of production planning in these kinds of environments.

The production planning process was manipulated by three workers (the scheduler, his assistant, and the production planning supervisor) using several Excel spreadsheets before implementing the ERP in the case company. From the annual inspection reports of ISO 9001, one could see that the promised delivery time, a main key performance indicator (KPI) of the company, was seven working days during this time (including one day for taking orders, five days for production planning, out of which four days were used for product structure configuration, and one day was used for the final assembly and delivery). The difficult and high-pressure production planning process caused the product to be overdue in 42% of cases, of which 33% were due to product structure configuration issues.

More importantly, the ability in implementing the framework for the PSCM to reuse the available components was found to reduce the total number of product structure data records from one hundred thousand in the previous system to merely eleven thousand in the new system. In addition, the case company's annual inspection report after the ERP implementation project also revealed significant improvements in the company's performance indicators. The promised delivery time was reduced to four working days, of which one day was for taking the orders and transferring related data to the production planning department, another day for the final assembly and delivery, and only two days were required for the whole production planning process. Overdue delivery due to product structure configuration issues was also reduced to 16%, as a result of controlling the negative effects of uncertainties on delivery by utilizing the new system's capabilities in the area of production planning. The implemented ERP also had a visible effect on human resource use all over the enterprise, particularly in production planning, as the new production planning process could be conducted by a single employee, and more efficiently than it was in the past.

The characteristics of the ERP, as they are related to the PSCM process, should be taken into consideration as the three critical success factors for the ERP implementation in the customer driven environment. Meanwhile, a further analysis on this critical process in both the initialization and utilization phases may lead to a diagnosis of more factors which affect the ERP performance in

the customer driven environment. Taking into account the above-mentioned CSFs in designing ERP software and focusing on PSCM process issues can lead to developing ERPs that are more compatible with the customer driven environment and one which can play a significant role as a business process management tool.

REFERENCES

Apostol, Tom M. (1967). "Calculus", Vol. 1: One-Variable Calculus with an Introduction to Linear Algebra (2nd Edn.). Wiley.

Berglund, M. and Karltun, J. (2007). Human, technological and organizational aspects influencing the production scheduling process. *International Journal of Production Economics*, *110*, 160–174.

Beheshti, H.M. (2006). What managers should know about ERP/ERP II. *Management Research News*, *29*(4), 184-193.

Carlson, John, G. H. and Yao, Andrew, C. (2008). Simulating an agile, synchronized manufacturing system. *International Journal of Production Economics*, *112*, 714-722.

Enns, S.T. (2001). MRP performance effects due to lot size and planned lead time settings. *International Journal of Production Research*, *39*, 461-80.

Hegge, H.M.H. and Wortmann, J.C. (1991). Generic bill of material: A new product model. *International Journal of Production Economics*, *23*, 117-128.

Hernandez Matias, J.C., Perez Garcia, H., Perez Garcia, J. and Vizan Idoipe, A. (2008). Automatic generation of a bill of materials based on attribute patterns with variant specifications in a customer-oriented environment. *Journal of Materials Processing Technology*, *199*, 431–436.

Jianxin Jiao and Tseng, M.M. (2004). Customizability analysis in design for mass customization. *Computer-Aided Design*, *36*, 745–757.

Jodlbauer, H. (2008). Customer driven production planning. *International Journal of Production Economics*, *111*, 793–801.

Koh and Simpson. (2007). Could enterprise resource planning create a competitive advantage for small businesses? *Benchmarking: An International Journal*, *1*, 59-76.

Koh, S.C.L. and Saad, S.M. (2003). MRP-controlled manufacturing environment disturbed by uncertainty. *International Journal of Robotics and Computer Integrated Manufacturing*, *19*, 157-71.

Koh, S.C.L. and Saad, S.M. (2002). Development of a business model for diagnosing uncertainty in ERP environments. *International Journal of Production Research*, *40*, 3015-39.

Olsen, K.A., Saetre, P. and Thorstenson, A. (1997). A procedure-oriented general bill of materials. *Computers and Industrial Engineering*, *32*(1), 29-45.

Persona, A., Regatttieri, A. and Romano, P. (2004). An integrated reference model for production planning and control in SMEs. *Journal of Manufacturing Technology and Management*, *15*, 626–640.

Philip L.Weaver, Nicholas, L. and Mathew, W. (1998). *Practical SSADM Version 4+: A Complete Tutorial Guide* (2nd Edn.). London: Pitman Publishing.

Vollmann, T.E., Berry, W.L. and Whybark, D.C. (1997). *Manufacturing Planning and Control Systems*. New York: Irwin/McGraw-Hill.

ISSN: 0128-7680
Pertanika J. Sci. & Technol. **19 (1)**: 93 – 107(2011)

Anthropogenic Concentrations of Cd, Ni and Zn in the Intertidal, River and Drainage Sediments Collected from North Western Peninsular Malaysia

Yap, C. K.* **and Pang, B. H.**
Department of Biology, Faculty of Science,
Universiti Putra Malaysia, 43400 UPM, Serdang,
Selangor, Malaysia
**E-mail: yapckong@hotmail.com*

ABSTRACT

Surface sediments were collected from the north western intertidal area (14 sites), drainage (3 sites), and rivers (3 sites) of Peninsular Malaysia in April 2005. The samples were analyzed for their concentrations of Cd, Ni, and Zn. The ranges for the total concentrations (µg/g dry weight) of Cd, Ni, and Zn were found to be 0.79-2.48, 6.46-73.92, and 33.6-484.14, respectively. Factory drainage site at Juru exceeded the established sediment quality values (Effect Range Median-ERM) for Zn and Ni, while the concentrations of Zn were also found to have exceeded the ERM at drainages at Kuala Kurau Town and Sg. Juru sites. The geochemical study, based on the sequential extraction technique on the sediments, revealed that the metal percentages of non-resistant fractions of the drainage at Kuala Kurau Town (drainage), Sg. Juru (river), Kuala Juru (intertidal), and factory drainage site at Juru were higher than the resistant fractions of the metals. These indicated that the sites (intertidal, river, and drainages) received anthropogenic inputs of these metals. Therefore, the point source of anthropogenic input in these sites should be given attention in future in order to mitigate the environmental problem on the living resources in the north western of Peninsular Malaysia. The present monitoring data are useful for future establishment of sediment quality guideline for Malaysian aquatic environment.

Keywords: Cd, Ni and Zn, north western Peninsular Malaysia

INTRODUCTION

Literatures on heavy metal concentrations in the surface sediments of the west coast of Peninsular Malaysia have been reported based on the samples collected between 1999-2004 (Yap *et al.*, 2002: 2003: 2005: 2006). Besides, the east coast sediments of Peninsular Malaysia have also been documented (Shazili *et al.*, 1987:1989; Shazili and Mawi, 1988; Yap *et al.*, 2008a). All of these monitoring studies imply the importance of such data from the environmental management point of view. In order to establish the local sediment quality guidelines of metals for this area, monitoring the data throughout a timeframe is therefore necessary. The findings of the present study are aimed to serve as a part of the monitoring work towards achieving the Malaysian sediment quality guidelines for heavy metals in future.

Reviewing the published work of heavy metal concentrations in sediment from Peninsular Malaysia by Yap *et al.* (2002) and Yap *et al.* (2003) is interesting; nonetheless, a question this crops up from it is, "What are the metal levels after 5 years at the same sampling sites based on the sediment samples?" Yap *et al.* (2002: 2003) reported the metal data based on the sediments collected in 1999-2001. It is therefore interesting to know the metal levels in the sediments collected from the west coast of Peninsular Malaysia in 2005.

Received: 25 November 2009
Accepted: 31 May 2010
*Corresponding Author

In this paper, surface sediments were collected in April 2005, using the method described by Yap *et al.* (2002, 2003). The advantages of using sediment as an indicator of heavy metal pollution is well-known in the literature (Yap *et al*., 2002: 2003a, b, c: 2005: 2006). The significance of this work is to compare the levels of Cd and Zn with those reported by Yap *et al.* (2003) and to set continued monitoring data for future references. Therefore, the objective of this study was to determine the concentrations of Cd, Ni, and Zn in the sediment from the north western part of Peninsular Malaysia collected in April 2005. Besides, this study was also done to determine the Cd, Ni, and Zn pollution based on the geochemical distribution (non-resistant and resistant fractions) of these metals in the sediments that were collected from the north western part of Peninsular Malaysia. The three geochemical fractions (easily, freely, leachable or exchangeable or EFLE, acid-reducible and oxidisable-organic), based on the sequential extraction technique, are useful in identifying the polluted sites in Malaysia (Yap *et al.*, 2007b). The data of this study were compared with those reported in the studies carried out in this region and Malaysia, as well as the established sediment quality values proposed by Long *et al.* (1995).

MATERIALS AND METHODS

The samples of sediment were collected on 18-20 April 2005 from 20 sampling sites that are located in the north western intertidal area (17 sites) and drainage (3 sites) of Peninsular Malaysia (see *Fig. 1*). The positions, sampling dates and site descriptions are given in Table 1. The top 3-5 cm of the surface sediments were collected at each sampling site. Each sediment sample was put in a plastic bag and frozen prior to analysis. The parameters of the surface water (0-20cm) samples recorded directly in the field at each sampling station were temperature, pH, specific conductivity (SpC), total dissolved solid (TDS), as well as salinity and dissolved oxygen (DO) using a Hydrolab Datasonae 4a water quality multi-probe.

The sediment samples were dried using an oven at 60°C until constant dry weights. Later, the dried sediments were pounded using a clean pestle and mortal and they were also sieved through a 63 μm stainless steel aperture. While sifting, the sieve was shaken vigorously to produce homogeneity (Yap *et al.*, 2002a) before they were stored in clean and new plastic bags.

In this study, the direct aqua-regia method was used to determine the concentrations of Cd, Ni, and Zn in the dried sediment samples. Firstly, about 1 g of each dried sample was weighed and digested in a combination of concentrated nitric acid (HNO3, AnalaR grade, BDH 69%) and perchloric acid (HClO4, AnalaR grade, BDH 60%) in the ratio of 4:1. After that, the tubes were put into the digestion block at the low temperature (40°C) for 1 hour and the temperature was then increased to 140°C for at least 3 hours. The digested samples were diluted to 40 ml in double distilled water and filtered through Whatman No.1 (filter speed: medium) filter paper in a funnel into acid washed pillboxes. After that, they were stored until metal determination.

The geochemical fractions of Cd, Ni, and Zn in the sediment were obtained using the Sequential Extraction Technique (SET), as described by Badri and Aston (1983) and modified by Yap *et al*. (2002). They are four fractions considered in this method, namely 'easily, freely, leachable or exchangeable' (EFLE), acid-reducible, oxidisable-organic, and resistant fractions.

Prior to the next fractionation, the residue for each fraction was weighed. The residue was then rinsed using 20 ml of double distilled water. After that, it was filtered through a Whatman No.1 (Filter speed: medium) filter paper in a funnel and the filtrates were stored for the next step. For each fraction of the sequential extraction procedure, a blank was employed using the same procedure to ensure that the samples and chemicals used were free of contamination.

After the filtration, the sample was determined using an air-acetylene flame Atomic Absorption Spectrophotometer (AAS), an inorganic analytical instrument made by Perkin-Elmer Model AAnalyst 800. All the data are presented in μg/g dry weight basis.

TABLE 1
Positions, sampling dates and description of the sampling sites for the intertidal sediment collected from the north western part of Peninsular Malaysia

St	Location	Sampling date	Latitude	Longitude	Description
1	Kampung Kuantan, Selangor	18 April 2005	101º18.093' E	03º21.745' N	River; A riverside, recreational park
2	Kampung Penambang, Selangor	18 April 2005	101º18.096' E	03º21.744' N	Intertidal; A small jetty, the fishing village
3	Sungai (Sg.) Bernam, Selangor	18 April 2005	101º14.965' E	03º21.599' N	River; Under a bridge of a main highway
4	Hutan Melintang, Perak	18 April 2005	100º55.965' E	03º52.345' N	Intertidal; A fishing village
5	Pelabuhan Hutan Melintang, Perak	18 April 2005	101º14.965' E	03º21.599' N	Intertidal; An abundant port, fishing village in the other side
6	Bagan Datoh, Perak	18 April 2005	100º47.150' E	03º59.563' N	Intertidal; A fishing village
7	Jambatan Raja Permaisuri Bainon (JRPB), Perak	18 April 2005	100º39.335' E	04º16.803' N	Intertidal; Under an overhead bridge
8	Kuala Kurau (jetty), Perak	19 April 2005	100º25.867' E	05º00.928' N	Intertidal; A jetty
9	Kuala Kurau (town), Perak	19 April 2005	100º26.017' E	05º01.052' N	Drainage; A small town, many kind of shops
10	Batu 14 Jalan Pantai, Kurau, Perak	19 April 2005	100º24.779' E	05º01.106' N	Drainage; A highway side
11	Bagan Tiang (offshore), Perak	19 April 2005	100º22.459' E	05º08.517' N	Intertidal; An offshore, fishes and mussel aquacultura
12	Bagan Tiang (jetty), Perak	19 April 2005	100º23.840' E	05º06.702' N	Intertidal; A jetty and fishing village
13	Sungai (Sg.) Berembang, Kedah	19 April 2005	100º08.787' E	06º21.313' N	Intertidal; A rocky shore
14	Kuala Perlis, Perlis	19 April 2005	100º07.740' E	06º23.927' N	Intertidal; A jetty
15	Alor Setar, Kedah	20 April 2005	100º21.595' E	06º07.420' N	Drainage; An urban area, many kind of shops and vehicles
16	Kuala Kedah, Kedah	20 April 2005	100º17.149' E	06º06.333' N	Intertidal; A jetty and fishing village
17	Kampung Kuala Muda, Kedah	20 April 2005	100º21.735' E	05º34.343' N	Intertidal; A jetty and fishing village
18	Sungai (Sg.) Juru, Penang	20 April 2005	100º26.083' E	05º19.772' N	River; roadside near the industrial site
19	Jetty Kuala Juru, Penang	20 April 2005	100º24.518' E	05º20.410' N	Intertidal; A fishing village and a jetty
20	A drainage near factory site at Juru, Penang	20 April 2005	100º26.011' E	05º20.105' N	Drainage; An industrial area

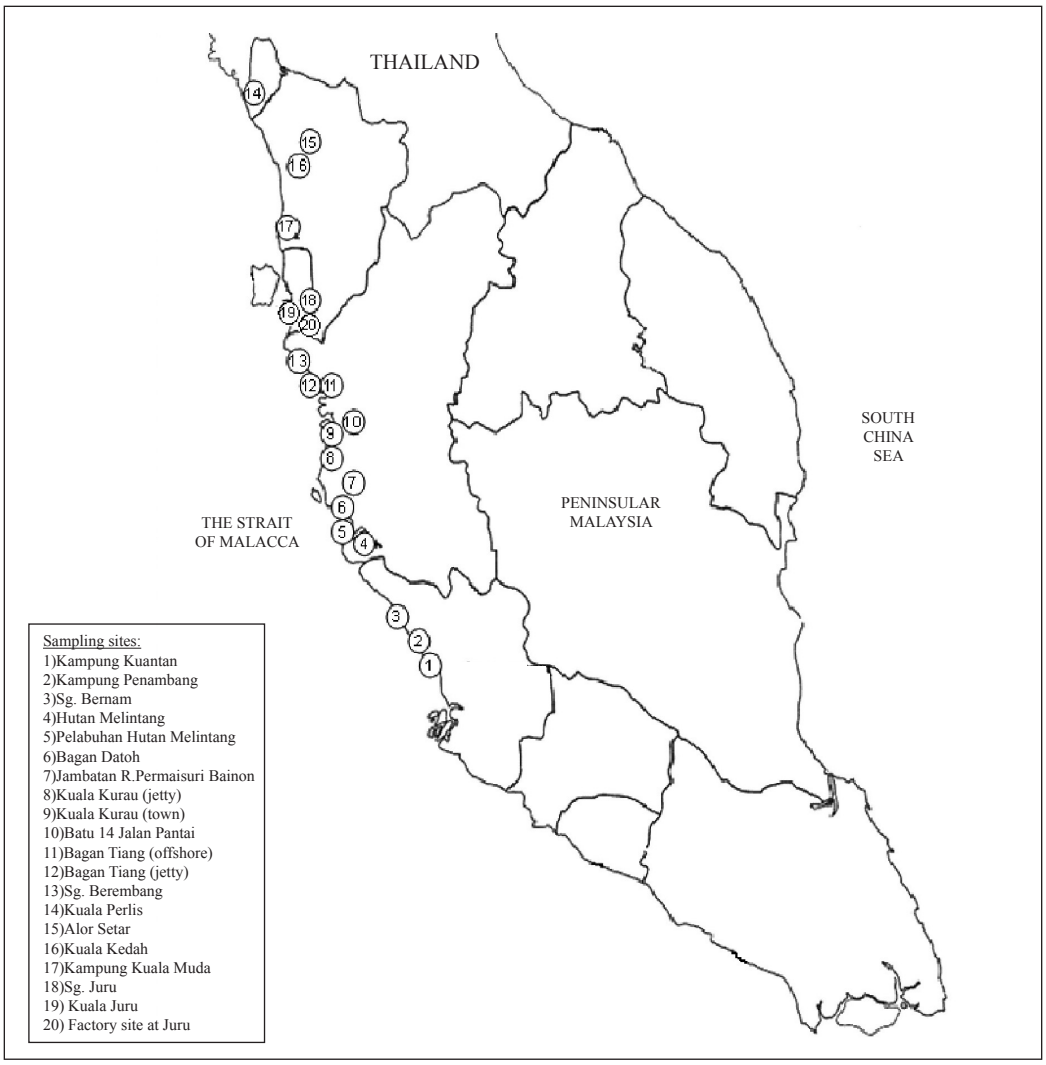

Fig. 1: Sampling locations of the surface sediments in the north western coast of Peninsular Malaysia

The quality of the method used was checked using the Certified Reference Material (CRM) for Soil (International Atomic Energy Agency, Soil-5, Vienna, Austria). The agreement between the analytical results for the reference material and its certified values for each metal were found to be satisfactory with the percentages of recovery ranging between 144% for Cd, 124.6% for Ni and 87% for Zn (Table 2). Meanwhile, the procedural blanks and quality of the control samples, made from the standard solutions for Cd, Ni, and Zn prepared from 1000 mg/L stock solution (MERCK Titrisol) of each metal, were analyzed for every five to ten samples to check for the sample accuracy.

TABLE 2
A comparison of the measured and certified concentrations (µg/g dry weight) of Cd, Ni, and Zn f or the Certified Reference Material for soil

Metal	Certified value (C)	Measured value (M)	Percentage of recovery (M/C)
Cd	1.5	2.16	144.0
Ni	1.3	1.62	124.6
Zn	368	323.24	87.8

TABLE 3
Some surface water parameters recorded *in-situ* during the sampling for all the 20 sampling sites

No.	Sampling sites	Temp (ºC)	SpC (µS/cm)	TDS (mg/L)	Salinity (ppt)	DO (mg/L)	pH
1	Kampung Kuantan	29.26	87	0.52	0.04	2.17	7.63
2	Kampung Penambang	30.18	12366	7.27	6.33	5.87	8.73
3	Sungai Bernam	31.27	765	0.44	0.33	3.09	7.62
4	Hutan Melintang	33.15	12504	7.03	6.06	4.65	8.66
5	Pelabuhan Hutan Melintang	34.30	17423	9.62	8.48	7.26	9.53
6	Bagan Datoh	33.71	10529	5.87	4.98	7.14	9.30
7	JRPB	33.02	52039	29.3	28.96	NA	10.29
8	Kuala Kurau (Jetty)	31.44	25081	14.5	13.34	3.92	8.94
9	Kuala Kurau (Town)	29.47	476.330	0.29	0.21	0.75	8.70
10	Batu 14 Jalan Pantai	29.53	380	0.23	0.16	0.79	8.40
11	Bagan Tiang (Offshore)	32.18	47416	27.1	26.51	9.03	10.13
12	Bagan Tiang (Jetty)	32.14	7971	4.559	3.81	2.49	8.51
13	Sungai Berembang	32.36	54219	30.9	30.71	6.76	9.82
14	Kuala Perlis	31.43	49657	28.9	28.53	5.58	9.70
15	Bandar Alor Setar	30.04	141	0.08	0.06	0.48	8.31
16	Jetty Kuala Kedah	30.29	1853	1.09	NA	4.60	8.81
17	Kuala Muda	33.40	33576	18.8	17.68	7.62	9.80
18	Sungai Juru	35.28	87	0.05	0.04	2.17	7.63
19	Kuala Juru	33.02	40324	40324	21.80	8.59	9.27
20	Factory site at Juru	32.11	1436	0.82	0.62	0.42	8.54

Note: Temp = temperature; SpC = specific conductivity; TDS = total dissolved solid; DO = dissolved oxygen

RESULTS AND DISCUSSION

The temperature, pH, SpC, TDS, salinity and DO recorded *in-situ* on the water surface from 20 sampling sites are given in Table 3. The range of these parameters are 29.26-35.28ºC for temperature, 87-54219 µS/cm for SpC, 0.05-40324 mg/L for TDS, 0.04-30.71 ppt for salinity, 0.42-9.03 mg/L for DO and 7.62-10.29 for pH. From the salinity data, it is clear that Kg. Kuantan (0.04 ppt), Sg. Bernam (0.33 ppt), and Sg. Juru (0.04 ppt) are the rivers with little influence from the marine seawater, while Kuala Kurau Town (0.21 ppt), Batu 14 Jalan Pantai at Kurau (0.16 ppt), Bandar Alor

TABLE 4
Total concentrations (µg/g dry weight ± standard error) Cd, Zn and Ni in the surface sediments collected from 20 sampling sites, based on the aqua-regia method

No.	Sampling site	Cd			Zn			Ni		
1	Kampung Kuantan	1.74	±	0.19	119.72	±	2.09	28.01	±	0.05
2	Kampung Penambang	1.46	±	0.03	54.68	±	0.38	25.86	±	0.30
3	Sungai Bernam	2.23	±	0.08	101.32	±	0.46	36.33	±	0.45
4	Hutan Melintang	1.63	±	0.20	83.80	±	2.14	34.33	±	0.26
5	Pelabuhan Hutan Melintang	1.69	±	0.07	71.15	±	0.90	33.78	±	0.51
6	Bagan Datoh	2.09	±	0.08	87.99	±	0.53	31.76	±	0.35
7	J.Raja Permaisuri Bainon	1.63	±	0.14	38.95	±	0.33	6.46	±	0.41
8	Kuala Kurau (Jetty)	1.70	±	0.10	74.64	±	1.05	21.82	±	0.25
9	Kuala Kurau(Town)	2.48	±	0.09	429.46	±	1.19	47.90	±	0.67
10	Batu 14 Jalan Pantai	1.69	±	0.05	88.74	±	2.06	14.21	±	0.43
11	Bagan Tiang (Offshore)	2.24	±	0.17	106.04	±	3.81	27.72	±	0.48
12	Bagan Tiang (Jetty)	1.60	±	0.09	73.22	±	3.42	25.40	±	0.30
13	Sungai Berembang	1.38	±	0.22	57.32	±	0.80	23.50	±	1.22
14	Kuala Perlis	1.42	±	0.11	55.73	±	1.32	25.02	±	0.45
15	Bandar Alor Setar	1.47	±	0.25	187.21	±	1.84	24.23	±	0.26
16	Jetty Kuala Kedah	1.09	±	0.17	53.21	±	0.73	25.75	±	0.29
17	Kuala Muda	0.79	±	0.08	33.60	±	1.01	21.08	±	0.44
18	Sungai Juru	1.40	±	0.19	461.33	±	1.86	46.61	±	0.71
19	Kuala Juru	1.24	±	0.10	317.39	±	2.48	50.28	±	0.75
20	Factory site at Juru	1.46	±	0.20	484.14	±	3.01	**73.92**	±	0.28

Setar (0.06 ppt) and the factory site in Juru (0.62 ppt) are concrete drainages potentially receiving effluents from industrial discharges or domestic wastes. Although these water parameters are difficult to explain the present metal data on the surface sediments, these aquatic parameters can, at least, indicate whether or the influence of marine seawater is significant.

The total concentrations of Cd, Ni, and Zn based on aqua-regia method for all the sampling sites are shown in Table 4, while the overall mean metal concentrations for each fraction with their total concentrations are presented in Table 5. The ranges for the total concentrations of Cd, Ni, and Zn were 0.79-2.48 µg/g dw, 6.46-73.92 µg/g dw, and 33.6-484.14 µg/g dw, respectively. In particular, the Kuala Kurau Town drainage was found to have the highest concentrations of Cd (2.48 µg/g dw), while the lowest concentration of Cd was recorded at Kuala Muda (0.79 µg/g dw). As for Zn and Ni, the highest concentration was recorded at a drainage site at the factory site at Juru Industrial area, while the lowest levels for both metals were found at Jambatan Raja Permaisuri Bainon (JRPB).

Meanwhile, the total concentrations of Cd, Ni, and Zn in the sediments collected from the north western part of Peninsular Malaysia were compared with those reported from Malaysia, as shown in Table 6. For Cd, four sites were shown to have recorded higher Cd levels [St-3 (2.23 µg/g dw), St-6 (2.09 µg/g dw), St-9 (2.48 µg/g dw), and St-11 (2.24 µg/g dw)] than the reported data in the intertidal and offshore of Peninsular Malaysia (Yap *et al.*, 2003), but significantly lower than the Cd concentrations at the Serdang industrial drainage sediments (Cd: 10.6-15.9 µg/g dw) (Yap *et*

TABLE 5
The overall mean concentrations (µg/g dw) of Cd, Zn, and Ni in the different geochemical fractions and their total concentrations in the surface sediments collected from the northern part of Peninsular Malaysia (based on 20 sampling sites)

Metal	Fraction	Min - Max	Mean ± SE
Cd	Total	0.79-2.48	1.622 ± 0.090
	Summation	0.95-4.68	2.712 ± 0.265
	F1	0.03-0.43	0.162 ± 0.025
	F2	0.04-0.38	0.187 ± 0.024
	F3	0.03-0.69	0.405 ± 0.044
	F 4	0.54-3.91	1.958 ± 0.242
Zn	Total	33.6-484.14	148.98 ± 32.962
	Summation	50.06-619.95	165.51 ± 32.567
	F1	0.37-59.37	11.447 ± 4.468
	F2	1.92-63.35	21.765 ± 5.165
	F3	11.75-86.58	39.366 ± 6.120
	F 4	17.54-413	92.932 ± 19.518
Ni	Total	6.46-73.92	31.199 ± 3.285
	Summation	10.12-75.36	29.157 ± 3.699
	F1	0.007-1.67	0.607 ± 0.113
	F2	0.007-3.3	0.926 ± 0.207
	F3	2.73-42.35	11.915 ± 2.308
	F 4	5.36-29.01	15.709 ± 1.338

Note: F1 = easily, freely, leacheable or exchangeable (EFLE), F2 = acid-reducible, F3 = oxidisable-organic and F4 = resistant

al., 2006a: 2008c) and within the Cd ranges of 6 intertidal areas in Selangor (Yap *et al.*, 2008c) and Kelana Jaya urban lakes (Ismail *et al.*, 2004) (*see* Table 6).

The range of Ni obtained from this study (6-74 µg/g dw) was comparable to that of the Kelana Jaya urban lakes (0.48-2.68 µg/g dw) (Ismail *et al.*, 2004), although wider to the Ni concentrations found in the Strait of Johore at 21.2-46.8 µg/g dw (Wood *et al.*, 1997); however, it was lower than the drainages near the industrial area in Peninsular Malaysia (121 µg/g dw) (Yap *et al.*, 2007b: 2008b). Other comparisons are also shown in Table 6.

In the study, four sites were found to have recorded higher levels of Zn than the previously reported data in Malaysia (Table 6); these were Kuala Kurau Town (429.46 µg/g dw), Sg. Juru (461.33 µg/g dw), Kuala Juru (317.4 µg/g dw) and a factory site at Juru (484.14 µg/g dw). Apparently, the three sites exceeding 400 µg/g were also comparable to most polluted drainages including the sites near a petrochemical plant, an electronic factory, a metal factory and two townships (Yap *et al.*, 2007a) and Kelana Jaya urban lakes (Ismail *et al.*, 2004) in Peninsular Malaysia (Table 6). The present Zn ranges were also found to be much higher than the Zn concentration (22.3 µg/g dry weight) found in the surface sediment of Kerteh Mangrove Forest in Terengganu (Yunus and Ong, 2008). In general, the concentrations of Cd and Zn found in the intertidal, river, and drainage sediments from the present study were also much higher than those reported in the east coast of Peninsular Malaysia, as reviewed by Shazili *et al.* (2006).

TABLE 6
Comparison of Cd, Zn, and Ni (µg/g dry weight) of the surface sediment data reported from Malaysia and this region

No.	Location	Cd	Zn	Ni	Reference
	Malaysian studies				
1.	Coast of Penang, Malaysia	BDL-6.8	73-109	NA	Seng *et al.* (1987)
2.	South China Sea	0.41-2.39	12-50	NA	Shazili *et al.* (1987)
3.	Offshore Sarawak	BDL-0.01	25-112	NA	Shazili and Mawi (1988)
4.	Offshore Terengganu, Pahang, Sarawak and Sabah	BDL-5.6	5-107	NA	Shazili *et al.* (1989)
5.	Langat River, Malaysia	3.0-37.9	71-374	NA	Sarmani (1989)
6.	Port Kelang, Malaysia	< 6.0	11-66	NA	Ismail *et al.* (1989)
7.	Bintulu coastal waters, Malaysia	1-5	39-91	NA	Ismail (1993)
8.	West of Peninsular Malaysia	<10.0	50-1400	NA	Ismail *et al.* (1993)
9.	Straits of Johore	1.70	26.1	5.4	Mat *et al.* (1994)
10.	Juru River, Malaysia	-	29-316	NA	Lim and Kiu (1995)
11.	Sarawak River, East Malaysia	-	8-48.4	NA	Lau *et al.* (1996)
12.	Johore Straits	0.11-0.36	68-231	21-47	Wood *et al.* (1997)
13.	Sepang Besar River, Malaysia	0.1-2.1	4-550	NA	Ismail and Ramli (1997)
14.	South China Sea Off Peninsular Malaysia and Borneo	0.1-0.91	18-98	NA	Shazili *et al.* (1997)
15.	Seberang Prai, Penang	0.27-4.68	30-513	NA	Ismail and Asmah. (1999)
16.	Intertidal area of the west coast of Peninsular Malaysia	0.03-1.98	3-306	NA	Yap *et al.* (2003)
17.	Kelana Jaya Lakes, Selangor	0.48-2.68	107-529	NA	Ismail *et al.* (2004)
18.	Sri Serdang Industrial Area	2.40-10.2	169-296	35-582	Yap *et al.* (2006a)
19.	Tg. Piai, Malaysia	0.72–1.19	40–43	10-11	Yap *et al.* (2006b)
20.	Sepang River, Selangor	NA	34-421	NA	Yap *et al.* (2007a)
21.	Drainage sediments from Peninsular Malaysia (6 sites)	1.46-15.9	330-484	47.0-121	Yap *et al.* (2007b)
22.	East coast of Peninsular Malaysia (10 sites)	NA	55-86	NA	Yap *et al*. (2008a)
23.	South coast of Peninsular Malaysia (5 sites)	NA	38.1-221	NA	Yap *et al.* (2008a)
24.	West coast of Peninsular Malaysia (5 sites)	NA	36-395	NA	Yap *et al.* (2008a)
25.	Intertidals and drainages, Selangor	NA	50-336	15-121	Yap *et al.* (2008b)
26.	Sri Serdang Industrial Area, Selangor	15.9	NA	NA	Yap *et al.* (2008c)
27.	Six intertidal area and 4 urban drainage sites, Selangor	1.39-3.41	NA	NA	Yap *et al.* (2008c)
28.	Kerteh Mangrove Forest in Terengganu	NA	22.3	NA	Yunus and Ong (2008)
29.	Sri Serdang Industrial Area, Selangor (1 site)	NA	219	NA	Yap *et al.* (2009)
30.	Northern part of Peninsular Malaysia	0.79-2.48	33-484	6-74	This study

Table 6: Continued

	Regional Studies				
1.	Pearl River Delta, China	1.2-3.9	46.4-533.3	6.3-71	Cheung *et al.* (2003)
2.	Coastal Alang–Sosiya, India	8.57–45.9	718.02–1,483	60–222	Reddy *et al.* (2004)
3.	Semarang, Indonesia	NA	84-259	17-36	Takarina *et al.* (2004)
4.	Mangrove area, Singapore	0.18–0.27	51–120	7.44–11.7	Cuong *et al*. (2005)
5.	Kranji and Pulau Tekong, Singapore	0.06–0.19	49–62	17–26	Cuong and Obbard (2006)
6.	Gaunabara Bay, Brazil	NA	5–755	1–3,516	Baptista-Nito *et al.* (2006)
7.	Mandovy estuary, India	NA	19.9–86	NA	Alagarsamy (2006)
8.	Western Xiamen Bay, China	0.33	139	37.4	Zhang *et al.* (2007)
9.	Kaoshiung Harbor, Taiwan	0.1–6.8	52–1,369	NA	Chen *et al.* (2007)
10.	Pearl River Estuary, China	1.84-6.43	120-478	13-318	Li *et al.* (2007)
11.	Victoria Harbour, Hong Kong	NA	52-221	NA	Chloe *et al.* (2008)
12.	Dumai coastal sediment, Indonesia (23 sites)	NA	32-88	NA	Bintal *et al.* (2008)
13.	Yantze River (intertidal zone), China	0.12–0.75	47-154	17-48	Zhang *et al.* (2009)
14.	Dumai coasts Indonesia (23 site)	0.46–1.89	31–87	7–19.9	Bintal *et al.* (2009)

Based on the cluster analysis in *Fig. 2*, it can be summarized that St-9, St-18, St-19, and St-20 (the four sites mentioned above) are grouped into the same sub-cluster, indicating that these four sites have received more contamination of Cd, Ni, and Zn, due to their higher concentrations as shown in Table 4. Among the four sites, St-18, St-19 and St-20 are located in Juru area, which was previously reported to have been polluted by heavy metals (Lim and Kiu, 1995; Yap *et al*., 2002). Therefore, the present data also confirm continued point source of industrial discharge into the Juru basin area.

The data obtained in the present study are comparable or within the range of most regional studies summarized in Table 6. The present Cd ranges are lower than those of the Coastal Alang–Sosiya (India), Kaoshiung Harbor (Taiwan) and Pearl River Estuary (China), as well as comparable to other areas. The present Zn ranges were also found to be lower than the most polluted sites from the Coastal Alang–Sosiya (India), Gaunabara Bay (Brazil) and Kaoshiung Harbor (Taiwan) and were comparable to the river in other countries, such as the Pearl River Estuary in China. As for Ni, once again, the present Ni ranges were shown to be lower than the coastal Alang–Sosiya (India), Gaunabara Bay (Brazil) and Pearl River Estuary (China), and within the ranges of those from the other areas. However, it should be noted that the elevated concentrations of metals found in the present ranges were mostly recorded at St-9, St-18, St-19 and St-20, while the metal ranges of the other sites were in fact very much comparable to other coastal areas in this region, including the recently reported from Dumai (Indonesia) (Bintal *et al.*, 2008: 2009).

Although comparisons with other reported data may give a picture of the overall contamination level in Malaysia, the environmental consequences of these metals remain uncertain. Therefore, in order to estimate possible environmental consequences of Cd, Zn, and Ni at the studied sites, the metals were compared to the Sediment Quality Guidelines of Effect Range Low (ERL) and

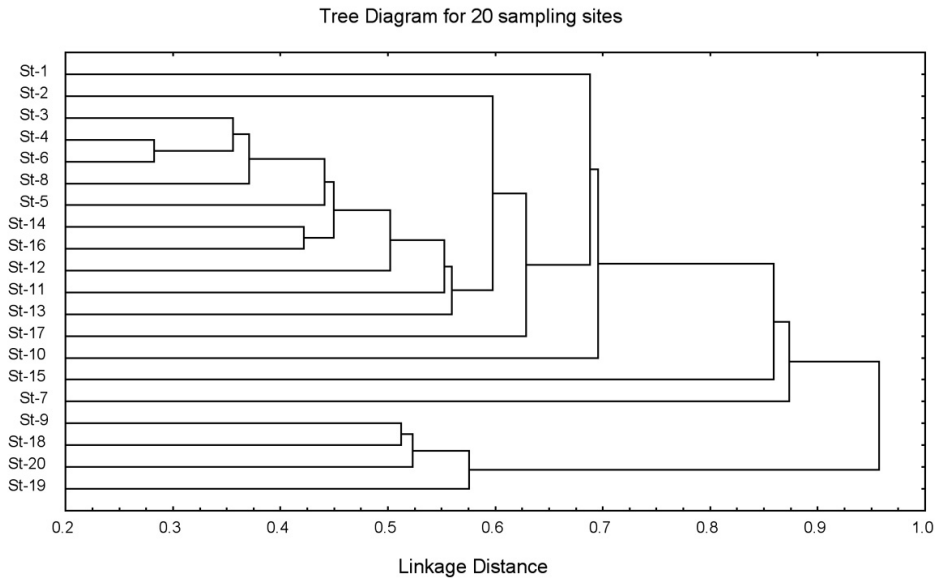

Fig. 2: Cluster analysis based on the Single Linkage Euclidean distances, on the Cd, Ni, and Zn concentrations in the sediments collected from 20 sampling sites, based on log_{10}(mean + 1) transformed data. All the sampling site numbers follow the names of the sampling sites in Table 1

Effect Range Median (ERM) proposed by Long *et al.* (1995). The findings of the present study showed that the Cd concentrations in most of the sites were between the values for ERL (1.2 µg/g) and ERM (9.6 µg/g). However, the Cd concentrations in all the sites were above the background concentration of non-contaminated sediment (0.17 µg/g), as suggested by Salomons and Forstner (1984). When compared to the Cd Sediment Quality Values (SQV) for Hong Kong (Chapman *et al.*, 1999), the present Cd ranges fell between SQV-low (1.5 µg/g) and SQV-high (9.6 µg/g), indicating a 'moderately polluted' status.

Meanwhile, the Zn concentrations in all the sites were still well below the values for the ERL (150 µg/g), except for Bandar Alor Setar and Kuala Juru (exceeding ERL value) and Kuala Kurau Town, Sg. Juru and the factory site in Juru (exceeding ERM: 410 µg/g). Similarly, all the sites were reported to be well below the SQV-low (200 µg/g) for Zn when compared to SQV for Zn (Chapman *et al.*, 1999), except for Kuala Juru which exceeded SQV-low, while Kuala Kurau Town, Sg. Juru and the factory site in Juru were found to have exceeded the SQV-high (410 µg/g), suggesting a 'highly polluted' status for the three sites.

For the concentrations of Ni, only two sites were found to be below the ERL value (20.9 µg/g), while the other sites exceeded the ERL value and the factory site in Juru exceeded the ERM value (51.6 µg/g). All the sampling sites, except for the factory site at Juru, were even still below the background concentration of non-contaminated sediment (52 µg/g for Ni), as suggested by Salomons and Forstner (1984). When compared to Ni SQV (Chapman *et al.*, 1999), all the present Ni ranges were found to exceed the SQV-low for Ni (40 µg/g for Ni), indicating a 'moderately polluted' status. However, the SQV-high for Ni has not been established.

Table 7 shows the percentages (%) of the four geochemical fractions of Cd, Zn, and Ni in the sediments collected from the northern part of Peninsular Malaysia. It is difficult to decide on the metal with the highest percentage of non-resistant fractions, but this is highly dependent on the sampling sites. In particular, cadmium was partitioned at 0.58-14.63% in the EFLE fraction,

TABLE 7
The percentages (%) of four geochemical fractions of Cd, Zn and Ni in the sediments

	CdF1	CdF2	CdF3	CdF4	NRCd	ZnF1	ZnF2	ZnF3	ZnF4	NRZn	NiF1	NiF2	NiF3	NiF4	NRNi
St-1	10.41	13.92	11.50	64.16	35.83	0.66	21.80	30.86	46.67	53.32	2.03	2.42	**22.75**	72.80	27.20
St-2	13.87	23.15	19.52	43.47	56.54	0.95	10.85	21.37	66.82	33.17	3.02	3.26	26.44	67.28	32.72
St-3	14.32	15.08	13.95	56.65	43.35	0.74	5.82	15.86	77.58	22.42	**0.03**	**0.03**	30.71	69.23	30.77
St-4	9.21	10.71	11.43	68.65	31.35	0.92	10.24	21.61	67.23	32.77	0.88	0.87	38.07	60.18	39.82
St-5	2.30	**1.30**	13.93	82.46	17.53	**0.39**	4.33	14.46	**80.82**	**19.18**	2.17	4.24	35.16	58.43	41.57
St-6	0.99	5.48	11.07	82.46	17.54	0.78	10.65	19.21	69.37	30.64	0.59	1.83	23.34	**74.24**	**25.76**
St-7	**14.63**	9.57	17.47	58.33	41.67	10.67	**28.59**	29.66	**31.07**	**68.92**	**9.24**	5.84	31.93	52.99	47.01
St-8	2.27	4.27	14.87	78.59	21.41	0.82	6.28	26.59	66.31	33.69	1.17	0.77	35.67	62.39	37.61
St-9	9.39	10.00	29.54	51.07	48.93	**15.77**	19.24	26.30	38.68	61.31	2.18	6.68	43.37	47.77	52.23
St-10	3.33	4.07	16.06	76.54	23.46	3.96	16.46	31.91	47.68	52.33	0.36	1.62	28.25	69.76	30.23
St-11	9.76	12.59	11.93	65.72	34.28	1.30	**3.13**	**35.57**	60.00	40.00	2.55	4.98	40.66	51.81	48.19
St-12	3.15	3.79	13.35	79.71	20.29	1.25	1.92	25.02	71.80	28.19	2.57	2.90	34.58	59.96	40.05
St-13	9.74	**23.65**	23.67	**42.94**	**57.06**	2.63	4.47	51.28	41.62	58.38	3.96	**7.24**	44.45	44.35	55.65
St-14	7.08	6.75	**8.43**	77.73	22.26	1.57	5.68	29.46	63.29	36.71	3.76	1.22	31.30	63.72	36.28
St-15	4.17	9.46	**30.47**	55.91	44.10	4.46	22.94	34.00	38.60	61.40	0.81	1.37	30.90	66.91	33.08
St-16	9.63	4.33	1.22	**84.82**	**15.18**	1.02	9.57	17.74	71.67	28.33	1.35	1.37	27.44	69.84	30.16
St-17	2.65	2.71	15.96	78.68	21.32	7.86	11.12	23.47	57.54	42.45	1.95	3.04	40.49	54.52	45.48
St-18	**0.58**	1.53	14.36	83.53	16.47	13.46	14.76	20.03	51.75	48.25	3.59	4.27	52.65	39.48	60.51
St-19	6.28	3.07	13.67	76.98	23.02	8.22	19.11	27.88	44.79	55.21	0.67	2.19	54.72	42.43	57.58
St-20	3.44	5.09	21.80	69.67	30.33	9.58	10.20	**13.60**	66.62	33.38	2.04	3.27	**56.20**	**38.50**	**61.51**

Note: Values in bold indicate minimum or maximum concentrations for each fraction. F1 = EFLE

1.30-23.65% in the acid-reducible fraction, 8.43-30.47% in the oxidisable-organic fraction and 42.94-84.82% in the resistant fraction.

Meanwhile, 19.18 to 68.92% of non-resistant Zn fraction was shown. In these non-resistant Zn fractions, Zn is highly associated with the oxidisable-organic fraction, accounting for 13.60-35.57% of the total Zn. Generally, the 'oxidisable-organic' fraction contributed the largest percentage of metals among the other three anthropogenic-related fractions which had been reported for intertidal and drainage sediments of Selangor (Yap *et al.*, 2008b). In particular, Zn was partitioned at 0.39-15.77% in the EFLE fraction, 3.13-28.59% in the acid-reducible fraction, and 31.07-80.82% in the resistant fraction. The Ni in the sediments is also strongly associated with the resistant fraction (38.50-74.24) and slightly bound to EFLE (0.03-9.24%), while acid-reducible phase accounts for 0.03-7.24% and oxidisable-organic fraction accounts for about 22.75-56.20% of Zn in the sediments. Meanwhile, Zn in the non-resistant fraction was found to be 25.76-61.51%. The present results on Cd and Zn are within the range reported by Yap *et al.* (2008b: 2008c) for the drainage sediment from the industrial area in Selangor.

Based on the data presented in Table 7, it was found that almost 50% (48.9%) of the total Cd concentrations were contributed by non-resistant fraction at St-9, which recorded the highest total Cd concentration. However, the highest percentage (57.1%) of Cd non-resistant was found at Sg. Berembang (St-13) although it had 1.38 μg/g dw of the total Cd concentration. This might indicate the fact that the majority (>50%) of the total Cd was contributed by anthropogenic origins. The percentages of the non-resistant fractions for Zn could also be clearly contributed by anthropogenic sources at St-9 (61.3%) and St-19 (55.2%), while the total Ni concentrations at St-9, St-18, St-19, and St-20 were mostly (>50%) contributed by anthropogenic sources. An increase in the relative importance of the non-resistant fraction was associated with contaminated conditions and this has been well documented in the literature (Ismail and Ramli, 1997; Ismail *et al.*, 2004; Yap *et al.*, 2007: 2008a, b, c). A higher percentage (>50%) of the non-resistant fraction of metals indicates the anthropogenic sources of these metals for Sepang River (Yap *et al.*, 2007a) and drainage sediments in Selangor (Yap *et al*., 2008b, c) and Sri Serdang Industrial Area (Yap *et al.*, 2009). These non-resistant metal percentages indicated that the metal concentrations were dominated by the anthropogenic sources since the non-resistant fraction of metals was mostly contributed by the anthropogenic sources (Badri and Aston, 1983; Yap *et al.*, 2002).

CONCLUSIONS

The wider ranges of Zn and Ni concentrations for the sediment collected from the north western intertidal area of Peninsular Malaysia were found when compared to the previously reported studies. The geochemical study revealed that the same sampling sites (namely Kuala Kurau town and 3 sites at Juru River basin) were clustered together, indicating a high contaminations of Cd, Zn, and Ni. The higher percentages of non-resistant fractions gathered in this study based on geochemical fractions also indicated the anthropogenic sources in the northwestern part of Peninsular Malaysia. Although this paper is just another monitoring work reporting the same phenomenon as those by Yap *et al.* (2002) and Yap *et al.* (2003), monitoring of the intertidal environment in the current study should be conducted on a regular basis. As ecotoxicologist who is concerned with the fate of the environment, the present data should provide a continued effort for future reference. Meanwhile, the elevated concentrations of Cd, Zn, and Ni that were found in some sampling sites should prompt proper actions, as well as better management and control to enhance environmentally sustainable development in Malaysia.

ACKNOWLEDGEMENTS

The authors wish to acknowledge the financial support provided through the Research University Grant Scheme (RUGS), (Vot no: 91230 and 91986) by Universiti Putra Malaysia.

REFERENCES

Alagarsamy, R. (2006). Distribution and seasonal variation of trace metals in surface sediments of the Mandovi estuary west coast of India. *Estuarine Coastal and Shelf Science*, *67*, 333–339.

Badri, M.A. and Aston, S.R. (1983). Observation on heavy metal geochemical associations in polluted and non-polluted estuarine sediments. *Environmental Pollution (Series B)*, *6*, 181-193.

Baptista-Nito, J. A., Gingele, F. X., Liepe, T. and Brehme, I. (2006). Spatial distribution of heavy metals in surficial sediments from Guanabara Bay: Rio de Janeiro, Brazil. *Environmental Geology*, *49*, 1051–1063.

Bintal, A., Ismail, A. and Yap, C. K. (2008). Distribution and speciation of Zn and Pb in coastal sediments of Dumai Sumatera, Indonesia. *Toxicological and Environmental Chemistry*, *90*, 609-623.

Bintal, A., Ismail, A., Arshad, A., Yap, C. K. and Kamarudin, M. S. (2009). Anthropogenic impacts on heavy metal concentrations in the coastal sediments of Dumai, Indonesia. *Environmental Monitoring and Assessment*, *148*, 291-305.

Chapman, P.M., Allard, P. J. and Vigers, G. A. (1999). Development of sediment quality values for Hong Kong special administrative region: A possible model for other jurisdictions. *Marine Pollution Bulletin*, *38*, 161-169.

Chen, C. W., Kao, C. M., Chen, C. F. and Dong, C. D. (2007). Distribution and accumulation of heavy metals in sediments of Kaoshiung Harbor, Taiwan. *Chemosphere*, *66*, 1431–1440.

Chloe, W.Y.T., Carman, C.I., Zhang, G., Paul, K.S.S., Qian, P. and Xiang-Dong, L. (2008). The spatial and temporal distribution of heavy metals in sediments of Victoria Harbour, Hong Kong. *Marine Pollution Bulletin*, *57*, 816–825.

Cuong, D. T. and Obbard, N. (2006). Metal speciation in coastal marine sediments from Singapore using a modified BCR sequential extraction procedure. *Applied Geochemistry*, *21*, 1335–1346.

Cuong, D. T., Bayen, S., Wurl, O., Subramaniam, K., Wong, K. K. S., Sivasothi, N. and Obbard, J. P. (2005). Heavy metal contamination in mangrove habitats of Singapore. *Marine Pollution Bulletin*, *50*, 1713-1744.

Ismail, A. (1993). Heavy metal concentration in sediment of Bintulu, Malaysia. *Marine Pollution Bulletin*, *26*, 706-707.

Ismail, A. and Asmah, M. I. N. (1999). Copper, zinc, lead and cadmium in intertidal mollusks and sediment of Seberang Perai coastline, Malaysia. Paper presented at the *Fourth Princess Chulabhorn International Science Congress*, Bangkok, Thailand.

Ismail, A., Badri, M. A. and Ramlan, M. N. (1993). The background levels of heavy metals concentration in sediments of the west coast of Peninsular Malaysia. *The Science of the Total Environment, Supplement*, *1993* (suppl), 315-323.

Ismail, A., Yap, C. K. and Chan, F. F. (2004). Concentrations of Cd, Cu and Zn in sediments collected from urban lakes at Kelana Jaya, Peninsular Malaysia. *Wetland Science*, *2*(4), 248-258.

Ismail, A., Idris, B. A. G. and Sukal, R. (1989). Distribution of heavy metals in sediment of Port Kelang. In *Proceeding of 12th Anniversary Seminar Malaysian Society of Marine Sciences* (pp. 79-282). November 1989, Universiti Malaya, Kuala Lumpur.

Ismail, A. and Ramli, R. (1997). Trace metals in sediments and molluscs from an estuary receiving pig farms effluent. *Environmental Technology*, *18*, 509-515.

Lau, S., Mohamed, M. and Suut, S. (1996). Logam berat di dalam sediment sebagai penyurih kepada punca pencemaran Sungai Sarawak. *Malaysian Journal of Analytical Sciences*, *2*, 365–371 (In Malay).

Li, Q. S., Wu, Z. F., Chu, B., Zhang, N., Czi, S. S. and Fang, J. H. (2007). Heavy metals in the coastal wetland sediments of the Pearl River Estuary, China. *Environmental Pollution*, *149*, 158-164.

Lim, P. E. and Kiu, M. Y. (1995). Determination and speciation of heavy metals in sediments of the Juru River, Penang, Malaysia. *Environmental Monitoring and Assessment*, *35*, 85-95.

Long, E.R., Macdonald, D.D., Smith, S.L. and Calder, F.D. (1995). Incidence of adverse biological effects within ranges of chemical concentrations in marine and estuarine sediments. *Environmental Management*, *19*, 81-97.

Mat, I., Maah, M. J. and Yahya, M. S. (1994). The status of trace metal pollution in inter-tidal sediments from the Straits of Tebrau, Malaysia. *Jurnal Sains*, *2*(2), 221-228.

Reddy, M. S., Basha, S., Kumar, V. G. S., Joshi, H. V. and Ramachandraiah, G. (2004). Distribution, enrichment and accumulation of heavy metals in coastal sediments of Alang-Sosiya ship scrapping yard, India. *Marine Pollution Bulletin*, *48*, 1055–1059.

Salomons, W. and Förstner, U. (1984). *Metal in Hydrocycle*. Berlin: Springer.

Sarmani, S.B. (1989). The determination of heavy metals in water, suspended materials and sediment from Langat River, Malaysia. *Hydrobiologia*, 176/177, 233–238.

Seng, C.E., Lim, P. P. E. and Ang, T. T. (1987). Heavy metal concentrations in coastal seawater and sediments off Prai Industrial Estate, Penang, Malaysia. *Marine Pollution Bulletin*, *18*, 611-612.

Shazili, N. A. and Mawi, S. (1988). Trace metals in sediment cores from the South China Sea off Sarawak. In A.K.M. Mohsin and M. I. Mohamed (Eds.), *Ekspedisi Matahari '87. A study of the offshore waters of the Malaysian EEZ* (pp. 69-75). Faculty of Fisheries and Marine Sciences, UPM. Occasional Publication, No. 8.

Shazili, N. A., Mohammad, A. R., Arima, S. and Higashikawa, S. (1987). Trace metals in sediments and benthic organisms from the south western portion of the South China Sea. In A.K.M. Mohsin, A. R. Rahman and M. A. Ambak (Eds.), *Ekspedisi Matahari '86. A study of the offshore waters of the Malaysian EEZ* (pp. 77-84). Faculty of Fisheries and Marine Sciences, UPM. Occasional Publication, No. 4.

Shazili, N. A., Mohamed, C. A. R. and Yaakod, R. (1989). Heavy metals in the sediments of the South China Sea. In *Proceedings of the 12th Annual Seminar of the Malaysian Society of Marine Sciences* (pp. 99-106).

Shazili, N. A., Husain, M. L., Rashid, M. K. A. and Nordin, A. (1997). Surface sediment metal distribution of the South China Sea off Peninsular Malaysia and Borneo. Paper presented at the *International Marine Science Conference*, 25th-27th August, 1997, Terengganu.

Shazili, N. A. M., Yunus, K., Ahmad, A. S., Abdullah, N. and Rashid, M. K. A. (2006). Heavy metal pollution status in the Malaysian aquatic environment. *Aquatic Ecosystem Health and Management*, *9*(2), 137-145.

Takarina, N. D., David, R. B. and Micheal, J .R. (2004). Speciation of heavy metal in coastal sediments of Semarang, Indonesia. *Marine Pollution Bulletin*, *49*, 854-874.

Wood, A. K., Ahmad, Z., Shazili, N. A., Yaakob, R. and Carpenter, R. (1997). Geochemistry of sediments in Johore Strait between Malaysia and Singapore. *Continental Shelf Research*, *10*, 1207-1228.

Yap, C. K., Ismail, A. and Tan, S. G. (2002). Concentrations of Cu and Pb in the offshore and intertidal sediments of the west coast of Peninsular Malaysia. *Environment International*, *28*, 467-479.

Yap, C. K., Ismail, A. and Tan, S. G. (2003). Cd and Zn concentrations in the Straits of Malacca and intertidal sediments of the west coast of Peninsular Malaysia. *Marine Pollution Bulletin*, *46*, 1341-1358.

Yap, C. K., Ismail, A., Pang, B. H., Yeow, K. L., Tan, S, G. and Siraj, S. S. (2006a). Elevated heavy metal concentrations in surface sediments collected from the drainages of the Sri Serdang Industrial Area, Malaysia. *Malaysian Applied Biology*, *35*(2), 35-40.

Yap, C. K., Choh, M.S., Franklin, E.B., Ismail, A. and Tan, S.G. (2006b). Comparison of heavy metal concentration in surface sediment of Tanjung Piai Wetland with other sites receiving anthropogenic inputs along the southwestern coast of Peninsular Malaysia. *Wetland Science*, *4*, 48-57.

Yap, C. K., Ismail, A., Low, C. H. and Tan, S. G. (2007a). Interpretation of Cu and Zn contamination in the aquatic environment of Peninsular Malaysia with special reference to a polluted river, Sepang River. *Wetland Science*, *5*(4), 311-321.

Yap, C. K., Pang, B. H., Fairuz, M. S., Hoo, Y. I. and Tan, S. G. (2007b). Heavy metal (Cd, Cu, Ni, Pb, and Zn) pollution in surface sediments collected from drainages receiving different anthropogenic sources from Peninsular Malaysia. *Wetland Science*, *5*(2), 97-104.

Yap, C. K., Cheng, W. H. and Tan, S. G. (2008a). Comparative studies of concentrations of Cu and Zn in the surface intertidal sediments collected from east, south and west coasts of Peninsular Malaysia. *Asian Journal of Water, Environment and Pollution*, *5*(2), 23-29.

Yap, C. K., Fairuz, M. S., Cheng, W. H. and Tan, S. G. (2008b). Distribution of Ni and Zn in the surface sediments collected from drainages and intertidal area in Selangor. *Pertanika Journal of Tropical Agricultural Science*, *31*(1), 79-90.

Yap, C. K., Fairuz, M. S. and Cheng, W. H. (2008c). How elevated of Cd, Cu and Pb levels in the surface sediments collected from drainage receiving metal industrial effluents ? Comparison with metal industrial drainage and intertidal sediments in Selangor, Malaysia. *Asian Journal of Microbiology, Biotechnology and Environmental Sciences*, *10*(2), 385-391.

Yap, C. K., Yazdani, M. and Tan, S.G. (2009). The importance of the identification of point sources in a river receiving industrial metal effluents at the Serdang Industrial Area, Selangor. *Journal of Sustainability Science and Management*, *4*(2), 18-26.

Yunus, K. and Ong, M. C. (2008). Distribution of some geochemical elements in the surface sediment of Kerteh Mangrove Forest, Terengganu, Malaysia. *Sains Malaysiana*, *37*(4), 337–340.

Zhang, L., Ye, X., Feng, H., Jing, Y., Ouyang, T., Yu, X., Liang, R., Gao, C. and Chen, W. (2007). Heavy metal contamination in western Xiamen Bay sediments and its vicinity, China. *Marine Pollution Bulletin*, *54*, 974–982.

Zhang, W., Feng, H., Chang, J., Qu, J., Xie, H. and Yu, X. (2009). Heavy metal contamination in surface sediments of Yangtze River intertidal zone: An assessment from different indexes. *Environmental Pollution*, *157*, 1533–1543.

ISSN: 0128-7680
Pertanika J. Sci. & Technol. **19 (1)**: 109 – 116 (2011)

A Description of an Automorphism of a Non-Split Metacyclic *p*-Group

Idham Arif Alias
Institute for Mathematical Research, Universiti Putra Malaysia,
43400 UPM, Serdang, Selangor, Malaysia
E-mail: idham@math.upm.edu.my

ABSTRACT

A map on a group is not necessarily an automorphism on the group. In this paper we study the necessary and sufficient conditions for a map on a non-split metacyclic *p*-group to be an automorphism, where we only consider *p* as an odd prime number. The metacyclic group can be defined by a presentation and it will be beneficial to have a direct relation between the parameters in the presentation and an automorphism of the group. We consider the action of an automorphism on the generators of the group mentioned. Since any element of a metacyclic group will be mapped to an element of the group by an automorphism, we can conveniently represent the automorphism in a matrix notation. We then use the relations and the regularity of the non-split metacyclic *p*-group to find conditions on each entry of the matrix in terms of the parameters in its presentation so that such a matrix does indeed represent an automorphism.

Keywords: Automorphism, matrix notation, non-split metacyclic *p*-group

INTRODUCTION

An automorphism of a non-split metacyclic *p*-group *P* where *p* is an odd prime, will be represented by a matrix notation $\left[\begin{smallmatrix} i & r \\ j & s \end{smallmatrix}\right]$ and denoted by φ, and we write $\varphi \sim \left[\begin{smallmatrix} i & r \\ j & s \end{smallmatrix}\right]$. Our aim is to find conditions on the integers i, j, r and s in terms of parameters in a presentation of the group *P*. We are able to prove that the conditions are sufficient by using the result established by Menegazzo (1993) regarding the order of the automorphism group of a non-split metacyclic *p*-group for an odd prime *p* so that φ does indeed represent an automorphism of the group *P*.

In this paper we show explicitly that the structure of the automorphism group *Aut(P)* of the group *P* mentioned above, depends on the parameters in the presentation of *P*. This result paves the way to find a set of generators and then the class of the automorphism group. This will be the subject of further work. Our approach is direct and computational and therefore different from approach by Bidwell and Curran (2006) who have previously studied the automorphism group of a non-split metacyclic *p*-group.

MATERIALS AND METHODS

We represent an automorphism of the group *P* in a matrix notation and find the direct connection between the entries of the matrix, and the parameters in a presentation of *P*. We recall that if *P* is a metacyclic *p*-group where *p* is a prime number, then the presentation of *P* can be written as

$$P = < x, y \mid x^{p^m} = 1, y^{p^t} = x^{p^q}, yxy^{-1} = x^{1+p^n} > \quad (1)$$

Received: 31 December 2009
Accepted: 10 June 2010

where the parameters m, t, q and n satisfy certain conditions as established by King (1973). We also define any map on the group P by $\varphi(x) = x^i y^j$ and $\varphi(y) = x^r y^s$ where we consider i and r as integers modulo p^m while j and s are considered modulo p^t. The third relation in the presentation above implies that any element of P can be written uniquely in the form $x^\mu y^\upsilon$, where $0 \le u < p^m$ and $0 \le v < p^t$. Therefore we represent φ by the matrix notation $\begin{bmatrix} i & r \\ j & s \end{bmatrix}$ and write $\varphi \sim \begin{bmatrix} i & r \\ j & s \end{bmatrix}$. This method is similar to the method used by Schulte (2001).

By referring to Theorem 3.2 in a paper written by King (1973), we find that the non-split case can be divided into four cases:
Case 1: $2 \le n < q < m \le t$ where $m \le 2n$,
Case 2: $1 \le n < q < m \le t$ where $2n < m \le q + n$,
Case 3: $3 \le n < q < t < m \le 2n$ and
Case 4: $2 \le n < q < t < m$ where $2n < m \le q + n$.

We will need the following results which will be used throughout this paper.

Lemma 2.1 $(g_1 g_2)^{p^k} = g_1^{p^k} g_2^{p^k}$ for any $g_1, g_2 \in P$ and $k \ge m - n \ge 1$.

Proof. The proof is straightforward using the fact that the metacyclic p-group is a regular group.▪

From the third relation in (1) we have $yx = x^{1+p^n} y$. By putting $\alpha = 1 + p^n$ then it follows that $yx = x^\alpha y$. Note that α will have this meaning throughout this paper.

Lemma 2.2 Let x, y, be the generators of P and u, v be integers with $v > 0$. Then $y^v x^u = x^{u\alpha^v} y^v$.

Proof. This result follows from the third relation in P which is $yx = x^{1+p^n} y$. ▪

Before we proceed we need the following definition.

Definition 2.1 Let u > 0 and $v \ge 1$.

We define $\Lambda(u, v)$as

$$\Lambda(u,v) = \begin{cases} 1 + \alpha^u + \alpha^{2u} + \ldots + \alpha^{(v-1)u}, & v > 1 \\ 1, & v = 1 \end{cases}$$

The following lemma is the result of direct calculation.

Lemma 2.3 Let u and v be integers, $u > 0, v > 1$. Then $\Lambda(u, v)(\alpha^u - 1) = \alpha^{uv} - 1$.

We need to write a power of $(x^u y^v)$ as a product of a power of x and a power of y and we write the proof by using induction.

Lemma 2.4 If x and y are the generators of the group P, u is any integer, $v > 0$ and $w > 1$ then $(x^u y^v)^w = x^{u\Lambda(v,w)} y^{vw}$.

Proof. For $u = 0$ the result is trivial.

Consider $u > 0$. For $w = 1$ the result is clear. Assume the result is true for $w - 1$. Then

$$(x^u y^v)^w = (x^u y^v)^{w-1} x^u y^v = x^{u\Lambda(v,w-1)} y^{v(w-1)} x^u y^v = x^{u\Lambda(v,w-1)} x^{u\alpha^{v(w-1)}} y^{vw} = x^{u\Lambda(v,w)} y^{vw}.$$

By induction the result is true for integers $w \ge 1$.

For $u < 0$ the same proof applies on replacing u by $-u'$ for a positive integer u'.▪

Next, we need quite precise information about the smallest power of p dividing terms in binomial coefficients. Thus we have the following series of lemmas and corollaries where we use the notation $p^k \| c$ to indicate that p^k divides c but p^{k+1} does not divide c.

Lemma 2.5 Let $p^{\epsilon} \| w$ where $\epsilon > 0$. If $2 \le k \le w$ then the power of p dividing $\binom{w}{k} p^{ku}$ is at least $p^{\epsilon + 2u}$ for all $u \ge 1$.

Proof. We first consider the case $2 \le k < p^{\epsilon}$.

Write $k = lp^{v}$ for a positive integer l where $(l, p) = 1$. It is clear that the power of p dividing k is the same as the power of p dividing $w– k$, so that the power of p dividing $(k–1)!$ is the same as that dividing $(w–1)\,(w-2)...(w–k+1)$. Now since $k < p^{\epsilon}$ we have $v < \epsilon$. Hence the power of p dividing

$$\binom{w}{k} p^{ku} = \frac{w(w-1)(w-2)...(w-k+1)}{k(k-1)!} p^{ku}$$

is $p^{\epsilon - v + ku}$.

If $v = 0$ then the proof is complete since $\epsilon + ku \ge \epsilon + 2u$ for $2 \le k < p^{\epsilon}$.

For $v \ne 0$, since $u \ge 1$ and $lp^{v} \ge 2 + v$ for $p \ge 3$ then

$$\epsilon - v + ku = \epsilon - v + lp^{v}u = \epsilon + 2u + (lp^{v} - 2)u - v \ge \epsilon + 2u.$$

This completes the proof for the case $2 \le k < p^{\epsilon}$.

We now consider the case $k \ge p^{\epsilon}$.

Then it is enough to observe that $ku \ge p^{\epsilon}u \ge (\epsilon + 2)u \ge \epsilon + 2u$ since $p^{\epsilon} \ge \epsilon + 2$ for $p \ge 3$. Hence $p^{\epsilon + 2u}$ divides $\binom{w}{k} p^{ku}$ for $k \ge p^{\epsilon}$. ▪

Corollary 2.6 If $p^{\epsilon} \| w$ for $w \ge 2$ and u and c are integers with $u \ge 1, (c, p) = 1$, then for an integer k

$$(1 + cp^{u})^{w} = 1 + cwp^{u} + kp^{\epsilon + 2u}.$$

By using Corollary 2.6 we have:

Corollary 2.7 Let p be an odd prime number and n be a positive integer. Then

a) $p^{n+k} \| (\alpha^{p^{k}} - 1)$ for all integers $k \ge 0$.

b) $\Lambda(u, v) \equiv v + 2^{-1}uv(v-1)p^{n} (mod\ p^{2n})$.

The following corollary relies on Lemma 2.3 and Corollary 2.7(b).

Corollary 2.8 Let u and v be integers, $u > 0$, $v > 1$. Then

$$\alpha^{u} - \alpha \equiv (u-1)p^{n} + 2^{-1}u(u-1)p^{2n} (mod\ p^{3n}).$$

Lemma 2.9 Let φ be an automorphism of P where $\varphi \sim \begin{bmatrix} i & r \\ j & s \end{bmatrix}$. If x, y are generators of P and m, n are parameters in the presentation (1) of P then

$$x^{r + i\alpha^{s} - r\alpha^{j}} = x^{i(\Lambda(j,\, p^{n}) + \alpha^{jp^{n}})} y^{jp^{n}}.$$

In particular, if $m \le 2n$ then by Corollary 2.7, we obtained

$$x^{r + i\alpha^{s} - r\alpha^{j}} = x^{i\alpha} y^{jp^{n}}.$$

Proof. These results are derived by applying the automorphism φ to both sides of the relation $yxy^{-1} = x^{1+p^n}$ and using the Lemmas 2.1, 2.2 and 2.4.▪

Definition 2.2 Let G be a group. Then G is a 2-generator group if G can be generated by two elements but no smaller set of elements generates G.

We note that if G is a group then $GL(n, G)$ is to denote the general linear group over G of dimension n.

We also note that the intersection of all the maximal subgroups of a non-trivial finite group G is called the Frattini subgroup of G and is denoted by $\Phi(G)$.

Lemma 2.10 If $\varphi \in Aut(P)$ where $\varphi \sim \begin{bmatrix} i & r \\ j & s \end{bmatrix}$ then $is - rj$ is not congruent to zero modulo p.
Proof. Since P is a 2-generator group, $P/\Phi(P) \cong Z_p \times Z_p$, and φ defines an automorphism on $P/\Phi(P)$ with matrix $\begin{bmatrix} i & r \\ j & s \end{bmatrix}$, where i, j, r and s are taken modulo p. The matrix is thus in $GL(2, P)$ and so $is - rj$ is not congruent to zero modulo p. ▪

RESULTS AND DISCUSSIONS

In the following theorem we provide the necessary and sufficient conditions for φ to be an automorphism of the group P.

Theorem 3.1 Let P be a non-split metacyclic p-group and φ is a map on P which is represented by $\varphi \sim \begin{bmatrix} i & r \\ j & s \end{bmatrix}$. Then $\varphi \in Aut(P)$ if and only if
i) $j \equiv 0 (mod\ p^{t-n})$,
ii) $j \equiv 1 (mod\ p^{m-q})$ (for cases 1 & 2) or $i \equiv 1 + rp^{t-q} (mod\ p^{m-q})$ (for cases 3 & 4),
iii) $s \equiv 1 + cp^{q-n} (mod\ p^{m-n})$ where $j = cp^{t-n}$ for $0 \le c < p^n$ and
iv) $r \in Z_{p^m}$.

Proof. Let $\varphi \sim \begin{bmatrix} i & r \\ j & s \end{bmatrix}$ and $\varphi \in Aut(P)$.
i) For all cases, $j \equiv 0 (mod\ p^{t-n})$ follows immediately from Lemma 2.9 since $jp^n \equiv 0 (mod\ p^t)$. This result also implies that i and s are not congruent to zero modulo p since from Lemma 2.10, $is - rj$ is not congruent to zero modulo p.
ii) Write $j = cp^{t-n}$ for an integer c where $0 \le c < p^n$.

In cases 1 and 2 where $m \le t$, using Corollary 2.6 we have $\alpha^j \equiv 1 (mod\ p^t) \equiv 1 (mod\ p^m)$, which also implies $\alpha^{jp^n} \equiv 1 (mod\ p^m)$ and $\Lambda(j, p^n) \equiv p^n (mod\, p^m)$. So by Lemma 2.9 we have $x^{r+i\alpha^s - r} = x^{i\alpha} y^{cp^t} = x^{i\alpha} x^{cp^q}$. This implies that

$$i(\alpha^s - \alpha) \equiv cp^q (mod\, p^m). \tag{2}$$

In case 1, $\alpha^s - \alpha \equiv (s-1)p^n (mod\ p^m)$ by Corollary 2.8 since $m \le 2n$. Hence putting this into (2) we obtain

$$i(s-1)p^n \equiv cp^q (mod\ p^m) \tag{3}$$

and so,

$$s \equiv 1 + i^{-1} cp^{q-n} (mod\ p^{m-n}). \tag{4}$$

In case 2, since $m > 2n, \alpha^s - \alpha = (s-1)p^n + kp^{2n}$, for an integer k by the same corollary. Putting this into (2) we have $i((s-1)p^n + kp^{2n}) \equiv cp^q (mod\ p^m)$. Hence

$i((s-1)+kp^n) \equiv cp^{q-n}(mod\ p^{m-n})$ so that

$$s \equiv 1 + i^{-1}cp^{q-n} - kp^n(mod\ p^{m-n}). \tag{5}$$

We now calculate i modulo p^{m-q} in cases 1 and 2. By using the relation $y^{p^t} = x^{p^q}, t \geq m-n, q \geq m-n$ and Lemma 2.1 we have $\varphi(y^{p^t}) = (x^r)^{p^t}(y^s)^{p^t} = (y^s)^{p^t} = x^{sp^q}$

where $(x^r)^{p^t} = 1$ since $t \geq m$ and
$\varphi(x^{p^q}) = (x^i)^{p^q}(y^j)^{p^q} = (x^i)^{p^q}y^{cp^{t-n+q}} = (x^i)^{p^q}(y^{p^t})^{cp^{q-n}} = (x^i)^{p^q}(x^{p^q})^{cp^{q-n}} = x^{ip^q+cp^{2q-n}}$.

Hence $sp^q \equiv ip^q + cp^{2q-n}(mod\ p^m)$. Therefore

$$i \equiv s - cp^{q-n}(mod\ p^{m-q}). \tag{6}$$

In modulus p^{m-q}, from (4) and (5) we see that $s \equiv 1 + i^{-1}cp^{q-n}$ since $n \geq m-q$. Putting this s into (6) and calculating modulo p^{m-q} we have

$$\begin{aligned} i &\equiv 1 + i^{-1}cp^{q-n} - cp^{q-n} \\ &\equiv W - (W-1)i \\ &\equiv W - Wi + i \end{aligned}$$

where $W = 1 + i^{-1}cp^{q-n}$. Thus $Wi \equiv W\ (mod p^{m-q})$ or $W(i-1) \equiv 0 (mod p^{m-q})$ which implies $i \equiv 1 (mod p^{m-q})$ since $W \equiv 1 (mod p)$ and so W is invertible modulo p^{m-q}. Hence we obtain necessity of condition (ii) for cases 1 and 2.

In cases 3 and 4 it is a bit more complicated due to the fact that $t < m$. We first calculate α^j and $\Lambda(j, p^n)$ modulo p^m.

By Corollary 2.6, $\alpha^j = (1+p^n)^{cp^{t-n}} = 1 + cp^t + kp^{t+n} \equiv 1 + cp^t (mod p^m)$ and so, $(\alpha^j)^l \equiv (1+cp^t)^l \equiv 1 + lcp^t + kp^{2t+\epsilon} \equiv 1 + lcp^t (mod p^m)$ for integers l, k and ϵ where $\epsilon \geq 0$. Hence by calculating modulo p^m,

$$\begin{aligned} \Lambda(j, p^n) &\equiv 1 + (1+cp^t) + ... + (1+cp^t)^{p^n-1} \\ &\equiv p^n + cp^t(1 + 2 + ... + (p^n - 1)) \\ &\equiv p^n + 2^{-1}cp^t p^n(p^n - 1) \\ &\equiv p^n. \end{aligned}$$

It is also clear that $\alpha^{jp^n} \equiv 1 (mod p^{n+t}) \equiv 1 (mod p^m)$.
So by Lemma 2.9 we have $x^{r+i\alpha^s - r\alpha^j} = x^{i\alpha}\ y^{cp^t} = x^{i\alpha}\ x^{cp^q}$. This implies

$$i(\alpha^s - \alpha) \equiv r(\alpha^j - 1) + cp^q \equiv rcp^t + cp^q (mod\ p^m). \tag{7}$$

In case 3, $\alpha^s - \alpha \equiv (s-1)p^n (mod\ p^m)$ by Corollary 2.8 since $m \leq 2n$. Hence putting this into (7), $i(s-1)p^n \equiv rcp^t + cp^q (mod\ p^m)$ and so,

$$s \equiv 1 + i^{-1}cp^{q-n}(1 + rp^{t-q})(mod\ p^{m-n}). \tag{8}$$

In case 4 since $m > 2n, \alpha^s - \alpha = (s-1)p^n + k'p^{2n}$, for an integer k' by the same corollary. Putting this into (7) we have $i((s-1)p^n + k'p^{2n}) \equiv rcp^t + cp^q (mod\ p^m)$ and so,

$$s \equiv 1 + i^{-1}cp^{q-n}(1 + rp^{t-q}) - k'p^n (mod\ p^{m-n}). \tag{9}$$

We now calculate i modulo p^{m-q} in cases 3 and 4. By using the relation $y^{p^t} = x^{p^q}, t \geq m-n$ and $q \geq m-n$ and Lemma 2.1 we have

$$\varphi(y^{p^t}) = (x^r)^{p^t}(y^s)^{p^t} = x^{rp^t + sp^q} \text{ and}$$

$$\varphi(x^{p^q}) = (x^i)^{p^q}(y^j)^{p^q} = x^{ip^q}\, y^{cp^{t-n+q}} = x^{ip^q + cp^{2q-n}}.$$

Hence $rp^t + sp^q \equiv ip^q + cp^{2q-n} (mod\ p^m)$ and so we have

$$i \equiv s + rp^{t-q} - cp^{q-n} (mod\ p^{m-q}). \tag{10}$$

In modulus p^{m-q}, from (8) and (9) we see that $s \equiv 1 + i^{-1}cp^{q-n}(1 + rp^{t-q})$since $n \geq m-q$. Putting this s into (10) and calculating modulo p^{m-q} we have

$$\begin{aligned} i &\equiv 1 + i^{-1}cp^{q-n}(1 + rp^{t-q}) + rp^{t-q} - cp^{q-n} \\ &\equiv (1 + rp^{t-q})(1 + i^{-1}cp^{q-n}) - cp^{q-n} \\ &\equiv (1 + rp^{t-q})W - (W-1)i \end{aligned}$$

where $W \equiv 1 + i^{-1}cp^{q-n} (mod p^{m-q})$ as seen in cases 1 and 2. It follows that $W(i-1) \equiv Wrp^{t-q} (mod p^{m-q})$ and since W is invertible modulus p^{m-q}, this gives $i \equiv (1 + rp^{t-q}) (mod p^{m-q})$ which is the necessity of condition (ii) of the theorem for cases 3 and 4.

(iii) In cases 1 and 3, calculating s modulo p^{m-n} is more simple due to the fact that $m \leq 2n$.

Since $i \equiv 1 (mod p^{m-q})$ in case 1, we have $i = 1 + zp^{m-q}$ for an integer z. Note that $p^{q-n} \equiv p^{q-n}(1 + zp^{m-q}) (mod\ p^{m-n})$. Substituting this into (4) so that calculating modulo p^{m-n},

$$\begin{aligned} s &\equiv 1 + i^{-1}cp^{q-n} \\ &\equiv 1 + i^{-1}cp^{q-n}(1 + zp^{m-q}) \\ &\equiv 1 + i^{-1}cp^{q-n}i \\ &\equiv 1 + cp^{q-n}. \end{aligned}$$

This gives the necessity of condition (iii) for case 1.
Similarly, since $i \equiv 1 + rp^{t-q} (mod\ p^{m-q})$ in case 3, we have $i = 1 + rp^{t-q} + z'p^{m-q}$ for an integer z'. Note that $p^{q-n}(1 + rp^{t-q}) \equiv p^{q-n}(1 + rp^{t-q} + z'p^{m-q}) (mod\ p^{m-n})$ so that substituting this into (8) and calculating modulo p^{m-n},

$$\begin{aligned} s &\equiv 1 + i^{-1}cp^{q-n}(1 + rp^{t-q}) \\ &\equiv 1 + i^{-1}cp^{q-n}(1 + rp^{t-q} + z'p^{m-q}) \end{aligned}$$

$$\equiv 1 + i^{-1}cp^{q-n}i$$

$$\equiv 1 + cp^{q-n}.$$

This gives the necessity of condition (iii) for case 3.

Now we calculate s modulo p^{m-n} in cases 2 and 4. Since $m > 2n$ in these two cases, the proof is harder and we divide into two subcases as follows:

a) If $q \leq 2n$

then $m \leq q + n \leq 3n$. Hence from Corollary 2.8,

$$\alpha^s - \alpha \equiv (s-1)p^n + 2^{-1}s(s-1)p^{2n}(mod\ p^m).$$

But from (5) and (9), $s - 1 \equiv 0(mod\ p^{q-n})$ since $n \geq q - n$ and so $(s-1)p^{2n}$ is divisible by $p^{q-n}p^{2n} = p^{q+n} \equiv 0(mod\ p^m)$. Thus $\alpha^s - \alpha \equiv (s-1)p^n(mod\ p^m)$.

In case 2, using this in (2) we obtain $i(s-1)p^n \equiv cp^q(mod\ p^m)$ so that $i(s-1) \equiv cp^{q-n}(mod\ p^{m-n})$ which implies $s \equiv 1 + i^{-1}cp^{q-n}(mod\ p^{m-n})$. Then the rest of the proof to obtain $s \equiv 1 + cp^{q-n}(mod\ p^{m-n})$ is the same as in case 1.

In case 4, using this in (7) we obtain $i(s-1)p^n \equiv rcp^t + cp^q \,(\mathrm{mod}\ p^m)$ and so $s \equiv 1 + i^{-1}cp^{q-n}(1 + rp^{t-q})(mod\ p^{m-n})$. Then the rest of the proof to obtain $s \equiv 1 + cp^{q-n}(mod p^{m-n})$ is the same as in case 3.

b) If $q > 2n$

then from (5) and (9), $s = 1 + fp^v$ where f is prime to p and $v \geq n$. Now we calculate $\alpha^s - \alpha$ modulo p^q.

We have i and α are invertible modulo p^q since both are congruent to one modulo p. Hence from (2) and (7) and calculating modulo p^q,

$$\begin{aligned} 0 &\equiv (\alpha^s - \alpha) \\ &\equiv (\alpha^{s-1} - 1) \\ &\equiv (\alpha^{fp^v} - 1) \\ &\equiv (1 + \alpha^{p^v} + \alpha^{2p^v} + ... + \alpha^{(f-1)p^v})(\alpha^{p^v} - 1) \text{ (by Lemma 2.3).} \end{aligned}$$

But $(1 + \alpha^{p^v} + \alpha^{2p^v} + ... + \alpha^{(f-1)p^v}) \equiv f\ (mod\ p)$ and thus it is not congruent to zero modulo p since f is prime to p. Hence $\alpha^{p^v} - 1 \equiv 0\ (mod\ p^q)$. Since by Corollary 2.7 the highest power of p dividing $\alpha^{p^v} - 1$ is p^{n+v}, we must have p^{n+v} is divisible by p^q so that p^v is divisible by p^{q-n}. Thus $s - 1 = fp^v \equiv 0(mod\ p^{q-n})$. We now calculate $\alpha^s - \alpha$ modulo p^m.

By Corollary 2.6, $\alpha^{s-1} = (1 + p^n)^{fp^v} = 1 + (s-1)p^n + kp^{(q-n)+2n}$. Since $q + n \geq m$ this gives $\alpha^{s-1} \equiv 1 + (s-1)p^n(mod\ p^m)$. Hence modulo p^m,

$\alpha^s - \alpha \equiv \alpha(\alpha^{s-1} - 1) \equiv \alpha(s-1)p^n \equiv (1 + p^n)(s-1)p^n \equiv (s-1)p^n$

since $(s-1)p^{2n} \equiv 0(mod\ p^{q+n}) \equiv 0(mod\ p^m)$ where $m \leq q + n$. Then the rest of the proof is similar to case (a) above to obtain $s \equiv 1 + cp^{q-n}(mod\ p^{m-n})$.

(iv) In all cases, we have no further restriction about r and so r can be any element in Z_{p^m}.

On the other hand, we now show that the conditions of the theorem are sufficient by calculating the number of distinct mappings allowed by these conditions.

In all cases, it is clear that the number of choices for j is p^n and the number of choices for r is p^m since $r \in Z_{p^m}$.

In addition for each $j = cp^{t-n}$ where $0 \leq c < p^n$, the number of choices for s is $p^{t-(m-n)} = p^{t-m+n}$. From this, we see that the number of choices for the pair (s, j) is $p^{t-m+n}p^n = p^{t-m+2n}$ in all cases.

Now, for cases 1 and 2 we have $i \equiv 1 (mod\ p^{m-q})$ and thus, it is clear that the number of choices for i is p^q.

Therefore the number of distinct mappings in cases 1 and 2 is $p^q p^{t-m+2n} p^m = p^{2n+q+t}$ which is also the order of *Aut(P)* as established by Menegazzo (1993).

Now, for cases 3 and 4 we have $i \equiv 1 + rp^{t-q} (mod\ p^{m-q})$ so for each r there are p^q choices of i. As in cases 1 and 2, the number of choices for the pair (s, j) is $(p^{t-m+n})(p^n) = p^{t-m+2n}$. Hence for a distinct $r \in Z_{p^m}$, the number of distinct mapping s allowed is $p^m p^{2n+q+t-m} = p^{2n+q+t}$ which is also the order of *Aut(P)* as established by Menegazzo (1993).

Therefore in all cases, the conditions of the theorem are sufficient. ▪

CONCLUSIONS

In this paper we have found the necessary and sufficient conditions for a map of a non-split metacyclic p-group where p is an odd prime number, to be an automorphism. This result is beneficial since it is directly related to the parameters in the presentation of the metacyclic group, and this may open the way to do further research on the class of the automorphism group of non-split metacyclic p-groups.

ACKNOWLEDGEMENT

I would like to thank very much Dr. Elizabeth Ormerod of The Australian National University for many valuables suggestions.

REFERENCES

Bidwell, J. N. S. and Curran, M. J. (2006). The automorphism group of a split metacyclic p-group. *Archives of Mathematics (Basel.)*, *87*(6), 488-497.

King, B. W. (1973). Presentations of metacyclic groups. *Bulletin of the Australian Mathematical Society*, *8*, 103-131.

Menegazzo, F. (1993). Automorphisms of p-groups with cyclic commutator subgroup. *Rendiconti del Seminario Matematics dell' Universitá di Padova*, *90*, 81-101.

Schulte, M. (2001). Automorphisms of metacyclic p-groups with cyclic maximal subgroups. *Rose-Hulman Undergraduate Research Journal*, *2*(2). Retrieved from http://www.rose-hulman.edu/mathjournal.

ISSN: 0128-7680
Pertanika J. Sci. & Technol. **19 (1)**: 117 – 127 (2011)

Biodiesel from Pungam Seed Oil and Its Effects on Engine Performance with a Computerized Engine Test Rig

T. MohanRaj[1*], K. Murugu Mohan Kumar[2] and Perumal Kumar[3]
[1]Department of Mechanical Engineering,
SASTRA UNIVERSITY –Thanjavur, Tamilnadu-613403, India
[2]M.A.M Engineering College, Trichy, India
[3]School of Engineering and Science,
Curtin University Technology, Sarawak Campus,
98009 Miri, Sarawak, Malaysia
[*]E-mail: tmraj@mech.sastra.edu

ABSTRACT

Vegetable oil has become more attractive recently because of its environmental benefits and better quality exhaust emission. A well-known transesterification process made biodiesel, pungam seed oil was selected for biodiesel production. Pungam seed oil is non-edible oil, thus, food versus fuel conflict will not arise if this is used for biodiesel production. A maximum of 75% biodiesel was produced with 20% methanol in the presence of 0.5% sodium hydroxide. The experimental investigations were carried out in an engine that is coupled with an eddy current dynamometer. The engine is a single cylinder water-cooled, direct injection diesel engine developing a power output of 3.7 kW at 1500 rev/min. The crank angle encoder measured the engine speed, whereas the piezo electric sensors measured the cylinder pressure and the fuel injection pressure. The experimental investigations were carried out for bio-diesel and diesel and the results were compared. From the experimental results, it is concluded that the use of bio-diesel as an alternative fuel leads to significant reduction in emissions and improved performance of diesel engines. This paper discusses the production process of biodiesel from Pungam seed oil and its performance in the compression ignition engine.

Keywords: Biodiesel, alternative fuel, Pungam seed oil, esterification

NOMENCLATURE

BD	Biodiesel
CI	Compression ignition engine
CO	Carbon monoxide
CO_2	Carbon dioxide
CRBO	Crude rice bran oil
DI	Direct injection
KOH	Potassium hydroxide
NA	Naturally aspirated
NaOH	Sodium hydroxide
NO	Nitrogen oxide
PM	Particulate matter
PSO	Pungam seed oil
PSOME	Pungam seed oil methyl ester
THC	Total unburned hydrocarbon

Received: 8 January 2010
Accepted: 10 June 2010
[*]Corresponding Author

INTRODUCTION

The concept of using vegetable oil, as fuel for diesel engine, has dated back to Dr. Rudolf Diesel's Development of diesel engine to run on vegetable oil. Demonstrated at the 1900 world exhibition in Paris, Rudolf tested peanut oil as a fuel for the engine. Bio-diesel meeting modern specifications has successfully been used in Europe for more than 20 years (Georing, 1982; Bagby, 1987). Transesterification is the process of reacting a triglyceride with alcohol in the presence of a catalyst to produce glycerol and fatty acid esters. The molecular weight of the ester molecule is roughly one-third that of a neat vegetable oil molecule and the ester has a viscosity approximately twice that of diesel fuel. In contrast, raw vegetable oil has a viscosity of 10-20 times that of diesel fuel. Viscosity of the fuel is of prime concern because of its spray pattern and deposit formation (Felderman, 1988; Mittlbach, 1992). Meanwhile, methyl esters of high erotic acid rapeseed oil perform similarly to diesel in both short- and long-run engine tests.

In the recent years, systematic efforts have been made by several researchers (Agarwal *et al*., 2001) to use vegetable oil like sunflower, peanut, soybean, rapeseed, palm, olive, cottonseed, linseed, jatropha, coconut, pungam, rubber seed, etc., as an alternative fuel for diesel. Most of the vegetable oil is edible in nature, and its continuous use has been suggested to have caused shortages in food supply and proven far expensive to be used as fuel at present. Very few non-edible vegetable oil types have been tried on diesel engine, and this leaves a lot of scope for further investigation in this area. It is important to note that the high viscosity of vegetable oil is responsible for these problems. Therefore, reducing the viscosity of vegetable oil is of the prime importance to make it suitable for diesel engines. Ramadhas *et al*. (2004) have suggested several ways for this purpose; among other, they proposed blending or diluting it with other oil, while pre-heating and transesterification are pre-dominant.

In India, only a small portion (<10%) of the total production of CRBO is processed into edible oil (Zullaikah *et al*., 2005), while the remaining high FFA CRBO is utilized for industrial applications such as cosmetics. Hence, more attention should be focused on this non-edible CRBO to test its suitability as a substitute for diesel oil. Even though the properties of high FFA CRBO-diesel blends are comparable with that of diesel (Saravanan *et al*., 2008a), there may be engine durability issues in the long run. In its unmodified form, glycerin that is present in the CRBO may create problems in the engine fuel injection system. By reducing the viscosity of the CRBO through Transesterification process (Meher *et al*., 2006), its structure will be modified and this makes it compatible with the engine fuel injection system.

Pungam oil has been converted into biodiesel by the transesterification method and the viscosity has been reduced to 4.8 centistokes from 21.4 centistokes. The free fatty acid (FFA) present in pungam oil has a greater influence in the process of converting it into bio diesel. This has been observed during the time of producing the biodiesel in the laboratory level. However, high viscosity and poor volatility lead to reduced thermal efficiency and increased hydrocarbon, carbon monoxide, and smoke emissions (Barsic, 1981; Ali, 1995; Joseph, 1982). Meanwhile, transesterification is one of the methods by which viscosity could drastically be reduced and the fuel could be adopted for use in diesel engine. The transesterification process involves reacting vegetable oil with alcohol, such as methanol or ethanol, in the presence of a catalyst (usually sodium hydroxide) at about 70°C to give the ester and the by-product, glycerin (Korbitz, 1995).

However, the dual fuel engine gives a poor part load performance, and HC and CO emissions are higher (Kumar *et al*., 2001). For agricultural applications, where small amounts of fuel are consumed in every engine, the use of neat vegetable oil is likely to be more attractive than the transesterified oil (biodiesel), as no chemical processing is needed. As mentioned earlier, several vegetable oil types have been tested in engines. Among these, jatropha oil was found to be promising. It is non-edible, as well as possesses a high calorific value and cetane number. In addition, it is also non-toxic. More importantly, water requirement for the jatropha plant is negligible and it can also grow anywhere even on sandy oil. Meanwhile, the calorific value and the cetane number of jatropha oil are comparable to diesel, but the density is higher. Carbon residue of jatropha oil is very high, and this can lead to high smoke levels and injector coking. It is important to note that coking of the injector leads to poor fuel atomization (Srinivasa *et al*., 1991). The flash point of jatropha oil is higher than the diesel, and hence, it is safer to use it in the engine. With advanced injection timing, there is more time available for mixture formation, and this can further lead to a better combustion, as well as improved performance and also reduction in HC and CO emissions (Karim, 1983; Narayana, 2004). In particular, increased injector opening pressure has a significant effect on the performance and the emissions of diesel engines. Meanwhile, an increase in injection pressure has been found to enhance the atomization at the nozzle outlet, resulting in a more distributed vapour, and hence, a better mixing. When the injection pressure is increased, fuel particle diameter reduces. Since mixing of fuel and air improves during the ignition delay period, HC and smoke levels will also reduce. A very high injection pressure will lead to fine droplets and this can adversely affect fuel distribution in air.

The main objectives of the present work were to produce biodiesel from non-edible pungam seed oil and to find the fuel properties of the biodiesel with the engine performance and to compare them with diesel fuel.

EXPERIMENTAL METHODS

The engine is coupled with an eddy current dynamometer. The ester of pungam oil was injected into the engine through the existing conventional injection system. However, two separate fuel tanks were used; one for diesel fuel and the other for the ester of pungam oil. Both the fuels were injected at the room temperature only. A fuel changing arrangement was provided to change one fuel mode to another.

The Experimental Setup

The experimental setup is a computerized test rig, as shown in *Fig. 1*. As stated earlier, the engine is coupled with an eddy current dynamometer. The instrument, like crank angle encoder, pressure sensor, injection sensor, and the flow transducers for measuring the fuel flow and airflow, have also been incorporated in the experimental setup.

Fig. 1: Computerized engine experimental setup

The Experimental Procedure

Diesel and biodiesel were injected into the engine cylinder through the existing fuel injector without any modification made to the engine. The fuels were injected at the room temperature only. A fuel-changing mode was provided to change one fuel mode to another. The engine was first made to run by supplying the diesel fuel to the engine, and then the fuel cock was shifted to supply the bio diesel fuel to the engine from a separate tank. The crank angle encoder measured the engine speed, while the piezo electric sensors, which have been mounted in the cylinder head, were used to measure the cylinder peak pressure, cylinder peak temperature and fuel injection pressure. The flow transducers measured the fuel flow and the airflow. The signals that were obtained from various sensors were fed into the engine indicator so as to store the data and interface with the computer. The stored data were analyzed using the engine software. The respective sensors carried out observations, i.e. the crank angle encoder measured the engine speed, while the cylinder pressure and fuel injection pressure were measured by the piezo electric sensors. The signals that were obtained from various sensors were fed into the engine indicator to store the data and interface with the computer.

Specification of the Engine

The specifications of the engine are as follows:

TABLE 1
Specifications of the engine

Engine model	COMET
No of cylinder	One
Orientation	Vertical
No of stroke	4 strokes
Ignition system	Compression ignition
Bore and stroke	80 mm x110 mm
Arrangement of valves	Overhead
Rated power	3.5 kW @ 1500 rpm
Cooling medium	Water cooled
Combustion chamber	Open chamber (Direct injection)
Compression ratio	18:1
Displacement volume	553 cc

Fuel Properties

It is important to note that the performance of the CI engines is greatly dependent upon the properties of the fuel, among which viscosity, volatility, lubricity, calorific values are very important. In this work, the effects of temperature on viscosity with neat diesel fuel and different biodiesel mixture were investigated. The properties of the neat diesel fuel and PSOME were determined and tabulated in Table 2.

Since there are no direct volatility data available for biodiesel, it can be explained with the help of distillation temperature. The higher the volatile fuels, the lower the distillation temperature. Similarly, since the diesel fuel (90% = 325°C) has lower distillation temperature than that of biodiesel (90% = 360°C), the neat biodiesel has a low volatility.

TABLE 2
Properties of the pungam oil

Properties	Diesel fuel	PSOME	Raw PSO	ASTM method
Density kg/m^3@15°C	840	915	938	D1298
Kinematic viscosity Cst @ 40°C	4.59	10.33	46.53	D445
Flash point °C	174	200	275	D2500
ASH (% by mass)	0.06	0.04	Nil	D3176
Calorific value (Cal/gm)	10127	9824	9767	D5865

PERFORMANCE RESULTS

TABLE 3

Performance results for the pungam oil

Load	Brake power	TFC	Air	SFC	Vol Eff	Torque	BMEP	HBP	HJW	HGAS
kg	kW	CC/m	mmWC	kg/kW-hr	%	kgm	Bar	%	%	%
0.12	0	8.19	40.88	10.214	67.5	0	0	0.84	19.69	20.07
0.76	0.25	0	38.97	0	66.11	0.15	0.34	0	18.43	0
3.03	0.98	12.41	38.15	0.631	65.96	0.61	1.35	13.58	17.2	17.16
5.79	1.86	16.53	36.88	0.443	65.31	1.16	2.58	19.35	16.02	16.02
8.84	2.82	16.12	36.21	0.285	65.17	1.77	3.94	30.09	20.75	20.75

TABLE 4

Performance result for the diesel fuel

Load	Brake power	TFC	Air	SFC	Vol Eff	Torque	BMEP	HBP	HJW	HGAS
kg	kW	CC/m	mmWC	kg/kW-hr	%	kgm	Bar	%	%	%
0.12	0	10.54	91.89	15.085	80.84	0	0	0.57	48.68	22.31
0.76	0.23	11.28	89.55	12.37	73.19	0.14	0.26	3.17	47.22	22.24
3.03	0.91	13.50	82.55	4.22	50.24	0.55	1.03	10.97	42.84	22.05
5.79	1.88	16.37	85.41	0.48	37.07	1.15	2.14	19.21	39.01	23.59
8.84	2.54	18.24	91.39	0.357	34.1	1.56	2.9	23.99	37.13	25.21

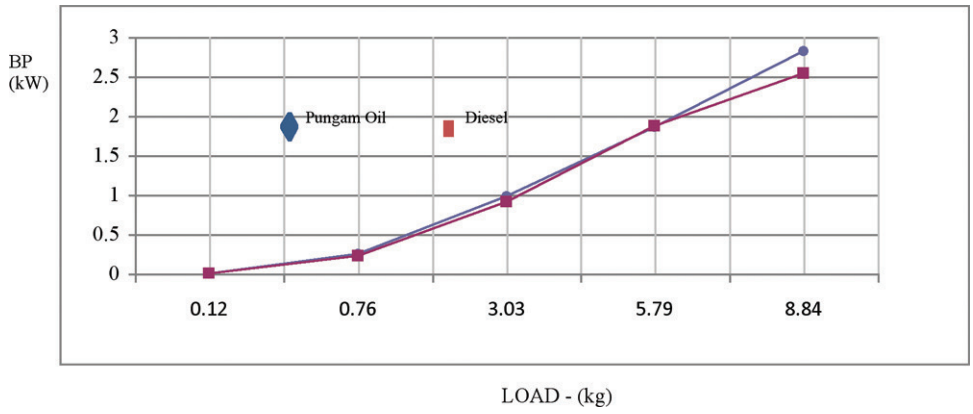

Fig. 2: Brake power vs. load

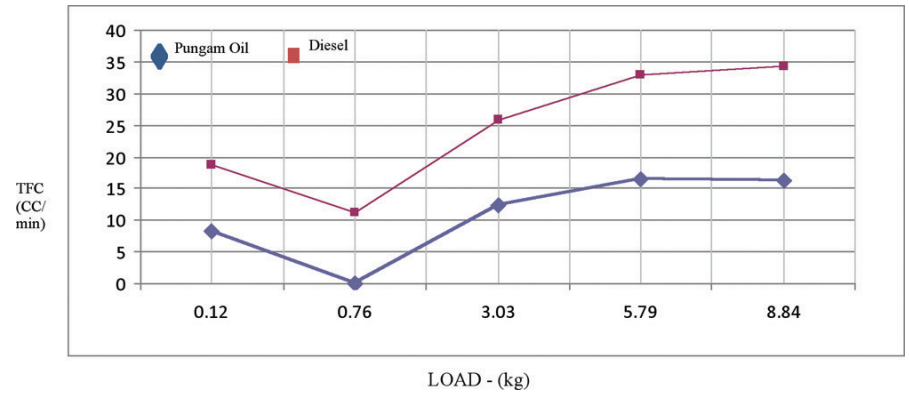

Fig. 3: Total fuel consumption vs. load

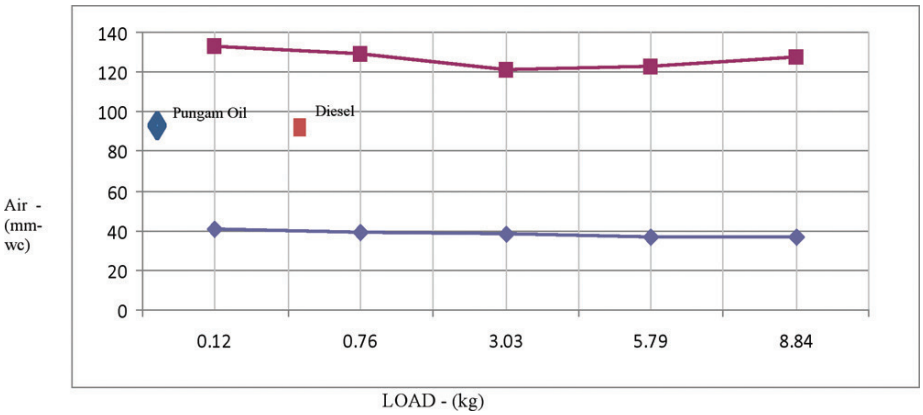

Fig. 4: Air flow vs. load

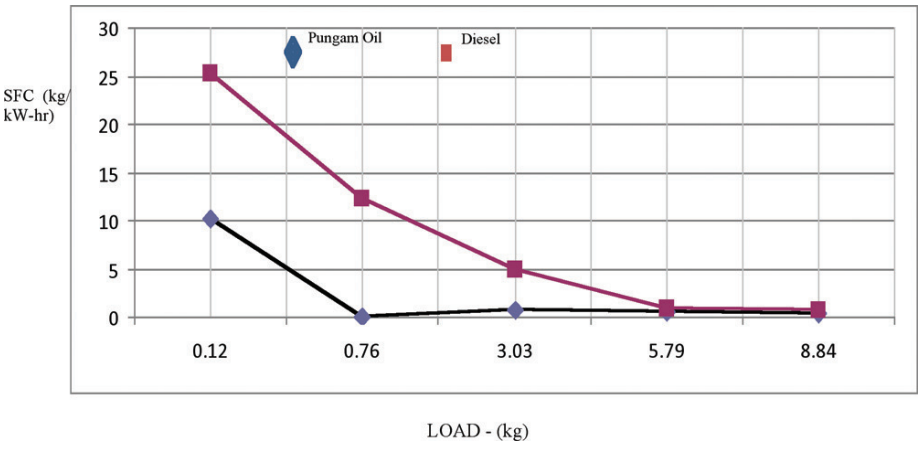

Fig. 5: Specific fuel consumption vs. load

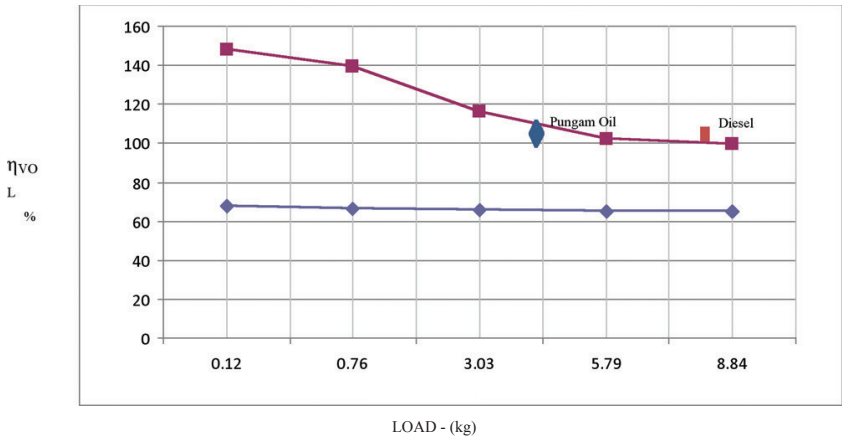

Fig. 6: Volumetric efficiency vs. load

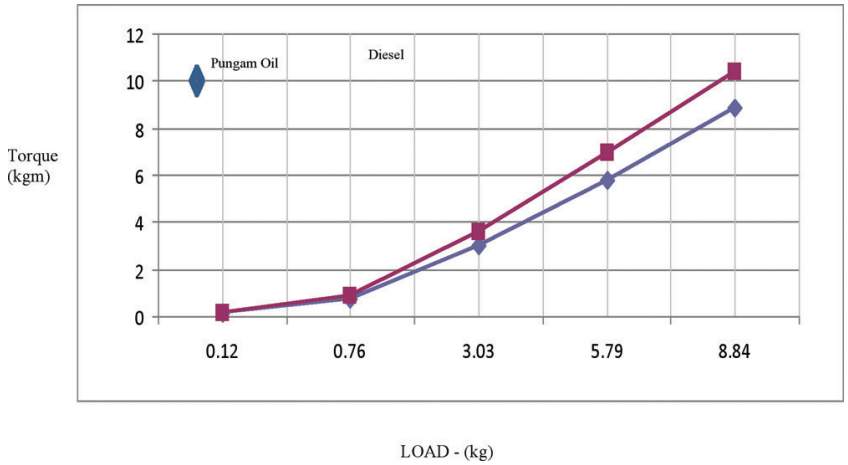

Fig. 7: Torque vs. load

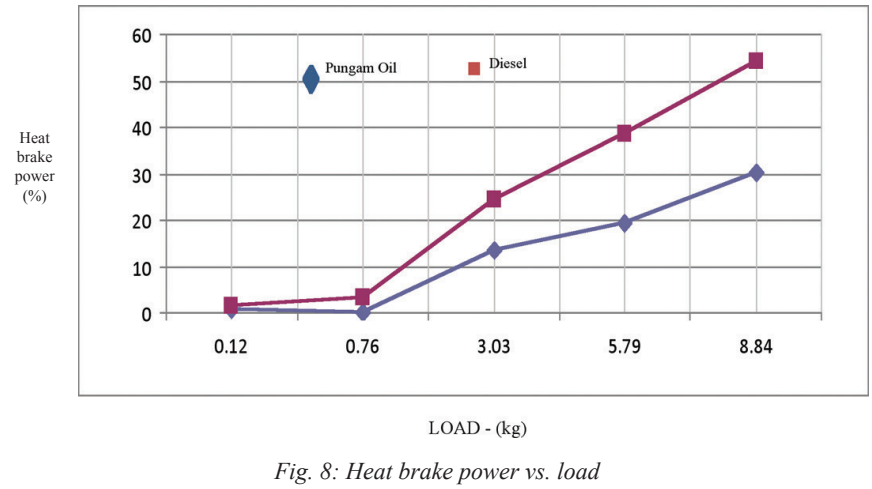

Fig. 8: Heat brake power vs. load

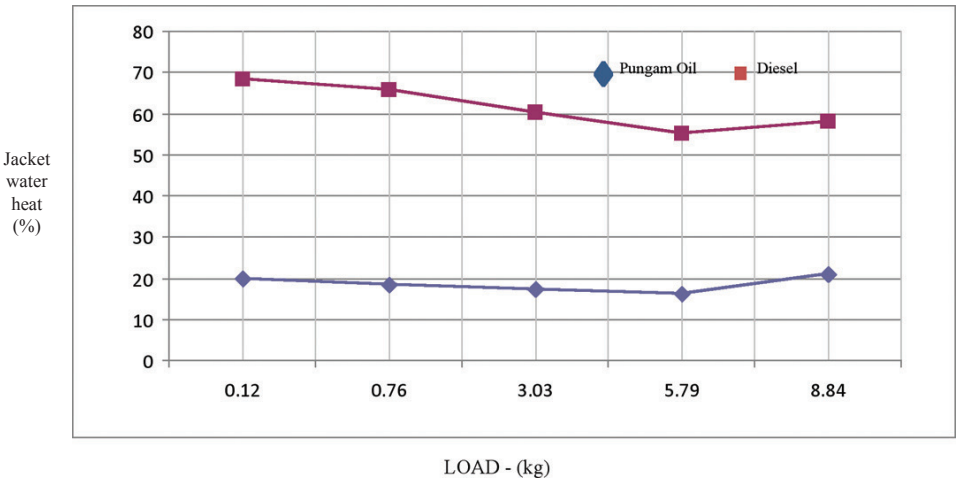

Fig. 9: Jacket water heat vs. load

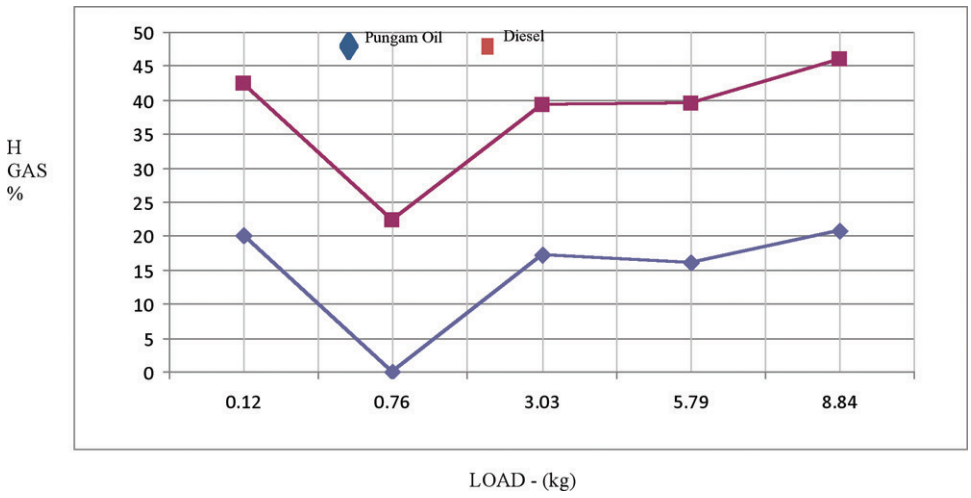

Fig. 10: Exhaust gas heat vs. load

RESULTS AND DISCUSSION

Based on the performance curves, there is not much variation in term of the volumetric efficiency under various loads for the pungam oil, whereas there is a drastic variation for diesel. Moreover, it could also be observed that when operating with pungam oil, the break thermal efficiency of the engine increased only marginally, ensuring the suitability of the pungam oil as a replacement for diesel fuel. Meanwhile, the total fuel consumption is less for pungam oil than diesel fuel. The specific fuel is almost the same for both pungam oil and diesel fuel after reaching 50 percent of load. Consequently, pungam oil can be effectively used in diesel engine without any modification. In other words, the use of the pungam oil as diesel fuel can improve the agriculture economy, diminish the indecision of fuel availability and achieve more environmental benefits at the same time.

CONCLUSIONS

The experimental results have shown the comparison between the performance and the combustion characteristics of the C.I engine using the pungam oil as a fuel, which are almost matching the diesel mode of operation. This justifies that the attempt made to use of pungam oil as a fuel in the C.I engine is very effective and that the oil can be used as an alternative fuel without having to do any modification to the engine. Due to the lower calorific value of the pungam oil, however, it was found that the brake power of the engine was higher when the load was increased. Meanwhile, the specific fuel consumption was also lower for the pungam oil as compared to diesel.

REFERENCES

Agarwal, A.K. and Das, L.M. (2001). Bio diesel development and characterization for use as fuel foe diesel engines. *Energy Converse Manage*, *123*, 440-7.

Bagby, M.O., Freedman, B. and Schwab, A.W. (1987). Seed oils for diesel fuels: Sources properties, ASAE Paper, Paper Number 871583.

Barsic, N.J. and Humke, A.L. (1981). Performance and emissions characteristics of a naturally aspirated diesel with vegetable oils and fuels, SAE Paper 810262, 1981.

Barsic, N.J. and Humke, A.L. (1985). Performance and emissions characteristics of a naturally aspirated diesel engine with vegetable oil fuels. SAE paper No. 810262.

Goering, C.E., Schwab, A.W., Daugherty, M.J., Pryde, E.H. and Heakin, A.J. (1982). Fuel properties of eleven vegetable oils. *Transactions of the ASAE*, *25*(6), 1472-1477.

Karim GA, Amoozegar. (1983). Determination of performance of dual fuels engine with addition of various liquid fuels to the intake charge. SAE Paper No. 830265.

Korbitz, W. (1995). Status and development of bio diesel production and projects in Europe and North America, SAE Paper No. 925768, Society of Automotive Engineers, Warren Dale.

Meher, L.C., Vidya Sagar, D. and Naik, S.N. (2006). Technical aspects of bio-diesel production by transesterification-a review. *Renewable & Sustainable Energy Reviews*, *10*, 248-68.

Mittlbach, M., Poktis, B. and Silberholz, A. (1992). Production and fuel properties of fatty acid methyl esters from used frying oil. In *Proceedings of an Alternative Energy Conference*. Nashville, USA, American Society of Agriculture Engineers (ASAE).

Narayana, R. J. and Ramesh, J. (2004). Experimental studies on a straight vegetable oil-biogas dual fuel engine. SAE Paper No. 2004-28-031, 2004.

Zhang, Q., Feldman, M. and Peterson, C.L. (1988). Diesel engine durability when fuelled with methyl ester of winter rapeseed oil, ASAE Paper, Paper Number 881562.

Ramadhas, A.S., Jayaraj, S. and Muraleedharan, C. (2004). Use of vegetable oils as IC engine fuels-a review. *Renew Energy*, *l29*, 727-42.

Saravanan, S., Nagarajan, G. and Lakshmi Narayana Rao, G. (2008a). Effect of FFA of crude rice bran oil on the properties of diesel blends. *Journal of the American Oil Chemist Society*, *85*, 663-6.

Senthil, K. M., Ramesh, A. and Nagallingam, B. (1981). Experimental investigation ON Jatropha oil methanol dual engines. SAE Paper No. 810262, 1981.

Senthil, K. M., Ramesh, A. and Nagalingam, B. (2003). Use of hydrogen to enhance the performance of vegetable oil fuelled compression ignition engine. *International Journal of Hydrogen Energy*, *28*, 1143-54.

Srinivasa Rao P. and Gopalakrishnan, K.V. (1991). Vegeable oils and methyl esters as fuels for diesel engines. Indian *Journal of Science and Technology*, *29*, 292-7.

Varaprasad, C.M., Muralikrishna, M.V.S. and Prabhakar, R. C. (1997). Investigations on bio diesel (Esterified Jatropha Curcus Oil) in diesel engines. *XV National Conference on I.C. Engines and Combustions*. Anna University, Chennai, Tamil Nadu, India.

Zullaikah, S., Lai, C.C., Vali, S.R. and Ju, Y.H. (2005). A two-step acid-catalyzed process for the production of biodiesel from rice bran oil. *Bio Resource Technology*, *96*, 1889-96.

ISSN: 0128-7680
Pertanika J. Sci. & Technol. **19 (1)**: 129 – 140 (2011)

Review Article

Adenoviral based Gene Therapy for Cancer in Human and Animals: A Review

Tan Seok Shin, Zeenathul Nazariah Allaudin* and Mohd. Azmi Mohd. Lila
Department of Veterinary Pathology and Microbiology,
Faculty of Veterinary Medicine, Universiti Putra Malaysia,
43400 UPM, Serdang, Selangor, Malaysia
**E-mail: zeenathul@putra.upm.edu.my*

ABSTRACT

Adenovirus vector is the most common used vector in clinical gene therapy. The development of adenovirus from the first generation until the helper-dependent adenovirus vector has greatly reduced toxicity and immunogenicity. The helper-dependent adenovirus can also prolong transgene expression. Tissue- or disease-specific approach has been used to improve the specificity of adenoviral vector for cancer gene therapy. This review summarizes some adenoviral gene therapy and targeting approaches available for human cancer as well as animal cancer.

Keywords: Adenovirus vector, clinical, gene therapy, human cancer, animal cancer

ABBREVIATIONS

Adenovirus (Ad)
Alternative reading frame (ARF)
Arg-Gly-Asp (RGD)
Carcinoembryonic antigen (CEA)
Complementary DNA (cDNA)
Coxsackie adenovirus receptor (CAR)
Cytomegalovirus (CMV)
Human papillomavirus (HPV)
Interferon (IFN)
Interleukin 2 (IL-2)
Interleukin 12 (IL-12)
Non-small-cell lung cancer (NSCLC)
Tumour necrosis factor (TNF)
Tumour protein 53 (p53)

INTRODUCTION

Adenoviruses (Ad) are among the most commonly used vectors for the delivery of genetic material into human and animal cells, and in selected stable germ-line (Stephan and Kelly, 2002; Takehashi *et al.*, 2006). In addition, adenoviruses have a number of advantages as vectors; these include a rapid infection of both dividing and non-dividing cells, DNA stability, ease of manipulation and propagation, and low pathogenicity in humans. Adenoviruses became the most widely used vector for gene therapy clinical trials in 2009, with 23.9% out of a total 1579 clinical trials (Michael, 2009), especially for cancer gene therapy using intratumoral injection (Shirakawa, 2008).

Over the years, Ad vectors have been passed through a serial of evolution mounting evidence of anti-Ad immunological responses (both innate and adaptive) prompted the development of improved Ad versions (Hartman *et al.*, 2007). The first generation adenovirus vectors were developed by deleting one or two early genes, E1 and/or E3. This vector induced strong host immune responses that rapidly remove transgene expression, and thus gene expression became

Received: 29 September 2009
Accepted: 29 June 2010
*Corresponding Author

low and could only offer transient gene expression (Cao *et al.*, 2004). Newer Ad vectors have improved the ability to persist *in vivo*, facilitating the avoidance of adaptive immune responses (Hartman *et al.*, 2007). An additional deletion in the early genes, E2 and/or E4 was manipulated for the second and third generation vectors (Zhou *et al.*, 1996). Meanwhile, toxicity was found to be reduced in animal models with these vectors (Lusky *et al.*, 1998; O'Neal *et al.*, 1998; Andrews *et al.*, 2001). The deleted all viral genes' helper-dependent adenoviruses, which contain solely the cis acting elements, were the most advanced vector that has been developed (Morsy and Caskey, 1999). These Ad vectors improve the prospects for a long-term gene therapy (Morsy and Caskey, 1999).

In March 2003, 63.4% of all the gene therapy clinical trials were for cancer according to the Journal of Gene Medicine (Clare *et al.*, 2003). Two adenoviral-based gene therapeutics for cancer treatment have been commercialized in China (Peng, 2005; Yu and Fang, 2007). These two constructs have been used as alternative treatments for cancer, in combination with chemotherapy in China (Shirakawa, 2008). This article summarizes the use of adenovirus in the preclinical and clinical trials of cancer gene therapy.

ADENOVIRUS BASED GENE THERAPY IN HUMAN CANCER

Colon Cancer

Colon cancer is the third most frequent cancer for both men and women in Malaysia, which accounts for 7.8% and 5.6% respectively for the two genders (NCR, 2002). The main treatment for colon cancer is surgical resection of the entire tumour, but the result often remains unsatisfactory due to the metastases of the tumour (Faye *et al.*, 2000). Thus, gene therapy may provide an alternative approach to the conventional treatment.

In particular, p53 protein acts as a multifunctional regulator for the cell cycle that is capable of causing apoptosis and becoming tumour suppressor (Levine, 1997). Harris *et al.* (1996) have used adenovirus encoding wild type TP53, a gene that encoded p53 protein, as their construct for their colon cancer study. The researchers found a complete regression and a doubling survival time as compared to the control mice model with intratumoral injection of the construct to the subcutaneous implant p53-mutated colon cancer mice model. A phase I clinical trial, with this construct, showed no tumour regression but with the combination with chemotherapy, those patients revealed partial responses to the treatment (Veenok *et al.*, 1998).

Meanwhile, anti-tumour effects were shown in the murine model with liver metastases colon cancer cell line transduced with adenovirus encoding IL-12 (Caruso *et al.*, 1996). There was a synergistic effect found in a combination treatment of adenovirus encoding TP53 and chemotherapy in immunodeficiency mice (Ogawa *et al.*, 1997).

Carcino-embryonic antigen (CEA) is a cell surface protein that was presumed to play a role in cellular adhesion. Richards *et al.* (1995) found the over-expressing of CEA in 90% of the colon cancer cells, but this was only at a low level in the normal cells. Lan *et al.* (1996: 1997) have developed adenovirus with CEA promoter to provide tumour specific transgene expression. However, the researchers found that the gene expression of this modified vector was weaker compared with the non-specific cytomegalovirus (CMV) promoter. With that, the development of tumour specific vector that is capable of maintaining the transgene expression remains challenging.

Lung Cancer

Lung cancer is the most common cancer among Malaysian men, with 13.9% of all the male cancer patients in the year of 2002 (NCR, 2002). Besides, lung cancer is also in the list of the most

frequent cancers in women, which was ranked at number six, with 4.3% of all the women cancer patients in 2002 (NCR, 2002). Thus, it is important to find an alternative treatment for lung cancer other than the conventional treatment that is available at present. The progressively delineated of the molecular biology of lung cancer, over the past three decades, has allowed the development of lung cancer gene therapy towards targeting (Toloza, 2005). Adenoviruses, with a tropism for lung cancer cells (Stratford-Perricaudet and Perricaudet, 1994), have gained an advantage as a gene therapy vector for lung cancer.

Swisher *et al.* (1999) designed a Phase I clinical trial using adenovirus encoding wild-type TP53 cDNA for advanced non-small-cell lung cancer (NSCLC) after finding a tumour regression in the animal model, following the intratumoral injection of the construct. From this study, the authors concluded that repeated intratumoral injection of the E1-deleted replication-defective recombinant adenovirus containing wild-type TP53 was well tolerated, while transient transgene expression was found to mediate the patients' anti-tumour activity. Besides, vector-related adverse events were also found to be minimal.

The targeting approach for lung cancer, with the use of adenovirus vector such as adenovirus vector with double expression cassette consisting of secretory leukoprotease inhibitor promoter gene that is highly expressed in almost all NSCLCs and CMV promoter (Maemondo *et al.*, 2004), adenovirus-mediated herpes simplex virus thymidine kinase (Fukunaga *et al*., 2002) and polylysine coated adenovirus encoding proto-oncogenec-kit (Schwarzenberger *et al.*, 1996) have shown a promising result for lung cancer treatment.

Breast Cancer

Breast cancer is the most frequent cancers among the women in Malaysia (NCR, 2002). According to the NCR database, 30.4% of the females in Malaysia were newly diagnosed breast cancer patients in the year 2002. A Malaysian woman has 1 in 19 chances of getting breast cancer in her life time (NCR, 2002). Therefore, it is crucial to develop a gene therapy treatment for breast cancer due to the limited success of conventional treatment (Zhang *et al.*, 1996).

Zhang *et al.* (1996) developed an adenovirus containing human interferon consensus gene and tested it on human breast cancer (MDA-MB-435) implanted nude mice. A complete regression, accompanied by the decreased of p53 gene expression, was found in this study. They also found a partial regression of the tumour in the control group, based on which, they concluded that the rapid regression of the breast tumour was due to the combination of the virus oncolysis and the effectiveness of the interferon gene therapy.

An alternative product from the family of cyclin-dependent kinase inhibitors, human INK4a/ARF (alternative reading frame) locus, $p14^{ARF}$, has been identified as a potent tumour suppressor for both *in vitro* and *in vivo* (Serrano *et al.*, 1996; Kamijo *et al.*, 1997; Sherr, 2000). Overexpression of $p14^{ARF}$ will result in cell cycle arrest (Quelle *et al.*, 1995; Kamijo *et al.*, 1997; Weber *et al.*, 2002) and apoptosis (Radfar *et al.*, 1998; Yang *et al.*, 2000; Hemmati *et al.*, 2002). Deng *et al.* (2002) constructed a recombinant adenovirus expressed human $p14^{ARF}$ cDNA for the treatment of human breast cancer. They found an increase in the number of cells in the G_0/G_1 phase but a decrease in the S and G_2/M phases during the time-course study. In addition, there was an increased amount of p53 at the same time. Besides, the findings of their study also indicated a significant increase in the sensitivity of the cells to chemotherapy drug upon $p14^{ARF}$ recombinant adenovirus expression.

A study that evaluated the infection efficiencies of three most promising vectors, namely human adenovirus type 5, canine adenovirus type 2, and human adeno-associated type 2 vectors, was carried out by Lucas *et al.* (2003) in breast cancer cell lines. Meanwhile, the real-time PCR, flow cytometry and antibody blocking studies achieved an agreement in this study that coxsackie adenovirus receptor (CAR) or αv integrin levels are not the main influence to the infection

efficiencies of human adenovirus vector and canine adenoviral vector. They concluded that human adenovirus vector served as the best choice of carrier for gene therapy as compared to canine adenovirus vector and human adeno-associated vector due to the excellent infection efficacy of the human adenovirus vector. This was supported by a study by Mountain (2000), in which a majority of more than 3500 patients who had been enrolled in cancer gene therapy trials approaches were found to have used human adenovirus.

Prostate Cancer

Prostate cancer ranks as the sixth most frequent cancers among men in Malaysia and this accounted for 5.7% in 2002 (NCR, 2002). As for males above the age of 70 years, prostate cancer becomes the top two most common cancers (NCR, 2002). In United States, prostate cancer is the second leading cause of cancer deaths in men (ACS, 2005). The slow growth rate of the prostate cancer as compared with other solid tumour (Schmid *et al.*, 1993) caused no major improvement in patient's survival with chemotherapy (Visakorpi *et al.*, 1991; Kallioniemi *et al.*, 1991). Gene therapy might be an alternative treatment choice for prostate cancer or in combination with conventional therapy to prolong the survival rate of prostate cancer patients.

Tissue- or disease-specific treatments have gained advantages for prostate cancer in gene therapy. The were an estimated 200 prostate-specific genes available for transcriptionally targeting prostate cells (Xu *et al.*, 2001; Nelson *et al.*, 2000). Meanwhile, cancer-specific gene mutation such as p53 (Navone *et al.*, 1993; Bookstein *et al.*, 1993; Brooks *et al.*, 1996) added advantage to prostate-targeting therapy. Adenovirus vector provides a highly tailored therapy that gives different qualities to prostate cancer cell (Lupold and Rodriguez, 2005). Promising results have been reported in several studies, involving the use of oncolytic and suicide gene therapy strategies (Lupold and Rodriguez, 2005). In particular, oncolytic virotherapy uses adenovirus that selectively kills cancer cells by competent replication in tumour cells, but not in normal cells (Hemminki *et al.*, 2003). Thus, a strong cytolytic effect is achieved by oncolytic virotherapy that targets cancer cells (Meerani and Yang, 2010). On the other hand, adenovirus can be used as a vector in suicide gene therapy to deliver non-toxic gene or prodrug to the cancer cells, which eventually triggers the maximum therapeutic effect with limited systemic toxicity (Yazawa *et al.*, 2002). A combination of radiation therapy with replicating adenoviruses shows synergistic effects to radiation and this study is in phases I and II of clinical trials (Freytag *et al.*, 2007).

Ovarian Cancer

Ovarian cancer is the fourth most common cancers among women in Malaysia, and this constituted about 5.0% of the total female cancer (NCR, 2002). Ovarian cancer is also the fourth leading cause of gynaecology malignancy deaths among the female population (Greenlee *et al.*, 2001). The lack of effective screening strategies and the unavailability of clear symptoms at the early stage of the disease caused 70% of the women to be at the advanced stage at the time of get initial diagnosis (Barnes *et al.*, 2002). This leads to the low long-term survival rate over the past 20 years even when advanced surgical technique and chemotherapy are available (Barnes *et al.*, 2002). With that, more advanced gene therapy might be a choice to increase the survival rate of ovarian cancer patients.

The deficiency of coxsackie adenovirus receptor (CAR) in ovarian cancer cells has caused a relative resistance of ovarian cancer cells to adenovirus infection (Vanderkwaak *et al.*, 1999). Retargeting adenovirus receptor to a common receptor of ovarian cancer cells is crucial to improve the tropism of the adenovirus vector to ovarian cancer cells. Wickham *et al.* (1993) added RGD peptide sequences into the penton base with the secondary host cell receptor integrins. Meanwhile,

Vanderkwaak *et al.* (1999) found the RGD-modified adenoviral vector to have shown a promising gene expression to primary ovarian cancer cells compared to human mesothelial tissue.

Cervical Cancer

Cervical cancer was ranked among the most common cancers in Malaysian female population in 2002. The cancer of cervix uteri is the second most common among Malaysia women, comprising of 12.0% of the total female cancers (NCR, 2002). Malaysia had higher age-standardized incidents of cervical cancer as compared to western countries and other countries in Asia (NCR, 2002). Nonetheless, the reason for the high age-standardized incidents in Malaysia remains unknown and it requires further investigation.

Human papillomavirus (HPV) has generally been recognized as the main contributor to cervical cancer. Hamada *et al.* (1996) found that the recombinant adenoviral incorporated wild type p53 was a potential therapy for HPV-positive cervical cancer cells. Further evaluation by Woong *et al.* (2002) indicated significant cell growth suppression by p53 recombinant adenovirus in HPV 18-infected cells (HeLa and HeLaS3) as compared to HPV 16-infected cells (CaSki and SiHa). Besides, the researchers also concluded that different cancer cell lines would have different cell cycles arrest phases and different roles of cell growth suppression through apoptosis in the event of over-expression of wild type p53 in those cell lines.

Table 1 summarizes the clinical trials in cancer gene therapy involving adenoviral vector. Adenovirus is the most used vector for cancer gene therapy in those trials.

ADENOVIRAL-BASED GENE THERAPY FOR ANIMAL CANCER

Canine

Biological and environmental similarities among dogs and humans have made dogs one of the appropriate preclinical models for gene therapy (Kruth, 1996). Andrawiss *et al.* (1999) studied the potential of adenoviral gene transfer in dog prostate, aiming that dog as a basic preclinical model for human prostate cancer gene therapy. The researchers found transgene expression in prostates and epithelial cells with no side effects on the dogs.

Meanwhile, Von Euler *et al.* (2008) have reported the usage of adenoviral vector for the gene therapy in canine malignant melanoma. Two dogs with oral and conjunctiva malignant melanoma respectively were given recombinant adenovirus encoding human CD40L gene as a treatment. CD40L protein is a member of the tumour necrosis factor (TNF) that is mainly expressed on activated T cells. The dog with oral melanoma was in stage III at the time it was diagnosed. This dog showed a complete regression of melanoma after 2 intratumoral injections of recombinant adenovirus. However, no recurrence of the tumour and no abnormality were found after the gene therapy. The other dog with conjunctival melanoma was in stage I with a rapid progression. This dog was treated with the same recombinant adenovirus just like the dog with oral melanoma but it was given 6 injections over 60 days. The tumour regressed dramatically within 60 days of post treatment with no sign of progression or metastasis. Adenoviral immunotherapy was efficient for canine melanoma and could be considered for human melanoma treatment, especially when aggressive surgical excision shortens the survival life span (< 10 months) (Dow *et al.*, 1998; MacEwen *et al.*, 1999).

Canine osteosarcoma is the most common cancer in large dogs, with over 8000 cases in Unites States annually and there is no curative treatment for this particular disease at the moment (Hemminki *et al.*, 2003). Due to the unlikely replication of human adenovirus in canine cells, Hemminki *et al.* (2003) have generated the first non-human oncolytic adenovirus. They found that

TABLE 1
The use of adenoviral vector for clinical trials in cancer gene therapy

Gene	Route	Phase	Tumour type	No. of patients
IL-2	ex vivo/ s.c.	I	Stage IV melanoma	15
IL-2	Intratumor	I	Stage IV melanoma	23
IL-2	Intratumor + prostectomy	I	Localized prostate cancer	12
IL-2	Intratumor	I	non-small-cell lung cancer (NSCLC)	21
p53	Intratumor	I	Advanced NSCLC	21
p53	Intratumor + chemotherapy	I	Advanced NSCLC	24
p53	Intratumor	I	Advanced NSCLC	15
p53	Intratumor + chemotherapy	II	Advanced NSCLC	25
p53	Intratumor or intravesical instillation+ cystectomy	I	Bladder cancer	12
p53	Intravesical instillation	I	Bladder cancer	13
p53	i.p. + chemotherapy	I/II	Recurrent ovarian cancer	36
p53	Intratumor	I	Advanced NSCLC	27
p53	Intratumor + radiotherapy	II	Advanced NSCLC	19
p53	Intratumor + surgery	I	Recurrent glioma	15
Anti-erbB2 single chain antibody	i.p.	I	Ovarian cancer	15
HSV-TK	Intratumor	I	Recurrent glioblastoma	13
HSV-TK	Intratumor	I/II	Recurrent glioblastoma	14
HSV-TK	Intratumor + surgery	I	Recurrent glioblastoma	14
HSV-TK	Intratumor	I	Prostate carcinoma	18
HSV-TK	Intratumor + radiotherapy	I/II	Prostate carcinoma	30
HSV-TK	Intratumor	I	Prostate carcinoma	11
*dl*1520	Intratumor	I	Recurrent head and neck cancer	22
*dl*1520	Intratumor	I	Hepatocellular carcinoma	3
*dl*1520	Intrahepatic artery or iv	I	Colon cancer liver metastases	6
*dl*1520	Intrahepatic artery+ chemotherapy	II	Liver metastases from colon cancer or unknown primary	7
*dl*1520	i.v. on day 1 and intratumor on subsequent days	II	Hepatocellular carcinoma	5
*dl*1520	Intratumor	I	Pancreatic carcinoma	23
*dl*1520	Intratumor + chemotherapy	I	Metastatic solid tumours	10
*dl*1520	i.p.	I	Advanced ovarian cancer	16
*dl*1520	Intratumor + chemotherapy	I/II	Advanced pancreatic carcinoma	21
*dl*1520	Intratumor + chemotherapy	II	Recurrent head and neck cancer	37
*dl*1520	Intratumor	II	Head and neck cancer	40
*dl*1520	Intrahepatic artery+ chemotherapy	II	Gastrointestinal carcinoma metastasis to the liver	27
CN706	Intratumor	I	Recurrent prostate cancer	20
Ad5-CD	Intratumor	I	Recurrent prostate cancer	16

(Obtained and modified from Baron *et al.,* 2004. Endocrine aspects of cancer gene therapy. *Endocrine Reviews*, *25*(1), 1-44)

this virus could effectively kill the primary canine osteosarcoma cells from a dog that underwent osteosarcoma surgery. Besides, the advantage of the *in vivo* therapeutic was attained from the development of this conditionally replicated canine adenovirus (Hemminki *et al.*, 2003).

A preparation study for phase I clinical trail of the recombinant adenoviral gene therapy for locally recurrent prostate cancer was carried out by Dwyer *et al.* (2005). This study showed no vector-related toxicity and the successful introduction of gene expression in the prostate gland of dogs. More importantly, no animal experienced surgical complications and no significant change was shown in the serum chemistry panels following the therapy. These results provide insight for further translation of this experiment into clinical setting.

Lung, colon or breast cancer in canine is not a good model for human cancer. This is due to the low prevalence of these cancers in dogs and the biologically difference of these organs between dog and human (Kruth, 1996).

Feline

Siddiqui *et al.* (2007) conducted a study using adenovirus harbouring feline interleukin-12 (IL-12) for feline soft tissue sarcomas gene therapy. The study was in phase I clinical trial. Thirteen cats with confirmed diagnosis of sarcoma underwent a gene therapy using recombinant adenovirus following a prior radiation therapy of 22 days. The recombinant adenovirus cloned feline IL-12 was intratumorally injected and the tumour was heated at 24-hours post-injection. This clinical trial was carried out to check the systemic toxicity and tumour expression of IL-12. From this study, Siddiqui *et al.* (2007) found that hyperthermia-induced gene therapy capable of localizing gene expression and limiting systemic toxicity.

The successes in using adenovirus system for preclinical or clinical study in canine and feline species have provided future insight into the development of cancer vaccine for animals. However, the unlikely replication of the human adenoviral vector in canine and feline cells might reduce the efficiency of vector. Therefore, a study on Ad dosage is crucial to inhibit tumour progression or enhance tumour regression effectively. Besides, the limited number of canine or feline in those trials might influence the validity of data. More trials are required for validating the use of the Ad vector as a carrier for cancer gene therapy in canine or feline.

Hamster

Recombinant hamster interferon (IFN)-α adenovirus can effectively suppress hamster pancreatic tumour growth in Syrian hamster (Hara *et al.*, 2007). Tumour regression was discovered in both the injected subcutaneous tumours and untreated tumours in the peritoneal cavity and at distant sites. No significant difference was found in the systemic toxicity among the treated and untreated groups. Thus, local IFN- α gene therapy has been proven to be a promising therapeutic strategy for pancreatic cancer (Hara *et al.*, 2007).

Another study that made use of the Syrian golden hamster as a biliary cancer model was conducted by Kim *et al.* (2006) who used genetically modified bone marrow stromal cells containing adenoviral harbouring human interleukin-2 (IL-2) gene as a treatment. All the hamsters in the treatment group survived with no evidence of disease during the 12 weeks' observation period. However, the hamsters in the untreated and control group showed disseminated metastases that involved lungs as early as 4 weeks. Thus, the researchers made a conclusion that adenovirus vector carrying IL-2 as an effective treatment for biliary cancer.

CONCLUSIONS

The advancing field of gene therapy promises survival remedies for the ever raising number of cancer patients worldwide. Moreover, innovative and combinatory treatment of Ad gene therapies with the aid of the advanced molecular biology tools have shown promising results in the treatment of cancer. Meanwhile, a continual evaluation on the specificity, transgene expression and safety of Ad gene therapy in cancer will ensure feasible approach for successful outcomes.

REFERENCES

American Cancer Society. (2005). *Cancer Facts and Figures 2005*. American Cancer Society: Atlanta.

Andrawiss, M., Opolon, P. and Benihoud, K. *et al.* (1999). Adenovirus-mediated gene transfer in dog prostate: A preclinical study of a relavant model system for gene therapy of human prostatic cancer. *Prostate Cancer and Prostatic Disease*, *2*, 25-35.

Andrews, J.L., Kadan, M.J., Gorziglia, M.I., Kaleko, M. and Connelly, S. (2001). Generation and characterization of E1/E2a/E/E4-deficient adenoviral vectors encoding human factor VIII. *Molecular Therapy*, *3*, 329-336.

Barnes, M.N., Coolidge, C.J., Hemminki, A., Alvarez, R.D. and Curiel, D.T. (2002). Conditionally replicative adenoviruses for ovarian cancer therapy. *Molecular Cancer Therapeutics*, *1*, 435-439.

Barzon, L., Boscaro, M. and Palu, G. (2004). Endocrine aspects of cancer gene therapy. *Endocrine Reviews*, *25*(1), 1-44.

Bookstein, R., MacGrogan, D. and Hilsenbeck, S.G. *et al.* (1993). p53 is mutated in a subset of advanced-stage prostate cancers. *Cancer Research*, *53*, 3369-3373.

Brooks, J.D., Bova, G.S. and Ewing, C.M. *et al.* (1996). An uncertain role for p53 gene alterations in human prostate cancers. *Cancer Research*, *56*, 3814-3822.

Cao, H.B., David, R.K. and Hu. J. (2004). Review: Adenoviral vectors for gene replacement therapy. *Viral Immunology*, *17*(3), 327-333.

Caruso, M. *et al.* (1996). Adenovirus-mediated interleukin 12 gene therapy for metastatic colon carcinoma. *Proceedings of the National Academy of Sciences U. S. A.*, *93*, 11302–11306.

Clare, E.T., Anja, E. and Mark, A.K. (2003). Progress and problem with the use of viral vectors for gene therapy. *Nature Reviews: Genetics*, *4*, 346-358.

Deng, X.Y., Kim, M. and Vandier, D. *et al.* (2002). Recombinant adenovirus-mediated $p14^{ARF}$ overexpression sensitizes human breast cancer cells to cisplatin. *Biochemical and Biophysical Research Communications*, *296*, 792–798.

Dow, S.W., Elmslie, R.E. and Willson, A.P. *et al.* (1998). *In vivo* tumor transfection with superantigen plus cytokine genes induces tumor regression and prolongs survival in dogs with malignant melanoma. *The Journal of Clinical Investigation*, *101*, 2406–2414.

Dwyer, R.M., Schatz, S.M., Bergert, E.R., Myers, R.M. and Harvey, M.E. *et al.* (2005). A preclinical large animal model of adenovirus-mediated expression of the sodium–iodide symporter for radioiodide imaging and therapy of locally recurrent prostate cancer. *Molecular Therapy*, *12*(5), 835-841.

Faye, G.A.C., Kerr, D.J., Young, L.S. and Searle, P.F. (2000). Gene therapy strategies for colon cancer. *Molecular Medicine Today*, *6*, 82-87.

Freytag, S.O., Movsas, B., Ibrahim, A., Stricker, H. and Peabody, J. *et al.* (2007). Phase I trials of replication-competent adenovirus-mediated suicide gene therapy combined with IMRT for prostate cancer. *Molecular Therapy*, *15*(5), 1016-1023.

Fukunaga, M., Takamori, S., Hayashi, A., Shirouzu, K. and Kosai, K.I. (2002). Adenoviral herpes simplex virus thymidine kinase gene therapy in an orthotopic lung cancer model. *The Annals of Thoracic Surgery*, *73*, 1740-1746.

Greenlee, R., Hill-Harmon, M. and Murray, T. (2001). Cancer Statistics, 2001. *CA: A Cancer Journal for Clinicians*, *51*, 15–36.

Hamada, K., Zhang, W.W., Alemany, R., Wolf, J., Roth, J.A. and Mitchell, M.F. (1996). Growth inhibition of human cervical cancer cells with the recombinant adenovirus p53 *in vitro*. *Gynecologic Oncology*, *60*, 373–379.

Hara, H., Kobayashi, A., Yoshida, K., Ohashi, M., Ohnami, S., Uchida, E., Higashihara, E., Yoshida, T. and Aoki1, K. (2007). Local interferon-α gene therapy elicits systemic immunity in a syngeneic pancreatic cancer model in hamster. *Cancer Science*, *98*, 455–463.

Harris, M.P. *et al.* (1996). Adenovirus-mediated p53 gene transfer inhibits growth of human tumor cells expressing mutant p53 protein. *Cancer Gene Therapy*, *3*, 121–130.

Hartman, Z.C., Kiang, A., Everett, R.S., Serra, D., Yang, X.Y., Clay, T.M. and Amalfitano, A. (2007). Adenovirus infection triggers a rapid, MyD88-regulated transcriptome response critical to acute- phase and adaptive immune responses in vivo. *Journal of Virology*, *81*(4), 1796-1812.

Hemmati, P.G., Gillissen, B., Von Haefen, C., Wendt, J., Starck, L., Guner, D., Dorken, B. and Daniel, P.T. (2002). Adenovirus-mediated overexpression of p14(ARF) induces p53 and Bax-independent apoptosis. *Oncogene*, *21*, 3149–3161.

Hemminki, A., Kanerva, A., Kremer, E.J., Bauerschmitz, G.J. and Smith, B.F. *et al.* (2003). A canine conditionally replicating adenovirus for evaluating oncolytic virotherapy in a syngeneic animal model. *Molecular Therapy*, *7*(2), 163-173.

Kallioniemi, O.P., Visakorpi, T. and Holli, K. *et al.* (1991). Improved prognostic impact of S-phase values from paraffin-embedded breast and prostate carcinomas after correcting for nuclear slicing. *Cytometry*, *12*, 413-421.

Kamijo, T., Zindy, F. and Roussel, M.F. *et al.* (1997). Tumor suppression at the mouse INK4a locus mediated by the alternative reading frame product p19ARF. *Cell*, *91*, 649-659.

Kim, M.H., Lee, S.S., Lee, S.K., Lee, S.G., Suh, C.W., Gong, G.Y., Park, J.S., Kim, Y.H. and Kim, S.H. (2006). Interleukin-2 gene-encoded stromal cells inhibit the growth of metastatic cholangiocarcinomas. *World Journal of Gastroenterology*, *12*(12), 1889-1894.

Kruth, S. (1996). Canine models for gene therapy. *Transfusion Science*, *17*(1), 71-77.

Lan, K.H. *et al.* (1996). Tumor-specific gene expression in carcinoembryonic antigenproducing gastric cancer cells using adenovirus vectors. *Gastroenterology*, *111*, 1241–1251.

Lan, K.H. *et al.* (1997). *In vivo* selective gene expression and therapy mediated by adenoviral vectors for human carcinoembryonic antigen-producing gastric carcinoma. *Cancer Research*, *57*, 4279–4284.

Levine, A.J. (1997). p53, the cellular gatekeeper for growth and division. *Cell*, *88*, 323–331.

Lucas, A., Kremer, E.J., Hemmi, S., Luis, J., Vignon, F. and Lazennec, G. (2003). Comparative transductions of breast cancer cells by three DNA viruses. *Biochemical and Biophysical Research Communications*, *309*, 1011–1016.

Lupold, S.E. and Rodriguez, R. (2005). Adenoviral gene therapy, radiation, and prostate cancer. *Reviews in Urology*, *7*(4), 193-202.

Lusky, M. *et al.* (1998). *In vitro* and *in vivo* biology of recombinant adenovirus vectors with E1, E1/E2A, or E1/E4 deleted. *Journal of Virology*, 72, 2022-2032.

MacEwen, E.G., Kurzman, I.D. and Vail, D.M. *et al.* (1999). Adjuvant therapy for melanoma in dogs: Results of randomized clinical trials using surgery, liposome-encapsulated muramyl tripeptide, and granulocyte macrophage colony-stimulating factor. *Clinical Cancer Research*, *5*, 4249-4258.

Maemondo, M., Saijo, Y. and Narumi, K. *et al.* (2004). Gene therapy with secretory leukoprotease inhibitor promoter-controlled replication-competent adenovirus for non-small cell lung cancer. *Cancer Research*, *64*, 4611-4620.

Meerani, S. and Yang, Y. (2010). Oncolytic viruses in cancer therapy. *European Journal of Scientific Research*, *40*(1), 156 -171.

Michael, E. (2009). Gene therapy clinical trials worldwide. *Journal of Gene Medicine*. Retrieved on April 10, 2010 at http://www.wiley.co.uk/genmed/clinical/.

Morsy, M.A. and Caskey, C.T. (1999). Expended-capacity adenoviral vectors- the helper dependent vectors. *Molecular Medicine Today*, *5*, 18-24.

Mountain, A. (2000). Gene therapy: The first decade. *Trends in Biotechnology*, *18*, 119-128.

National Cancer Registry. (2002). *The First Report of The National Cancer Registry Cancer Incident in Malaysia*. NCR, Malaysia.

Navone, N.M., Troncoso, P. and Pisters, L.L. *et al.* (1993). p53 protein accumulation and gene mutation in the progression of human prostate carcinoma. *Journal of the National Cancer Institute*, *85*, 1657-1669.

Nelson, P.S., Clegg, N. and Eroglu, B. *et al.* (2000). The prostate expression database (PEDB): Status and enhancements in 2000. *Nucleic Acids Research*, *28*, 212-213.

Ogawa, N. *et al.* (1997). Novel combination therapy for human colon cancer with adenovirus-mediated wild-type p53 gene transfer and DNA-damaging chemotherapeutic agent. *International Journal of Cancer*, *73*, 367-370.

O'Neal, W.K. *et al.* (1998). Toxicology comparison of E2a-deleted and first-generation adenoviral vector expressing α1-antitypsin after systemic delivery. *Human Gene Therapy*, *9*, 1587-1598.

Peng, Z. (2005). Current status of gendicine in China: recombinant human Ad-p53 agent for treatment of cancers. *Human Gene Therapy*, *16*, 1016-1027.

Quelle, D.E., Zindy, F., Ashmun, R.A. and Sherr, C.J. (1995). Alternative reading frames of the INK4a tumor suppressor gene encode two unrelated proteins capable of inducing cell cycle arrest. *Cell*, *83*, 993-1000.

Radfar, A., Unnikrishnan, I., Lee, H.W., DePinho, R.A. and Rosenberg, N. (1998). p19(Arf) induces p53-dependent apoptosis during abelson virus-mediated pre-B cell transformation. *Proceedings of the National Academy of Sciences USA*, *95*, 13194-13199.

Richards, C.A. *et al*. (1995). Transcriptional regulatory sequences of carcinoembryonic antigen: Identification and use with cytosine deaminase for tumor-specific gene therapy. *Human Gene Theraphy*, *6*, 881–893.

Schmid, H.P., McNeal, J.E. and Stamey, T.A. (1993). Clinical observations on the doubling time of prostate cancer. *European Urology*, *23*(suppl. 2), 60-63.

Schwarzenberger, P., Spence, S.E. and Gooya, J.M. *et al.* (1996). Targeted gene-transfer to human hematopoietic progenitor cell lines through the c-kit receptor. *Blood*, *87*(2), 472-478.

Serrano, M., Lee, H. and Chin, L. *et al.* (1996). Role of the INK4a locus in tumor suppression and cell mortality. *Cell*, *85*, 27-37.

Sherr, C.J. (2000). The Pezcoller lecture: Cancer cell cycles revisited. *Cancer Research*, *60*, 3689-3695.

Shirakawa, T. (2008). The current status of adenovirus-based cancer gene therapy. *Molecules and Cells*, *25*(4), 462-466.

Siddiqui, F., Li, C.Y., LaRue, S.M., Poulson, J.M. and Avery, P.R. *et al.* (2007). A phase I trial of hyperthermia-induced interleukin-12 gene therapy in spontaneously arising feline soft tissue sarcomas. *Molecular Cancer Therapeutics*, *6*(1), 380-389.

Stephan, A.V. and Kelly, K.H. (2002). Adenoviral gene therapy. *The Oncologist*, *7*, 46-59.

Stratford-Perricaudet, L.D. and Perricaudet, M. (1994). *Gene therapy: The advent of adenovirus*. In J.A Wolff (Ed.), *Gene therapeutics: Methods and applications of direct gene transfer* (pp. 344-62). Boston (MA): Birkhauser.

Swisher, S.G., Roth, J.A. and Nemunaitis, J. *et al.* (1999). Adenovirus-mediated p53 gene transfer in advance non-small-cell lung cancer. *Journal of the National Cancer Institute*, *91*(9), 763-771.

Takehashi, M., Kanatsu, S.M., Inoue, K., Ogonuki, N., Miki, H., Toyokuni, S., Ogura, A. and Shinohara, T. (2006). Adenovirus-mediated gene delivery into mouse spermatogonial stem cells. *PNAS*, *104*(8), 2596-2061.

Toloza, E.M. (2005). Gene therapy for lung cancer. *Thoracic and Cardiovascular Surgery*, *17*, 205-212.

Vanderkwaak, T., Wang, M., Navarro, J., Rancourt, C., Dmitriev, I., Krasnykh, V., Barnes, M., Siegal, G. P., Alvarez, R. and Curiel, D. T. (1999). An advanced generation of adenoviral vectors selectively enhances gene transfer for ovarian cancer gene therapy approaches. *Gynaecologic Oncology*, *74*, 227-234.

Venook, A.E. *et al.* (1998). Gene therapy of colorectal liver metastases using a recombinant adenovirus encoding wt p53 (SCH 58500) via hepatic artery infusion: A Phase I study (abstr.) *American Society of Clinical Oncology (ASCO) Proceedings 17*, 431a.

Visakorpi, T., Kallioniemi, O.P. and Paronen, I.Y. *et al.* (1991). Flow cytometric analysis of DNA ploidy and S phase fraction from prostatic carcinomas: Implications for prognosis and response to endocrine therapy. *British Journal of Cancer*, *64*, 578-582.

Von Euler, H., Sadeghi, A., Carlsson, B., Rivera, P., Loskog, A., Segall, T., Korsgren, O. and Tötterman, T. H. (2008). Efficient adenovector CD40 ligand immunotherapy of canine malignant melanoma. *Journal of Immunotherapy*, *31*(4), 377-384.

Weber, H.O., Samuel, T., Rauch, P. and Funk, J.O. (2002). Human p14 (ARF)-mediated cell cycle arrest strictly depends on intact p53 signaling pathways. *Oncogene*, *21*, 3207-3212.

Wickham, T., Mathias, P., Cheresh, D. and Nemerow, G. (1993). Integrins α v β 3 and α v β 5 promote adenovirus internalization but not attachment. *Cell*, *73*, 309-319.

Woong, S. A., You, J. H., Su, M. B., Kim, T.H., Rho, M. S., Lee, J. M., Sung, E. N., Yong, S. P., Chong, K. K. and Sin, J. I. (2002). Differential suppression of human cervical cancer cell growth by adenovirus delivery of p53 in vitro: Arrest phase of cell cycle is dependent on cell line. *Japanese Journal of Cancer Research*, *93*, 1012-1019.

Xu, L.L., Su, Y.P. and Labiche, R. *et al.* (2001). Quantitative expression profile of androgen regulated genes in prostate cancer cells and identification of prostate-specific genes. *International Journal of Cancer*, *92*, 322-328.

Yang, C.T., You, L., Yeh, C.C., Chang, J.W., Zhang, F., McCormick, F. and Jablons, D.M. (2000). Adenovirus-mediated p14(ARF) gene transfer in human mesothelioma cells. *Journal of the National Cancer Institute*, *92*, 636-341.

Yazawa, K., Fisher, W.E. and Brunicardi, F. C. (2002). Current progress in suicide gene therapy for cancer. *World Journal of Surgery*, *26*(7), 783-789.

Yu, W. and Fang, H. (2007). Clinical trials with oncolytic adenovirus in China. *Current Cancer Drug Targets*, *7*, 141-148.

Zhang, J.F., Hu, C.J. and Geng, Y.P. *et al.* (1996). Treatment of a human breast cancer xenograft with an adenovirus vector containing an interferon gene results in rapid regression due to viral oncolysis and gene therapy. *Proceedings of the National Academy of Sciences USA*, *93*, 4513-4518.

Zhou, H., O'Neal, W.K. and Morral, N. *et al.* (1996). Development of a complementing cell line and a system for construction of adenovirus vectors with E1 and E2a deleted. *Journal of Virology*, *70*, 7030-7038.

ISSN: 0128-7680
Pertanika J. Sci. & Technol. **19 (1)**: 141 – 146 (2011)

Review Article

Multimodality Diagnostic Imaging in Tuberculous Lymphadenitis – A Case Review

Abdul Jalil Nordin[1*], Suraini Mohd Saini[1], Hairil Rashmizal Abdul Razak[2] and Noraini Abdul Rahim[3]

[1]Diagnostic Nuclear Imaging Unit, Faculty of Medicine and Health Sciences, Universiti Putra Malaysia, 43400 UPM, Serdang, Selangor, Malaysia
[2]RMIT University, Melbourne, Australia
[3]Radiology Department, Serdang Hospital, 43400 Serdang, Selangor, Malaysia
[*]E-mail: drimaging@yahoo.com

ABSTRACT

The purpose of this article is to demonstrate the appearance of active TB lymphadenitis using multimodality imaging apparatus. Multi-modality diagnostic imaging tools, including chest radiograph, Ultrasound (US), Computed Tomographic Scan (CT), Magnetic Resonance Imaging (MRI), and integrated 18F-FDG Positron Emission Tomography/CT examination, were performed to demonstrate TB lymphadenitis in the neck and superior mediastinum of a 26 year old female patient. There was widening of superior mediastinum on chest radiograph. Meanwhile, the ultrasound carried out detected superficial cystic lesions in the cervical region. The MRI found multiple gadolinium enhanced cervical and mediastinal lymphadenophaties. Contrast enhanced CT found heterogeneous enhancing lymphadenopathies in the same anatomical region. FDG PET/CT demonstrated a high metabolic activity in all lesions, as demonstrated by conventional imaging modalities. Mycobacterium tuberculosis was isolated from 1ml aspirate using US guidance. Post-treatment FDG PET CT scan demonstrated a complete metabolic remission of active lesions FDG PET CT can be used to demonstrate metabolic activity of active TB lesions in addition to guide clinicians in treating TB lesions.

Keywords: Extra pulmonary tuberculosis, 18F-FDG PET/CT, SUVmax, treatment response

INTRODUCTION

Tuberculosis (TB) infection has become a global health issue than a mere exclusive tropical disease owing to the increasing migration pattern and immuno compromised patients (Peter and Paul, 2009). Investigations performed on patients with suspicious extrapulmonary TB infection are often too exhaustive, while the time taken to confirm the diagnosis is usually prolonged. TB is highly infective during active form of infection. Therefore, it is important to diagnose the disease early and to start treatment that will arrest its further spread (Elad, Charles and Sally, 2001).

Conventional diagnostic imaging modalities, like plain radiographs, ultrasound, MR and CT scan, have limited ability in demonstrating active TB lesions although iodine-based contrast and gadolinium that enhanced the properties of lesions on CT and MR can be utilized as an indicator for active disease (Yeon and Kyung, 2008).

Received: 13 October 2009
Accepted: 24 May 2010
[*]Corresponding Author

PET/CT imaging modality is a relatively new imaging tool used in the diagnosis of infection. This modality is capable of providing morphological and metabolic information during a single examination (Hongming, Jian and Abbas, 2005). In this study, active extrapulmonary TB lesions in the form of cervical lymphadenitis utilizing multi modality diagnostic imaging including 18F-FDG PET/CT were demonstrated.

This study was approved by the medical ethic review committee of Universiti Putra Malaysia and the Ministry of Health, Malaysia.

CASE REVIEW

A 26 year old female factory worker presented with painless right neck swelling for the past few months. She was otherwise healthy. Clinically, there were no abnormalities found aside from small soft tissue swelling in the right side, at the base of her neck. All lab investigations, including Erythrocyte Sedimentation Rate (ESR), total white count, sputum AFB were negative for TB infection. Meanwhile, an ultrasound examination found several neck lymphadenopathies. Magnetic Resonance Imaging (MRI) of the neck and upper thorax was performed to assess disease extension. A whole body low dose unenhanced 18F-FDG PET/CT examination was also performed for this patient. Ultrasound guided aspiration using 12-gauge needle yielded 1 ml of yellowish aspirate, isolating M. Tuberculosis organism on culture, confirming the diagnosis of cervical TB lymphadenitis. The patient was treated with anti-TB drugs for 6 months. A repeat FDG PET/CT was done for the patient during follow up.

RESULTS

The blood and sputum laboratory workout for the diagnosis of TB in this patient before the intervention procedure was rather inconclusive. The results of imaging studies are as follows.

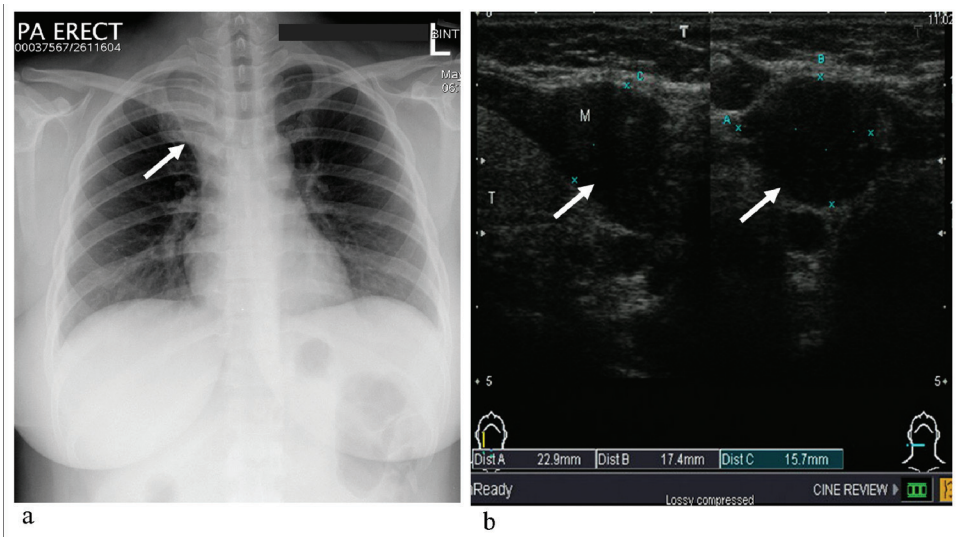

Fig. 1: (a) Frontal chest radiograph showing an enlarged mediastinum; (b) Ultrasound examination demonstrating a superficial cystic lesion measuring 22.9 mm x 17.4 mm on the right side at the base of the neck

Frontal chest radiograph demonstrated widening of the superior mediastinum (*Fig.1a*). Meanwhile, the ultrasound examination was done using a high frequency (7.5MHz) linear probe. The palpated lesion in the right base of the neck appeared as a low ecchogenicity mass with well defined border (as shown by arrows in *Fig.1b*).

Magnetic resonance imaging with gadolinium injection was done and it showed multiple low signal intensity lesions on T1 weighted images and high signal on T2 weighted images at the base of the neck. The cystic masses showed a thickened wall which enhanced following intravenous gadolinium injection (*Fig. 2*).

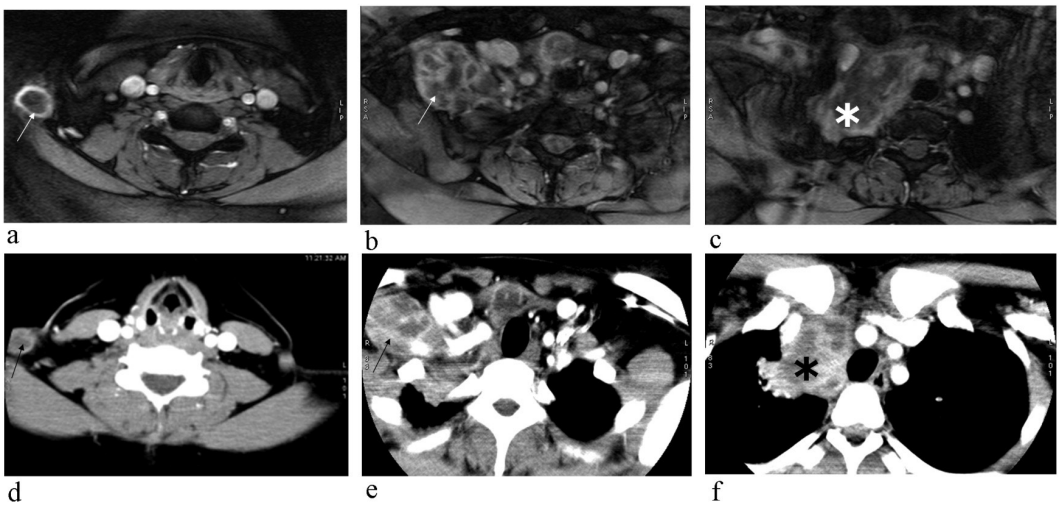

Fig. 2: Post gadolinium MRI of the neck and upper thorax in axial sections (first row a-c) in comparison to contrast enhanced CT (second row d-f). There are multifocal lesions seen in the right superficial cervical region (arrows) and deep mediastinal lesions (asterisks). Variable enhancement pattern noted following intravenous gadolinium and contrast media injection

Upon FDG PET/CT examination, several neck and mediastinal lesions were visually high intensity in keeping with increased metabolism (indicated by the arrows in *Fig. 3a*). These include the right base of the neck, para thyroid, infraclavicular, retrosternal, and left pretracheal groups of lymph nodes. The maximum standardized uptake value (SUVmax) obtained from within the region of interest (ROI) drawn over these lesions ranged between 6.9 and 14.4, as depicted in *Fig. 3b*. The most superficially located active lesion in the infraclavicular region was chosen for aspiration under ultrasound guidance where M. Tuberculosis was isolated, confirming the diagnosis.

Upon completion of the 6-month anti-TB treatment, a repeat FDG PET/CT scan revealed partial and complete metabolic remission of the lesions, indicating the response to treatment (see *Fig. 4*). Morphologically, residual nodes were found to be 20% smaller. Functionally, there was 30% to 100% reduction in the SUVmax.

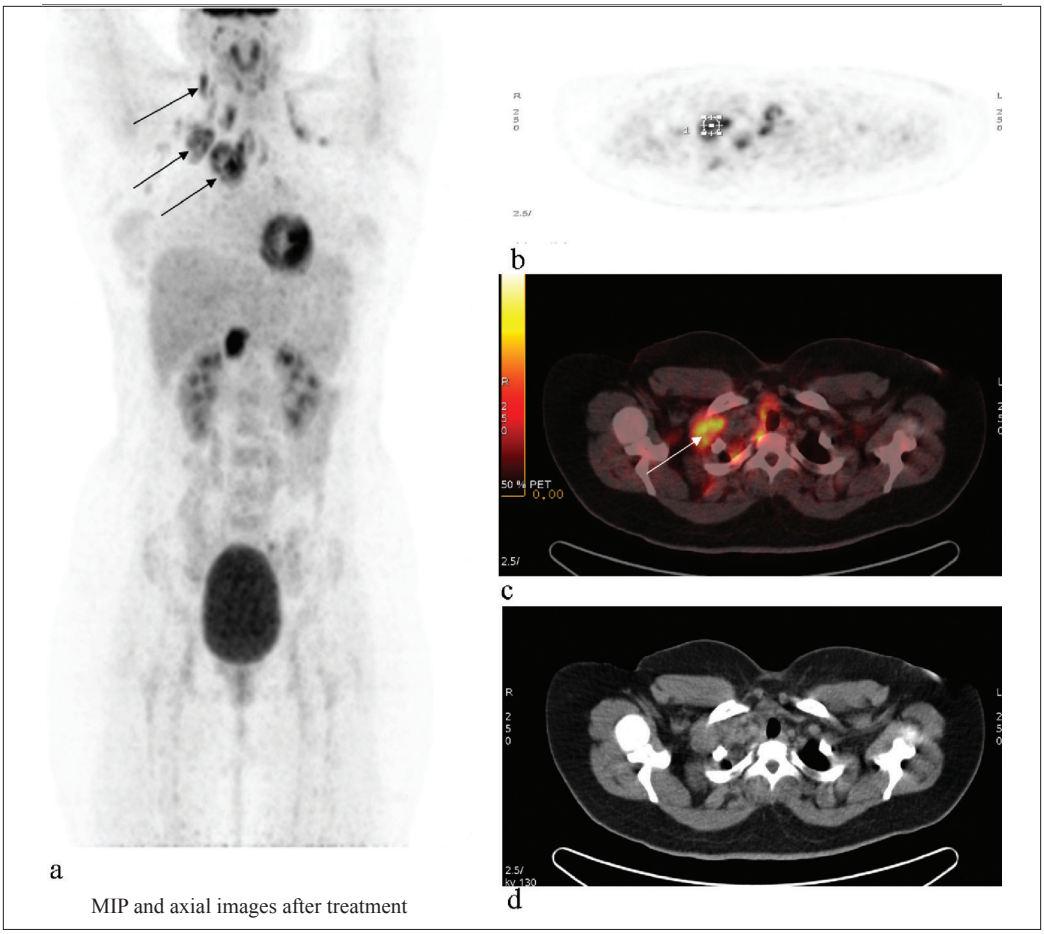

Fig. 3: Whole body 18F-FDG PET/CT examination demonstrating visually high intensity nodular lesions in the neck and superior mediastinum before the treatment (arrows). The white ROI cursor in (b) demonstrate SUVmax 14.4

DISCUSSION

There are two important aspects to be resolved in this patient before starting the anti-TB treatment. These include confirming the diagnosis and the state of lesional activity. Since TB is highly infective during its active stage, the TB treatment should be commenced immediately upon adequate clinical and laboratory evidence of active TB infection to prevent further spread.

Plain radiographs like chest X-ray can be useful in providing additional information on the possibility of co-existing pulmonary TB infection, where the incidence is far more common than extrapulmonary infection alone (Yeon and Kyung, 2008). Ultrasound is an excellent modality to be utilized in demonstrating superficial soft tissue lesions using suitable probes and technical settings. If there is a clinical need, as in the case of the present study, it can be a useful modality in assisting guided interventional procedures like aspiration biopsy.

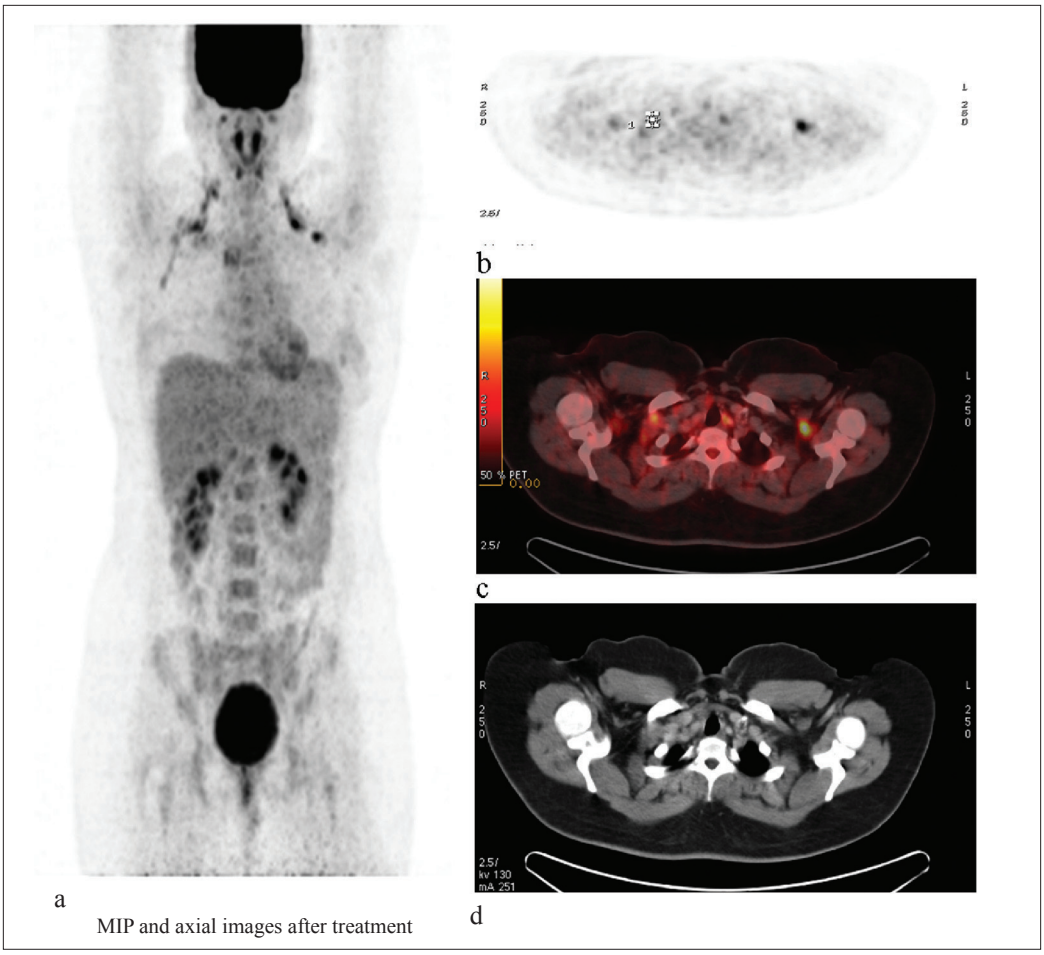

Fig. 4: Repeat FDG PET/CT examination during the follow up at 6 months interval upon completion of the anti-TB treatment revealed partial and complete metabolic remissions of the previously active lesions. On CT, these lesions were smaller, i.e. less than 1 cm in diameter with no significant enhancement pattern following the intravenous contrast administration

MR and CT are excellent imaging modalities for mapping deep seated lesions. Meanwhile, the multi planar imaging capability of the MRI enables 3 dimensional viewing of the lesions. With the latest technological advancement, multi-slice CT has tremendously improved the quality of image by increasing its spatial resolution. CT has become a routine modality in demonstrating soft tissue lesions in the upper chest and abdomen. The accessibility of this imaging modality, with its short acquisition time, makes CT a popular choice over other modalities in mapping thoracic lesions (Yeon and Kyung, 2008). In addition, CT also plays an important role in delineating the precise anatomical location of metabolically active lesions on PET in fusion imaging. However, both modalities require intravenous contrast injection to demonstrate the activity of lesions. Thus, contrast-related hypersensitivity reaction and its complications are standing risks.

The patho-physiology of the FDG uptake in tumour and infection has been elaborated in many publications. Among all other imaging modalities, the FDG PET/CT is exceptional in demonstrating the functionality of a lesion through its metabolic activity. There are two methods in its assessment.

This can be accomplished by visual intensity of the FDG uptake within the lesions or a semi-quantitative evaluation by means of a standardized uptake value (SUV). A value of the maximum SUV or SUVmax >2.5 is generally regarded as an abnormal high uptake of FDG in most PET/CT centres. In the present study, the SUVmax of the active TB lesions was found to range between 6.9 and 14.4 at diagnosis. The most superficial lesion was aspirated using the US guidance, where TB was isolated. The patient was treated using the anti-TB drugs for 6 months. A repeat FDG PET/CT at follow up revealed a near complete metabolic remission of the previously active lesions.

Although more than 80% of the FDG PET/CT work is oncology-related, the present study has demonstrated the ability of this new integrated diagnostic fusion modality being utilized in demonstrating active lesions of chronic extrapulmonary TB infection (Demura *et al.*, 2009; Park, Ryu and Shim, 2008). When a diagnostic CT scan is performed during a PET CT image acquisition and integrated with the PET images, useful clues can be obtained in a single seating which may influence the correct investigations to be performed finding the correct path to the final diagnosis.

CONCLUSIONS

In practice, multiple imaging modalities have been used for the diagnosis of Tuberculosis infection. This approach can be improved using the new integrated FDG PET CT imaging modality which provides functional information of the active extra pulmonary TB lesions. This fusion imaging technique is a useful modality in guiding biopsy procedure for the diagnosis and evaluating active lesions following the treatment.

REFERENCES

Demura, Y., Tsuchida, T., Uesaka, D., Umeda, Y., Morikawa, M. and Ameshima, S. *et al.* (2009). Usefulness of 18F-fluorodeoxyglucose positron emission tomography for diagnosing disease activity and monitoring therapeutic response in patients with pulmonary mycobacteriosis. *European Journal of Nuclear Medicine and Molecular Imaging*, *36*, 632-639.

Elad, Z., Charles, L. D. and Sally, M. B. (2001). Early therapy for latent tuberculosis infection. *The American Journal of Epidemiology*, *153*, 381-385.

Hongming, Z., Jian, Q.Y. and Abass, A. (2005). Applications of fluorodeoxyglucose-PET imaging in the detection of infection and inflammation and other benign disorders. *Radiologic Clinics of North America*, *43*, 121–134.

Park, I.N., Ryu, J.S. and Shim, T.S. (2008). Evaluation of therapeutic response of tuberculoma using F-18 FDG positron emission tomography. *Clinical Nuclear Medicine*, *33*, 1-3.

Peter, R.D. and Paul, D.V.H.(2009). The global burden of tuberculosis — Combating drug resistance in difficult times. *The New England Journal of Medicine*, *360*, 2393-95.

Yeon, J.J. and Kyung, S. L.(2008). Pulmonary tuberculosis: Up-to-date imaging and management. *AJR*, *191*, 834-844.

ISSN: 0128-7680
Pertanika J. Sci. & Technol. **19 (1)**: 147 – 152 (2011)

Effects of Process Parameters on Selected Properties of Liquid Compression-Molded Vinyl Ester Sheets

Mohamed Abd. Rahman[1*], Mohd. Sapuan Salit[2] and Khalina Abdan[3]
[1,2]Department of Mechanical and Manufacturing Engineering, Faculty of Engineering,
[3]Institute of Tropical Forest and Forest Products,
Universiti Putra Malaysia, 43400 UPM,
Serdang, Selangor, Malaysia
**E-mail: mabdrahman2@gmail.com*

ABSTRACT

Vinyl esters combine the best of polyesters and epoxies in terms of properties and processing. Without complicating presence of reinforcing fibres, this study investigated the effects of catalyst amount, preheating time, molding temperature, and pressure on flexural and water absorption properties of cast vinyl ester (VE) using a factorial experiment. Longer preheating time enhanced the stiffness of VE, while higher molding pressure reduced the flexural modulus. All the four factors did not affect the flexural strength and elongation at the break of molded VE significantly. Using a high molding pressure also caused molded VE to have higher water absorption for a long water exposure period. Meanwhile, greater water absorption at bigger amount of catalyst and higher preheating temperature indicate possible interactions between these factors. The results suggest possible negative effects of high molding pressure through the increase in the network of micro-cracks, and thus lowering the integrity of cast VE sheets. Judicious selection of the process parameters was required in order to obtain good quality molded VE sheets and by extension fibre-reinforced VE composites. Molded VE-unsaturated polyester (UP) blend is a significantly different material which is 1.49 times stronger, 2.38 times more flexible, but it is 0.69 less stiff than neat VE and with significantly higher water absorption. The results obtained warrant for a further investigation in process optimization of VE molding and the use of VE-UP blend as a matrix for natural fibre-reinforced composites.

Keywords: Vinyl ester, compression molding, factorial experiment, flexural properties, water absorption

INTRODUCTION

Thermoplastics and thermosets have been used as the continuous phase to bind the discontinuous fibrous or particulate phase in polymer composites. Thermosets are relatively easy to process and are well-suited for structural applications (Mallick, 1993). Though not directly recyclable, thermosets may still make positive environmental contributions through lower energy usage and air emissions (Joshi *et al*., 2004). Combining the best properties of epoxies and polyesters, VE resins are much less researched despite being tougher, more resilient, and less susceptible to water degradation by hydrolysis (Li, 1998). Nevertheless, there has been little use of VE with natural fibres like pineapple leaf fibres (PALF) (Arib *et al*., 2004) and more so of VE-UP blends.

The properties of the final composites depend on the individual properties of the matrix, fibre, and the nature of the interface between the two phases. Research has normally been carried out to understand either ingredient-structure-property relationships of resins or those of the fibre-resin combinations (Anon, 2008; Li, 1998). Therefore, there is a need to study the effects of processing

Received: 3 January 2010
Accepted: 5 March 2010
*Corresponding Author

parameters of liquid compression molding (LCM) on the cast matrix properties with the aim to optimize the process, particularly when fibre samples are scarce. LCM is seldom used to fabricate natural fibre-reinforced composites (Arib *et al*., 2004) and results have been varying, apart from the fact that it is limited to composite mechanical properties only (de Deus *et al*., 2005; de Sousa *et al*., 2004; Takagi and Asano, 2008; Mwaikambo and Ansell, 2003). As reported, molding pressure may not have any effect on the composite mechanical properties (de Deus *et al*., 2005) or even decrease them (Mwaikambo and Ansell, 2003).

Literature search indicates that there has been no previous work conducted on any simultaneously studying the effects of processing parameters on the mechanical and physical properties of molded VE and VE-UP blend. In this study, sheets of VE were compression-molded while varying the catalyst amounts, resin preheating time, molding temperature, and pressure. Their effects on the flexural and water absorption of this resin cast using LCM were also studied. Some comparative work was also done on VE-UP blend.

MATERIALS AND METHODS

Sample Preparation

The resins used were Bisphenol-A epoxy VE, Hetron 922, supplied by Act (UK) Ltd., whereas Synolac standard UP resin was supplied by Cray Valley Resins (M) Sdn. Bhd. Antonox-90 methyl ethyl ketone peroxide (MEKP) was used as the catalyst. VE was catalyzed with MEKP (*see* Table 1) and the mixture was stirred well before pouring it into the cavity of a flat three-piece mold and molded using a Technopress 40HC-B (Technovation) compression molding machine. Catalyzed resin preheating time, molding temperature, and pressure were varied as stipulated. Samples were molded for 10 minutes before cooling at 20°C without pressure and left to cure at ambient temperature for a minimum of 72 hours. Specimens were cut into required dimensions using a Pro-light Machining Centre (Light Machines Corp.). Sheet samples of VE-UP (50:50) blend were also press-molded.

TABLE 1
Processing parameters and their levels

Factor level	Catalyst (phr)*	Preheat time (minutes)	Molding temp. (°C)	Molding pressure (MPa)
Low	1.0	3	40	2.8
High	2.0	7	60	5.6
Centre-point	1.5	5	50	4.2

*phr – parts per hundred resin

Testing

Sample flexural properties were evaluated using an Instron 3365 tensile testing machine with a 5 kN load cell utilizing specimens of 63 mm long, 10 mm wide and 3 mm thick and ASTM D790 as a reference. In each case, five specimens with a span/thickness ratio of 16 and 2 mm/min test speed were used. Square specimens with 10 mm by 10 mm and 3 mm thickness were used to study water absorption as per ASTM D570. Samples were dried for 24 hours at 50°C in an air oven until constant weights were obtained. Conditioned samples were immersed in distilled water at ambient temperature. The samples were periodically taken out for weighing to the nearest 0.1 mg using

a Sartorius CP224S balance before they were immediately re-immersed. The specimens were carbon-coated using a Polaron SC7640 sputter coater before they were examined under a JEOL JSM – 5600 scanning electron microscope operated at 5 - 15 kV.

RESULTS AND DISCUSSION

The flexural properties and water absorption of the tested samples presented in Table 2 were analyzed following the examples in Wadsworth *et al*. (2002) and using Statsoft Statistica Release 7. The property change observed in optimizing matrix properties might turn out to be larger than those obtained by optimizing composite properties (Anon, 2008), and this would be valuable especially for composites with low fibre volume fractions. With only eight runs, effects of the four independent factors may be analyzed independently even though the isolation of interaction effects is not possible. The centre points chosen were not significantly different from the overall mean of all the points, and this suggested that the selected factors were linearly related to the dependent variables.

The calculations of student's t test and analysis of variance (ANOVA) of the results led the researchers to the following observations:

a. Increasing the catalyzed resin preheating time was found to significantly increase vinyl ester flexural modulus, while higher molding pressure significantly reduced the bending stiffness. On the other hand, the amount of MEKP and molding temperature did not affect flexural modulus. Though requiring further tests, it may be suspected that too high a molding pressure may affect the structural integrity of cast matrix and thus influence the mechanical properties especially the flexural modulus.
b. All four independent process parameters did not have any significant impact on the bending strength and elongation at the break of molded vinyl ester.
c. Increasing the molding pressure significantly increased the 432-hour water absorption of the molded vinyl ester. Though not significant, the trend might be observed in the case of 24-hour water absorption as well. Apparently, some finite amount of time was required for water molecules to diffuse through the networks of micro-crack and voids.
d. The average water absorbed by VE was 0.179% higher for 5.6 MPa molding pressure than for 2.8 MPa, representing a 32.8% increase. It was evident that water absorption was different between the two molding pressures. Though pressure consolidated the molding by significantly reducing the micro-crack network and voids in non-pressed moldings (*Fig. 2a*), too high a pressure might possibly reverse that effect and adversely affect the VE sheet by extension fibre-reinforced VE composites (Takagi and Asano, 2008; Mwaikambo and Ansell, 2003). Possible increase in the network of micro-crack could be indicated by the increase in water absorption.
e. Combining the high levels of MEKP and molding temperature (2.0% and 60^{o}C) led to the average amount of water absorbed 0.149% higher than the average difference between the catalysts over both molding temperatures (40^{o}C and 60^{o}C); a value not less significant than 0.179% given in (b) above (see *Fig. 2b*). The intersection in *Fig. 2b* indicated a possible strong interaction between catalyst amount and molding temperature, as highlighted by the ANOVA table in *Fig. 1*.

Molding of hybrid VE-UP (50:50) produced a significantly different material. The cast hybrid matrix was 1.48 times stronger and 2.38 times more flexible, but 0.69 less stiff than neat VE. However, its water absorption was substantially worse than that of the neat VE. This combination of properties may be suitable for applications requiring high toughness and may be further explored.

TABLE 2
Half-fractional factorial design with 2-level (2**(4-1)) standard design with the responses

Run	Factor				Response				
	Catalyst (phr)	Preheating time (min)	Molding temp (°C)	Molding pressure (MPa)	Flexural modulus (MPa)	Flexural strength (MPa)	EAB* (%)	24h water absorption (%)	432h water absorption (%)
1	-	-	-	-	2498.2	68.5	4.0	0.159	0.518
2	+	-	-	+	2352.9	54.1	3.2	0.226	0.652
3	-	+	-	+	2466.3	56.9	3.2	0.325	0.756
4	+	+	-	-	2778.6	52.2	2.7	0.192	0.495
5	-	-	+	+	2381.0	64.9	3.7	0.246	0.576
6	+	-	+	-	2598.2	57.5	3.2	0.270	0.651
7	-	+	+	-	2710.5	57.3	2.9	0.177	0.520
8	+	+	+	+	2371.9	59.4	3.2	0.273	0.917
9	0	0	0	0	2713.3	62.5	3.2	0.297	0.651
10	0	0	0	0	2674.3	57.3	3.0	0.183	0.571
11	0	0	+	+	1760.3	88.1	7.7	0.605	1.391

*EAB – extension at break

Effect Estimates; Var.:Var5; R-sqr=.97185; Adj:.87331 (Spreadsheet26)
2**(4-1) design; MS Residual=.0020926
DV: Var5

Factor	Effect	Std.Err.	t(2)	p	-95.% Cnf.Limt	+95.% Cnf.Limt	Coeff.	Std.Err. Coeff.	-95.% Cnf.Limt	+95.% Cnf.Limt
Mean/Interc.	0.630762	0.014466	43.60309	0.000526	0.568520	0.693004	0.630762	0.014466	0.568520	0.693004
(1)Var1	0.086516	0.032347	2.67462	0.115971	-0.052662	0.225693	0.043258	0.016173	-0.026331	0.112847
(2)Var2	0.072649	0.032347	2.24592	0.153787	-0.066529	0.211826	0.036324	0.016173	-0.033264	0.105913
(3)Var3	0.060601	0.032347	1.87348	0.201866	-0.078576	0.199779	0.030301	0.016173	-0.039288	0.099889
(4)Var4	0.179156	0.032347	5.53857	0.031087	0.039978	0.318333	0.089578	0.016173	0.019989	0.159167
1 by 2	-0.018095	0.032347	-0.55939	0.632181	-0.157272	0.121083	-0.009047	0.016173	-0.078636	0.060542
1 by 3	0.149440	0.032347	4.61992	0.043797	0.010263	0.288618	0.074720	0.016173	0.005131	0.144309
1 by 4	0.032350	0.032347	1.00009	0.422614	-0.106828	0.171528	0.016175	0.016173	-0.053414	0.085764

Var 1 - Catalyst Amount
Var 2 - Preheat Time
Var 3 - Molding Temperature
Var 4 - Molding Pressure

Fig. 1: Statistical R7 output of the main effects and interactions of the process parameters on 432h water absorption

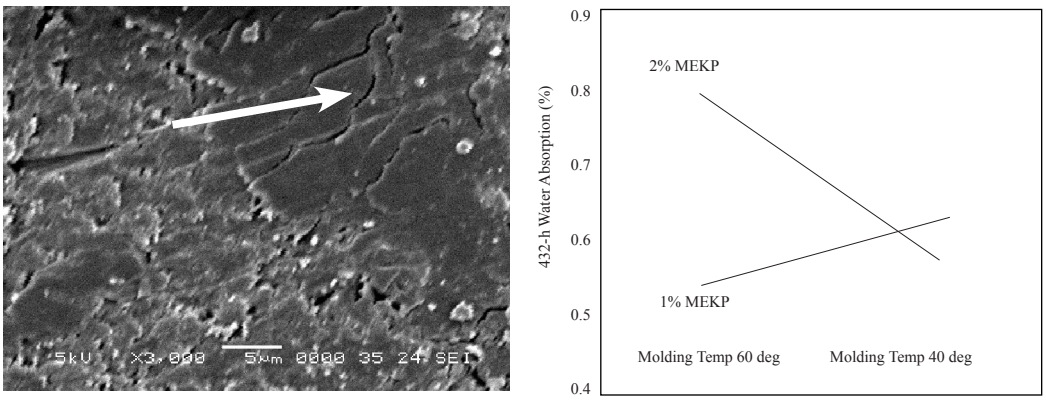

Fig. 2: (a) Microcrack network in the VE cast without pressure, and (b) interaction plot between catalyst amount and molding temperature

CONCLUSIONS

Based on the present study, it may be concluded that matrix optimization should be carried out not only to arrive at approximately optimal processing parameters before loading of reinforcement, the results may also provide clues to the resultant composite properties. Factorial experiments should be used as interactions of factors that may cause unsolicited significant property changes. Thus, further studies may be warranted on matrix optimization and the use of VE-UP blend as matrix for natural fibre-reinforced eco-composites.

ACKNOWLEDGEMENTS

The authors would like to thank Syahrul Hilmi, P. from INTROP, UPM, M. Noor, Z.A., Ibrahim, R., Syamsul Kamal, A. and Mohd. Hairi, M.R. from Engineering Faculty, International Islamic University, Malaysia, and Muhammad Wildan Ilyas, M.G. from the Faculty of Engineering, Universiti Putra Malaysia, for the assistance received in carrying the tests.

REFERENCES

Anonymous,http://www.interplastic.com/UserFiles/File/T_ProperCure.VinylEsters5_07.pdf. Retrieved on June 12, 2008.

Arib, R.M.N., Sapuan, S.M., Hamdan, M.A.M.M., Paridah, M.T. and Zaman, H.M.D.K. (2004). A literature review of pineapple fibre reinforced polymer composites. *Polymer & Polymer Composites*, *12*, 341-348.

de Deus, J.F., Monteiro, S.N. and d'Almeida, J.R.M. (2005). Effect of drying, molding pressure, and strain rate on the flexural mechanical behavior of piassava (*Attalea funifera Mart*) fiber–polyester composites. *Polymer Testing*, *24*, 750-755.

de Sousa, M.V., Monteiro, S.N. and d'Almeida, J.R.M. (2004). Evaluation of pre-treatment, size and molding pressure on flexural mechanical behavior of chopped bagasse–polyester composites. *Polymer Testing*, *23*, 253-258.

Joshi, S.V., Drzal, L.T., Mohanty, A.K. and Arora, S. (2004). Are natural fiber composites environmentally superior to glass fiber reinforced composites*? Composites Part A*, *35*, 371-376.

Li, Hui III. (1998). Synthesis, characterization and properties of vinyl ester matrix resins, PhD Thesis, Virginia Polytechnic Institute and State University.

Mallick, P.K. (1993). *Fiber-reinforced Composites – Materials, Manufacturing, and Design*. New York: Marcel Dekker.

Mwaikambo, L.Y. and Ansell, M.P. (2003). Hemp fibre reinforced cashew nut shell liquid composites. *Composites Science and Technology*, *63*, 1297-1305.

Takagi, H. and Asano, A. (2008). Effects of processing conditions on flexural properties of cellulose nanofiber reinforced "green" composites. *Composites Part A: Applied Science and Manufacturing*, *39*, 685-689.

Wadsworth, H.M., Stephens, K.S. and Godfrey, A.B. (2002). *Modern Methods for Quality Control and Improvement* (2nd Edn.). New York: John Wiley & Sons.

ISSN: 0128-7680
Pertanika J. Sci. & Technol. **19 (1)**: 153 – 159 (2011)

The Effects of Chemical Modifiers on the Thermal Properties of Calcium Carbonate Filled Polypropylene/Ethylene Propylene Diene Terpolymer Composites

Siti Rohana Ahmad[1*], Salmah Husseinsyah[2] and Kamarudin Hussin[2]
[1]Mechanical Section, Universiti Kuala Lumpur Malaysian Spanish Institute (UniKL MSI), Lot 13 - 16, Kulim Hi-Tech Park, 09000 Kulim, Kedah, Malaysia
[2]School of Material Engineering, Universiti Malaysia Perlis (UniMAP), 02600 Jejawi, Perlis, Malaysia
[*]E-mail: sitirohana@msi.unikl.edu.my

ABSTRACT

A chemical modifier (acrylic acid) was used to improve the thermal properties of polypropylene/ethylene propylene diene terpolymer/calcium carbonate (PP/EPDM/$CaCO_3$) composites. Treated and untreated PP/EPDM composites were filled by $CaCO_3$ at 0, 20 and 40% wt. The composites were prepared using Z-blade mixer machine at 180°C and 50 rpm of rotor speed. Thermogravimetric analysis (TGA) and differential scanning calorimetry (DSC) methods were used to analyze the thermal properties of the composites. Thermogravimetric analysis indicated that the total weight loss of PP/EPDM/$CaCO_3$ composites decreased with the increasing filler loading for the treated and untreated composites. Meanwhile, the presence of acrylic acid was found to have increased the thermal stability and crystallinity of PP/EPDM/$CaCO_3$.

Keywords: Calcium carbonate, polypropylene, ethylene propylene diene terpolymer, chemical modifiers, composites

INTRODUCTION

Nowadays, the application of polymer composites has increased tremendously because it is a relatively easy way to obtain new materials with balanced properties. The name polyolefinic thermoplastic elastomer (TPE) has been coined to refer to a specific family of thermoplastic alloys that offers the main advantages of two types of polymeric materials, namely elastomeric behaviour at room temperature and thermoplastic behaviour at processing temperatures. This dual behaviour is obtained because the morphology consists of small rubber particles dispersed in a continuous thermoplastic matrix.

Since the past decade, the use of inorganic filler to improve the physical properties of polymer composites has become widespread, particularly in the production of high-performance materials. Adding inorganic filler can enhance their stiffness but it also results in a decrease of toughness. In order to overcome the drawback resulted by only adding elastomer or filler, a lot of work has been done on polymer/elastomer/filler ternary system, where both elastomer and filler were used to enhance the toughness and stiffness simultaneously (Zhang *et al.*, 2000; Jancar and Dibenedetto, 1995).

Acrylic acid is classified as a surface modifier in polymer composite industry. One of the methods used for rubber surfaces is surface modification using acrylic acid. Okrasa *et al*. (2001) reported that a larger modification of the molecular relaxation processes was observed in

Received: 3 January 2010
Accepted: 5 March 2010
[*]Corresponding Author

the hydroxypropyl cellulose: poly (acrylic acid), (HPC:poly(AA)) composites, where stronger intermolecular interactions were also present.

Thermogravimetric analysis (TGA) and differential scanning calorimetry (DSC) are commonly used to investigate the thermal properties of polymer. Thermal analysis of polymers is very important in determining their utility under various environmental conditions, high temperature application, decomposition mechanism, etc. Thermogravimetric analysis furnishes data on weight loss as a function of temperature and provides a means to estimate kinetic parameters or thermal decomposition reaction. It is also possible to establish a pyrolysis mechanism, a rapid comparison of thermal stabilities and a decomposition temperatures of different polymers. In addition, Differential Scanning Calorimetry (DSC) is thermoanalytical technique used to investigate the difference in the amount of heat required to increase the temperature of a sample while reference is measured as a function of temperature (Alonso *et al*., 1997; Dudic *et al*., 2001; Salmah *et al*., 2005).

In the previous study based on tensile properties, water absorption and morphology analysis, the present of acrylic acid on polypropylene/ ethylene propylene diene terpolymer/ calcium carbonate (PP/EPDM/$CaCO_3$) composites showed an improvement compared to untreated composites. Meanwhile, the incorporation of chemical modifiers, acrylic acid (AA) increased the tensile strength and modulus of elasticity but decreased the elongation at break. A better water resistance was shown in the treated composites with acrylic acid compared to untreated composites. The presence of acrylic acid has improved the filler-matrix distribution, adhesion and compatibility between $CaCO_3$ and PP/EPDM matrix, and it has consequently improved the properties of the composites that can be seen through the morphology analysis (Siti Rohana *et al*., 2008).

In this analysis, acrylic acid was used as a chemical modifier in order to increase the thermal properties of polypropylene/ethylene propylene diene terpolymer/ calcium carbonate (PP/EPDM/$CaCO_3$) composites.

EXPERIMENTAL DESIGN

Materials

Polypropylene used was grade S12232 G112 from Polypropylene Malaysia Sdn. Bhd. Meanwhile, ethylene propylene diene terpolymer (EPDM) grade Vistalon 2504N was obtained from Exxonmobile Chemical while calcium carbonate ($CaCO_3$) was supplied by Ipoh Ceramic Sdn. Bhd. in Perak, Malaysia. With an average particle size of 8.3µm, $CaCO_3$ was dried in a vacuum oven at 100°C for 4 hours to remove its moisture. Acrylic acid anhydrous coupling agent grade 01730 was supplied by Fluka. Table 1 shows the formulation for both the untreated and treated PP/EPDM/$CaCO_3$ composites used in this study.

Filler Treatment

Calcium carbonate was modified using 3% acrylic acid in ethanol and stirred for 1 hour. The calcium carbonate was filtered out, washed with distilled water and dried in oven at 80°C for 24 hours.

Mixing Procedure

The mixing of composites was prepared in Z-blade mixer machine for 15 minutes at the temperature of 180°C and rotor speed of 50 rpm. Firstly, polypropylene was discharged to the chamber and allowed to melt. The polypropylene was completely melted in 7 minutes. Then, $CaCO_3$ was added, and this was followed by EPDM at tenth minute. Mixing was continued for 5 more minutes, and was completed in 15 minutes. For the treated composites, the sequences were similar to that of the untreated composites.

The formulation of PP/EPDM/$CaCO_3$ composites with acrylic acid was similar to the preparation of the untreated PP/EPDM/$CaCO_3$ composites with different filler loadings. After 7 minutes, $CaCO_3$ treated with acrylic acid was added into the mixing chamber. *Fig. 1* shows the chemical reaction of $CaCO_3$ with acrylic acid.

Then, the composites were taken out from the mixing machine and sheeted with roll mill to obtain composites with 2.0 mm thickness. The samples were press-moulded in a compression moulding machine model GT 7014A to perform 1.0 mm sheet of composites. The hot–press procedures involve pre-heating at 180°C for 6 minutes, followed by compressing for 4 minutes at the same temperature and subsequent cooling under pressure for 4 minutes. The samples were cut from the moulded sheets by using Wallace die cutter model S/6/1/4 to obtain the dumbbell specimens (ASTM D-638).

Measurement of the Thermal Properties

Differential scanning calorimetry (DSC)

Differential scanning calorimetry (DSC) is a thermo analytical technique. It is used to study the behaviour of heated polymer, as well as to determine the thermal transitions that take place in polymer when it is heated. In addition, DSC measures the difference in the amount of heat required to increase the temperature of a sample, while a reference is measured as a function of temperature.

The melting characteristics and crystallization behaviour of the composite samples were carried out using Perkin Elmer DSC Q10 V8.2 Build 268 analyser equipments. Samples of about 10 - 25 mg were heated from 20 to 220°C in nitrogen air flow of 50 ml/min and the heating rate of 20°C/min. The crystallinity percentage of composites (X_{com}) was determined using equation (1):

$$X_{com}\ (\%\ crystalinity) = \Delta H_f / \Delta H^0_f\, x\ 100\% \quad (1)$$

Where ΔH_f and ΔH^0_f are enthalpy of the system's fusion and enthalpy of fusion of perfectly (100%) crystalline PP, respectively. As for ΔH^0_f (PP), a value of 209 J/g was used for 100% crystalline PP. X_{com}, which is calculated using this equation. However, it gives only the overall crystallinity of the composites based on the total weight of composites including non-crystalline fractions. Also, it is not the true crystallinity of the PP phase. The value of crystallinity for PP phase of the fraction (X_{pp}) was normalized using equation (2):

$$X_{pp} = (X_{com}) / Wf_{pp} \quad (2)$$

Where Wf_{pp} is the weight fraction of PP in the composites.

Thermogravimetric analysis (TGA)

Thermogravimetric analysis (TGA) is an analytical method where the change of mass of a sample as a function of the temperature and time is measured. The thermogravimetric analysis of composites was carried out using the Perkin Elmer analyzer equipments. The samples with the weight between 15 to 25 mg were scanned from 50 to 600°C using a nitrogen air flow of 50 ml/min and a heating rate of 20°C/min. The sample size was kept almost the same for all the sample tests.

RESULTS AND DISCUSSION

Differential Scanning Calorimetry (DSC)

Fig. 2 shows the differential scanning calorimetry (DSC) curve of the untreated and treated PP/EPDM/$CaCO_3$ composites with AA at 40 php $CaCO_3$. The highest melting temperature occurred at 40 php calcium carbonate loading of the treated composites with AA. It could be seen from Table 2 that the value of $\Delta H^0_{f(\mathrm{com})}$ and X_{com} decreased with the increase in the calcium carbonate loading. This might be due to the decreasing PP concentration at a higher $CaCO_3$ loading. At a similar filler loading, composites with AA exhibited a higher value of $\Delta H^0_{f(\mathrm{com}),}$ X_{com} and X_{pp} than the composites without AA. The increase in crystallization of esterification with acrylic acid of PP/EPDM/$CaCO_3$ composites might be due to the enhancement of calcium carbonate as a nucleation agent.

Thermogravimetric Analysis

The comparison of thermogravimetric analysis curves of the untreated and treated PP/EPDM/$CaCO_3$ composites with AA composites at 0, 20 and 40 php $CaCO_3$ is shown in *Fig. 3*. For all the composites, the weight loss in a nitrogen atmosphere is very similar, proceeding principally in a single step which leads to significant weight losses above 350ºC with the maximum rate at 480 - 500ºC. The subsequent weight loss above 600ºC was due to the degradation of the calcium carbonate filler. It could be seen from Table 3 that degradation temperature corresponding to the major total weight loss decreased with esterification of the composite. From this table, it could clearly be observed that the treated composites with AA at higher loading of calcium carbonate have more resistance against degradation and a better thermal stability compared to the untreated composites. Consequently, this indicates that the presence of acrylic acid has increased the thermal stability in PP/EPDM/$CaCO_3$ composites.

Acrylic acid polymers are known to show a significant decomposition at 360ºC (McNeill and Sadeghi, 1990). Higher thermal stability of the polymers is due to an interaction between calcium ions and carboxylate ions. McNeill and Sadeghi (1990), McNeill (1997), and Kramer *et al*. (2007) observed that polymers formed by the reaction of calcium carbonate of acrylic acid are stable up to the temperature of 440ºC

TABLE 1
The formulation of PP/EPDM/$CaCO_3$ composites with and without AA at different loadings

Materials	PP/EPDM/$CaCO_3$ (without AA)	PP/EPDM/$CaCO_3$ (with AA)
Polypropylene (PP) (wt%)	70	70
Ethylene propylene diene terpolymer (EPDM) (wt%)	30	30
Calcium carbonate ($CaCO_3$) (wt%)	0, 10, 20, 30, 40	0, 10, 20, 30, 40
Acrylic acid (AA) (wt%)	-	3

TABLE 2
Parameters of DSC of the untreated and treated PP/EPDM/$CaCO_3$ composites with AA at different filler loadings

Composites	Melting temperature *Tm* (°C)	$\Delta H^0_{f(com)}$ (J/g)	X_{com} (% crystalinity)	X_{pp} (%)
PP/EPDM/$CaCO_3$: 70/30/0 (Untreated)	163.33	55.50	26.56	37.94
PP/EPDM/$CaCO_3$: 70/30/20 (Untreated)	163.86	46.49	22.24	38.15
PP/EPDM/$CaCO_3$: 70/30/40 (Untreated)	162.87	43.41	20.73	41.54
PP/EPDM/$CaCO_3$: 70/30/20 (Treated with AA)	163.91	70.63	33.79	57.97
PP/EPDM/$CaCO_3$: 70/30/40 (Treated with AA)	164.30	82.33	39.39	78.78

TABLE 3
Percentage of weight loss for the untreated and treated PP/EPDM/$CaCO_3$ composites with AA at different filler loadings and temperatures

Temperature (°C)	Weight loss (%)				
	Untreated			Treated with AA	
	70/30/0	70/30/20	70/30/40	70/30/20	70/30/40
100	0.00	0.21	0.07	0.01	0.02
200	0.05	0.03	0.03	0.03	0.01
300	0.73	0.47	1.14	0.12	0.06
400	11.91	8.92	12.14	1.12	0.78
500	86.96	73.15	57.68	77.28	68.05
600	0.23	0.05	0.12	2.59	1.65
Total	99.88	82.83	71.18	81.15	70.57

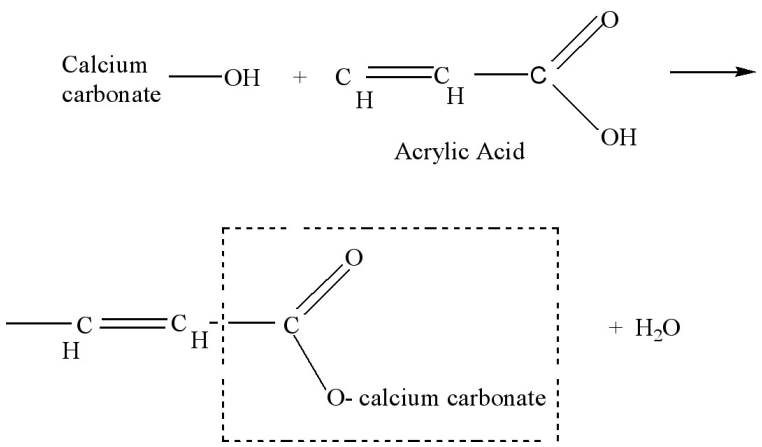

Fig. 1: Chemical reaction of calcium carbonate with AA

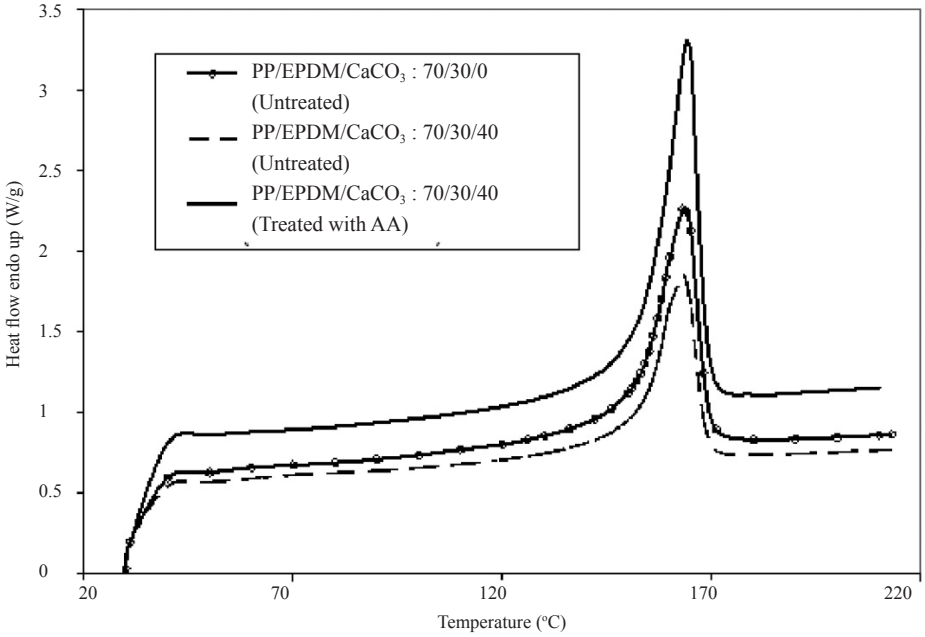

Fig. 2: Comparison of differential scanning calorimetry (DSC) curves of the untreated and treated PP/EPDM/$CaCO_3$ composites with AA at 40 php $CaCO_3$

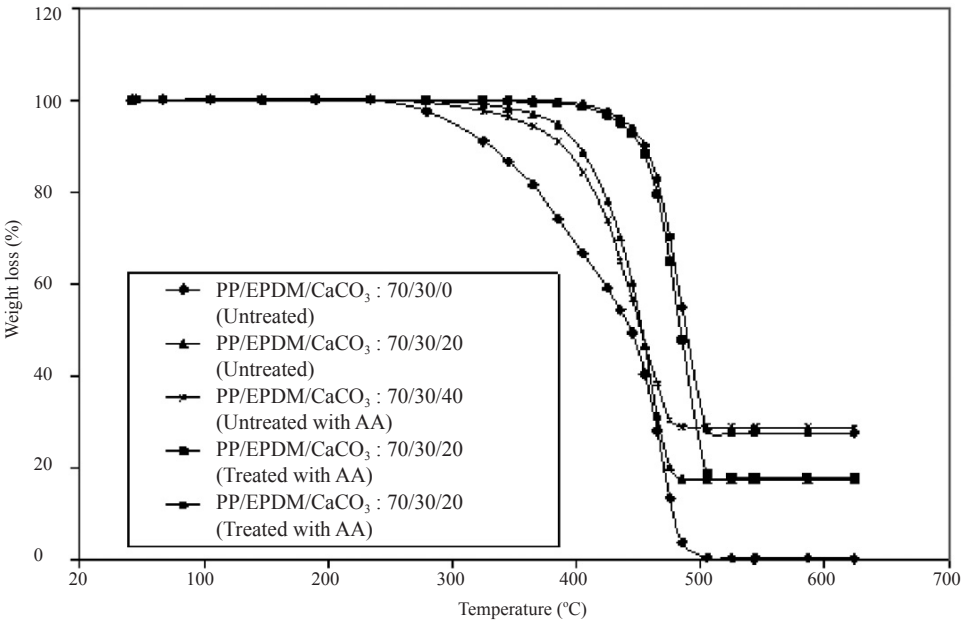

Fig. 3: Comparison of thermogravimetric analysis curves of the untreated and treated PP/EPDM/$CaCO_3$ composites with AA at different loadings

CONCLUSIONS

The thermogravimetric analysis indicates the improved thermal stability of the treated acrylic acid composites. The crystallinity of PP/EPDM/$CaCO_3$ composites increased with the presence of AA as chemical modifiers. The improvement of thermal properties could be achieved by the presence of AA due to the interaction between calcium ions and carboxylate ions.

REFERENCES

Alonso, M., Velasco, J. I. and de Saja, J. A (1997). Constrained crystallization and activity of filler in surface modified talc polypropylene composites. *European Polymer Journal*, *33*, 255-262.

Dudic, D., Kostoski, D., Djokovic, V. and Dramicanin, M.D. (2001). Formation and behaviour of low-temperature melting peak of quenched and annealed isotactic polypropylene. *Polymer International*, *51*, 111-116.

Jancar, J. and Dibenedetto, A.T. (1995). Failure mechanics in ternary composites of polypropylene with inorganic fillers and elastomer inclusions. Part II. Fracture toughness. *Journal of Materials Science*, *30*, 2438-2445.

Kramer, R.H., Raza, M.A. and Gedde, U.W., (2007). Degradation of poly(ethylene-co-methacrylic acid)-calcium carbonate nanocomposites. *Polymer Degradation and Stability*, *92*, 1795-1802.

McNeill, I.C. (1997). Thermal degradation behaviour of acrylic acid salt polymers and ionomers. *Angewandte Makromolekulare Chemie*, 157-172.

McNeill, I.C. and Sadeghi, S.M.T. (1990). Thermal stability and degradation mechanisms of poly(acrylic acid) and its salts: Part 1 poly(acrylic acid). *Polymer Degradation and Stability*, *29*, 233-246.

Okrasa, L., Boiteux, G., Ulanskia, J. and Seytre, G. (2001). Molecular relaxation in anisotropic composites based on (hydroxypropyl) cellulose and acrylic polymer. *Polymer*, *42*, 3817-3825.

Salmah, H. Ismail and Bakar, A. (2005). A comparison study on the effects of paper sludge and kaolin on properties of polypropylene (PP)/ethylene diene terpolymer (EPDM) composites. *Iranian Polymer Journal*, *14*, 705-713.

Siti Rohana, Salmah, H. and Kamarudin, H. (2008). Effects of surface modifiers on the properties of calcium carbonate filled polypropylene/ ethylene propylene diene terpolymer composites. *Proceeding Paper: International Conference for Young Chemists (ICYC 2008)*. Universiti Sains Malaysia (USM), Pulau Pinang.

Zhang, Q., Fu, Q., Jiang, L. and Lei, Y. (2000). Preparation and properties of polypropylene/montmorillonite layered nanocomposites. *Polymer International*, *49*(12), 1561–1564.

ISSN: 0128-7680
Pertanika J. Sci. & Technol. **19 (1)**: 161 – 170 (2011)

Thermogravimetric Analysis (TGA) and Differential Scanning Calometric (DSC) Analysis of Pineapple Leaf Fibre (PALF) Reinforced High Impact Polystyrene (HIPS) Composites

Januar Parlaungan Siregar[1*], Mohd. Sapuan Salit[1], Mohd. Zaki Ab. Rahman[2] and Khairul Zaman Hj. Mohd. Dahlan[3]

[1]Department of Mechanical and Manufacturing Engineering, Faculty of Engineering,
[2]Department of Chemistry, Faculty of Science,
Universiti Putra Malaysia, 43400 UPM, Serdang, Selangor, Malaysia
[3]Radiation Processing Technology Division,
Malaysia Nuclear Agency Bangi, 43000 Kajang, Selangor, Malaysia
[*]E-mail: januarjasmine@yahoo.com

ABSTRACT

This paper studied the thermal behaviour of pineapple leaf fibre (PALF) reinforced high impact polystyrene (HIPS) composite. Thermogravimetric analysis (TGA) and differential scanning calorimetric (DSC) analysis were used to measure the thermal characteristic of HIPS/PALF composites. In particular, the TGA analysis was utilized to measure the degradation and decomposition of materials in neat polystyrene, pineapple fibre, and the composites. The measurements were carried out in the temperature of 25°C – 800°C, at a heating rate of 20°C min^{-1} and the nitrogen gas flow was 50 mL min^{-1}. The temperature of the DSC analysis was programmed to be between 25°C – 300°C. The results from TGA analysis show that the addition of pineapple fibre has improved the thermal stability of the composites as compared to neat HIPS. In addition, the effects of compatibilising agent and surface modification of PALF with alkali treated were also determined and compared.

Keywords: Pineapple leaf fibre, natural fibre composites, high impact polystyrene (HIPS), TGA, DSC

INTRODUCTION

Thermal analysis is a very useful and important method to be used to characterize any materials, including thermoplastic or thermosetting polymer matrix, as well as to determine the influence of natural fibres addition into the polymers (George *et al*., 1996; Luz *et al*., 2008). One of the accepted methods for studying the thermal properties of polymeric materials is the thermogravimetric analysis (TGA). TGA is a thermal analysis technique that has been used to measure changes in the weight loss (mass) of sample that is subjected to a steady increase of temperature so as to quantify reactions involving gaseous emissions (Villain *et al*., 2007; Reis *et al*., 2007). Meanwhile, the differential scanning calorimetric analysis (DSC) was used to measure a melting point and phase transition of the composites.

The degradation of natural fibre with TGA analysis has been investigated in some previous studies. The decomposition natural fibres occurs in two or three stages of loss weight processes under controlled temperature between 25°C to 800°C (Araujo *et al*., 2008; Brigida *et al*., 2010; Arbelaiz *et al*., 2006). It is important to note that the different loss weight processes are dependent upon

Received: 3 January 2010
Accepted: 8 April 2010
[*]Corresponding Author

the types and sources of natural fibres. Meanwhile, the degradation of polymeric matrix materials, particularly the HIPS, has taken place in a single stage between 350°C and 500°C (Vilaplana *et al*., 2007). The temperature of the maximum decomposition of HIPS is around 430°C and the weight of residue is about 1.2%.

In the DSC analysis, glass transition temperature (Tg) is related to the mobility of the polymeric chains and it determines the transition between the glassy and the rubbery polymeric state (Vilaplana *et al*., 2007). The investigation of glass transition PS/sisal composites with dynamic mechanical analysis was carried out by Nair *et al*. (2001) who found that the glass transition temperature (Tg) of neat polystyrene was higher compared to the composites that contained a sisal fibre. The glass transition temperature of neat polystyrene was found to be 107.55°C, while the composites with 10, 20, and 30 wt% sisal fibre were at 89.71°C , 94.28°C, and 100.05°C, respectively. The objective of this study was to observe the thermal properties of the HIPS/PALF composites under the TGA and DSC analysis.

MATERIALS AND METHODS

Materials

The high impact polystyrene (HIPS) that has been used as the polymer matrix is Idemitsu PS HT 50, which was supplied by Petrochemical (M) Sdn. Bhd., Pasir Gudang, Johor, Malaysia. The pineapple leaf fibre (PALF) was obtained from Pemalang, Central of Java, Indonesia. The size of the pineapple leaf fibre used in this study was 10-40 mesh. There are two types of compatibilising agent used in this research, namely polystyrene-block-poly(ethylene-ran-butylene)-block-poly(styrene-graft-maleic anhydride), and poly(styrene-co-maleic anhydride). Sodium hydroxide (NaOH) that was also used to treat the pineapple leaf fibres was supplied by Aldrich Chemical Company, Malaysia.

Compatibilising Agent

Three different weight concentrations (2, 4, and 6 wt%) of compatibilising agent were applied for both types of compatibiliser. The weight of the short PALF (i.e. 50 wt% of the total formulation) was kept constant while the ratio of HIPS and compatibilising agent were also varied, as given in Table 1 below.

TABLE 1
Denotation of sample

Sample	Materials			
	HIPS [%]	PALF [%]	Compatibilising agent [%]	
			Polystyrene-block-poly (ethylene-ran-butylene)-block-poly (styrene-graft-maleic anhydride)	Poly (styrene-co-maleic anhydride)
HIPS 100	100	0	0	0
HIPS/PALF	50	50	0	0
CFA2	48	50	2	0
CFA4	46	50	4	0
CFA6	44	50	6	0
CFB2	48	50	0	2
CFB4	46	50	0	4
CFB6	44	50	0	6

Alkali (NaOH) Treatment

The PALF was soaked in two different concentrations (2% and 4%) of NaOH solution in a water bath for 1 hour at room temperature. The ratio of the fibres to the solution was 1:20 (w/v). After the treatment, the fibres were washed, rinsed several times with distilled water, and then dried in an oven at 80°C for 24 hours. The fibre treated with 2% NaOH and denoted with TFA2 for 4% is TFA4.

Composite Processing

The PALF fibres were incorporated into the HIPS matrix using a Brabender Plasticorder intensive mixer, model PL2000-6 at 165°C. The mixing process was performed in the following order. First, the HIPS and compatibilising agent were placed inside the mixing chamber for about 2 minutes at 50 rpm; later, the PALF was added into the mixing chamber for 10 minutes. The total mixing process took about 12 minutes.

Thermogravimetric Analysis (TGA)

Thermogravimetric analysis was carried out using a Mettler Toledo SDTA 851 analyzer. The samples weighing between 7-20 mg were placed in ceramic crucibles, while the tests were carried out in nitrogen atmosphere. The heating rate of the samples was 20°C min^{-1}.

Differential Scanning Calorimetric (DSC)

The preparation of the samples that were used for the differential calorimetric was similar to the TGA. Meanwhile, the analysis in the DSC was performed using the Mettler Toledo DSC822 analyzer. The temperature was programmed in the range of 25°C to 300°C, under nitrogen atmosphere.

RESULTS AND DISCUSSIONS

Thermogravimetric Analysis (TGA)

In this study, the Thermogravimetric (TGA) curves were used to determine the thermal degradation and thermal stability of each material. The TG analysis of neat high impact polystyrene (HIPS), pineapple leaf fibre (PALF) and their composites are presented in *Fig. 1*. The thermal decomposition of each sample took place in a programmed temperature range of 25°C to 800°C. The neat HIPS showed only one stage of weight loss process, which had a transition temperature that began from 341°C and the final transition at 483°C, and it was clear that the peak transition temperature of HIPS at 418°C. The weight loss and residual weight of HIPS for the TG analysis were found to be 98% and 2.4%, respectively (*see* Table 2). Previous studies (Vilaplana *et al.*, 2007) have observed thermogravimetric of virgin HIPS using the same instrument analyzer. They found that the thermal decomposition of HIPS occurred in one single stage, i.e. between 369°C – 490°C and temperature maximum transition at 433°C. The percentage of the residual weight of HIPS gathered in their study was 1.2%. The other investigation (Nair *et al*., 2001) of the thermogravimetric neat polystyrene showed that the decomposition of PS started at 288°C and there are four stages of weight loss process.

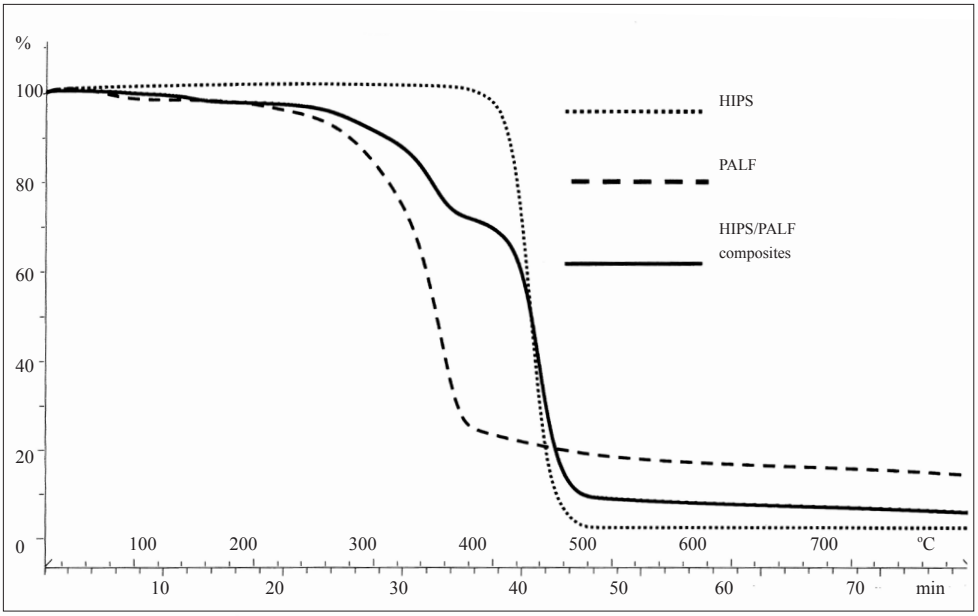

Fig. 1: The TG analysis of HIPS, PALF and HIPS/PALF composites

The thermal decomposition of PALF under nitrogen atmosphere comprises of a two-step process. The first step process that was shown at temperature 25°C to 103°C had a weight loss of 2.4%. Several previous studies (e.g. Threepopnatkul *et al*., 2009; De Rosa *et al*., 2010) revealed that the loss weight of this stage was due to the release of absorbed moisture or vaporization of the water from the fibres. George *et al*. (1996) reported that the weight loss of pineapple fibre at 100°C was about 6%, while at 200°C and 300°C, the weight loss were about 7.6% and 16%, respectively. The second stage of weight loss occurred at 126°C - 542°C, with the peak of this transition at 339°C. This weight loss indicated the decomposition of cellulose (George *et al*., 1996). In their study, the thermal decomposition of pineapple fibre was obtained at 350°C. Meanwhile, the thermal decomposition for other natural fibres, such as sisal and flax fibres, occurred at 340°C and 345°C, respectively (Manfredi *et al*., 2006). Compared to these natural fibres, the thermal decomposition of pineapple fibre in this study was slightly lower than the thermal stability. Meanwhile, the residual weight of PALF in the temperature that ranged between 25°C - 800°C was 17% (*see* Table 2). Devallencourt *et al*. (1996) reported that the residual weight of cellulose, after heating from 20 to 900°C, was about 17% and they explained that the results for the final products from the degradation of cellulose under an inert atmosphere were carbonaceous residues plus undegraded fibres when they did not remain after heating.

As illustrated in Table 2, the degradation steps are in the temperature range of 72°C - 182°C, 202°C - 367°C, and 371°C - 479°C, while the maximum peak of the transition temperature for these steps were 139°C, 338°C, and 425°C. The percentage of the loss weight composites at corresponding transition was 2.6, 26, and 62%, respectively. Therefore, it can be concluded that the thermal stability of the composites had a higher value as compared to neat HIPS.

TABLE 2
Results of the TG analysis HIPS, PALF and its composites

Sample	No. of transition	Transition temperature (°C)			Weight loss at transition (%)	Residual weight (%) at 800°C
		T_i	T_m	T_f		
HIPS	1	341	418	483	98	2.4
PALF	1	36	69	104	2.4	17
	2	126	339	542	81	
HIPS/PALF composites	1	72	139	182	2.6	9
	2	202	338	367	26	
	3	371	425	479	62	

The Effects of Compatibilizing Agent and Alkali Treated Fibre on the TG Analysis

Fig. 2 presents the effects of compatibilising agent and alkali-treated PALF fibre on the thermal degradation of the composites. All the sample materials exhibited a three-stage degradation process. Meanwhile, the composites using compatibilizer of *polystyrene-block-poly(ethylene-ran-butylene)-block-poly(styrene-graft-maleic anhydride)* showed the maximum peak temperature decomposition of composites at 428°C. It was clear that the TG curve of the modified HIPS/PALF composites was higher compared to the untreated ones. The modification of the natural fibre reinforced polymer composite using modifier or compatibilizer was found to improve the thermal resistance of the composites due to the stronger interaction between the natural fibre and the polymer matrix that was caused by the formation of the covalent bond at the interface (Doan *et al*., 2007). Meanwhile, the increase compatibilizer of *poly(styrene-co-maleic anhydride)* from 2-6 wt.% decreased the thermal stability of the composites. The thermal decomposition treated fibre composites, with 2% and 4% of NaOH, was found at the temperature 428°C. This result is similar to the modification of fibres using compatibilizer (CFA2, CFA4, and CFA6). Meanwhile, the fibres treated with caustic soda enhanced the thermal stability of natural fibre. This treatment removed natural and artificial impurities, produced a rough surface topography and made fibre fibrillation (Alawar *et al*., 2009).

Table 3 shows the weight loss of all composites at the first stage transition temperature (<200°C)

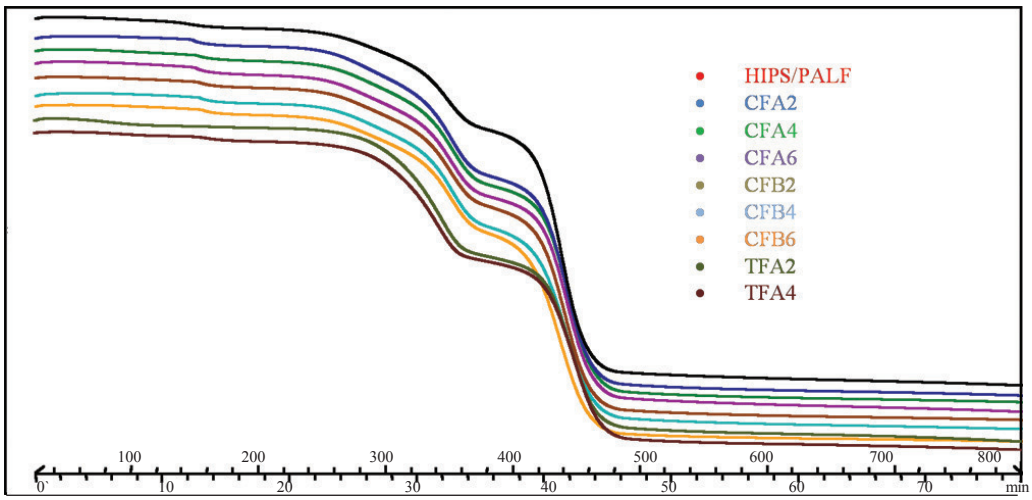

Fig. 2: The TG curves showing the effects of the compatibilising agent and alkali-treated fibre

in the range of 1.1% to 1.9%. At the second stage (<400°C), the weight loss of the composites was around 31%-36% and at the third stage of transition temperature (<600°C), the weight loss ranged from 48%-53%. The total residual weight of all the composites at 800°C was in the range of 12%-15%.

TABLE 3
The TG analysis of the effects of compatibilising agent and alkali-treated fibre

Sample	No. of transition	Transition temperature (°C)			Weight loss at transition (%)	Residual weight (%) at 800°C
		T_i	T_m	T_f		
CFA2	1	121	145	176	1.8	14.8
	2	204	339	372	32	
	3	373	428	483	51	
CFA4	1	125	149	178	1.7	12.1
	2	202	339	374	32	
	3	374	428	490	53	
CFA6	1	118	147	176	1.7	12.2
	2	204	338	375	32	
	3	374	428	483	52	
CFB2	1	128	150	182	1.8	13.1
	2	203	338	367	31	
	3	373	425	481	53	
CFB4	1	119	148	172	1.9	14.6
	2	200	338	367	32	
	3	370	423	480	50	
CFB6	1	132	150	177	1.6	12.6
	2	197	339	368	31	
	3	369	422	478	53	
TFA2	1	129	148	170	1.2	12.7
	2	220	327	361.	36	
	3	372	427	490.	48	
TFA4	1	134	151	172	1.1	12.8
	2	208	325	357	33	
	3	369	428	485	50	

Differential Scanning Calometric (DSC)

The DSC curve of the HIPS, PALF, and HIPS/PALF composites are shown in *Fig. 3*, while the values of these materials are summarized in Table 4. The glass transition (Tg) of HIPS at 105°C, while the melting point (Tm) at the temperature 150°C. The findings of other studies showed that the glass transition and melting point of HIPS were at 90°C and 120°C or 160°C, respectively (Vilaplana *et al*., 2007). The glass transition (Tg) of PALF from this study occurred at 75°C. Meanwhile, the addition of PALF to reinforce HIPS increased the Tg value of the composites. It could be seen that the temperature of Tg HIPS/PALF composite was at 123°C, indicating that the temperature Tg of the composite increased around 18°C as compared to neat HIPS.

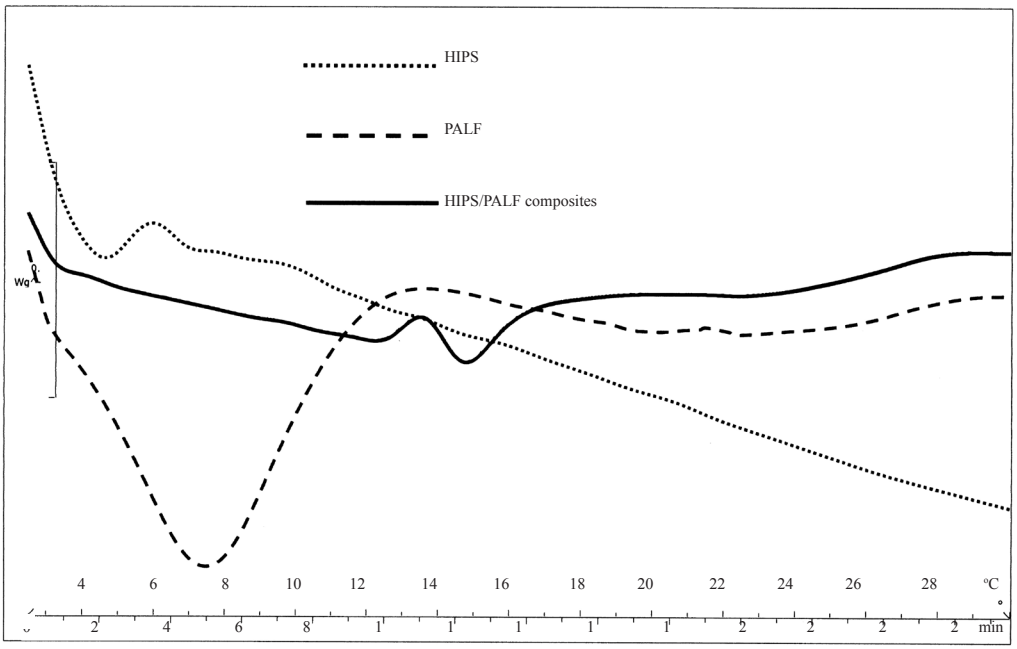

Fig. 3: The DSC analysis of HIPS, PALF and HIPS/PALF composites

The Effects of Compatibilizing Agent and Alkali-treated Fibres on the DSC Analysis

Fig. 4 presents the DSC curve of the composites using compatibilising agents. The addition of compatibilizer into the composites, with different weight concentrations of *polystyrene-block-poly(ethylene-ran-butylene)-block-poly(styrene-graft-maleic anhydride)*, decreased the glass transition and melting point of the composites. As shown in Table 4, the glass transition of the composites, denoted with CFA2, CFA4 and CFA6, was about 118°C, 104°C, and 102°C. The melting point also decreased at 149°C, 147°C, and 147°C, respectively. The increase of *poly(styrene-co-maleic anhydride)* that modified the HIPS/PALF composites (CFB2, CFB4, and CFB6) also decreased the glass transition of the composites, but the melting temperature of the composites was found to be similar to the untreated fibre composites.

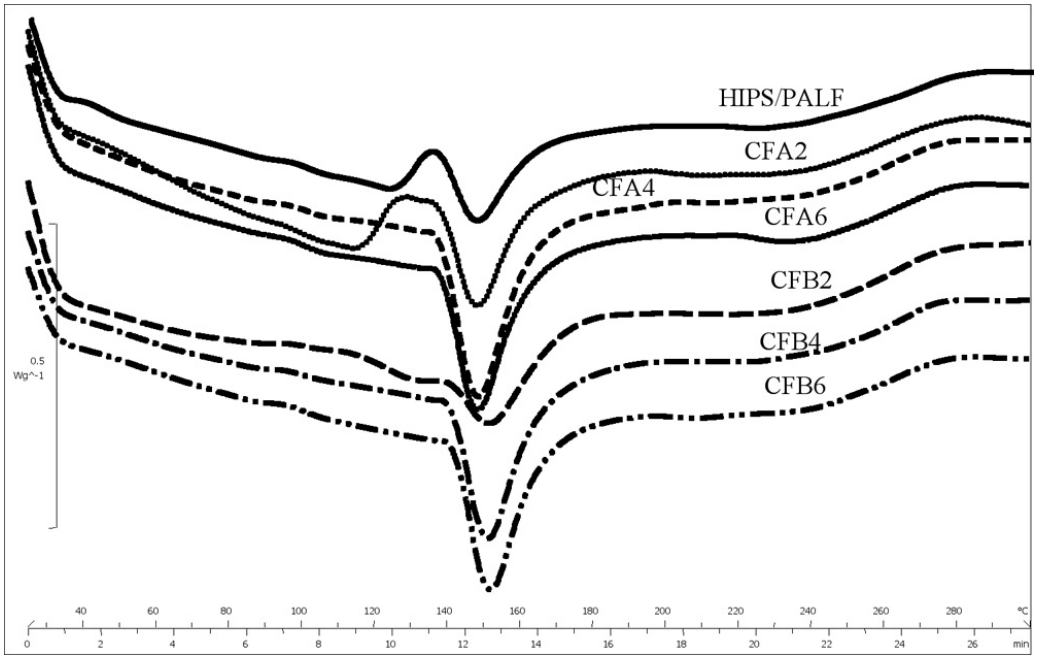

Fig. 4: The DSC curves of the composites using compatibilizer

TABLE 4
The DSC analysis of the HIPS/PALF composites

Sample	T_g, glass transition °C	T_m, melting point (°C)
HIPS	105	150
PALF	75	-
HIPS/PALF	123	149
CFA2	118	149
CFA4	104	147
CFA6	102	147
CFB2	99	150
CFB4	96	150
CFB6	95	151
TFA2	106	152
TFA4	105	151

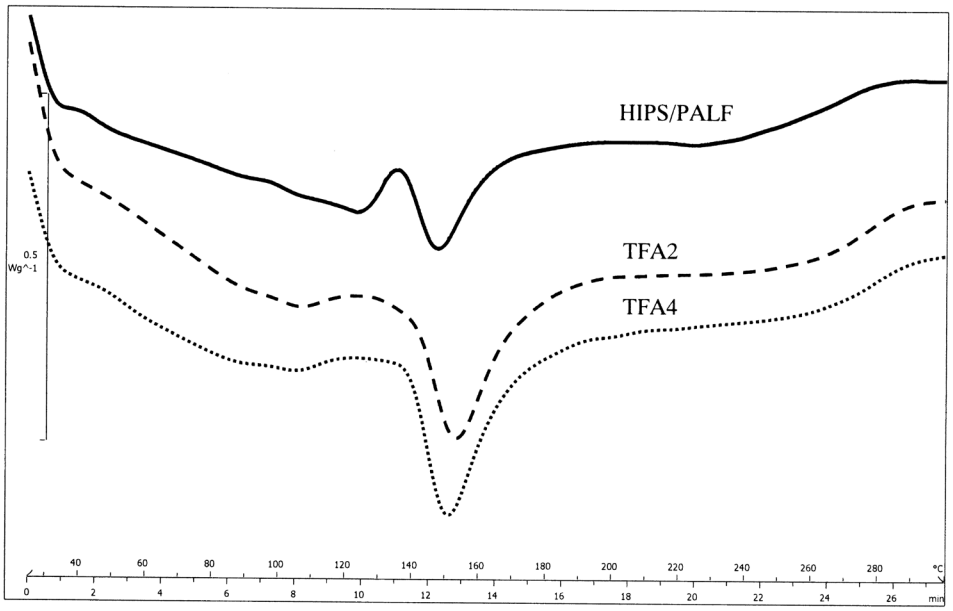

Fig. 5: The DSC curves of the alkali-treated fibre composites

Fig. 5 presents the DSC curves of the untreated and treated fibre composites. The glass transition (Tg) temperature of alkali-treated fibre composite, with 2% (TFA2) and 4% (TFA4) of NaOH, was shown at 106°C and 105°C. The melting temperature of these composites was 152°C and 151°C, respectively. This value is similar to the glass transition of neat HIPS and only small improvement was observed at the melting temperatue of the composites. As compared to the untreated fibre composite, the glass transition of the treated fibre composite was shown to be lower, but the melting temperature was higher.

CONCLUSIONS

Based on the results of this study, it can be concluded that the addition of PALF for the reinforced HIPS composites has increased the thermal decomposition and glass temperature (Tg) of the composites. The modification of the HIPS/PALF composites, using the compatibilising agent with different weight concentrations of *polystyrene-block-poly(ethylene-ran-butylene)-block-poly(styrene-graft-maleic anhydride)* and the fibres treated with alkali, has brought a slight improvement to the thermal decomposition of composites. Meanwhile, the modification composites using *poly(styrene-co-maleic anhydride)* decreased the thermal decomposition as compared to the untreated fibre. However, no significant improvement was found on the melting temperature of composites with the addition of compatibilizer and the fibre that was treated with alkali solution.

ACKNOWLEDGEMENTS

The authors wish to thank the Ministry of Higher Education, Malaysia, for funding the research through the Fundamental Research Grant Scheme (FRGS) grant number 5523413. Our appreciation also goes to the staff of the Malaysian Nuclear Agency, Selangor, Malaysia, for their support in carrying out this research.

REFERENCES

Alawar, A., Hamed, A. M. and Al-Kaabi, K. (2009). Characterization of treated palm tree fibre as composites reinforcement. *Composites: Part B*, *40*, 601-606.

Araujo, J.R., Waldman, W.R. and De Paoli, M.A. (2008). Thermal properties of high density polyethylene composites with natural fibres: Coupling agent effect. *Polymer Degradation and Stability*, *93*, 1170-1775.

Arbelaiz, A., Fernandez, B., Ramos, J.A. and Mondragon, I. (2006). Thermal and crystallization of short flax fibre reinforced polypropylene matrix composites: Effect of treatment, *Thermochimica Acta*, *440*, 11-121.

Brigida, A.I.S., Calado, V.M.A., Goncalves, L.R.B. and Coelho, M.A.Z. (2010). Effect of chemical treatments on properties of green coconut fibre. *Carbohydrate Polymers*, *79*, 832-838.

De Rosa, I.M., Kenny, J.M., Puglia, D., Santulli, C. and Sarasini, F. (2010). Morphological, thermal and mechanical characterization of okra (*Abelmoschus esculentus*) fibres as potential reinforcement in polymer composites. *Composites Science and Technology*, *70*, 116-122.

Devallencourt, C., Saiter, J.M. and Capitaine, D. (1996). Characterization of recycled cellulose: Thermogravimetry/Fourier transform infra-red coupling and thermogravimetry investigations. *Polymer Degradation and Stability*, *52*, 327-334.

Doan, T.T.L., Brodowsky, H. and Mader, E. (2007). Jute fibre/polypropylene composites II. Thermal hydrothermal and dynamic mechanical behaviour. *Composites Science and Technology*, *67*, 2707-2714.

George, J., Bhagawan, S.S. and Thomas, S. (1996). Thermogravimetric and dynamic mechanical thermal analysis of pineapple fibre reinforced polyethylene composites. *Thermal Analysis*, *47*, 1121-1140.

Luz, S.M., Del Tio, J., Rocha, G.J.M., Goncalves, A.R. and Del`Arco Jr., A.P. (2008). Cellulose and cellulignin from sugarcane bagasse reinforced polypropylene composites: Effect of acetylation on mechanical and thermal properties. *Composites Part A. Applied Science and Manufacturing*, *39*, 1362-1369.

Manfredi, L.B., Rodriquez, E.S., Przybylak, M.W. and Vasquez, A. (2006). Thermal degradation and fire resistance of unsaturated polyester, modified acrylic resins and their composites with natural fibres. *Polymer Degradation and Stability*, *91*, 255-261.

Nair, K.C.M., Thomas, S. and Groeninckx, G. (2001). Thermal and dynamic mechanical analysis of polystyrene composites reinforced with short sisal fibres. *Composites Science and Technology*, *61*, 2519-2529.

Reis, P.N.B., Ferreira, J.A.M., Antunes, F.V. and Costa, J.D.M. (2007). Flexural behaviour of hybrid laminated composites. *Composites Part A: Applied Science and Manufacturing*, *38*, 1612-1620.

Threepopnatkul, P., Kaerkitcha, M. and Anthipongarporn. (2009). Effect of surface treatment on performance of pineapple leaf fibre-polycarbonate composites. *Composites: Part B*, *40*, 628-632.

Vilaplana, F., Ribes-Greus, A. and Karlsson, S. (2007). Analytical strategies for the quality assessment of recycled high impact polystyrene: A combination of thermal analysis, vibrational spectroscopy, and chromatography. *Analytica Chimica Acta*, *604*, 18-28.

Villain, G., Thiery, M. and Platret, G. (2007). Measurement methods of carbonation profiles in concrete: Thermogravimetry, chemical analysis and gammadensimetry. *Cement and Concrete Research*, *37*, 1182-1192.

ISSN: 0128-7680
Pertanika J. Sci. & Technol. **19 (1)**: 171 – 176 (2011)

Microcellular Rubber: A Study on Reclaimed Natural Rubber (NR) Latex Gloves/Standard Malaysian Rubber (SMR) 20 Blends

Khaw Pei Chin*, Ngeow Yen Wan and Che Su Mt. Saad
Technology & Engineering Division, Advance Rubber Technology Unit,
Rubber Research Institute of Malaysia, Malaysian Rubber Board,
P.O. Box 10150, 40908 Kuala Lumpur, Malaysia
**E-mail: khawpc@lgm.gov.my*

ABSTRACT

Reclaimed rubber from rejected natural rubber (NR) latex gloves (r-NRG) was evaluated as partial replacement for Standard Malaysian Rubber (SMR) 20 in producing microcellular rubber. In the study, the amount of reclaimed rubber varied from 20 pphr to 95 pphr for the purpose of cost reduction, environmental interest and as processing aids in reducing internal porosity, swells and to minimize shrinkage and air-trapped problems in producing microcellular rubber. A typical formulation in making microcellular rubber slab was developed and two-roll mill was used for compounding. The cure characteristics and mechanical properties, such as density, hardness, tensile strength, and elongation at break, were evaluated. Scorch time and cure rate index performed marginal decreased with increasing of r-NRG content. 95 pphr r-NRG blends showed a consequential drop in hardness. Both tensile properties and elongation at break decreased as the r-NRG content was increased.

Keywords: Cure characteristic, mechanical properties, microcellular rubber, reclaimed natural rubber latex gloves, standard Malaysian rubber (SMR) 20

INTRODUCTION

Malaysia is currently the world's largest rubber glove producer and exporter (Tan, 2009; Xin Hwa News Agency, 2009). The export earnings for Malaysian rubber gloves were RM7.03 billion, and this was equivalent to nearly 49 billion pairs of gloves (Xin Hwa News Agency, 2009). The Malaysia latex industry has expanded over the years to meet the world demands and to comply with a more stringent defect standard of the US Food and Drug Administration (FDA) (Yew, 2009). Rajan *et al.* (2006) reported that about 15% of the final latex products were rejected due to the strict specifications and the unstable nature of latex. These rejects create a major disposal problem for the rubber industry. In order to alleviate this environmental issue, reclaiming is an important method rather than landfill or incineration. Since latex product waste represents a source of high quality rubber hydrocarbon and it is widely used to reduce compounding cost as additive in various rubber article formulations because it is easier to be broken down and hence reduced the mixing time. Besides, reclaimed rubber is used as a processing aid to give a better dimensional stability to the compounds and products, as well as to reduce internal porosity in the manufacturing of rubber goods. It is not a necessity to attain the physical properties of the final compound, with or without the addition of crude rubber or synthetic rubber (Dhingra). These non-black reclaimed rubbers have extra advantages in the manufacture of coloured rubber products. Thus, latex gloves from the local gloves manufacturers, which had undergone the reclamation process, were utilized in this study to produce microcellular rubber.

Received: 3 January 2010
Accepted: 8 April 2010
*Corresponding Author

Microcellular rubber is like any solid rubber, with an exception that the chemical blowing agent (CBA) is added into compounding. CBA is a combination of inorganic and organic compounds that are stable at room temperature, but decompose and liberate gas at suitable higher temperature. The cells structure of microcellular is normally closed with gas trapped within the cells and gives the material a porous or cellular structure, as well as a low specific gravity (lightweight). Microcellular polymers have been commercially accepted in a wide range of applications since 1940s because of the advantages of light weight, buoyancy, cushioning performance, thermal and acoustic insulation, impact damping, and cost reduction. Although microcellular rubber is widely manufactured, the available articles concerning their electrical and mechanical properties are still limited in number. The correlation between the experimental data in microcellular rubber is attractive from the experimental and theoretical point of view (Lee *et al.*, 2007). Therefore, an evaluation on the partial replacement of reclaimed rubber from rejected natural rubber latex gloves (r-NRG) was carried out. The amount of reclaimed rubber varied from 20 pphr to 95 pphr in a typical formulation in making microcellular rubber slab.

MATERIALS AND METHODS

Sample Preparation

Natural rubber (SMR 20) and natural rubber latex gloves reclaimed rubber (r-NRG) were purchased from KL Kepong Berhad and HSB Reclaimed Rubber Sdn. Bhd., respectively. The r-NRG was analyzed and natural rubber (74.6%), calcium carbonate (14.3%), ash (4%), total sulphur (0.85%) and others ingredients (6.25%) were found in the content. All the mixing ingredients used are shown in Table 1. Meanwhile, the compound formulation is given in Table 1. In this study, microcellular with 100/0, 80/20, 60/40, 40/20, 20/80, 5/95 pphr ratio of SMR20/r-NRG were prepared. All the blends possess the same chemical composition. The mixing was carried out in Carter 9" x 18" two-roll mill. The preparation process was started with the mastication of polymers to viscosity at about 25±5 in Mooney unit, followed by the addition of activators, fillers, chemical blowing agent, and curing agents. Then, the finished compounds were cured to t_{90} obtained from Monsanto Moving Die Rheometer MRD 2000P at 160°C using an electrical heated hydraulic press after conditioning for 24 hours.

TABLE 1
Compound formulation

Ingredients	p.p.h.r.
Natural rubber (SMR 20)	variable
Latex gloves reclaimed rubber (r-NRG)	variable
Zinc oxide (ZnO)	5.0
Stearic acid	2.0
Kaolin clay/Refined clay	50
Polymerized 2,2,4- Trimethyl-1, 2– dihydroquinoline (TMQ)	1.0
N-(1,3-Dimethylbutyl)-N´-phenyl-p-phenylenediamine (6PPD)	1.5
Sulphur	2.0
N-Cyclohexyl-2-benzothiazolesulfenamide (CBS)	0.6
Azodicarbonamide (ADC)	4.0

Testing

Cure characteristic of vulcanizates were tested with Monsanto Moving Die Rheometer MDR 2000P (Alpha Technologies) under ISO 6502. Both the density and hardness (Shore Instrument & Mfg. Co. Jamaica, New York 23352-00) of the vulcanizates were determined in accordance with ISO 1855 and ISO 48, respectively. In addition, the tensile properties of the specimens were measured according to ISO 1798, Type 1A. The crosshead rate for the tensile testing was 500mm/min, with an initial gauge length of 40mm, using Instron 5500R Series IX Automated Material Tester.

RESULTS AND DISCUSSION

The cure characteristics of microcellular rubber, with different natural rubber latex gloves reclaimed (r-NRG) contents, are presented in Table 2. Scorch time, t_{s2}, is the time taken for the minimum torque value to increase by two units. It is defined as time to incipient cure (measure of time) when the premature vulcanization occurs. The cure rate index is calculated as hundred divided by the difference between cure time, t_{90} and incipient scorch time, t_{s2} (Lee *et al.*, 2007). It can be seen that the scorch time and cure rate index performed marginal decreased with the increase of the r-NRG content. This observation might be attributed to the filler and sulphur content left in the reclaimed rubber (Farahani *et al.*, 2006). An increasing trend of the cure time, t_{90}, was also observed upon the increasing reclaimed rubber content.

TABLE 2
Rheometric characteristic of the SMR20/r-NRG microcellular rubber

r-NRG content, pphr	Minimum torque, ML (dNm)	Maximum torque, MH (dNm)	Scorch time, T_{S2} (minutes)	Cure time, T_{90} (minutes)	Cure rate index
0	0.27	9.77	2.72	6.54	26.18
20	0.18	7.46	2.14	5.57	29.15
40	0.30	8.46	2.18	5.85	27.25
60	0.34	8.89	2.25	6.06	26.25
80	0.33	9.18	2.40	5.94	28.25
95	0.14	7.61	2.15	5.75	27.78

TABLE 3
Variation of the tensile properties and hardness of the microcellular foam

SMR/r-NRG	Density, g/cm^3 ISO 1855	Hardness, IRHD (N) ISO 48	Tensile strength, MPa ISO 1798	Elongation at break, % ISO 1798
100/0	0.625	67.4	3.12	391.00
80/20	0.519	34.9	2.85	371.45
60/40	0.593	44.4	2.59	351.90
40/60	0.624	48.8	2.40	312.80
20/80	0.649	54.6	1.82	205.75
5/95	0.524	32.8	0.57	117.30

Table 3 shows the variation of the tensile properties and hardness of the microcellular foam. Both the density and hardness of vulcanizates are shown in *Figs. 1* and *2*, respectively. The r-NRG has less crosslink density as compared to virgin rubber due to the fact that chain scission has lowered the molecular weight of reclaimed rubber during the reclaiming process (Gonzalez *et al.*, 1996). Therefore, more cells could easily be formed with gas entrapped in between the matrix, with 20 pphr of r-NRG added and hence, the vulcanizate density was reduced and it also became softer. In contrast, 95 pphr r-NRG blends showed a consequential drop in hardness. It can be explained that the hemispherical indenter of Durometer penetrated and slightly broke the vulcanizates because the microcellular network was very dense and brittle (Srilathakutty *et al.*, 1999).

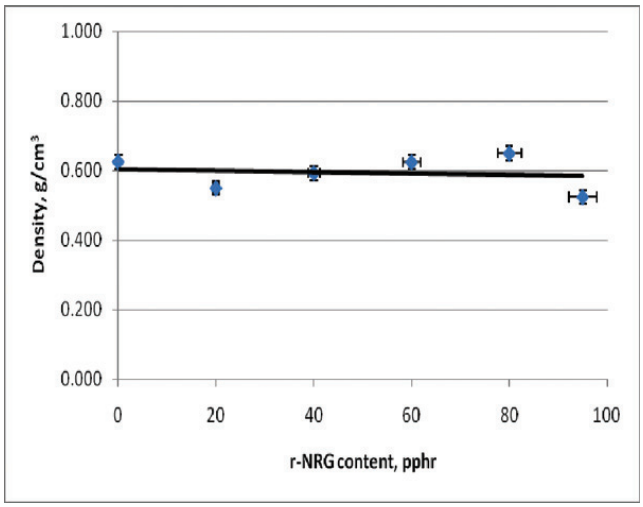

Fig. 1: The density of vulcanizates as a function of r-NRG blend ratio

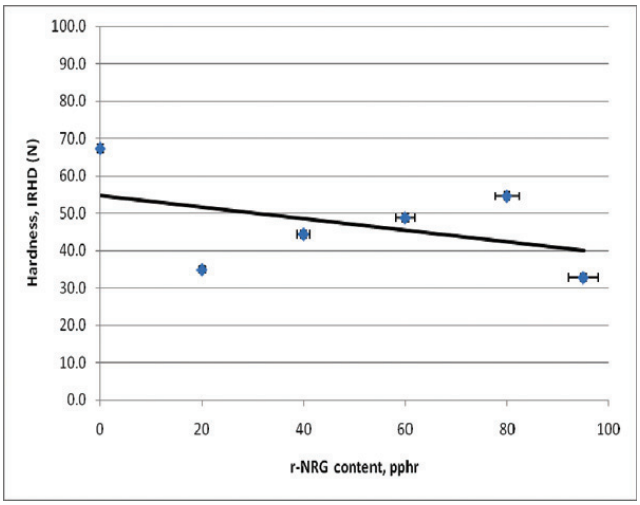

Fig. 2: Hardness of vulcanizates as a function of r-NRG blend ratio

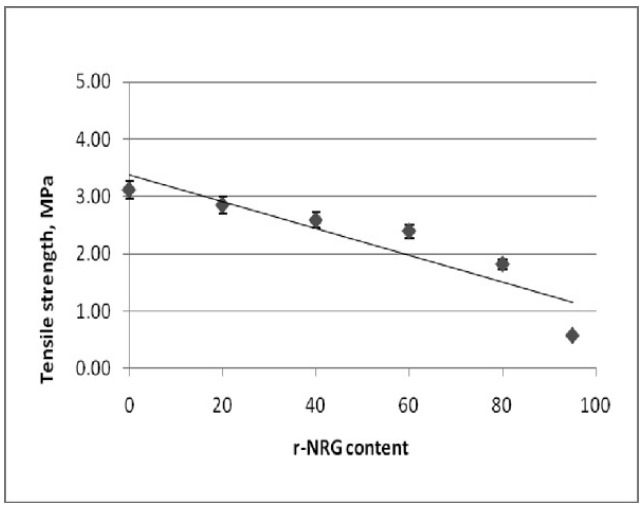

Fig. 3: Tensile strength of vulcanizates as a function of r-NRG blend ratio

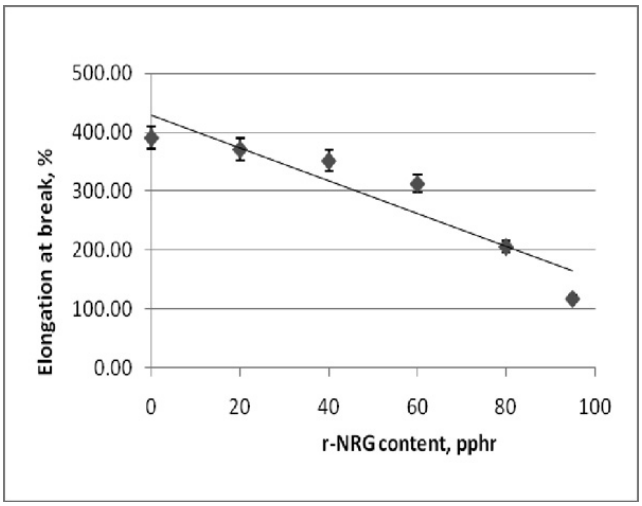

Fig. 4: Elongation at break of vulcanizates as a function of r-NRG blend ratio

Plots of tensile strength and elongation at break, as a function of r-NRG content of vulcanizates, are shown in *Figs. 3* and *4*, respectively. It is evident that both the properties decreased as the r-NRG content was increased. This might be attributed to the presence of the crosslinked gel in the matrix which originated from the reclaimed rubber gel that is difficult to disperse in the fresh rubber matrix. Such gels remained as weak sites for stress concentration; as a result, the tensile strength of reclaimed rubber is inferior to the virgin natural rubber (Adhikari *et al.*, 2000).

CONCLUSIONS

From the results of the study, it can be deduced that reclaimed natural rubber latex gloves (r-NRG) affect the curing characteristics due to the residual sulphurs and fillers in them. Moreover, the presence of the crosslinked gel from the reclaimed rubber remained as a weak site for stress concentration; its lower molecular weight (as a result of chain scission during reclaiming process) could cause reduction in density, hardness, tensile and elongation of Standard Malaysian Rubber (SMR) 20 with addition of r-NRG.

ACKNOWLEDGEMENTS

The author would like to thank Pn. Dayang Habibah and Dr. Mohamad Asri Ahmad for their advice and encouragement. She would also like to take this opportunity to thank Mr. Arumugan N, Khairudin Johari, Mohd Izami Muhamad and all the staff at the Advanced Rubber Technology Unit and Physical Testing Laboratory of the Rubber Research Institute of Malaysian Rubber Board for the assistance received in carrying the preparation of the samples and the tests.

REFERENCES

Adhikari, B., De, D. and Maiti, S. (2000). Reclamation and recycling of waste rubber. *Progress in Polymer Science*, *25*(7), 909-948.

Dhingra, K. Schemes on rubber goods manufacturing (part I: Rubber and modern rubber goods industries). *Handbook of rubber chemicals and rubber goods industries* (pp. 262-263). Delhi, India: Small Industry Research Institute.

Farahani, T. D., Bakhshandeh, G. R. and Abtahi, M. (2006). Mechanical and viscoelastic properties of natural rubber/ reclaimed rubber blends. *Polymer Bulletin*, *56*(4-5), 495-505.

Gonzalez, A., Rodriguez, A., Marcos, A. and Chamorro, C. (1996). *Rubber Chemistry and Technology*, *69*(2), 230.

Lee, E. K. and Choi, S. Y. (2007). Preparation and characterization of natural rubber foams: Effects of foaming temperature and carbon black content. *Korean Journal of Chemical Engineering*, *24*(6), 1070-1075.

Rajan, V. V., Dierkes, W. K., Joseph, R. and Noordermeer, J. W. M. (2006). Science and technology of rubber reclamation with special attention to NR-based waste latex products. *Progress in Polymer Science*, *31*(9), 811-834.

Srilathakutty, R., Joseph, R. and George, K. E. (1999). Studies on microcellular soles based on natural rubber/ polyethylene blends. *Journal of Materials Science*, *34*(7), 1493-1495.

Tan, C. S. (2009, August 3-9). Glove makers come of age. *The Edge Malaysia,* Cover story page.

XinHua News Agency. Malaysia exports 40 billion rubber gloves last year. Retrieved on October 15, 2009 from http://www.highbeam.com/doc/1P2-15398398.html.

Yew, P. L. (2009). Glove makers tighten standards. Retrieved on October 15, 2009. from http://biz.thestar.com.my/services/printerfriendly.asp?file=/2009/2/24/business/3280732.asp&sec=business.

ISSN: 0128-7680
Pertanika J. Sci. & Technol. **19 (1)**: 177– 187 (2011)

Fracture Toughness of Kenaf Mat Reinforced Polyester Composite

Zainab Shakir Radif [*] and Aidy Ali
Department of Mechanical and Manufacturing Engineering,
Faculty of Engineering,Universiti Putra Malaysia,
43400 UPM, Serdang, Selangor, Malaysia
[*]E-mail: zina_engi@yahoo.com

ABSTRACT

The fracture behaviour represents the most critical issue in the automotive and aerospace engine fields. Thus, the objective of this study was to estimate and analyze the crack criteria by using the Mathematical laws that were limited in E 1820 standard and the results affirmed by applying the numerical solutions of ANSYS to estimate the fracture toughness value KIC, besides the energy release rate of biomass composite. The specimens were prepared from different percentage of kenaf mat (KM) and unsaturated polyester resin (UP) 20% KM – 80% UP and 40% KM – 60% UP, respectively, as well the other composite properties which were calculated using the stress-strain data. The fracture characterizations of this composite were carried out using the compact tension (CT) specimen that was commonly used to determine Mode-I fracture properties. The fracture toughness has been found to be independent of pre-crack length. Meanwhile, the tests were performed at room temperature. The numerical simulations of the ANSYS model results demonstrated a good agreement between the experiments computed results of the fracture toughness. The fracture toughness KIC of 20% KM – 80% UP and 40% KM – 60% UP was equivalent to 0.76 MPa√m and 2.0 MPa√m, respectively. Thus, the fracture propagation is dependent on the fibre percentage of the composite. On the other hand, there are unlimited mechanisms of crack paths derived from randomly kenaf mat packs, particularly in the frontal process zone of crack tip.

Keywords: Fibre, fracture toughness, energy release rate, kenaf mat composite, unsaturated polyester resin

NOMENCLATURE

Ao	original measured crack length
Ai	current crack length
Ao	Initial measured crack length
Δa	= a(i)-ao
KIC	Fracture toughness
KI	Stress intensity factor
J	J-integral
JIC	Energy release rate
JPL	Plastic component of J
Jel	Elastic component of J
B	Specimen thickness
BN	Net specimen thickness BN=B if no side grooves are present

Received: 3 January 2010
Accepted: 8 April 2010
[*]Corresponding Author

Be Express as B-(B-BN)2/B
E Young's modulus
N Poisson's ratio
σY Yield stress
Σel Ultimate stress
KIC Fracture toughness
KI Stress intensity factor
JIC Energy release rate
H Initial half-span of the load points
R Radius of rotation of the crack centreline
Θ Angle of rotation of a rigid body element about the unbroken midsection line
E Young's modulus
ν Poisson's ratio
σY Yield stress
σel Ultimate stress
KIC Fracture toughness
KI Stress intensity factor
JIC Energy release rate
H Initial half-span of the load points
R Radius of rotation of the crack centerline
Θ Angle of rotation of a rigid body element about the unbroken midsection line

INTRODUCTION

The natural fibre composite reorganized exceptional benefits that were derived from the specific mechanical properties of the fibre and the adequate toughness that represents prerequisite issues of most engineering applications. Thus, the researchers' interest shifted to analyzing the fibre architecture effect at the toughness quantity (Maya and Sabu, 2008).

Liu and Hughes (2008) studied the toughness and fracture behaviour of the flax fibre woven reinforced epoxy resin. Hence, the results demonstrated the enhancement of composite resistance derived from the fibre distribution technique that controls the composite morphology by using regularly woven textiles. Thus, the random orientations of composite fibre lead to increasing the defects of the composites. Recently, numerous studies have been investigating on natural fibre reinforcement in polymeric composites. This fact is based on both fibres and matrixes that are derived from renewable resources. Thus, the formed composites have more compatibility with environmental preservation issues. In addition, biomass composites have recently gained extensive domination in the industrial field for their significant properties, such as renewal ability, degradable, density, high specific strength, being lightweight, as well as low cost and desired mechanical properties. Meanwhile, the plant fibres that originate from leaf or hard fibres, seed, fruit, wood, cereal straw and other grass fibres, whereby the cellulose fibrils embedded in lignin matrix. Liu and Hughes found an increase of fracture toughness in woven fabric and this improvement is most probably the result of an increase in the fibre volume fraction due to better packing of the fibres, rather than the woven textile. The fibre length and formation nature have influenced on the tensile strength, rigidity, fracture toughness, and flexural strengths values of the composites.

The polymers, such as elastomer, thermoplastic, thermosetting, rigid and flexible foams, represent the most essential substances entire of composites formation. The fibre-polyester composites are attractive due to their structural versatility which enables them to be used in the manufacture of load bearing composites (Farias *et al.*, 2008; Sharifah *et al.*, 2003). The natural

fibres suffer a few limitations like low compatibility with the polymeric matrix because of their typical hydrophilic characteristic. However, some selected elements of the composites must be more compatible for natural fibres and resins due to ability of the hydroxyl groups that contain hydrogen bond between the fibre and polymer to represent a major role in directing the crystalline packing (Matthews and Rawlings, 1994). Many studies have notable success in determining the fracture toughness of K_{IC} determinations and J-integral (e.g. Rodney and John, 1999; Dvorak, 2000). The procedures employed in this study are similar to those applied to metals in ASTM E1820. A number of investigations on the fracture mechanism at the crack tip of the fibre composites have described the microstructure behaviour of these areas (Patricia *et al.*, 2002). All materials, which are either ductile or brittle, homogenous or composite, have defects and cracks, which contribute to more degradation. Generally, the microstructure of materials is studied to better understand the fracture behaviour of the materials precisely under any situation for a wider application (Sami and Ridha, 2005). At the same time, the environment also has significant effects in the fracture toughness mechanism and energy absorption amount of the composite materials (Dash and Chatterjee, 2004). One of the accepted methods of analyzing the fracture behaviour is the application of the Linear Elastic Fracture Mechanics (LEFM), whereby the attention is focused on exploring the fracture mechanism in the crack tip of the fibre composite.

Most of composite material applications are fabricated from brittle matrices and high modulus fibres. However, the stress intensity factor and energy observation rate can be estimated using the linear elastic fracture mechanic concepts. The main energy observation mechanism can be interpreted as crack deflections that are generated from the crashing of the polymer bonds between agglomerate fibres. Meanwhile, tilting paths or twisting motion around the fibres can be produced according to the fibre distribution and the pullout fibre (extraction of fibres from the matrix) and fibre-bridging mechanism kind of the one distinct failure mode of the randomly fibre as the spatially mat fibres. Thus, it can be stated that no limitation mechanism can dominate to estimate the fracture behaviour (Atodaria *et al.*, 1997). Kao (2003) studied the fracture toughness of a laminated composite, and affirmed that the energy required before the onset of fracture was unexpectedly large, i.e. around five times larger for the separate Al-foil layer. Other studies have been focused at estimating the microstructure fracture mechanism (Wong and Mai, 1998; Silva *et al.*, 2005) as attempts to study the limited stability of fracture mechanism.

Preparation of the Sample

The material subject in the present study was constructed from kenaf mat for its significant property advantages, such as low cost, and high filling levels that possibly resulting in high stiffness properties unlike brittle fibres. A comparison was done between the fracture toughness amounts for the different percentages of the kenaf mat reinforced and unsaturated polyester (UP) resin.

Generally, the composites that are fabricated from the fibre-reinforced polymer encountered dramatic improvement in both their tensile and flexural properties. Unsaturated polyesters are used for a variety of industrial and consumer applications. This investigation split into two major computation scopes to estimate the fracture toughness and energy release rate; these include the numerical analysis of ANSYS and the experiment data for 20% KM – 80% UP and 40% KM – 60% UP specimens. Meanwhile, the compact tension (CT) specimen was constructed according to the E1820 standard for the fracture toughness measurement. All the parameters of the specimens are illustrated in *Fig. 1*.

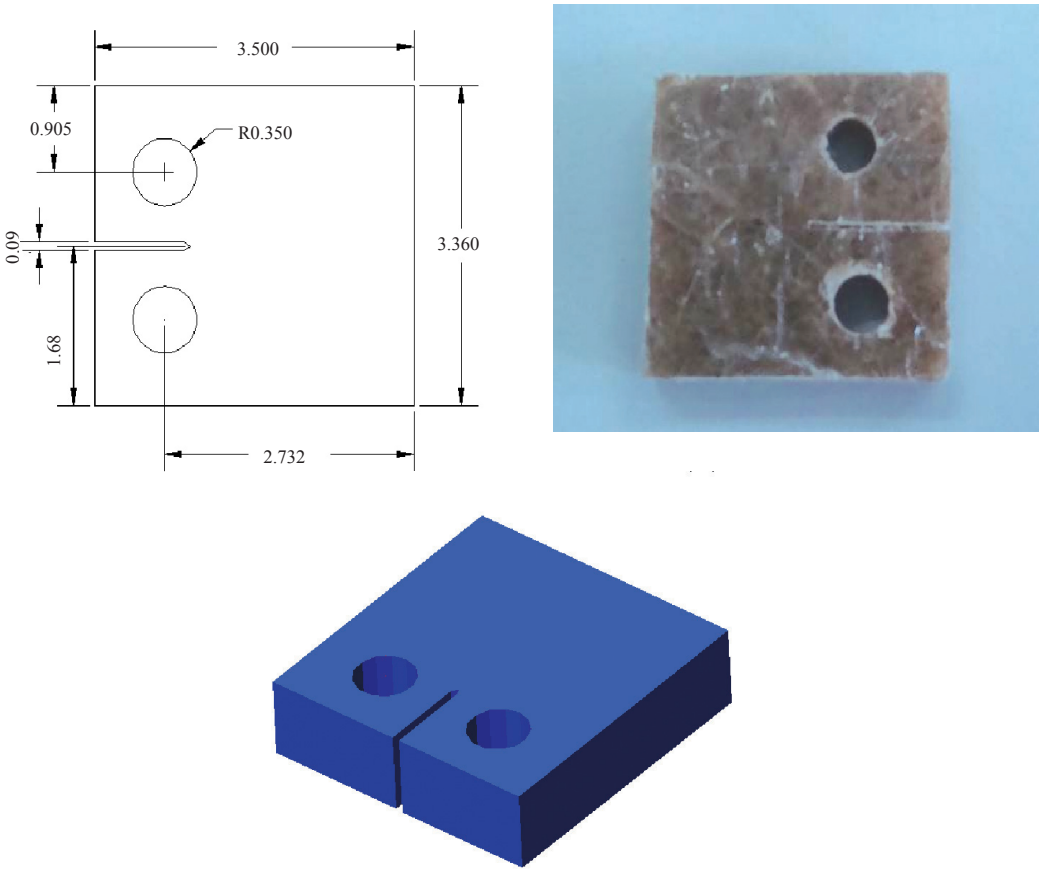

Fig. 1: (a) The front view of the CT specimen; (b) the compact tension specimen 20% KM -80% UP; and (c) Izo AutoCAD drawing of CT specimen

The thickness was 7 mm for all the specimens, while the initial notch length to specimen was between 12.6 mm and the notch tip was sharpened with a razor blade to simulate a sharp crack. The tensile test for 15 specimens was conducted to estimate the fracture toughness and J-integral for this particular composite. The tensile young modulus, yield load, and extension at yield point were calculated automatically.

Tensile Testing of Composites

The tensile specimen, i.e. 145 mm by 15 mm, was caught according to ASTM D3039 /D3039M-95M; the composite of the tensile specimen is as illustrated in *Fig. 2*. Testing was conducted and the data were digitally acquired. The tensile stress, tensile strain and young modulus of 20% KM – 80% UP and 40% KM – 60% UP were calculated automatically as indicated below. The young modulus for these composites was 4488 MPa and 4780 MPa, respectively. The test was performed in the instron machine 10 kN, series 2716 and 2736 under test speed that is limited by 2 mm/min. The specified test conditions for determining the tensile properties of specimen were conducted according to ISO 527.

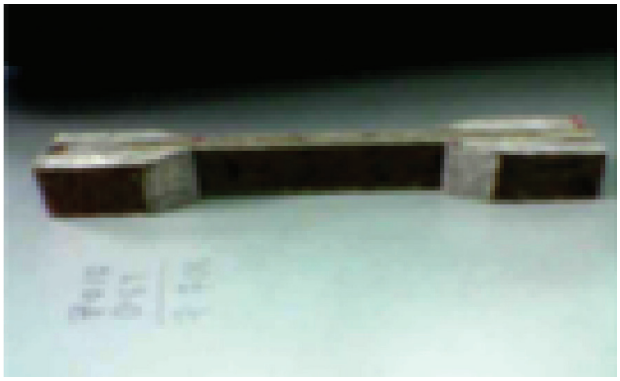

Fig. 2: ASTM D3039 tensile specimen

The tensile test was performed for fifteen compact specimens under stable speed rate to estimate the energy release rate and fracture toughness. Accurate evaluations were recorded for the limited the Poisson's ratio of the composite via recourse of the composite materials gage strain.

RESULTS AND DISCUSSIONS

The tensile results of 40% KM – 60% UP denote the dramatic improvement in the yield load of the composite which increase the fibre percentage. The tensile results are shown in Table 1, while the load-displacement graph is illustrated in *Fig. 3*.

TABLE 1
Tensile results of the kenaf–polyester composite

Kenaf–polyester percentage	Yield stress MPa	Young modulus Mpa	Tensile extension at yield point mm
20%KM – 80%PU	26.648	4488	1.836
40%KM – 60%PU	28.295	4780	1.6003

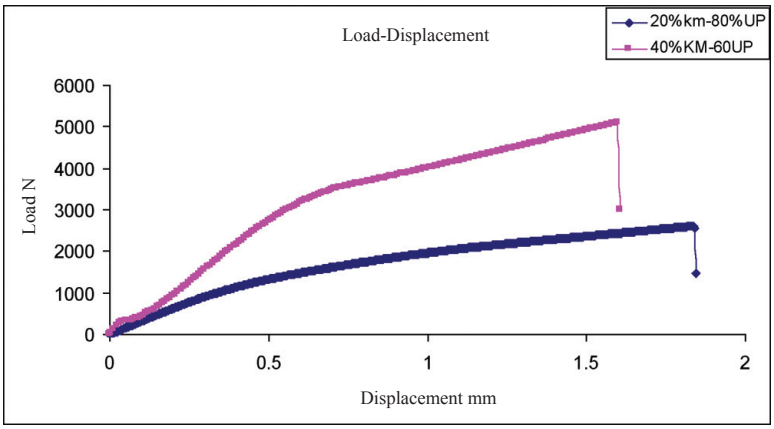

Fig. 3: The tensile load-displacement graph

The combat specimen was generally used only for the k_{IC} testing. At load $P_{(i)}$, the calculation of K_i was computed instantaneous at all the recorded points in the load-displacements curve, as follows:

The current crack length was calculated from the knowledge the instantaneous load-displacement slope that was required to find $C_{c(i)}$, as follows:

$$slope = \left(\Delta v / \Delta p\right)_i \tag{1}$$

with:

$$a_i / w = [1.000196 - 4.0631u + 11.242u^2 - 106.043u^3 + 464.335u^4 - 650.677u^5 \tag{2}$$

Hence:

$$u = \frac{1}{[B_e E C_{c(i)}]^{1/2} + 1} \tag{3}$$

Thus, the instantaneous fracture can be mathematically expressed using the following expression:

$$K_{(i)} = \frac{P_i}{(BB_N W)^{1/2}} f(a_i / W) \tag{4}$$

$$f(a_i / W) = \frac{[(2 + a_i / W)(0.886 + 4.64(a_i / W) - 13.32(a_i / W)^2 + 14.72(a_i / W)^3 - 5.6(a_i / W)^4)]}{(1 - a_i / W)^{3/2}} \tag{5}$$

Meanwhile, J for the compact specimen was calculated, as follows:

$$J = J_{el} + J_{pl} \tag{6}$$

The J calculations for the basic test method for the compact specimen are related to the Poisson's ratio and young modulus.

$$J = \frac{K^2(1 - v^2)}{E} + J_{Pl} \tag{7}$$

The plastic component of J was calculated, as follows:

$$J_{pl} = \frac{\eta A_{Pl}}{B_N b_o} \tag{8}$$

In order to account for the crack opening displacement, the crack length estimation shall be corrected for rotation, while the compliance is corrected, as follows:

$$C_{c(i)} = \frac{C_i}{[\frac{H}{R}\sin\theta_i - \cos\theta_i][\frac{D}{R}\sin\theta_i - \cos\theta_i]} \tag{9}$$

Where:

$$u = \frac{1}{[B_e E C_{c(i)}]^{0.5} + 1} \quad (10)$$

In addition, the crack length is given as follows:

$$a_i / W = [1.000196 - 4.06319u + 11.242u^2 - 106.043u^3 + 464.335u^4 - 650.677u^5] \quad (11)$$

The experimental results for the fracture toughness of 20% KM – 80% UP were equivalent to (0.95 MPa .√m) and in the 40% KM – 60 UP equal to (2 MPa. √m), this finding denoted the relationship between the fibre percentage and the increase in the fracture toughness value. The tolerance of K_{CL} value between the specimens is related with the fibre microdiameter or the kenaf picks diameters at the crack tip and the crack zone morphology, whereby no mechanism can dominate an accurate assessment for the fracture toughness of the mat composites. Thus, the K_{CL} releases, depending on the average of fracture toughness values to characterize the K_{CL} values of the composite, whereas in order to obtain more accurate calculations, the numerical analysis was performed to only the K_{CL} value.

TABLE 2
Experiments and numerical results for the fracture toughness and energy release rate

Specimen percentage contents	No. specimen	K_{Lc} experimental results MPa √m	Experiment energy release rate KJ/m^2	K_{Lc} numerical results MPa √ m	Numerical energy release rate KJ/m^2
	1	1.8899	0.716	1.515	0.465
	2	0.779	0.123	1.0406	0.219
	3	1.0287	0.214	0.9499	0.182
	4	0.855	0.148	0.8837	0.158
	5	1.6577	0.557	1.2877	0.336
	6	0.4319	0.037	0.787	0.125
20 KM-80UP	7	0.5046	0.051	0.922	0.172
	8	0.8405	0.143	1.058	0.226
	9	0.5546	0.062	0.785	0.124
average		0.95	0.182	1.025	0.213
	1	1.935	0.712	2.945	1.650
	2	1.452	0.401	2.185	0.908
	3	2.32	1.024	2.75	1.439
	4	2.14	0.871	2.5	1.189
40 KM-60UP	5	2.57	1.257	2.04	0.792
	6	1.36	0.352	2.593	1.279
average		2.0	0.761	2.49	1.180

The potential errors in the ANSYS module solutions were derived using homogenous material, while the experimental results dominate the heterogeneous of distribution and orientation of the fibre in the crack tip. *Fig. 4* illustrates the stress component that is concentrated at the yield point

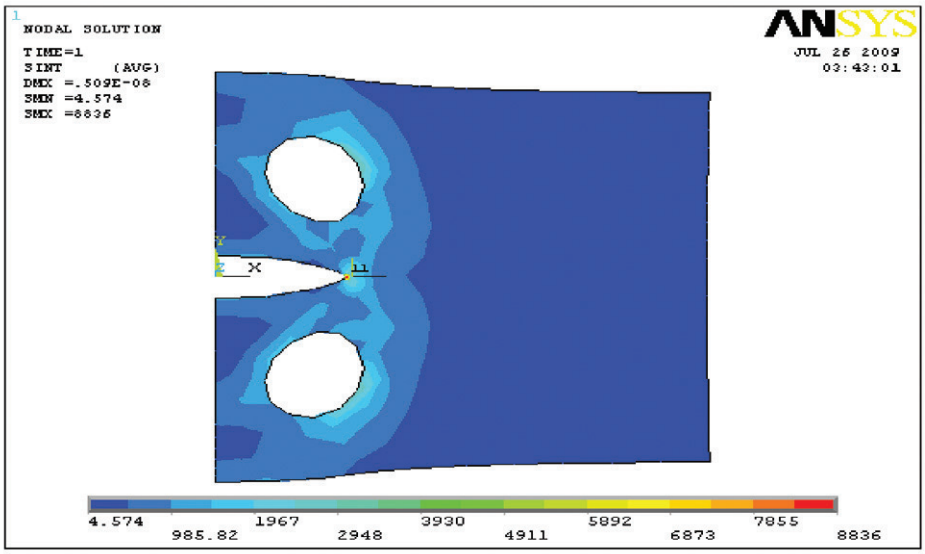

Fig. 4: The stress deformation of the simulation specimen

of the crack tip. Three deformation concentration zones were generated according to the forces compounds that influence the edges of the corresponding circular holes and crack tip. The plastic zone size in the crack tip, J_{max} and $\Delta a_{max,}$ could be estimated for the composite subject study, as illustrated in Table 3.

TABLE 3
The crack parameters and the maximum energy release

Composite percentages	r_p (m)	J_{max} (KJ/m^2)	Δa_{max} (m)
20%KM- 80% UP	6.74×10^{-5}	9.327×10^{-3}	1.75×10^{-3}
40%KM – 60% UP	2.65×10^{-4}	1.27×10^{-2}	2.25×10^{-3}

The J-integral values and the corresponding crack extension values must be plotted, as shown in *Fig. 5*. Hence, the J-R curve is defined as the data in a bounded region by the coordinate axes, J_{max} and Δa_{max}, as illustrated in *Fig. 5*.

Particularly in the ANSYS programme, there is a complexity of construct in the composite model, whereby the content kenaf mat acts as randomly reinforced fibre. Thus, the material properties of the Young's modulus and poisson's ratio of the composite can be dominated by recourse the tensile test results. The results exhibit a good agreement with the findings of the experiment, as shown in *Fig. 6*.

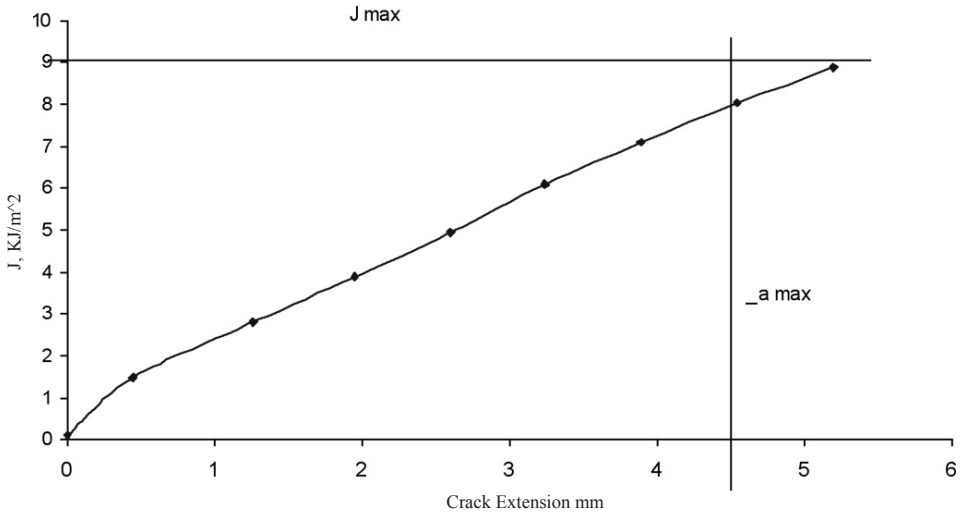

Fig. 5: Crack extension and energy release rate (J-R curve) of 20% KM – 80% UP

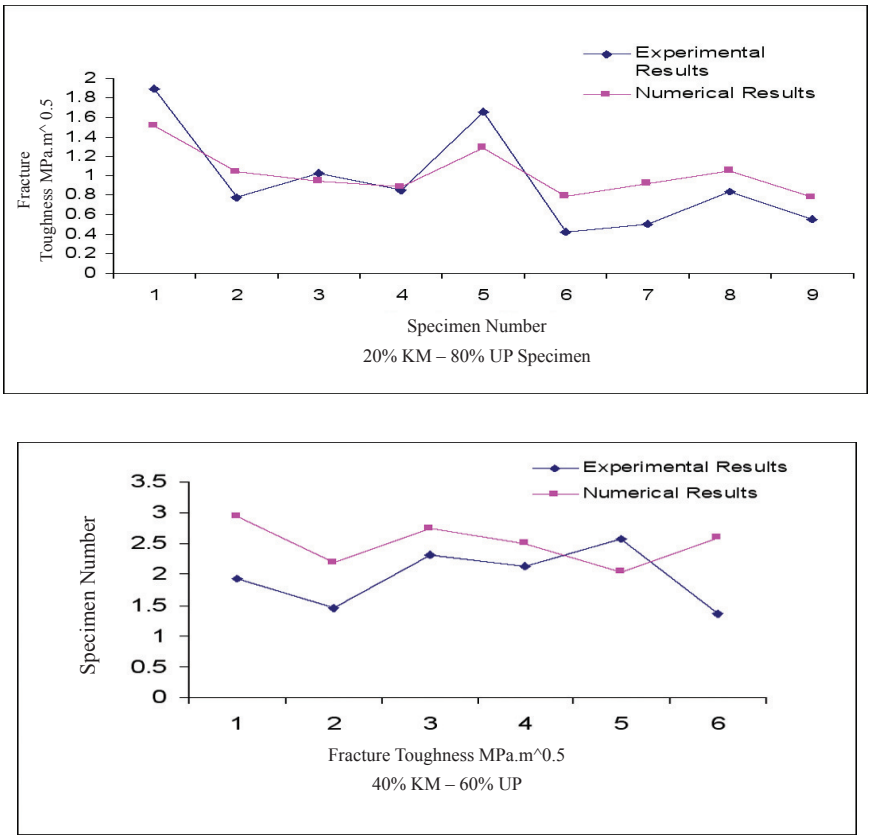

Fig. 6: The tolerances between experiment and the ANSYS results for (a) 20% KM – 80% UP and(b) 40% KM – 60% UP

CONCLUSIONS

From this investigation, a number of conclusions can be drawn, as listed below.

1. The tensile result of 40% KM – 60% UP demonstrated a dramatic improvement in the yield load of the composite with the increasing percentage of fibre.
2. Based on the experiment, the fracture toughness results of 20% KM – 80% UP were found to be equivalent to (0.95 MPa .√m) and this was equivalent to (2 MPa .√m) in the 40% KM – 60 UP, demonstrating the relationship between the fibre percentage and the increasing value of the fracture toughness.
3. The numerical results exhibited a good agreement with the results from the experiments.

ACKNOWLEDGEMENTS

The authors would like to thank the Ministry of Higher Education Malaysia and Universiti Putra Malaysia (UPM) for their generous support. In addition, the technical assistance from Mr. Muhammad Wildan Ilyas, Mr. Fasil, Miss Siti Hasnani Mohammad, Mr. Tajul Ariffin b. Md. Tajuddin is much appreciated.

REFERENCES

ASTM D3039/D3039M -95a, Standard test method for tensile properties of polymer matrix composite materials. *Annual book of ASTM Standards*, *14*, 02.

ASTM E1820-01. Standard test method for measurement of fracture toughness of metallic materials, 2003.

Atodaria, D.R., Putatunda, S.K. and Mallick, P.K. (1997). A fatigue crack growth model for random fiber composites. *Journal of Composite Materials*, *31*(18), 2645–59.

Dash, P. K. and Chatterjee, A. K. (2004). Effects of environment on fracture toughness of woven carbon/epoxy composite. Birla Institute of Technology.

Dvorak, G.J. (2000). Composite materials: Inelastic behaviour, damage, fatigue and fracture. *International Journal of Solids and Structures*, *37*(1/2), 155–70.

Farias, M.A. de., Farina, M.Z., Pezzin, A.P.T. and Silva, D.A.K. (2008). Unsaturated polyester composites reinforced with fiber and powder of peach palm: Mechanical characterization and water absorption profile. *Materials Science and Engineering* doi:10.1016/j.msec.2008.09.020.

Liu, Q. and Hughes, M. (2008). The fracture behaviour and toughness of woven flax fibre reinforced epoxy composites, Composites Part A: *Applied Science and Manufacturing*, *39*(10), 1644-1652.

Matthews, F.L. and Rawlings, R.D. (1994). *Composite Materials: Engineering and Science.* London: Chapman and Hall.

Maya Jacob John and Sabu Thomas. (2008). Biofibres and biocomposite. *Carbohydrate Polymers*, *71*, 343–364.

Patricia Kim Nelson, Victor C. Li, Asce, F. and Toshiro Kamada. (2002). Fracture toughness of microfiber reinforced cement composites. *Journal of Materials in Civil Engineering*, *14*(5), 384. 10.1061/(A SCE) 0899-1561.

Silva, R.V., Spinelli, D., Bose Filho, W.W., Claro Neto, S., Chierice, G.O. and Tarpani, J.R. (2005). Fracture toughness of natural fibers/castor oil polyurethane composites.

Rodney W. Trice and John W. Halloran. (1999). Mode I fracture toughness of a small-grained silicon nitride: Orientation, temperature and crack length effects. *Journal of the American Ceramic Society*, *82*(10), 2633–40.

Sami Ben Brahim and Ridha Ben Cheikh. (2007). Influence of fibre orientation and volume fraction on the tensile properties of unidirectional Alfa-polyester composite. *Composites Science and Technology*, *67*, 140–147.

Sharifah H. Aziz, Martin P. Ansell, Simon J. Clarke and Simon R. Panteny. (2005). Modified polyester resins for natural fibre composites. *Composites Science and Technology*, *65*, 525–535.

Sharon Kao-Walter. (2003). *Fracture Toughness of a Laminated Composite*. Elsevier Ltd. and ESIS. A.

Shinji Ochi. (2008). Mechanical properties of kenaf fibers and kenaf/PLA composites. *Mechanics of Materials*, *40*, 446–452.

Wong, S.C. and Mai, Y.W. (1998). Fracture resistance and microstructures of unreinforced and fiber reinforced PA6,6/PP/SEBS-g-MA. *Annual Technical Conference*, *56*, Atlanta, USA.

ISSN: 0128-7680
Pertanika J. Sci. & Technol. **19 (1)**: 189 – 197 (2011)

Effects of Soil Burial on Properties of Linear Density Polyethylene (LDPE)/ Thermoplastic Sago Starch (TPSS) Blends

Hanafi Ismail*, Rohani Abdul Majid and Razaina Mat Taib
School of Materials and Mineral Resources Engineering,
USM Engineering Campus, Universiti Sains Malaysia,
14300 Nibong Tebal, Penang, Malaysia
**E-mail: hanafi@eng.usm.my*

ABSTRACT

Linear density polyethylene (LDPE)/thermoplastic sago starch (TPSS), blended with and without the addition of compatibilizer [Polyethylene-grafted-Maleic Anhydride, (PE-g-MA)] were prepared for soil burial test. The test was conducted in the natural soil environment for 3 and 6 months. Different loading of TPSS (10, 20, 30, 40, and 50 wt. %) were used in this study. After soil burial, the blends were evaluated for their tensile properties and scanning electron microscopy (SEM) to observe the surface morphology properties after the test. For LDPE/TPSS, it was observed that the tensile strength decreased with the increase of soil burial time, as well as Young modulus and elongation at break (EB). The LDPE/TPSS/PE-g-MA also showed the same trend for the tensile properties, but with higher properties as compared to uncompatibilized blends. The tensile properties also decreased with the increase in the TPSS loading for both the LDPE/TPSS and LDPE/TPSS/PE-g-MA. Meanwhile, the scanning electron microscopy (SEM) on the blend surfaces after the soil burial test showed that degradability increased with the increase in the exposure time as well as the TPSS loading.

Keywords: Soil burial, mechanical properties, biodegradation, TPSS

INTRODUCTION

The increase in the plastic production through the whole nation had introduced the world to environmental problems because most of the plastic materials have remained in the garbage deposits and landfills for decades. These situations may contribute to serious environmental problems **(**Bikiaris *et al*., 1998; Chandra and Renu, 1997; Dash *et al*., 2002; Iionna, 2007; Ismail and Awang, 2008; Krishna Sastry *et al.*, 1998). However, the use of hydrocarbon plastic materials that are not readily biodegradable has increased. Meanwhile, some alternatives have been considered to increase the use of biopolymer in reducing environmental problems.

Biopolymer, such as starch, is a good example of degradable polymer that can be used to replace the hydrocarbon plastic material. The addition of starch and other plastic additives like plasticizers and fillers is usually susceptible to microbial attack. This leads to physical embrittlement of the polymer, leaving a porous and mechanically weakened polymer. The microbes, in turn, release non-specific oxidative enzymes that could attack the synthetic polymer. In addition, the gradual degradation of the natural polymer leads to increased surface area by erosion and pitting. This will accelerate the degradation of the synthetic polymer by diffusion of oxygen, moisture, and enzymes into the porous polymer matrix (Torabi *et al*., 2004; Usarat and Duangdao, 2006).

Received: 3 January 2010
Accepted: 8 April 2010
*Corresponding Author

In this article, LDPE/TPSS blends were subjected to soil burial. The objective of the paper is to study the behaviour of the samples after the soil burial environment and the effects of the addition of PE-g-MA. The tensile test and surface morphology were applied to characterize the change of tensile properties after the soil burial test. The difference between the uncompatibilized and compatibilized blends was also discussed in this article.

THE EXPERIMENT

Materials

Sago starch was obtained from the Land Custody Development Authority (LCDA), Sarawak. Its moisture content was determined at 13 wt. %. The granules sizes ranged from 9 to 35 μm, with an average granule size of 20 μm. It is crucial to note that sago starch decomposes at 230°C. Pellets of low density polyethylene (LDPE), with the melting temperature of 138°C, were obtained from Titan Polyethylene (M) Sdn. Bhd. Meanwhile, polyethylene-grafted-Maleic Anhydride (PE-g-MA) was obtained from Sigma-Aldrich (M) Sdn. Bhd. Glycerol was obtained from Merck Chemicals grade ACS Reag. Ph Eur.

Preparation of the LDPE/TPSS Blends

TPSS was melt-blended with LDPE in a Haake Rheomix Model R600/610. Mixing was performed at 150°C and 50 rpm for 10 minutes. LDPE was first added into the mixing chamber, followed by the TPSS after 3 minutes of mixing. The total mixing time was 10 minutes. The TPSS loadings varied from 10, 20, 30, 40, and 50 wt. %. PE-g-MA was used at an amount of 10 wt. % based on the TPSS weight. Both the melting temperature and torque were recorded during the mixing periods.

Compression Moulding

The LDPE/TPSS blends were compression moulded in an electrical heated hydraulic press. Hot press procedures involved preheating at 150ºC for 6 minutes, followed by compression with a pressure of 1000kg/m^3 for 3 minutes at the same temperature. All the compression moulded sheets (150 x 150 x 1mm) were cold pressed for 2 minutes.

Soil Burial Test

The soil burial test was conducted for 3 and 6 months. The reason for choosing 3 and 6 months of burying time was primarily to study the effects of biodegradation after the short period of time, as the material is partially biodegradable. In this method, the samples in a dumbbell shape size were buried in alluvial deposit soil environment, whereby all the samples were put in a box covered by soil and thus subjected to the action of micro-organisms, i.e. both fungi and bacteria which are normally present in the soil. After the test, the samples were removed, washed in distilled water and dried at 105ºC in an oven for 24 h and then kept in a desiccator.

Tensile Properties

The tensile tests for the unexposed and exposed samples were carried out with a universal testing machine, Instron 3366, according to ASTM D638. The dumbbell specimens of 1mm thickness were cut from the compression moulded sheets with a Wallace die cutter. A crosshead speed of 5 mm/min was used and the test was performed at 25 ± 3°C. Five specimens were used to obtain the average values for tensile strength, elongation at break and Young's modulus.

Morphology Study

Studies on the surface morphology of the exposed samples of the LDPE/TPSS blends were carried out using a field emission scanning electron microscope, FESEM SUPRA36VP-24-58. The surfaces of the sample were mounted on aluminium stubs and sputter coated with a thin layer of gold.

RESULTS AND DISCUSSION

Tensile Properties

Figs. 1 to *3* show the tensile properties of LDPE/TPSS and LDPE/TPSS/PE-g-MA blends that were buried in the soil. From the figures, it can be seen that the tensile strength, Young's modulus and elongation at break decreased with the increase in the TPSS loading, as well as the burying time. Meanwhile, the decrease in the tensile strength, Young's modulus and elongation at break was due to the pit and voids which occurred after the assimilation of the TPSS particles on the surface of LDPE/TPSS blends. The pit and voids act as stress concentrator and lead to a decrease in tensile strength and Young's modulus. In addition, micro-organism attacks starting with starch. As the micro-organisms consumed the surrounding starch, the blends lost their structural integrity. This process could lead to the deterioration of the tensile properties. The degradation of the blends normally occurs due to the vacation of starch sites, which are occupied by either microbes or water and thus, leads to extensive degradation of the blends. During the experiment, the water inside the soil diffuses into the polymer sample, causing swelling and enhancing biodegradation. In addition, extra cellular enzymes made by the microbes also attack the resin and may be responsible for the fine cracking and tearing that lower the elongation at break, and can lead to further degradation and lower the tensile properties. The blends containing a higher percentage of TPSS (40 and 50% TPSS content) degraded faster as compared to the blends with lower TPSS loading in first 3 months, during which the maximum starch content was accessed. Over the next 6 months, a gradual decrease of TPSS was observed.

The tensile properties of the LDPE/TPSS/PE-g-MA blends with the addition of compatibilizer buried in the soil showed a higher tensile strength as well as the Young's modulus and elongation at break. This result might be due to the compatibizing effect of the PE-g-MA in the blends that could prevent early degradation to the blends. Meanwhile, the effect of the PE-g-MA reduced the volumes of voids which created the stress concentration area in the blends. As a result, the mechanism of degradation was reduced.

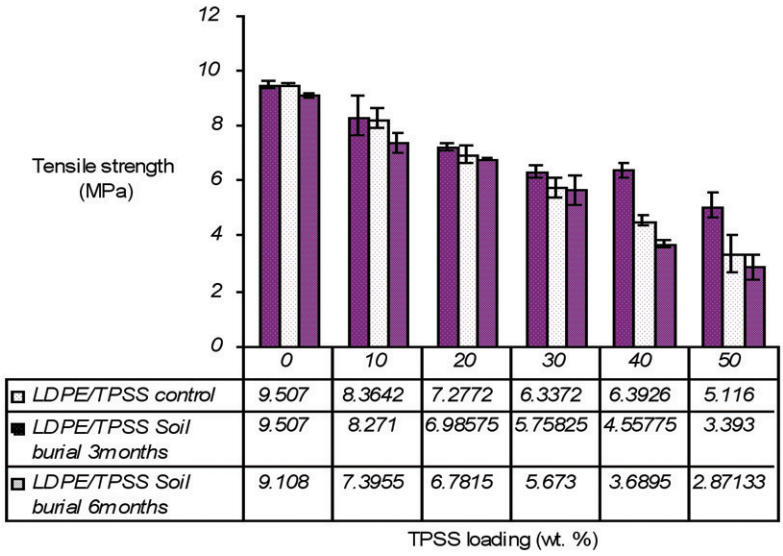

	0	10	20	30	40	50
LDPE/TPSS control	9.507	8.3642	7.2772	6.3372	6.3926	5.116
LDPE/TPSS Soil burial 3months	9.507	8.271	6.98575	5.75825	4.55775	3.393
LDPE/TPSS Soil burial 6months	9.108	7.3955	6.7815	5.673	3.6895	2.87133

(a)

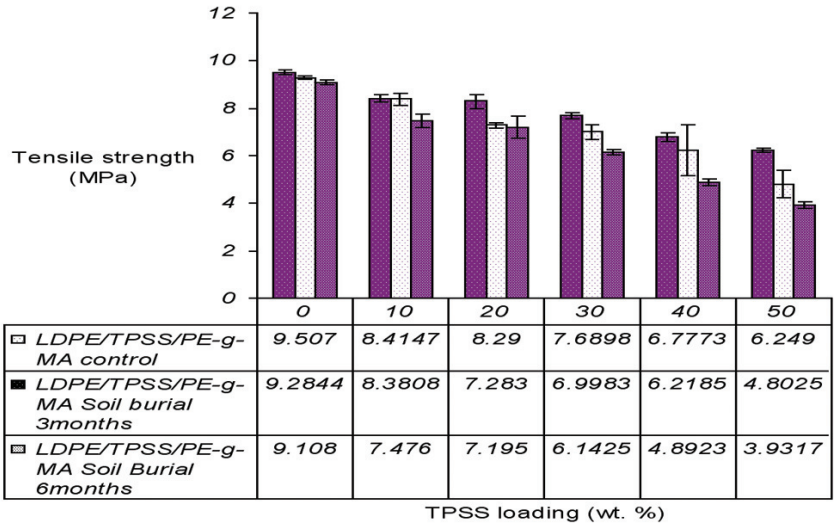

	0	10	20	30	40	50
LDPE/TPSS/PE-g-MA control	9.507	8.4147	8.29	7.6898	6.7773	6.249
LDPE/TPSS/PE-g-MA Soil burial 3months	9.2844	8.3808	7.283	6.9983	6.2185	4.8025
LDPE/TPSS/PE-g-MA Soil Burial 6months	9.108	7.476	7.195	6.1425	4.8923	3.9317

(b)

Fig. 1: Tensile strength of control and buried samples (a) LDPE/TPSS blends; (b) LDPE/TPSS/PE-g-MA blends

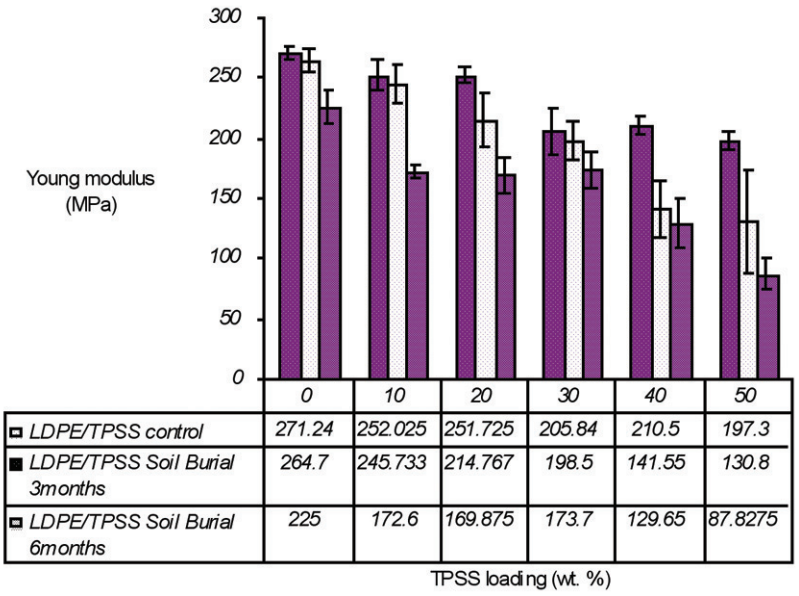

	0	10	20	30	40	50
LDPE/TPSS control	271.24	252.025	251.725	205.84	210.5	197.3
LDPE/TPSS Soil Burial 3months	264.7	245.733	214.767	198.5	141.55	130.8
LDPE/TPSS Soil Burial 6months	225	172.6	169.875	173.7	129.65	87.8275

(a)

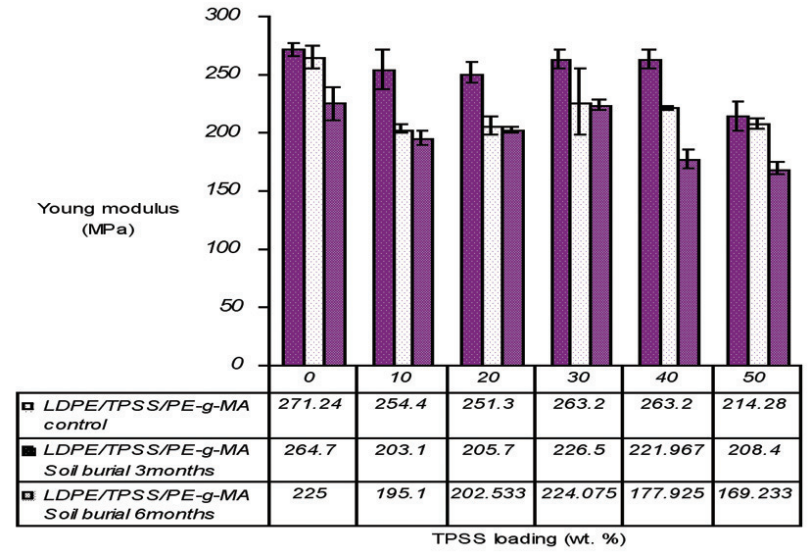

	0	10	20	30	40	50
LDPE/TPSS/PE-g-MA control	271.24	254.4	251.3	263.2	263.2	214.28
LDPE/TPSS/PE-g-MA Soil burial 3months	264.7	203.1	205.7	226.5	221.967	208.4
LDPE/TPSS/PE-g-MA Soil burial 6months	225	195.1	202.533	224.075	177.925	169.233

(b)

Fig. 2: Young modulus of the control and buried samples; (a) LDPE/TPSS blends; (b) LDPE/TPSS/PE-g-MA blends

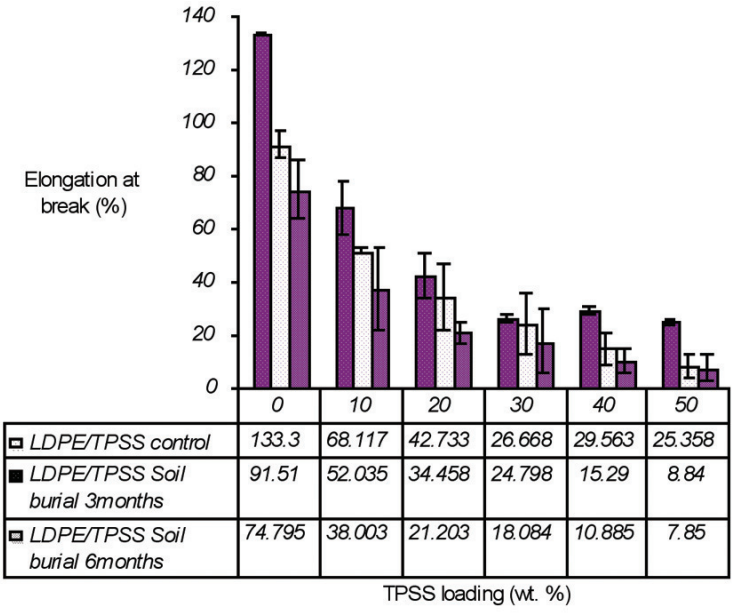

	0	10	20	30	40	50
LDPE/TPSS control	133.3	68.117	42.733	26.668	29.563	25.358
LDPE/TPSS Soil burial 3months	91.51	52.035	34.458	24.798	15.29	8.84
LDPE/TPSS Soil burial 6months	74.795	38.003	21.203	18.084	10.885	7.85

(a)

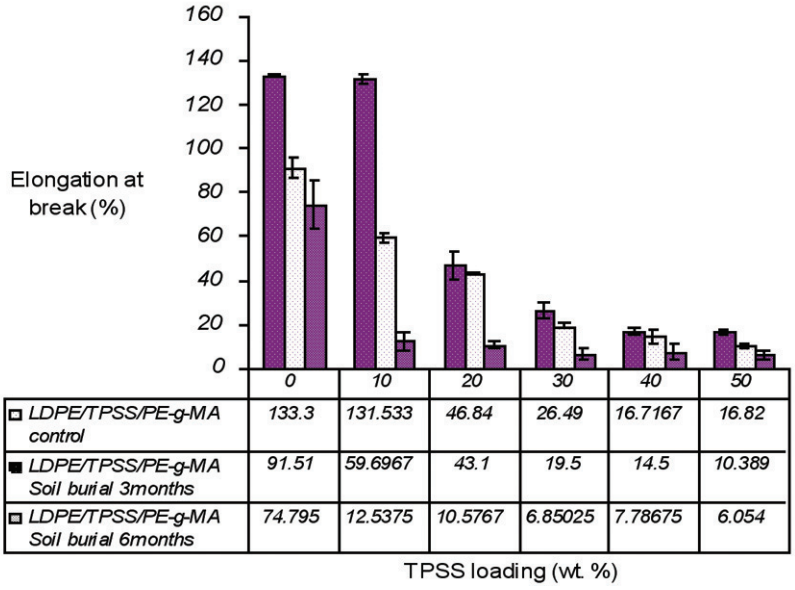

	0	10	20	30	40	50
LDPE/TPSS/PE-g-MA control	133.3	131.533	46.84	26.49	16.7167	16.82
LDPE/TPSS/PE-g-MA Soil burial 3months	91.51	59.6967	43.1	19.5	14.5	10.389
LDPE/TPSS/PE-g-MA Soil burial 6months	74.795	12.5375	10.5767	6.85025	7.78675	6.054

(b)

Fig. 3: Elongation at break of the control and buried samples; (a) LDPE/TPSS blends; (b) LDPE/TPSS/PE-g-MA blends

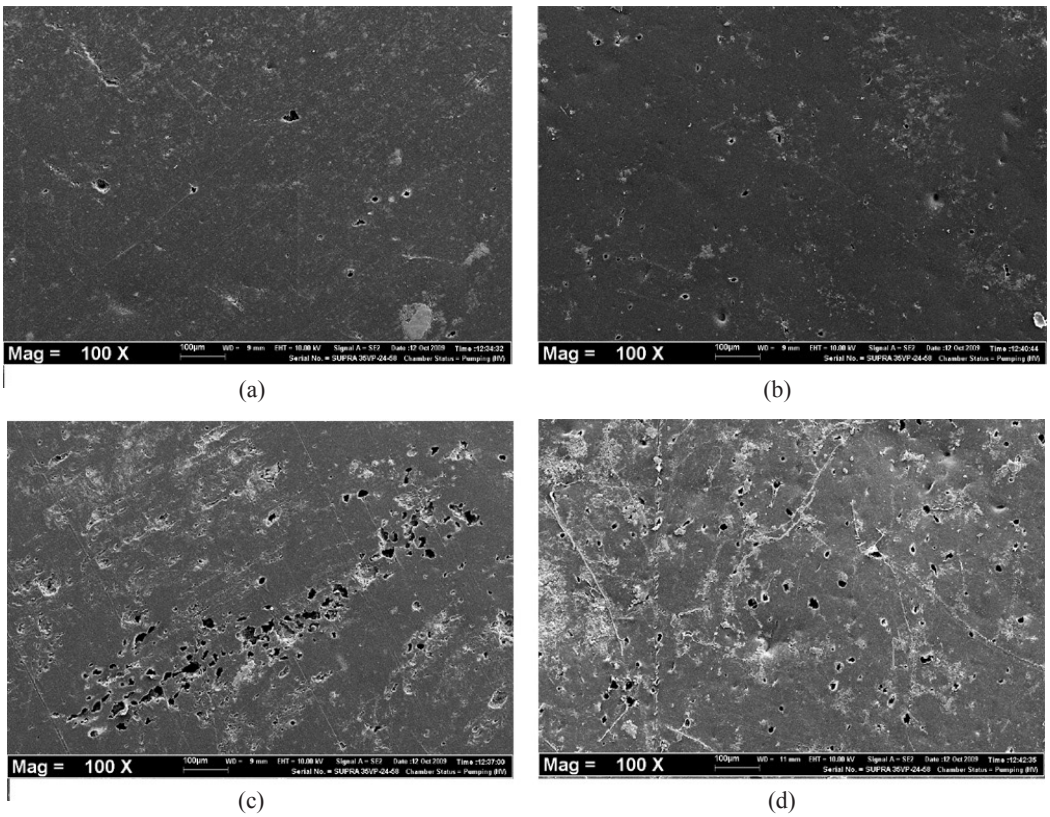

Fig. 4: The SEM Micrographs of LDPE/TPSS; (a) 10% TPSS loading, (c) 50% TPSS loading and LDPE/ TPSS/PE-g-MA after 6 months of soil burial; (b) 10% TPSS loading, (d) 50% TPSS loading

Morphological Properties

Fig. 4 shows the SEM micrographs of LDPE/TPSS and LDPE/TPSS/PE-g-MA blends after 6 months of soil burial. From the figures, it can be seen that the sample with higher TPSS loading yields higher degradation effects. At 50% TPSS loading, continuous holes and voids can be seen due to the starch that has leached out. In addition, the samples containing a higher percentage of starch supported fungal growth. TPSS, being a natural polymer, could be readily used as a carbon source by the fungus. For the LDPE/TPSS/PE-g-MA blends, it can be seen that the samples with the addition of compatibilizer show lower voids, especially for the sample with 50% TPSS loading. The voids can still be seen but the trend is different with the blend without compatibilizer. Similarly, the voids and holes can be seen but with better distribution. The samples without the addition of compatibilizer show continuous holes and voids that prove the agglomeration has occurred inside the blends. However, the SEM micrographs for the blends with the addition of compatibilizer show a lower agglomeration but a better distribution of voids and holes.

As an evident in the SEM surface micrograph, *Fig. 5* shows the percentage of weight loss for the LDPE/TPSS and LDPE/TPSS/PE-g-MA blends after soil burial for 3 months and 6 months. It is clear that the weight loss for the blends without the addition of compatibilizer is higher than the blends with the addition of compatibilizer. Meanwhile, the addition of PE-g-MA, as the compatibilizer reduced the water diffused inside the samples, has generated the degradation mechanism inside the blends.

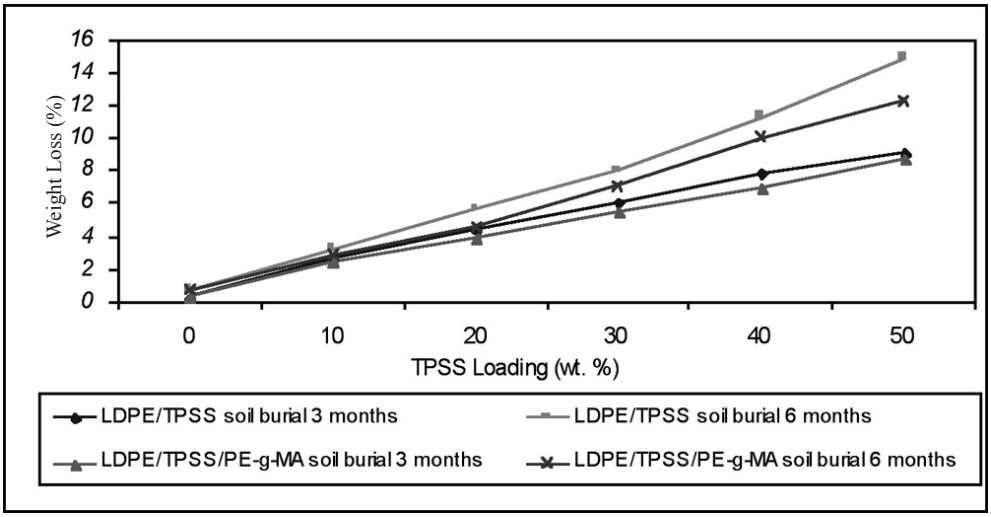

Fig. 5: Weight loss changes for the LDPE/TPSS and LDPE/TPSS/PE-g-MA blends after 3 months and 6 months of soil burial

CONCLUSIONS

After both exposure periods to soil burial test, the results from the tensile test indicated that the LDPE/TPSS/PE-g-MA blend exhibited higher tensile strength and Young modulus than LDPE/TPSS blends due to a good interfacial adhesion between the LDPE and TPSS, although both blends have shown a reduction in the tensile properties with the increase in the soil burial time. The tensile properties have also been found to decrease with the increase in the TPSS loading for both the LDPE/TPSS and LDPE/TPSS/PE-g-MA blends. Although holes were evident for both the blends, the surface morphology of LDPE/TPSS /PE-g-MA showed lower continuous holes and TPSS leached out due to the lower agglomeration and good interaction between the TPSS and LDPE.

ACKNOWLEDGEMENT

The authors gratefully acknowledge the financial support from the Research University Grant (Grant No. 1001/PBAHAN/814008).

REFERENCES

Bikiaris, D., Pavlidou, E., Prinos, J., Aburto, J., Alric, I., Borredonb, E. and Panayiotou, C. (1998). Biodegradation of octanoated starch and its blends with LDPE. *Polymer Degradation and Stability*, *60*, 437-447.

Chandra, R. and Renu Rustgi. (1997). Biodegradation of maleated linear low-density polyethylene and starch blends. *Polymer Degradation and Stability*, *56*, 185-202.

Dash, B.N., Sarkar, M., Rana, A.K., Mishra, M., Mohanty, A.K. and Tripathy S.S. (2002). A study on biodegradable composite prepared from jute felt and polyesteramide (BAK). *Journal of Reinforced Plastics and Composites*, *21*, 1493-1503.

Ioanna Kyrikou Demetres Briassoulis. (2007). Biodegradation of agricultural plastic films: A critical review. *Journal of Polymer Environment*, *15*, 125–150.

Ismail, H. and Awang, M. (2008). Natural weathering of polypropylene and waste tire dust (PP/WTD) blends. *Journal of Polymer Environment*, *16*, 147-153.

Krishna Sastry, P., Satyanarayana, D. and Mohan Rao, D. V. (1998). Accelerated and environmental weathering studies on polyethylene–starch blend films. *Journal of Applied Polymer Science*, *70*, 2251–2257.

Torabi Angaji, Mahmood Hagheeghatpadjooh and Hamid Reza Iran. (2004). Preparation of biodegradable low density polyethylene by starch – urea composition for agricultural applications. *Journal of Chemical & Chemical Engineering*, *23*, 7-11.

Usarat Ratanakamnuan and Duangdao Aht-Ong. (2006). Photobiodegradation of low-density polyethylene/ banana starch films. *Journal of Applied Polymer Science*, *100*, 2725–2736.

REFEREES FOR THE PERTANIKA JOURNAL OF SCIENCE AND TECHNOLOGY (JST)

August 2010 – January 2011

The Editorial Board of the Journal of Science and Technology wish to thank the following for acting as referees for manuscripts published in JST between August 2010 and January 2011.

Abd Fatah Wahab
Abdul Halim Ghazali
Abdul Rahman Omar
Adem Kilicman
Aileen Tan Shau Hwai
Asmah Rahmat
Badrul Munir Md Zain
Bujang B.K. Huat
Edi Syams Zainudin
Gwendoline Ee Cheng Lian
Hambali Arep@Ariff
Hanafi Ismail
Hazizan Md Akil
Karen A Crouse
Kartini Kamaruddin
Khalina Abdan
Lili Nurliyana Abdullah
M Iqbal Saripan
Megat Mohamad Hamdan Megat Ahmad
Mohamad Ridzwan Ishak
Mohammad Bakri Mustafa
Mohammad Ismail
Mohd Hasan Selamat
Mohd Sapuan Salit
Mustafa Abdul Rahman
Nik Muhamad Nik Ab Majid
Norazman Mohamad Nor
Rozi Mahmud
Sam Choon Kook
Sudhanshu Shekhar Jamuar
Suhaimi Napis
Suleyman Aremu Muyibi
Suraya Sulaiman
Suzana Ab Hamid
Tan Wee Tee
Wan Omar Abdullah
Yaakob Che Man
Yasmin Modassir
Yuzine Esa
Zainuddin Md Yusoff
Zaleha Kassim
Zubir Din
Zulkiflle Leman
Zuriati Zakaria

Special Acknowledgment

The JST Editorial Board gratefully *acknowledges* the assistance of Doreen Dillah, who served as the English language editor for the 2010 issues, during the period from 31 December 2009 through 31 December 2010.

While every effort has been made to include a complete list of referees for the period stated above, however if any name(s) have been omitted unintentionally or spelt incorrectly, please notify the Executive Editor, *Pertanika* Journals at ndeeps@admin.upm.edu.my.

Any inclusion or exclusion of name(s) on this page does not commit the *Pertanika* Editorial Office, nor the UPM Press or the University to provide any liability for whatsoever reason.

Pertanika

Our goal is to bring high quality research to the widest possible audience

Journal of Science & Technology

INSTRUCTIONS TO AUTHORS

(Manuscript Preparation & Submission Guidelines)

Revised January 2010

We aim for excellence, sustained by a responsible and professional approach to journal publishing.
We value and support our authors in the research community.

Please read the guidelines and follow these instructions carefully; doing so will ensure that the publication of your manuscript is as rapid and efficient as possible. The Editorial Board reserves the right to return manuscripts that are not prepared in accordance with these guidelines.

About the Journal

Pertanika is an international peer-reviewed journal devoted to the publication of original papers, and it serves as a forum for practical approaches to improving quality in issues pertaining to tropical agriculture and its related fields. *Pertanika* began publication in 1978 as Journal of Tropical Agricultural Science. In 1992, a decision was made to streamline *Pertanika* into three journals to meet the need for specialised journals in areas of study aligned with the interdisciplinary strengths of the university. The revamped Journal of Science and Technology (JST) is now focusing on research in science and engineering, and its related fields. Other *Pertanika* series include Journal of Tropical Agricultural Science (JTAS); and Journal of Social Sciences and Humanities (JSSH).

JST is published in **English** and it is open to authors around the world regardless of the nationality. It is currently published two times a year i.e. in **January** and **July**.

Goal of *Pertanika*

Our goal is to bring the highest quality research to the widest possible audience.

Quality

We aim for excellence, sustained by a responsible and professional approach to journal publishing. Submissions are guaranteed to receive a decision within 12 weeks. The elapsed time from submission to publication for the articles averages 5-6 months.

Indexing of *Pertanika*

Pertanika is now over 30 years old; this accumulated knowledge has resulted in *Pertanika* JST being indexed in EBSCO.

Future vision

We are continuously improving access to our journal archives, content, and research services. We have the drive to realise exciting new horizons that will benefit not only the academic community, but society itself.

We also have views on the future of our journals. The emergence of the online medium as the predominant vehicle for the 'consumption' and distribution of much academic research will be the ultimate instrument in the dissemination of the research news to our scientists and readers.

Aims and Scope

Pertanika Journal of Science and Technology aims to provide a forum for high quality research related to science and engineering research. Areas relevant to the scope of the journal include: *bioinformatics, bioscience, biotechnology and bio-molecular sciences, chemistry, computer science, ecology, engineering, engineering design, environmental control and management, mathematics and statistics, medicine and health sciences, nanotechnology, physics, safety and emergency management*, and related fields of study.

Editorial Statement

Pertanika is the official journal of Universiti Putra Malaysia. The abbreviation for *Pertanika* Journal of Science & Technology is *Pertanika J. Sci. Technol.*

Guidelines for Authors

Publication policies

Pertanika policy prohibits an author from submitting the same manuscript for concurrent consideration by two or more publications. It prohibits as well publication of any manuscript that has already been published either in whole or substantial part elsewhere. It also does not permit publication of manuscript that has been published in full in Proceedings.

Editorial process

Authors are notified on receipt of a manuscript and upon the editorial decision regarding publication.

Manuscript review: Manuscripts deemed suitable for publication are sent to the Editorial Advisory Board members and/or other reviewers. We encourage authors to suggest the names of possible reviewers. Notification of the editorial decision is usually provided within to eight to ten weeks from the receipt of manuscript. Publication of solicited manuscripts is not guaranteed. In most cases, manuscripts are accepted conditionally, pending an author's revision of the material.

Author approval: Authors are responsible for all statements in articles, including changes made by editors. The liaison author must be available for consultation with an editor of *The Journal* to answer questions during the editorial process and to approve the edited copy. Authors receive edited typescript (not galley proofs) for final approval. Changes **cannot** be made to the copy after the edited version has been approved.

Please direct all inquiries, manuscripts, and related correspondence to:

The Executive Editor
Pertanika Journals
Research Management Centre (RMC)
IDEA Tower II, UPM-MTDC Technology Centre
Universiti Putra Malaysia
43400 UPM, Serdang, Selangor
Malaysia
Phone: + (603) 8947 1622
ndeeps@admin.upm.edu.my

or visit our website at http://www.pertanika2.upm.edu.my/jpertanika/index.htm for further information.

Manuscript preparation

Pertanika accepts submission of mainly four types of manuscripts. Each manuscript is classified as **regular** or **original** articles, **short communications**, **reviews**, and proposals for **special issues**. Articles must be in **English** and they must be competently written and argued in clear and concise grammatical English. Acceptable English usage and syntax are expected. Do not use slang, jargon, or obscure abbreviations or phrasing. Metric measurement is preferred; equivalent English measurement may be included in parentheses. Always provide the complete form of an acronym/abbreviation the first time it is presented in the text. Contributors are strongly recommended to have the manuscript checked by a colleague with ample experience in writing English manuscripts or an English language editor.

Linguistically hopeless manuscripts will be rejected straightaway (e.g., when the language is so poor that one cannot be sure of what the authors really mean). This process, taken by authors before submission, will greatly facilitate reviewing, and thus publication if the content is acceptable.

The instructions for authors must be followed. Manuscripts not adhering to the instructions will be returned for revision without review. Authors should prepare manuscripts according to the guidelines of *Pertanika*.

1. Regular article
Definition: Full-length original empirical investigations, consisting of introduction, materials and methods, results and discussion, conclusions. Original work must provide references and an explanation on research findings that contain new and significant findings.
Size: Should not exceed 5000 words or 8-10 printed pages (excluding the abstract, references, tables and/or figures). One printed page is roughly equivalent to 3 type-written pages.

2. Short communications
Definition: Significant new information to readers of the Journal in a short but complete form. It is suitable for the publication of technical advance, bioinformatics or insightful findings of plant and animal development and function.
Size: Should not exceed 2000 words or 4 printed pages, is intended for rapid publication. They are not intended for publishing preliminary results or to be a reduced version of Regular Papers or Rapid Papers.

3. Review article
Definition: Critical evaluation of materials about current research that had already been published by organizing, integrating, and evaluating previously published materials. Re-analyses as meta-analysis and systemic reviews are encouraged. Review articles should aim to provide systemic overviews, evaluations and interpretations of research in a given field.

Size: Should not exceed 4000 words or 7-8 printed pages.

4. Special issues
Definition: Usually papers from research presented at a conference, seminar, congress or a symposium.

Size: Should not exceed 5000 words or 8-10 printed pages.

5. Others
Definition: Brief reports, case studies, comments, Letters to the Editor, and replies on previously published articles may be considered.

Size: Should not exceed 2000 words or up to 4 printed pages.

With few exceptions, original manuscripts should not exceed the recommended length of 6 printed pages (about 18 typed pages, double-spaced and in 12-point font, tables and figures included). Printing is expensive, and, for the Journal, postage doubles when an issue exceeds 80 pages. You can understand then that there is little room for flexibility.

Long articles reduce the Journal's possibility to accept other high-quality contributions because of its 80-page restriction. We would like to publish as many good studies as possible, not only a few lengthy ones. (And, who reads overly long articles anyway?) Therefore, in our competition, short and concise manuscripts have a definite advantage.

Format
The paper should be formatted in one column format with the figures at the end. A maximum of eight keywords should be indicated below the abstract to describe the contents of the manuscript. Leave a blank line between each paragraph and between each entry in the list of bibliographic references. Tables should preferably be placed in the same electronic file as the text. Authors should consult a recent issue of the Journal for table layout.

There is no need to spend time formatting your article so that the printout is visually attractive (e.g. by making headings bold or creating a page layout with figures), as most formatting instructions will be removed upon processing.

Manuscripts should be typewritten, typed on one side of the ISO A4 paper with at least 4cm margins and double spacing throughout. Every page of the manuscript, including the title page, references, tables, etc. should be numbered. However, no reference should be made to page numbers in the text; if necessary, one may refer to sections. Underline words that should be in italics, and do not underline any other words.

Authors are advised to use Times New Roman 12-point font. Be especially careful when you are inserting special characters, as those inserted in different fonts may be replaced by different characters when converted to PDF files. It is well known that 'μ' will be replaced by other characters when fonts such as 'Symbol' or 'Mincho' are used.

We recommend that authors prepare the text as a **Microsoft Word** file.

1. Manuscripts in general should be organised in the following order:

    - **Page 1: Running title.** (Not to exceed 60 characters, counting letters and spaces). This page should **only** contain your running title of your paper. In addition, the **Subject areas** most relevant to the study must be indicated on this page. Select one or two subject areas (refer to the *Scope Form)*.
      A **list** of number of **black and white / colour figures and tables** should also be indicated on this page**.** Figures submitted in color will be printed in colour. See "*5. Figures & Photographs"* for details.

    - **Page 2: Author(s) and Corresponding author information.** This page should contain the **full title** of your paper with name(s) of all the authors, institutions and corresponding author's name, institution and full address (Street address, telephone number (including extension), hand phone number, fax number and e-mail address) for editorial correspondence. The names of the authors **must** be abbreviated following the international naming convention. e.g. Salleh, A.B., Tan, S.G., or Sapuan, S.M.

      Authors' addresses. Multiple authors with different addresses must indicate their respective addresses separately by superscript numbers:

      George Swan[1] and Nayan Kanwal[2]

[1]Department of Biology, Faculty of Science, Duke University, Durham, North Carolina, USA.
[2]Research Management Centre, Universiti Putra Malaysia, Serdang, Malaysia.

- **Page 3**: This page should **repeat** the **full title** of your paper with only the **Abstract** (the abstract should be less than 250 words for a Regular Paper and up to 100 words for a Short Communication). **Keywords** must also be provided on this page (Not more than eight keywords in alphabetical order).
- **Page 4 and subsequent pages**: This page should begin with the **Introduction** of your article and the rest of your paper should follow from page 5 onwards.

Abbreviations. Define alphabetically, other than abbreviations that can be used without definition. Words or phrases that are abbreviated in the introduction and following text should be written out in full the first time that they appear in the text, with each abbreviated form in parenthesis. Include the common name or scientific name, or both, of animal and plant materials.

Footnotes. Current addresses of authors if different from heading.

2. **Text.** Regular Papers should be prepared with the headings **Introduction**, **Materials and Methods**, **Results and Discussion, Conclusions** in this order. Short Communications should be prepared according to "*8. Short Communications."* below.
3. **Tables.** All tables should be prepared in a form consistent with recent issues of *Pertanika* and should be numbered consecutively with Arabic numerals. Explanatory material should be given in the table legends and footnotes. Each table should be prepared on a separate page. (Note that when a manuscript is accepted for publication, tables must be submitted as data - .doc, .rtf, Excel or PowerPoint file- because tables submitted as image data cannot be edited for publication.)
4. **Equations and Formulae.** These must be set up clearly and should be typed triple spaced. Numbers identifying equations should be in square brackets and placed on the right margin of the text.
5. **Figures & Photographs.** Submit an original figure or photograph. Line drawings must be clear, with high black and white contrast. Each figure or photograph should be prepared on a separate sheet and numbered consecutively with Arabic numerals. Appropriate sized numbers, letters and symbols should be used, no smaller than 2 mm in size after reduction to single column width (85 mm), 1.5-column width (120 mm) or full 2-column width (175 mm). Failure to comply with these specifications will require new figures and delay in publication. For electronic figures, create your figures using applications that are capable of preparing high resolution TIFF files acceptable for publication. In general, we require **300 dpi or higher resolution for coloured and half-tone artwork** and **1200 dpi or higher for line drawings**. For review, you may attach low-resolution figures, which are still clear enough for reviewing, to keep the file of the manuscript under 5 MB. Illustrations may be produced at extra cost in colour at the discretion of the Publisher; the author could be charged Malaysian Ringgit 50 for each colour page.
6. **References.** Literature citations in the text should be made by name(s) of author(s) and year. For references with more than two authors, the name of the first author followed by 'et al.' should be used.

   Swan and Kanwal (2007) reported that …
   The results have been interpreted (Kanwal et al. 2009).

   - References should be listed in alphabetical order, by the authors' last names. For the same author, or for the same set of authors, references should be arranged chronologically. If there is more than one publication in the same year for the same author(s), the letters 'a', 'b', etc., should be added to the year.
   - When the authors are more than 11, list 5 authors and then et al.
   - Do not use indentations in typing References. Use one line of space to separate each reference. The name of the journal should be written in full. For example:
     - Jalaludin, S. (1997a). Metabolizable energy of some local feeding stuff. *Tumbuh, 1,* 21-24.
     - Jalaludin, S. (1997b). The use of different vegetable oil in chicken ration. *Malayan Agriculturist, 11,* 29-31.
     - Tan, S.G., Omar, M.Y., Mahani, K.W., Rahani, M., Selvaraj, O.S. (1994). Biochemical genetic studies on wild populations of three species of green leafhoppers *Nephotettix* from Peninsular Malaysia. *Biochemical Genetics*, *32,* 415 - 422.
   - In case of citing an author(s) who has published more than one paper in the same year, the papers should be distinguished by addition of a small letter as shown above, e.g. Jalaludin (1997a); Jalaludin (1997b).
   - Unpublished data and personal communications should not be cited as literature citations, but given in the text in parentheses. 'In press' articles that have been accepted for publication may be cited in References. Include in the citation the journal in which the 'in press' article will appear and the publication date, if a date is available.

7. **Examples of other reference citations**:
   Monographs: Turner, H.N. and Yong, S.S.Y. (2006). *Quantitative Genetics in Sheep Breeding*. Ithaca: Cornell University Press.

   Chapter in Book: Kanwal, N.D.S. (1992). Role of plantation crops in Papua New Guinea economy. In Angela R. McLean (Eds.), *Introduction of livestock in the Enga province PNG* (p. 221-250). United Kingdom: Oxford Press.

   Proceedings: Kanwal, N.D.S. (2001). Assessing the visual impact of degraded land management with landscape design software. In N.D.S. Kanwal and P. Lecoustre (Eds.), *International forum for Urban Landscape Technologies* (p. 117-127). Lullier, Geneva, Switzerland: CIRAD Press.

8. **Short Communications** should include **Introduction, Materials and Methods, Results and Discussion, Conclusions** in this order. Headings should only be inserted for Materials and Methods. The abstract should be up to 100 words, as stated above. Short Communications must be 5 printed pages or less, including all references, figures and tables. References should be less than 30. A 5 page paper is usually approximately 3000 words plus four figures or tables (if each figure or table is less than 1/4 page).

   *Authors should state the total number of words (including the Abstract) in the cover letter. Manuscripts that do not fulfill these criteria will be rejected as Short Communications without review.

STYLE OF THE MANUSCRIPT

Manuscripts should follow the style of the latest version of the Publication Manual of the American Psychological Association (APA). The journal uses British spelling and authors should therefore follow the latest edition of the Oxford Advanced Learner's Dictionary.

SUBMISSION OF MANUSCRIPTS

All articles submitted to the journal **must comply** with these instructions. Failure to do so will result in return of the manuscript and possible delay in publication.

The **four copies** of your original manuscript, four sets of photographic figures, as well as a CD with the **electronic copy in MS Word** (including text and figures) together with a **cover letter**, **declaration form**, **referral form A**, **scope form** need to be enclosed. They are available from the *Pertanika*'s home page at http://www.rmc.upm.edu.my/j*Pertanika*/index.htm or from the Executive Editor's office upon request.

Please do **not** submit manuscripts directly to the editor-in-chief or to the UPM Press. All manuscripts must be **submitted through the executive editor's office** to be properly acknowledged and rapidly processed:

Dr. Nayan KANWAL
Executive Editor
Research Management Centre (RMC)
IDEA Tower II, UPM-MTDC Technology Centre
Universiti Putra Malaysia
43400 UPM, Serdang, Selangor, Malaysia
email: ndeeps@admin.upm.edu.my; tel: + 603-8947 1622

Authors should retain copies of submitted manuscripts and correspondence, as materials can not be returned.

Cover letter

All submissions must be accompanied by a cover letter detailing what you are submitting. Papers are accepted for publication in the journal on the understanding that the article is original and the content has not been published or submitted for publication elsewhere. This must be stated in the cover letter.

The cover letter must also contain an acknowledgement that all authors have contributed significantly, and that all authors are in agreement with the content of the manuscript.

The cover letter of the paper should contain (i) the title; (ii) the full names of the authors; (iii) the addresses of the institutions at which the work was carried out together with (iv) the full postal and email address, plus facsimile and telephone numbers of the author to whom correspondence about the manuscript should be sent. The present address of any author, if different from that where the work was carried out, should be supplied in a footnote.

As articles are double-blind reviewed, material that might identify authorship of the paper should be placed on a cover sheet.

Note When your manuscript is received at *Pertanika*, it is considered to be in its final form. Therefore, you need to check your manuscript carefully before submitting it to the executive editor (see also **English language editing** below).

Electronic copy
Preparation of manuscripts on a CD or DVD is preferable and articles should be prepared using MS Word. File name(s), the title of your article and authors of the article must be indicated on the CD. The CD must always be accompanied by four hard-copies of the article, and the content of the two must be identical. The CD text must be the same as that of the final refereed, revised manuscript. CDs formatted for IBM PC compatibles are preferred, as those formatted for Apple Macintosh are not acceptable. Please do not send ASCII files, as relevant data may be lost. Leave a blank line between each paragraph and between each entry in the list of bibliographic references. Tables should be placed in the same electronic file as the text. Authors should consult a recent issue of the Journal for table layout.

Peer review
In the peer-review process, three referees independently evaluate the scientific quality of the submitted manuscripts. The Journal uses a double-blind peer-review system. Authors are encouraged to indicate in **referral form A** the names of three potential reviewers, but the editors will make the final choice. The editors are not, however, bound by these suggestions.

Manuscripts should be written so that they are intelligible to the professional reader who is not a specialist in the particular field. They should be written in a clear, concise, direct style. Where contributions are judged as acceptable for publication on the basis of content, the Editor or the Publisher reserves the right to modify the typescripts to eliminate ambiguity and repetition and improve communication between author and reader. If extensive alterations are required, the manuscript will be returned to the author for revision.

The editorial review process
What happens to a manuscript once it is submitted to *Pertanika*? Typically, there are seven steps to the editorial review process:

1. The executive editor and the editorial board examine the paper to determine whether it is appropriate for the journal and should be reviewed. If not appropriate, the manuscript is rejected outright and the author is informed.

2. The executive editor sends the article-identifying information having been removed, to three reviewers. Typically, one of these is from the Journal's editorial board. Others are specialists in the subject matter represented by the article. The executive editor asks them to complete the review in three weeks and encloses two forms: (a) referral form B and (b) reviewer's comment form along with reviewer's guidelines. Comments to authors are about the appropriateness and adequacy of the theoretical or conceptual framework, literature review, method, results and discussion, and conclusions. Reviewers often include suggestions for strengthening of the manuscript. Comments to the editor are in the nature of the significance of the work and its potential contribution to the literature.

3. The executive editor, in consultation with the editor-in-chief, examines the reviews and decides whether to reject the manuscript, invite the author(s) to revise and resubmit the manuscript, or seek additional reviews. Final acceptance or rejection rests with the Editorial Board, who reserves the right to refuse any material for publication. In rare instances, the manuscript is accepted with almost no revision. Almost without exception, reviewers' comments (to the author) are forwarded to the author. If a revision is indicated, the editor provides guidelines for attending to the reviewers' suggestions and perhaps additional advice about revising the manuscript.

4. The authors decide whether and how to address the reviewers' comments and criticisms and the editor's concerns. The authors submit a revised version of the paper to the executive editor along with specific information describing how they have answered' the concerns of the reviewers and the editor.

5. The executive editor sends the revised paper out for review. Typically, at least one of the original reviewers will be asked to examine the article.

6. When the reviewers have completed their work, the executive editor in consultation with the editorial board and the editor-in-chief examine their comments and decide whether the paper is ready to be published, needs another round of revisions, or should be rejected.

7. If the decision is to accept, the paper is sent to that Press and the article should appear in print in approximately two to three months. The Publisher ensures that the paper adheres to the correct style (in-text citations, the reference list, and tables are typical areas of concern, clarity, and grammar). The authors are asked to respond to any queries by the Publisher. Following these corrections, page proofs are mailed to the corresponding authors for their final approval. At this point, only essential changes are accepted. Finally, the article appears in the pages of the Journal and is posted on-line.

English language editing
Authors are responsible for the linguistic accuracy of their manuscripts. Authors not fully conversant with the English language should seek advice from subject specialists with a sound knowledge of English. The cost will be borne by the author, and a copy of the certificate issued by the service should be attached to the cover letter.

Author material archive policy
Authors who require the return of any submitted material that is rejected for publication in the journal should indicate on the cover letter. If no indication is given, that author's material should be returned, the Editorial Office will dispose of all hardcopy and electronic material.

Copyright
Authors publishing the Journal will be asked to sign a declaration form. In signing the form, it is assumed that authors have obtained permission to use any copyrighted or previously published material. All authors must read and agree to the conditions outlined in the form, and must sign the form or agree that the corresponding author can sign on their behalf. Articles cannot be published until a signed form has been received.

Lag time
The elapsed time from submission to publication for the articles averages 5-6 months. A decision of acceptance of a manuscript is reached in 2 to 3 months (average 9 weeks).

Back issues
Single issues from current and recent volumes are available at the current single issue price from UPM Press. Earlier issues may also be obtained from UPM Press at a special discounted price. Please contact UPM Press at penerbit@putra.upm.edu.my or you may write for further details at the following address:

UPM Press
Universiti Putra Malaysia
43400 UPM, Serdang
Selangor Darul Ehsan
Malaysia.

Pertanika

Our goal is to bring high quality research to the widest possible audience

Pertanika is Indexed in SCOPUS & EBSCO

Pertanika is an international peer-reviewed leading journal in Malaysia which began publication in 1978. The journal publishes in three different areas — Journal of Tropical Agricultural Science (JTAS); Journal of Science and Technology (JST); and Journal of Social Sciences and Humanities (JSSH).

JTAS is devoted to the publication of original papers that serves as a forum for practical approaches to improving quality in issues pertaining to tropical agricultural research or related fields of study. It is published twice a year in **February** and **August**.

JST caters for science and engineering research or related fields of study. It is published twice a year in **January** and **July**.

JSSH deals in research or theories in social sciences and humanities research with a focus on emerging issues pertaining to the social and behavioural sciences as well as the humanities, particularly in the Asia Pacific region. It is published twice a year in **March** and **September**.

Why should you publish in Pertanika Journals?

Benefits to Authors

PROFILE: our journals are circulated in large numbers all over Malaysia, and beyond in Southeast Asia. Recently, we have widened our circulation to other overseas countries as well. We will ensure that your work reaches the widest possible audience in print and online, through our wide publicity campaigns held frequently, and through our constantly developing electronic initiatives via Pertanika Online and e-pertanika.

QUALITY: our journals' reputation for quality is unsurpassed ensuring that the originality, authority and accuracy of your work will be fully recognised. Our double-blind peer refereeing procedures are fair and open, and we aim to help authors develop and improve their work. Pertanika JTAS is now over 30 years old; this accumulated knowledge has resulted in Pertanika being indexed in SCOPUS (Elsevier) and EBSCO.

AUTHOR SERVICES: we provide a rapid response service to all our authors, with dedicated support staff for each journal, and a point of contact throughout the refereeing and production processes. Our aim is to ensure that the production process is as smooth as possible, is borne out by the high number of authors who publish with us again and again.

LAG TIME: Submissions are guaranteed to receive a decision within 14 weeks. The elapsed time from submission to publication for the articles averages 5-6 months. A decision of acceptance of a manuscript is reached in 3 to 4 months (average 14 weeks).

Call for Papers

Pertanika invites you to explore frontiers from all fields of science and technology to social sciences and humanities. You may contribute your scientific work for publishing in UPM's hallmark journals either as a ***regular article, short communication,*** or ***a review article*** in our forthcoming issues. Papers submitted to this journal must contain original results and must not be submitted elsewhere while being evaluated for the Pertanika Journals.

Submissions in **English** should be accompanied by an abstract not exceeding 300 words. Your manuscript should be no more than 6,000 words or 10-12 printed pages, including notes and abstract. Submissions should conform to the Pertanika style, which is available at www.pertanika2.upm.edu.my/jpertanika/index.htm or by mail or email upon request.

Papers should be double-spaced 12 point type (Times New Roman fonts preferred). The first page should include the title of the article but no author information. Page 2 should repeat the title of the article together with the names and contact information of the corresponding author as well as all the other authors. Page 3 should contain the title of the paper and abstract only. Page 4 and subsequent pages to have the text - Acknowledgments - References - Tables - Legends to figures – Figures, etc.

Questions regarding submissions should only be directed to the Executive Editor, *Pertanika* Journals.

Remember, ***Pertanika is the resource to support you in strengthening research and research management capacity.***

An Award Winning International-Malaysian Journal

FEB. 2008

Mail your submissions to:

The Executive Editor
Pertanika Journals
Research Management Centre (RMC)
Publication Division
1st Floor, IDEA Tower II
UPM-MTDC, Technology Centre
Universiti Putra Malaysia
43400 UPM, Serdang, Selangor, Malaysia

Tel: +603-8947 1622
ndeeps@admin.upm.edu.my
www.pertanika2.upm.edu.my/jpertanika/index.htm